Interactive effects of ageing processes and early life stress on brain structure: a neuroimaging informatics approach.

Nathan Shaun Kindred

Supervisors: Dr Colline Poirier, Dr Yujiang Wang, Professor Christopher Petkov and Professor John-Paul Taylor

COVID-19 Impact Statement removed in published copy

Abstract

Though it is well established that ageing and early-life stress can cause changes in brain structure, there is less agreement on both region-specific changes and how interactions between ageing and early-life stress may impact on brain structure. Investigations in humans often rely on cross-sectional studies, and are confounded by a number of drawbacks and biases. These issues can be mitigated through the use of model animals, such as rhesus macaques. However, processing macaque MRI data comes with a number of issues, precluding the use of human MRI processing pipelines. Therefore, this project first involved the creation of a novel processing pipeline for macaque MRI data. The outputs of the AutoMacq pipeline had a low error-rate and high levels of reliability.

As the majority of previous studies focus on brain changes in late adulthood, this project focused on the under-researched period of early to mid-adulthood. Using a longitudinal approach, significant decreases, in both cortical thickness and grey matter volume, with ageing were identified, primarily within the frontal, temporal and parietal lobes.

Early weaning was utilised as a measure of early life stress. In an age-matched cross-sectional dataset, subjects weaned before 12 months showed significantly lower cortical thickness in regions of the temporal lobe, compared to those weaned after 12 months.

Significant interactions between weaning and ageing were found for grey matter volume in one area of the occipital lobe, as well for cortical thickness in regions of parietal and occipital lobes. Brain areas across the whole brain appeared sensitive to ageing, whereas regions specifically involved in visual processing seemed most affected by early weaning.

Overall, this project resulted in the creation of a novel macaque MRI processing pipeline, and provided new knowledge on the impacts of ageing and early-life stress on brain structure during early to mid-adulthood.

Acknowledgements

Dedicated to Alex, for all of your love and support.
Love and thanks to my mam, dad, brother, and the rest of my family.
Thank you to Isabella, Maria, Alix, Deighton, Janire, Chris and Genevieve for going through the trials and tribulations of a PhD with me.
With thanks to Dr Colline Poirier and Dr Yujiang Wang for their guidance throughout my PhD, as well as Professor Christopher Petkov and Professor John-Paul Taylor.

This project was funded by the MRC DiMeN Doctoral Training Partnership (MR/N013840/1).
With thanks to Dr Dirk Jan Ardesch and Professor Martijn van den Heuvel for their guidance on FreeSurfer and assistance in writing the initial FreeSurfer scripts. Thank you to Professor Hank P. Jedema and Dr Charles W Bradberry for sharing the NIDA dataset, Dr Jerome Sallet (Dpt of Experimental Psychology, Oxford, UK /INSERM U1208, Bron, France) for sharing the Oxford dataset, and the Cognitive Neuroscience Laboratory at the German Primate Center for sharing the DPZ dataset.

Table of Contents

List of Tables and Figures

Chapter 1: Rhesus Macaques as an Animal Model for Studying the Impacts of Stress and Ageing on Brain Structure

1.1 The Use of Rhesus Macaques as an Animal Model

Animal models are non-human species' which have similarities to humans that allow them to be utilised to investigate physiological changes and diseases seen in humans. Animal models allow for the carrying out of experiments which could not be carried out with human subjects, either due to ethical concerns or practical issues (Simmons 2008).

Mice and rats account for around 95% of the animal models utilised in biomedical research (https://www.nabr.org/biomedical-research/importance-biomedical-research). This is partially due to the relative ease and low cost of breeding, housing, and maintaining rodents (due to their small size). Additionally, the short lifespan and fast reproductive cycle of rodents allows for quick and efficient research, and their relatively docile temperament means they can be safely handled and manipulated. Furthermore, there is a strong foundation of information already available on the genetics, anatomy, and physiology of both rats and mice. In fact, it is possible to breed rodent models which have been genetically manipulated to better investigate specific research questions (Bryda 2013).

However, though rodents are relatively genetically similar to humans, they diverged evolutionarily over 80 million years ago meaning that they have evolved in different environments with different evolutionary pressures (Kumar *et al.* 2017). Because of this, it is difficult to accurately recreate human phenotypes in rodent models, which can make translating research from rodents to humans problematic. This is exemplified by the number of pharmaceutical studies that see success in rodent models which then cannot be translated to humans, either due to a lack of efficacy or issues with toxicity. Additionally, rodents lack the behavioural complexity of humans, and mice in particular do not live in social structures similar to humans, limiting their translatability further (Ellenbroek and Youn 2016). For the use of rodents as disease models, it is often not possible to fully replicate the suite of symptoms seen in humans, and for rodent models of physiological changes it can be difficult to see the full phenotypic impact that would be exhibited in humans.

When considering neuroscience research specifically, rodent brains do exhibit similar organisation to the human brain, with many homologous structures (Beauchamp *et al.* 2022). However, rodents are limited as neuroscience models due to the major differences in gross brain structure between rodents and humans. Not only are rodent brains lissencephalic, lacking the gyri and sulci of the human brain (Kelava, Lewitus and Huttner 2013), but they also lack multiple cortical areas which are unique to primates, such as the prefrontal cortex (Wise 2008). Clearly, though rodent models have their value, they are often not an ideal model, particularly when it comes to neuroscience research. An alternative which can overcome the outlined drawbacks of rodent models is the use of non-human primates (NHPs) as animal models.

Non-human primates have been utilised as animal models for decades and are of particular comparative and translational interest due to their relative evolutionary proximity to humans. Compared to rodents, non-human primates diverged evolutionarily from humans more recently, with some NHP species diverging as recently as 5 million years ago (Kumar *et al.* 2017). Many NHP species were therefore exposed to environments and evolutionary pressures far more similar to those experienced by humans. As a result of this, the evolutionary proximity of NHPs provides a much higher level of genetic similarity to humans, compared with other model organisms such as rodents (Phillips *et al.* 2014; Stonebarger *et al.* 2021). This genetic similarity corresponds to greater comparability to humans in terms of brain anatomy and cognitive abilities, which has made NHPs crucial model animals in neuroscience research (Phillips *et al.* 2014; Roefsema and Treue 2014; Stonebarger *et al.* 2021). The NHP species most closely related to humans are great apes, such as chimpanzees and bonobos, which diverged evolutionarily from humans less than 10 millions years ago (Kumar *et al.* 2017). However, the use of great apes in research has been banned due to ethical concerns in the UK since 1997 and in Europe since 2013 (EU directive 2010/63). As a consequence of this, rhesus macaques have now become one of the most commonly used NHP model animals (Phillips *et al.* 2014; Stonebarger *et al.* 2021).

Rhesus macaques are a member of the phylogenetic family of primates termed ‘old world monkeys’, which are the most evolutionarily proximal to humans after great apes (diverging around 29 million years ago) (Kumar *et al.* 2017). As

such, ‘old world monkeys’ show more genetic and neuroanatomical similarity to humans than ‘new world monkeys’ such as marmosets (which diverged around 45 million years ago and, like rodents, are lissencephalic) (Kumar *et al.* 2017). Rhesus macaques have been utilised extensively in biomedical research and, as a result, macaque studies are benefitted by considerable knowledge on their genetics and anatomy (Phillips *et al.* 2014; Roefsema and Treue 2014; Stonebarger *et al.* 2021). It is well established that rhesus macaques are social animals and display behaviours more similar to humans than rodents do. Consequently, macaques can more clearly display the phenotypic impacts of physiological changes, and are more likely to replicate the full suite of symptoms seen in humans when used as a disease model.

1.1.1 Benefits of rhesus macaque models for studies of ageing

Ageing is defined as the natural accumulation of changes over time, that increase susceptibility to disease and death (Harman 1991). As advances in medical science continue to extend the lifespan of humans, age-related frailty is becoming more common and age-related diseases are becoming more prevalent (Dall *et al.* 2013; Faye *et al.* 2021). Accordingly, there is a growing need for research into both healthy and unhealthy ageing processes, in order to determine how best to reduce the impact of ageing, and age-related diseases, on the population. In particular, there is a need for studies prior to late adulthood, as by that point in the life course the impacts of ageing, and any age-related diseases, are likely to have already manifested. By investigating ageing during early to mid-adulthood it may be possible to identify changes that can be targeted by therapies to then prevent or mitigate age-related problems later in life.

However, human studies of ageing are often limited by a cross-sectional study design in which outcome measures are simply compared between a group of older individuals and a group of younger individuals. A cross-sectional design is usually chosen because a longitudinal study of humans can be logistically difficult and time-consuming. The issue with this cross-sectional design is that it only allows for the investigation of between-subjects differences, which can be confounded by other factors. For example, genetic factors such as vulnerability genes for age-related diseases, environmental factors such as diet and exercise, as well as interactions between genetic and environmental factors such as the suppression of DNA repair

mechanisms by stress, can all confound a cross-sectional study of ageing (Song *et al.* 2021). Also, for ageing studies in particular, Di Biase *et al.* (2023) has recently highlighted an apparent underestimation of effects when utilising a cross-sectional approach as opposed to a longitudinal approach. Another potential issue with human studies of ageing comes from the nature of the recruitment used, which can bias the sample. For example, hospital samples may be biased towards those with greater age-related decline, whereas community samples may be biased towards healthier participants as those who are less healthy may find it more difficult to be involved in a study. These issues with human studies of ageing can be circumvented through the use of longitudinal studies with animal models, such as rhesus macaques.

Macaques are a particularly useful animal model for studies of ageing, as they have a longer lifespan than other models such as rodents but age at an accelerated rate compared to humans (3-4 times) (Mattison and Vaughan 2017). This allows for more efficient longitudinal studies of ageing than could be carried out in humans, as longer life periods can be studied in a shorter time frame, with reduced subject dropout. Additionally, despite their accelerated ageing rate, the life stages of rhesus macaques (development, maturation, reproduction and senescence) are comparable to those of humans in terms of their relative timing (Mattison and Vaughan 2017). When macaques reach old age they show a similar old age phenotype to humans, with reduced mobility, wrinkling of skin and thinning and greying of hair (Huneke *et al.* 1996; Uno 1997). Furthermore, similar to humans, macaques have been found to show age-related increases and redistribution of body fat, as well as decreases in both bone mineral density and muscle mass later in life (Uno 1997; Ramsey, Laatsch and Kemnitz 2000; Cerroni *et al.* 2000). As such, the marked age-related frailty seen in humans is likely well replicated in macaques.

Moreover, similar age-related brain changes to those observed in humans, such as a loss of dendritic spines and synapses and/or an increase in microglia density, have been identified in rhesus macaques (Peters and Kemper 2012; Robillard *et al.* 2016). These brain changes may relate to the development of mild cognitive impairment which has also been observed in both older macaques and older humans (Peters and Kemper 2012). Studies have found that macaques that reach very old age can develop neurofibrillary tangles and amyloid plaques, similar to those associated with Alzheimer's disease in humans. However, these macaques

have far fewer tangles and plaques than are seen in Alzheimer's patients, and there appears to be no correlation between the plaques/tangles and cognitive decline, nor do they go on to develop Alzheimer's disease itself (Peters and Kemper 2012; Arnsten *et al.* 2019). This indicates that macaques are a good model of healthy ageing but can also be informative for studying the early stages of age-related disorders such as Alzheimer's disease.

1.1.2 Benefits of rhesus macaque models for studies of stress

Stress is a natural response to both real and perceived threats. A stress response is generally thought to involve both physical aspects such as activation of the sympathetic nervous system and the hypothalamic-pituitary-adrenal (HPA) axis, as well as psychological aspects such as changes in mood and loss of focus (Ellenbogen *et al.* 2002; Lucini *et al.* 2005; Lovell, Moss and Wetherell 2011; Liu *et al.* 2020). Stress is a major risk factor for a wide array of diseases including diabetes, digestive disorders and cardiovascular disease, as well as for psychological conditions such as post-traumatic stress disorder, anxiety disorders and mood disorders (Faravelli and Pallanti 1989; Kessing *et al.* 2003; Grieger *et al.* 2006; Lee *et al.* 2015; Harris *et al.* 2017; Satyjeet *et al.* 2020). Stress can occur at any point in the life course and can have both acute effects, which are only present for a relatively short period soon after the stress occurs, and chronic effects, which can last long after the initial occurrence of stress. Generally, chronic effects are of greater interest as they are more likely to impact on an individual's quality of life, and as such there is a need to investigate the impacts long after a stressful event has occurred.

As with studies of ageing, investigating the chronic effects of stress can be difficult for human studies as a longitudinal design is often impractical. Cross-sectional human studies investigating the impacts of stress usually rely on self-reports of previous stressful events, which can introduce memory-related recall bias into the studies (Althubaiti 2016). This can occur either through patients completely forgetting past experiences, or misremembering past experiences as being more or less stressful than they actually were. As a result, the study's findings may be confounded, as subjects are incorrectly classified in terms of the amount or severity of stress they have experienced. Additionally, studies of stress in humans are often also confounded by a difficulty to control for all of the potential stressors throughout

the life course, as well as other unexpected nuisance variables, and any potential antistressors. This is due to the vast array of events that can be experienced through the human life course that may either be stressful in and of themselves or may in some way interact with the impacts of stress, and the fact that human subjects do not live their lives in a controlled environment. The lack of control over the events experienced by human subjects can cause further issues due to different events potentially also resulting in different types, and levels of severity, of stress. As a result of this, studies of a particular stressful event may be confounded by the fact some subjects have experienced other stressful events unknown to the researchers, that are either more stressful than the event of interest, or that have a cumulative effect with the stress of the event of interest. As with the problems faced by human studies of ageing, the issues outlined above can be minimised through the use of animal models, such as rhesus macaques, for studies of stress.

As was previously discussed, longitudinal studies are more feasible when using rhesus macaques as a model animal, owing to their accelerated rate of ageing and the fact their lifespan is longer than other common model animals such as rodents (Mattison and Vaughan 2017). This longer lifespan of macaques compared to other model animals provides a specific benefit for studies of stress, in that it allows for more efficient investigation of the chronic effects of stress. Additionally, laboratory macaques are closely monitored throughout their life course, allowing for easier identification of any potential stressors, antistressors and nuisance variables. This should allow for any of these variables that are not of interest in a study to be identified and controlled for in a way that is unlikely to be possible in a study utilising human subjects. The controlled nature of the environment that captive macaques live in when utilised for research, also may result in comparably fewer types of stressors than would be experienced by human subjects, and in turn, more comparable stressors between the captive macaques. Furthermore, being involved in research likely comes with intrinsically stressful events such as separation for weaning or training purposes, surgeries and the use of anaesthesia, and fluid/diet restrictions which are used as motivational tools (Pfefferle *et al.* 2018). These events, which are often common amongst groups of captive macaques, allow for the investigation of the impacts of stress taking advantage of stressors already existing in the animals' lives. This allows for the introduction of any additional stressors to be avoided, in line

with the ‘3Rs’ (Replacement, Reduction and Refinement) for studies using animal models.

Additionally, rhesus macaques are similar to humans in that they are highly social animals. This allows for investigation of stressors analogous to those experienced by humans, such as conflict or loss of a loved one. For example, stress caused by conflict with friends or family can be modelled by macaque social group instability, and stress due to social isolation can be modelled through removal of a macaque from its social group. It is also possible to model the stress humans can experience due to societal disadvantages such as poverty or general low social status, through the use of low-ranking macaques who are known to inherently experience high levels of stress (Meyer and Hamel 2014). The social nature of macaques also allows for the investigation of coping mechanisms, as it is likely the techniques macaques use to cope with stress are comparable to those used by humans (Wooddell *et al.* 2017).

The similar biology of macaques and humans also lends itself well to studies of stress. Both macaques and humans share a common system in the HPA axis, which is activated upon exposure to stress. The HPA axis produces the glucocorticoid cortisol when either a macaque or a human is exposed to stress, and studies will often measure this cortisol as a proxy of stress levels (Koch *et al.* 2014). Though the HPA axis is highly conserved across vertebrate species, there are likely subtle differences between species which will be less prominent between humans and NHPs due to their genetic similarity. This is exemplified by the fact that some animals which are less genetically similar to humans, such as rats and mice, produce another glucocorticoid, known as corticosterone, instead of cortisol when exposed to stress (Yu *et al.* 2015). Additionally, development of the HPA axis differs between rodents and primates, with rodents during early life displaying a lack of HPA axis activation in response to stress. This contrasts with primates which do show HPA axis activation in response to stress throughout the life course, and may mean that the impacts of early life stress in rodents will differ from those in both macaques and humans (Parker and Maestripieri 2011).

1.2 The Importance of Studying Brain Structural Changes

As was previously discussed, humans and rhesus macaques are highly similar in terms of brain structure, with the brains of both species being gyrencephalic. The brains of both humans and macaques are primarily composed of two tissue types, these being grey matter and white matter. These tissues are surrounded by cerebrospinal fluid which protects the brain from injury and provides it with nutrients. The majority of the brain is made up of white matter, which conducts information between different brain regions and the spinal cord. Loss of white matter can therefore make communication within the brain (and to the spinal cord) more difficult, which can lead to functional loss if there is no alternative to the pathway that is damaged (Kinnunen *et al.* 2011).

Grey matter makes up the outer layer of the brain and contains most of the neuronal cell bodies, where information processing occurs. Grey matter is therefore crucial for an array of functions, including memory, emotions and movement (Rosenbaum *et al.* 2005; Anderson *et al.* 2006; Gauthier *et al.* 2012). Consequently, unlike with white matter loss where alternative pathways can prevent functional loss, any grey matter loss can result in functional loss. In fact, the more extensive the grey matter loss the more extensive the corresponding functional loss tends to be. As such, grey matter changes are often of greater interest than white matter changes. Studies of brain injuries have shown a wide array of functional impairments dependent on which region of the brain is damaged. For example, damage to the hippocampus has been linked to difficulties with forming and retrieving memories (Rosenbaum *et al.* 2005), damage to the motor cortex results in issues with coordinating and carrying out movements (Gauthier *et al.* 2012), and damage to the prefrontal cortex can lead to problems with emotional regulation (Anderson *et al.* 2006). Additionally, there is evidence that the greater amount of grey matter that is lost, following a brain injury, the poorer the prognosis for recovery (Gauthier *et al.* 2012). Grey matter loss has also been linked to neurodegenerative disorders such as Alzheimer's disease and Parkinson's disease, as well as psychiatric disorders such as schizophrenia and mood disorders (Shad, Muddasani and Rao 2012; Vita *et al.* 2012; Wang *et al.* 2019; Zeighami *et al.* 2019; Wu *et al.* 2021).

It is clear that changes in brain structure, and in particular changes in the grey matter, correspond strongly to functional changes, and can have a major impact on

quality of life, as well as being hallmarks of neurological disorders. As such, there is great interest in not only studying how brain structure, and more specifically grey matter, changes over the life course, but also how other factors (for example stress) impact on it.

1.3 The Use of Magnetic Resonance Imaging to Investigate Brain Structural Changes

One popular method of investigating brain structural changes is through the use of magnetic resonance imaging (MRI). MRI is a non-invasive technique which can be utilised to produce highly detailed, three dimensional, anatomical images. Though MRI scanning can be carried out on the whole body, only MRI scans of the brain will be discussed in the current project.

The production of MRI images relies on the use of magnets to generate a magnetic field. When a subject is in an MRI scanner, the magnetic spin of protons in their body aligns with the magnetic field, creating a net magnetization aligned with the magnetic field. Radiofrequency pulses are then utilised to flip the magnetization. When the radiofrequency pulses end, the magnetization will emit a detectable electromagnetic signal while returning to its initial state. The amount of this energy released, along with the time taken for it to be released, will differ across different tissue types, allowing for the creation of detailed anatomical images. MRI scanning produces many two dimensional ‘slices’ of the subject which then make up a complete, three-dimensional image.

There are three parameters that affect the MRI signal of a tissue: proton density, longitudinal relaxation time (T1) and transverse relaxation time (T2). Proton density is a measure of how much initial magnetization there is. T1 is how fast the magnetization returns to its initial state, and T2 is how fast the signal decays after the radiofrequency pulse. MRI images will commonly be referred to as either T1- or T2-weighted. With T1-weighted images the signal is strongest for tissues with a fast magnetization recovery, like fat. This causes white matter to appear brighter than grey matter, and cerebrospinal fluid to appear darker than both of these tissues (see figure 1).

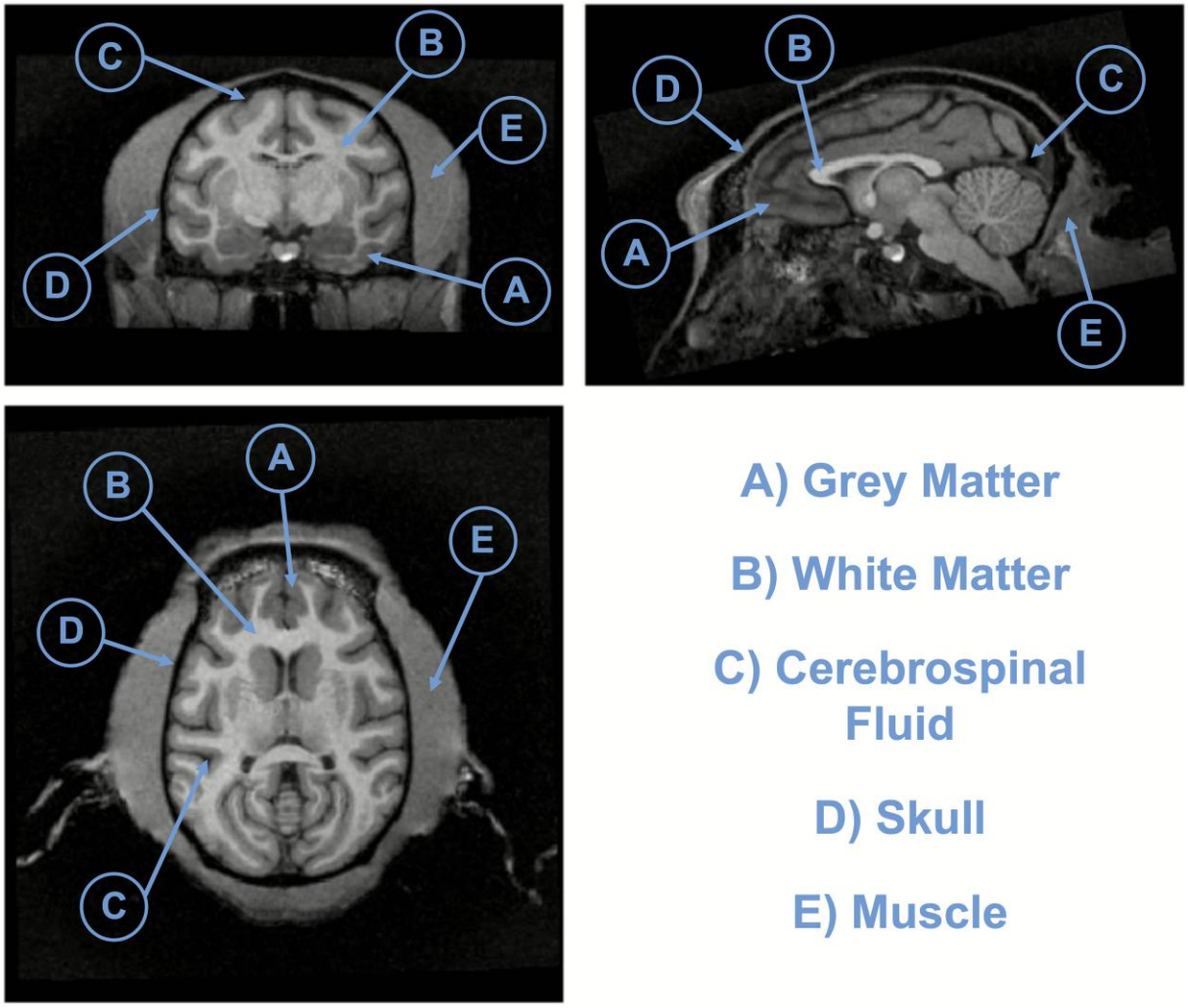

Figure 1: A Labelled Example of a T1-weighted Rhesus Macaque MRI Scan. Three standard views are presented, these being coronal (top left panel), sagittal (top right panel) and axial (bottom left panel).

In contrast, for T2-weighted images the signal is strongest for tissues with a long signal decay, like water. This results in cerebrospinal fluid appearing the brightest on scans, and grey matter appearing brighter than white matter (see figure 2). The differences in the contrast of T1- and T2-weighted images means than utilising both in tandem can aid in image processing, as it allows for easier distinction of the boundaries between different tissues.

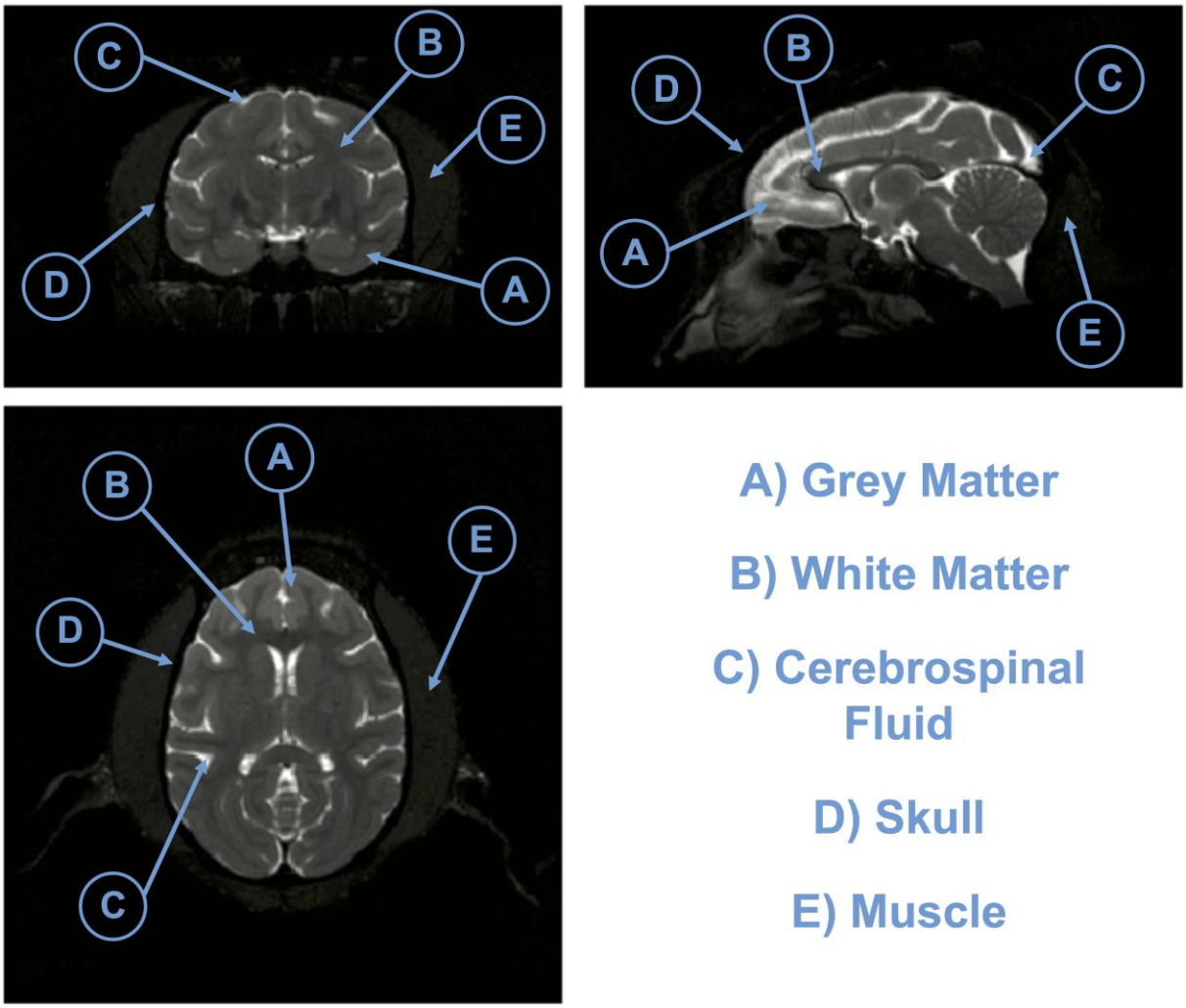

Figure 2: A Labelled Example of a T2-weighted Rhesus Macaque MRI Scan. Three standard views are presented, these being coronal (top left panel), sagittal (top right panel) and axial (bottom left panel).

1.3.1 Methods of processing MRI images

Once acquired, MRI images need to be further processed in order to allow for the analysis of different metrics (such as the volumes of different tissues in a specific region), and this processing can be done in a number of different ways. Early MRI studies tended to use manual methods to process scans, which generally involved tracing over structures in order to determine differences or changes in their size. However, this method is not only time consuming and difficult but also subjective, meaning it can introduce bias into studies. As such, more objective and efficient approaches to processing MRI data were needed. Voxel Based Morphometry (VBM) is one such method of investigating brain structural changes captured in MRI images.

VBM quantifies volumes of different tissues in each voxel (3-dimensional pixel) of the brain, allowing for both region-specific and global differences or changes to be identified. This is done by segmenting the brain into tissue classes (e.g., grey matter, white matter, and cerebrospinal fluid) and warping the segmented image to a template (Ashburner and Friston 2000). VBM is a well-established methodology which has been utilised in MRI research for decades to investigate changes in brain structure, with changes in grey matter volume being the most commonly investigated (Goto *et al.* 2022).

Surface-based morphometry (SBM) provides an alternative method, to voxel-based morphometry, to analyse changes in brain structure using MRI images, and has gained popularity over recent years (Goto *et al.* 2022). Surface-based morphometry works through the generation of brain surfaces (the white matter surface and the grey matter surface), which are then warped to a template in order to allow for computation of morphological metrics (Dale, Fischl and Sereno 1999; Fischl, Sereno and Dale 1999). SBM is commonly utilised to investigate surface area and/or cortical thickness, two metrics which contribute to tissue volume measurements (Storsve *et al.* 2014).

Importantly, Goto *et al.* (2022) recently recommended that studies utilise both voxel-based and surface-based morphometry in tandem, in order to exploit data to the fullest extent possible, capitalise on the benefits of both approaches, and allow for comparison to a wider range of previous studies. As such, the current project has utilised both voxel-based and surface-based morphometry for all of the analyses carried out.

1.3.2 The impacts of scan parameters on MRI image processing

When processing MRI images the accuracy of the final outputs, and the subsequent statistical analyses, can be greatly affected by the image quality. In particular, accurate tissue segmentation is crucial for MRI image processing, and this accuracy is affected by a number of factors related to image quality. These factors include contrast to noise ratio, signal homogeneity, image resolution and image artifacts. Figure 3 illustrates how the accuracy of tissue segmentation can be reduced by low contrast to noise ratio, poor signal homogeneity or low image resolution. Crucially, these different aspects of MRI image quality can be heavily influenced by

the parameters of both the scanner and the sequence utilised, meaning that these parameters must be considered when carrying out MRI research.

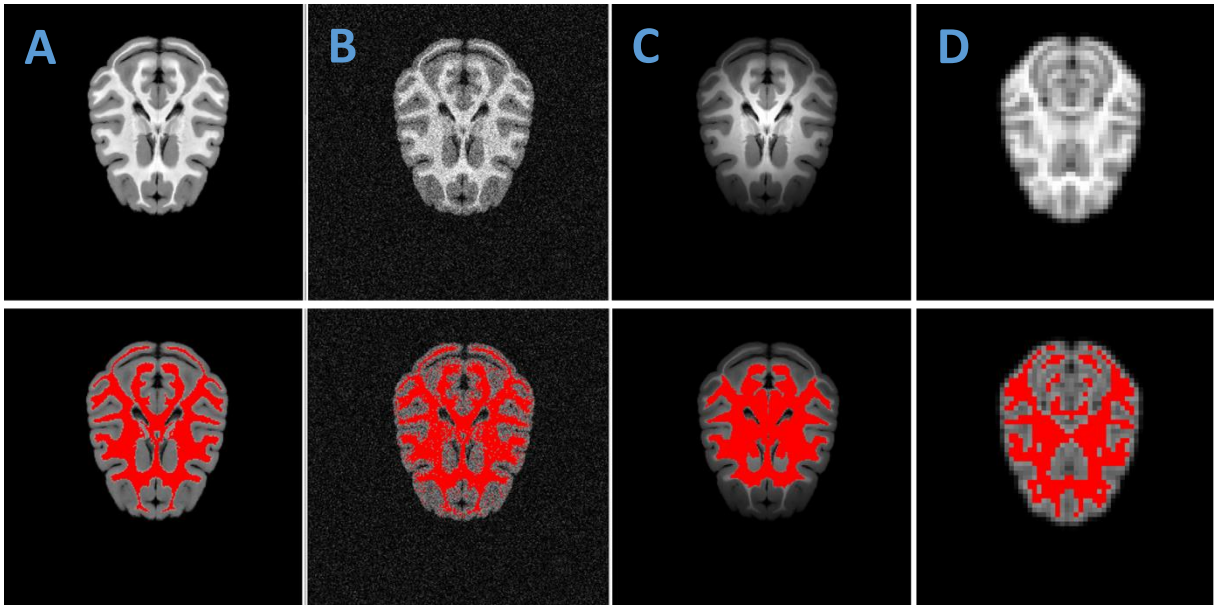

Figure 3: The Effect of Image Quality on the Segmentation of White Matter and Grey Matter. Top row: raw images; Bottom row: tissue segmentation. A: Good image quality, B: Low contrast to noise ratio, C: poor signal homogeneity, D: Low image resolution.

Perhaps the most important scan parameter is the magnetic field strength (also referred to as the scanner strength). Field strength is measured in tesla (T), and the higher the field strength the higher the signal to noise ratio (SNR). Higher SNR then results in clearer images, allowing for smaller brain structures to be more easily distinguished (Chow *et al.* 2015). The majority of MRI scanners have a strength of between 1.5T and 3T, though there are also scanners with a strength lower than 1.5T or higher than 3T (e.g., 7T and beyond). Though scanners with a very high field strength have a higher SNR, they also face additional issues such as variations in image intensity and artifacts, which can then make image processing more difficult (Milham *et al.* 2018).

A further scan parameter that can influence image processing is the voxel size. This is a measure, usually in millimetres, of how large the voxels (3D pixels) that make up the image are. Scans with a larger voxel size have a coarser image resolution, meaning that finer details (such as smaller brain structures) cannot be

distinguished. As a consequence of this, if the voxel size used is too large then the accuracy of the image processing will be reduced (Mulder *et al.* 2019). Though it is important to note that in order to acquire images with a smaller voxel size (and therefore a higher resolution) longer scanning times are needed, and the SNR will be decreased.

Another important factor affecting image quality is the radiofrequency coils that are utilised. These coils can have a direct effect on the image quality as they affect the coverage of the scan, meaning that the positioning of the coils directly impacts on signal strength and homogeneity across the brain (Milham *et al.* 2018). Additionally, utilising more coil elements allows for the signal to be acquired multiple times simultaneously. This can allow for faster image acquisition and increases the SNR. Though it should be noted that the SNR improvement tends to be towards the periphery of the image, and the SNR inside the brain can be poorer (Kim *et al.* 2019).

During image acquisition, consideration must be given to time intervals between consecutive radiofrequency pulses, and between radiofrequency pulses and signal acquisition, as this allows for modulation of the signal between tissues with different relaxation times. This then allows for differently weighted images to be produced. For instance, the repetition time (TR) is the chosen delay between radiofrequency pulses, whereas the echo time (TE) is the delay between the radiofrequency pulse and the signal being recorded. Shorter TR and TE results in the acquisition of T1-weighted images and longer TR and TE leads to the acquisition of T2-weighted images (Seeger 1989). As such, using the incorrect TR and TE for a scan can result in either the image not being weighted in the desired way or the contrast between tissue types being poor. Poor contrast between tissue types can then make it more difficult to separate them during processing, reducing the accuracy. It should also be noted that depending on the MRI sequence used, other parameters than TE and TR can also affect the contrast of the MRI image.

It should also be noted that the image quality, and thus the subsequent accuracy of image processing, can also be greatly impacted by how much the subject moves during scanning. Movement during an MRI scan introduces noise into the images in the form of motion artefacts, and this noise can make accurate processing of the images more difficult (PRIMatE Data Exchange [PRIME-DE] Global Collaboration Workshop and Consortium 2020).

In conclusion, there are a number of factors that can impacts on the quality of MRI images, and these need to be considered when acquiring and processing MRI images as they can greatly affect the accuracy of tissue segmentation and, therefore, MRI analysis. For Rhesus Macaque data there are a number of other issues which can further complicate MRI processing, as will be discussed in section 1.3.3.

1.3.3 MRI processing pipelines and the difficulties with processing rhesus macaque MRI images

MRI scanning of human subjects, and the subsequent processing of human MRI images, has become fairly commonplace. In fact, there are a multitude of well tested processing pipelines for human MRI data that are freely available (https://neuro-jena.github.io/cat/; https://surfer.nmr.mgh.harvard.edu/fswiki/FreeSurferAnalysisPipelineOverview; https://www.nipreps.org/smriprep/; https://www.fil.ion.ucl.ac.uk/spm/software/spm12/; Fischer *et al.* 2012; Glasser *et al.* 2013; Reuter *et al.* 2012). MRI processing pipelines essentially entail a series of steps that can be carried out in order to transform a raw MRI image into a processed image which statistical analyses can be carried out on. These pipelines usually are in the form of ready to run scripts or batches, and often involve separating a brain into different tissue types and matching the outputs to a template (created from many other MRI scans), so that the same brain regions can be compared in images from different time points or subjects. This is necessary due to the variability across images, both within-subject at different time points and between-subjects, in terms of brain shape and size. Metrics such as measures of tissue volumes, thickness or surface area can then be calculated from the outputs of processing pipelines. Notably, these pipelines can often be utilised with minimal expert knowledge of neuroanatomy as they require little to no manual processing of the images.

MRI scanning of model animals such as rhesus macaques is still a relatively new, though fast growing, field (Öz, Tkáč and Ugurbill 2013). The processing of macaque MRI data is complicated by the fact that it cannot be accurately processed using pipelines designed to process human MRI (Milham et al., 2018; PRIMatE Data Exchange [PRIME-DE] Global Collaboration Workshop and Consortium 2020). This

is due to a number of factors that differ between human and macaque MRI data, the first of which being neuroanatomical differences.

The average macaque brain has a volume which is around 12-16 times smaller than a human brain, and though there is a high level of homology, some brain regions account for different proportions of the brain in humans and macaques (Croxson *et al.* 2018). Macaques also have highly muscular heads, which means there is more tissue outside of the skull on macaque MRI images than there is on human MRI images. These anatomical differences already make macaque MRI data more difficult to process than its human counterpart, but this difficulty is compounded by interindividual variation and a lack of standardisation in macaque MRI scanning (Milham *et al.* 2018; PRIMatE Data Exchange [PRIME-DE] Global Collaboration Workshop and Consortium 2020).

The equipment used to scan macaques across different sites will often greatly vary, with the use of non-standardized surface coil arrangements (used to produce the radiofrequency pulses; see section 1.3) being common. This is often accompanied by differences in the parameters and image quality of the scans across sites. Ultimately this not only adds to the difficulty of processing macaque MRI data (as discussed in section 1.3.2) but also means that developing processing methods that can translate to data from other sites may be even more challenging (Milham *et al.* 2018).

Finally, there are further challenges when MRI scanning awake macaques. As was previously discussed, the quality of MRI images can be greatly reduced if the subject moves during scanning, as this introduces motion artefacts. With human scans it can be impressed upon the subject to remain as still as possible during scanning, but with macaques this is more difficult. Macaques will usually be head fixed during awake scanning and will be trained to be acclimatised to the scanning environment, in order to minimise stress and motion artefacts (PRIMatE Data Exchange [PRIME-DE] Global Collaboration Workshop and Consortium 2020). However, this is not a fool proof solution, and awake macaque scans are still more likely to have motion artefacts than scans in humans.

Due to all of these factors, custom methods are needed in order to accurately process macaques MRI data, and a handful of macaque processing pipelines have been recently released (Balbastre *et al.* 2017; Garcia-Saldivar et al. 2021; Lepage et

al. 2021). However, each of these pipelines require manual corrections which are, by nature of being manually carried out by human researchers, subjective and could introduce bias. Additionally, they have all been designed to process cross-sectional data, using a surface-based morphometry approach. As such, there appears to currently be no pipeline that can process macaque MRI data using a voxel-based morphometry approach, no pipeline that can process macaque MRI data without manual corrections, and no pipeline that has been tested on longitudinal macaque MRI data.

Consequently, the first aim of this project was to design, optimise and implement an analysis pipeline capable of processing structural MRI data from rhesus macaques. More specifically, this pipeline needed to incorporate both voxel-based and surface-based morphometry (as discussed in section 1.3) and had to be capable of handling both cross-sectional and longitudinal MRI data (see section 1. 6).

1.4 The Impacts of Ageing on Brain Structure

As was previously alluded to, brain structural changes are not limited to those caused by injury or disease. Over the life course, global brain structure is known to change dramatically, with the relative amounts of grey matter, white matter and cerebrospinal fluid all following different trajectories. These changes are likely caused both by natural ageing processes and the influence of lifestyle factors such as stress, physical activity, and social integration. Table 1 provides the ages ranges of humans and macaques during different life periods, demonstrating the previously discussed accelerated ageing rate of macaques.

Life Period	Age Range in Humans (Years)	Age Range in Macaques (Years)
Childhood	0 - 12	0 - 3
Adolescence	12 - 20	3 - 5
Early Adulthood	20 - 40	5 - 16
Mid-Adulthood	40 - 60	16 - 20
Late Adulthood	60+	20+

Table 1: Age Ranges of Different Life Periods in Humans and Rhesus Macaques.

There are a number of potential mechanisms of ageing that may impact on brain structure, with impacts on grey matter being particularly notable. For example, accumulation of genetic damage over the life course has been theorised to play a major role in ageing. This process involves the build-up of DNA which has been damaged by factors such as reactive oxygen species, which are generated in neurons of the brain during excitatory activity, and DNA replication errors (Cardozo-Pelaez et al. 2000; Schumacher et al. 2021). It has been shown that the quantity of damaged DNA in the brain increases with ageing, and the ability of cells to accurately repair this damage decreases during ageing (Schumacher *et al.* 2021). Notably, the quantity of damaged DNA appears to vary across brain regions, due to some regions being more vulnerable to oxidative stress than others (Cardozo-Pelaez *et al.* 2000). This could provide an explanation for why the impacts of ageing on brain structure are not uniform across different regions, and may be useful when considering therapeutics to minimise age-related functional changes. The accumulation of DNA damage with ageing appears to contribute to grey matter loss through increasing neuronal cell death and/or disrupting neuronal cell function (Schumacher et al. 2021).

However, neuronal cell death has been shown to only be one factor contributing to grey matter loss, with other factors potentially having a greater impact (von Bartheld 2018). One such factor is age-related decreases in the size of neuronal cell bodies, which in turn leads to shrinkage of the grey matter with ageing. This decrease in the size of neuronal cell bodies is believed to be due to a combination of the metabolic rate of neurons slowing with advancing age and age-related mitochondrial dysfunction (Castelli et al 2019). Mitochondria are essential to neuronal cell function as they produce adenosine triphosphate, which is the primary source of energy for neurons. With advancing age mitochondria undergo changes in both their structure (such as becoming enlarged or fragmenting [Morozov *et al.* 2017]) and function (for example, reduced capacity to synthesise adenosine triphosphate [Lam *et al.* 2009]) which can result in them becoming dysfunctional. This dysfunction has been linked to both neuronal cell death and decreases in the size of neuronal cell bodies, ultimately playing a role in age-related grey matter loss/shrinkage (Lam et al. 2009; Morozov et al. 2017).

Another factor which may contribute to age-related loss of grey matter is changes in the dendrites. Dendrites are branched structures through which neurons

receive information from other cells, meaning that changes to the dendrites alters the ability of neurons to communicate. Studies have shown that with ageing the number of dendritic spines decreases, limiting intercellular communication between neurons (Boros *et al.* 2019). Additionally, there is evidence for the length of dendrites decreasing with age, and for the amount of neuropil in these dendrites also decreasing with age (Jacobs, Driscoll and Schall 1997). Taken together these dendritic changes reduce intercellular communication in the brain which may impact on cognition, and contribute to an overall reduction in the size of neurons which is reflected in grey matter shrinkage (Jacobs, Driscoll and Schall 1997; Boros et al. 2019). As with DNA damage, age-related mitochondrial dysfunction, and changes in dendrites with ageing, have been suggested to vary across brain regions, further indicating that ageing is likely to have greater effects in some brain regions than others (Navarro *et al.* 2008; Duan *et al.* 2003; Young *et al.* 2014; Sotoudeh *et al.* 2020).

Figure 4 illustrates the impacts of ageing on brain structure through comparison of the brain of a macaque during early adulthood (equivalent of early 20s in humans) to that of a macaque during late adulthood (equivalent of late 60s in humans).

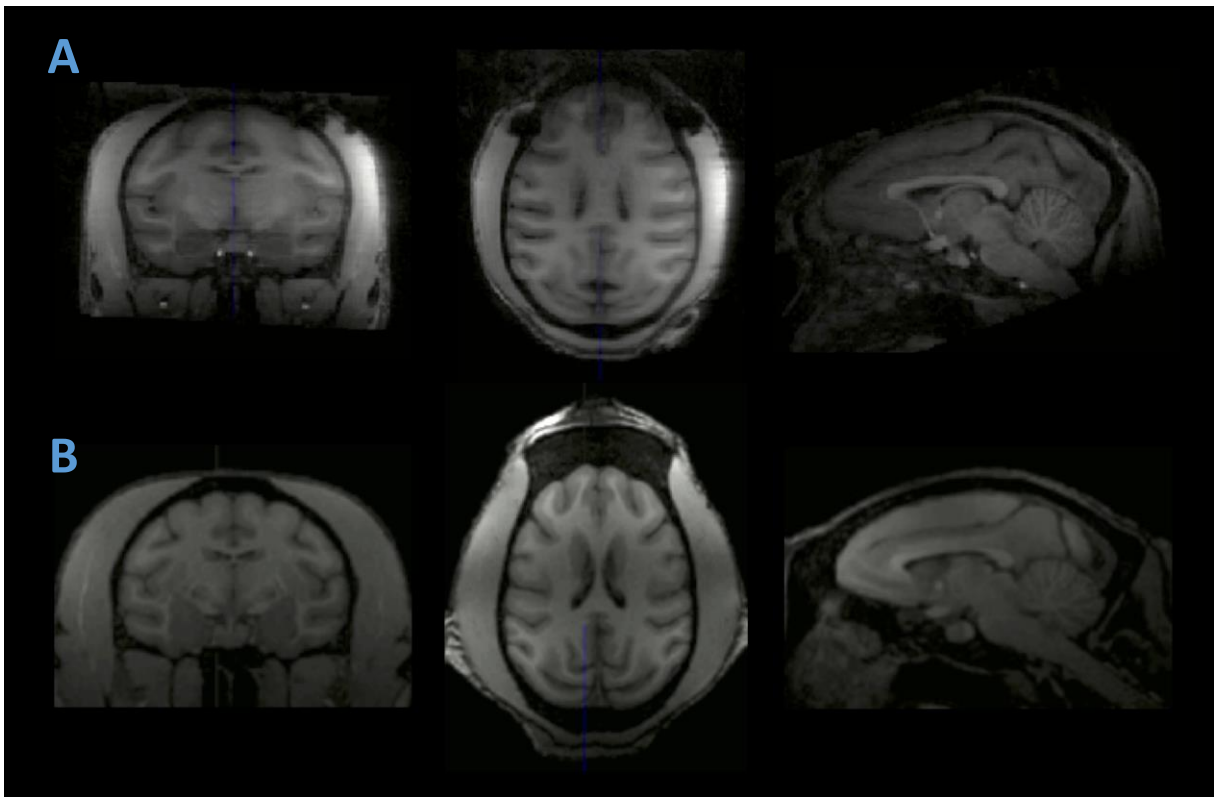

Figure 4: T1-weighted Scans of a Macaque During Early Adulthood (A) and a Macaque During Late Adulthood (B). Comparison images of the brain of a 5 year old macaque (A) and a 23 year old macaque (A), showing the clear brain structural changes that accompany ageing such as grey matter shrinkage and ventricular expansion.

1.4.1 Human MRI studies of the impacts of ageing on brain structure

Though the impacts of ageing on brain structure have been studied fairly extensively during late adulthood in humans, the results tend to be mixed and changes during other periods of adulthood are little understood. It is well established that total brain volume (the sum of whole brain grey matter and white matter volumes) decreases with ageing in humans, and there is general agreement that this decrease follows a non-linear trajectory (Schahill et al. 2003; Takao et al. 2012; Mills et al. 2016; Vinke et al. 2018, Bethlehem et al. 2022). This decrease appears to begin after the initial increase in brain volume during development, at around the age of 11-12 years (Bethlehem et al. 2022). However, there is less consensus as to the exact shape of this trajectory, with little agreement as to when the decline in total brain volume accelerates or decelerates. Schahill *et al.* 2003 found an acceleration after the age of 70 when studying a sample aged 31-84 years, whereas Vinke *et al.*

2018 demonstrated an acceleration after 50 years in a similarly aged sample (46-98 years old). Takao *et al.* 2012 also investigated a sample with a similar age range (38-83 years old), but they found an even earlier acceleration in the decline in total brain volume, this being from late 30s onwards. A study of a younger sample (8-30 years old) found a decline in total brain volume as early as adolescence, which then decelerated through early adulthood (20s and 30s) (Mills *et al.* 2016). This disagreement in terms of the exact trajectory of the age-related decline in total brain volume may be due to differences in the cohorts studied, differences in the age groups studied or differences in the methodologies utilised.

The impacts of ageing on total white matter volume have also been well studied in humans, with mostly consistent findings. Total white matter volume has been shown to initially increase until around the age of 40, followed by a decrease over the rest of the life course (Bartzokis et al. 2001; Good et al. 2001; Westlye et al. 2009; Bendlin et al. 2010; Michielse et al. 2010; Lebel et al. 2012; Mills *et al.* 2016; Vinke *et al.* 2018). In terms of region-specific changes in white matter, Nyberg *et al.* (2010) found decreases with ageing in older adults (55-84 years), localised to areas of the frontal, temporal and parietal lobes, as well as in the corpus callosum. Lebel *et al.* (2012) identified initial increases in white matter volume for most white matter tracts of the brain until the age of 20-42 (depending on the tract), followed by a decrease through the rest of the life course.

A non-linear decrease in total grey matter volume with ageing has also been highlighted by multiple studies (Lebel *et al.* 2012; Mills *et al.* 2016; Vinke *et al.* 2018). Both Lebel *et al.* (2012) and Mills *et al.* (2016) included children in their samples and identified a non-linear decrease in total grey matter volume from childhood (around 5 years for Lebel *et al.* [2012] and around 8 years for Mills *et al.* [2016]) onwards. Though the sample of Mills *et al.* (2016) only covered childhood through to early adulthood, Lebel *et al.* (2012) covered the entire life course and found that the age-related decrease in grey matter volume showed continuous deceleration, with the slowest rate of decline during late adulthood. Vinke *et al.* (2018) only investigated the age-related changes between the ages of 45 and 95, and though they identified a somewhat non-linear decrease in grey matter volume, this trajectory was much more linear than those observed by Lebel *et al.* (2012) and Mills *et al.* (2016). Notably, Vinke and colleagues showed a minor acceleration of the decrease in grey matter

volume in late adulthood, contrasting the deceleration identified by Lebel *et al.* (2012). Bethlehem *et al.* (2022) aggregated scans from across 100 different studies to investigate brain changes over the life course and found that grey matter volume peaked at the age of 5.9 years, fitting with the decrease from childhood onwards identified by Lebel *et al.* (2012) and Mills *et al.* (2016), and then showed a near-linear decrease across the rest of the life course. This near-linear decrease fits with the findings of Vinke *et al.* (2018), further contrasting the continuous deceleration identified by Lebel *et al.* (2012).

Results in terms of region-specific changes in grey matter volume with ageing tend to be the least consistent, though there is a wealth of evidence for regions in the frontal lobe being affected the most extensively (Good *et al.* 2001, Tisserand *et al.* 2004, Smith *et al.* 2007, Hutton *et al.* 2009, Peelle *et al.* 2012, Farokhian *et al.* 2017; Ramanöel *et al.* 2018). This is often followed by regions of the temporal lobe, which have also been frequently identified as showing reduced grey mater volume with ageing (Good *et al.* 2001; Tisserand *et al.* 2004, Smith *et al.* 2007, Hutton *et al.* 2009, Peelle *et al.* 2012; Ramanöel *et al.* 2018). However, this has been disputed, with conservation of temporal lobe regions with ageing also being observed (Farokhian *et al.* 2017). Age-related reductions in grey matter volume of parietal lobe regions have been reported much less frequently than those of the frontal and temporal lobes (Good *et al.* 2001, Smith *et al.* 2007; Ramanöel *et al.* 2018), and reductions in grey matter volume of occipital lobe regions are reported even more rarely (Tisserand *et al.* 2004; Ramanöel *et al.* 2018). Other regions occasionally implicated as showing reduced grey matter volume with ageing include the cerebellum (Good *et al.* 2001, Smith *et al.* 2007; Ramanöel *et al.* 2018) and insula (Good *et al.* 2001, Hutton *et al.* 2009, Peelle *et al.* 2012, Farokhian *et al.* 2017). The lack of consistency in the results of these studies may be due to differences in methodology or differences in the cohort or age group studied.

Though again there are some inconsistencies between studies, investigations of cortical thickness have found similar results to what has been seen for grey matter volume. Indeed, a whole brain, non-linear decrease in cortical thickness from childhood onwards has been noted by a number of studies (Lemaitre *et al.* 2012; Long *et al.* 2012; Fjell *et al.* 2015; Proskovec *et al.* 2020), and the frontal regions of the brain have been seen to be particularly vulnerable to ageing (Fjell *et al.* 2009;

Hogstrom *et al.* 2012; Lemaitre *et al.* 2012; Hurtz *et al.* 2014; Storsve *et al.* 2014; Fjell *et al.* 2015; Proskovec *et al.* 2020; Podgórski *et al.* 2021). Cortical thinning in other regions though appears more extensive than the grey matter volume decreases previously discussed, with age-related decreases in cortical thickness noted in the temporal (Fjell *et al.* 2009; Hurtz *et al.* 2014; Storsve *et al.* 2014; Fjell *et al.* 2015; Proskovec *et al.* 2020; Podgórski *et al.* 2021), parietal (Fjell *et al.* 2009; Long *et al.* 2012; Hurtz *et al.* 2014; Storsve *et al.* 2014; Fjell *et al.* 2015; Proskovec *et al.* 2020; Podgórski *et al.* 2021) and occipital (Fjell *et al.* 2009; Hurtz *et al.* 2014; Fjell *et al.* 2015; Proskovec *et al.* 2020; Podgórski *et al.* 2021) lobes, as well as the insula (Long *et al.* 2012) and cingulate cortex (Storsve *et al.* 2014). It should again be noted that the regions identified as showing cortical thinning with ageing are not completely consistent across studies, despite the more widespread nature of the changes.

Previous human studies have therefore highlighted extensive effects of ageing on brain structure, with frontal regions potentially showing the strongest impacts, and the impacts in other regions being less agreed upon. However, the vast majority of these studies of ageing focus on older adults or compare groups of young adults to groups of older adults, meaning that the impacts of ageing on brain structure prior to old age are more poorly understood. The period of early to mid-adulthood may be particularly important to investigate in terms of ageing effects as the onset of neurodegenerative disorders can begin during this period (Edwards-Lee *et al.* 2005; Vo *et al.* 2020). As such, the current project investigated the impacts of ageing on brain structure during early to mid-adulthood.

Additionally, the majority of humans studies utilise a cross-sectional approach. This may not only underestimate the impacts of ageing (Di Biase et al. 2023) but may also highlight results that are not ‘true’ age effects but are caused by the focus on between-subject, rather than within-subject, effects. For example, if a cross-sectional study of ageing includes a group of older subjects that have lived through a period of hardship (for example wartime) not experienced by the group of younger individuals they are being compared to, then this could result in brain changes resulting from stress being misinterpreted as being due to ageing. This confounder is termed a cohort effect and is due to cross-sectional studies of ageing only investigating differences between subjects rather than differences within subjects (Song et al. 2021). Longitudinal studies of the impacts of ageing are clearly needed, and they are

likely to be more logistically possible through the use of rhesus macaques as an animal model.

1.4.2 Rhesus macaque MRI studies of the impacts of ageing on brain structure

Results for the impacts of ageing on brain structure in rhesus macaques are far less numerous and consistent than in humans. This reduced consistency is likely to be partially explained by the difficulties in acquiring and processing macaque MRI data, which may then contribute to both a smaller pool of studies and a higher error rate in macaque research (Milham et al., 2018; PRIMatE Data Exchange [PRIME-DE] Global Collaboration Workshop and Consortium 2020). In terms of total brain volume, some previous macaque studies found no significant change with ageing (Andersen *et al.* 1999, Matochik *et al.* 2000, Chen *et al.* 2012), directly contrasting previous human studies (Schahill *et al.* 2003; Takao *et al.* 2012; Mills *et al.* 2016; Vinke *et al.* 2018). However, Chen *et al.* (2012) did find a trend towards reduced total brain volume with ageing. In terms of total grey matter volume, Andersen *et al.* (1999) identified significantly lower total grey matter volume in old macaques (aged 21 to 27 years, equivalent to around 63-81 years in humans) compared to younger macaques (aged 5 to 8 years, equivalent to around 20-24 in humans). Wisco *et al.* (2008) then found that old macaques (aged 24 to 30 years, equivalent to around 72-90 years in humans) had significantly lower forebrain grey matter volume than middle aged macaques (aged 16 to 19 years, equivalent to around 48-57 years in humans), but not young macaques (aged 5 to 12 years, equivalent to around 20 to 36 years in humans). Finally, Chen *et al.* (2012) found a significant linear decrease in total grey matter volume with ageing, using a sample of macaques aged 9 to 27 years (equivalent to around 27-81 in humans).

Similar to the discussed human studies, decreased grey matter volume for older macaques have been identified by a number of studies in regions of the frontal lobe (Wisco *et al.* 2008; Alexander *et al.* 2008; Colman *et al.* 2009; Dash *et al.* 2023), and the temporal lobe (Alexander *et al.* 2008; Colman *et al.* 2009). Wisco *et al.* 2008 also identified decreases in white matter volume with ageing, particularly localised to frontal lobe regions. Multiple studies have also highlighted reduced grey matter volume for older macaques in the caudate nucleus (Matochik *et al.* 2000; Lacreuse *et al.* 2005; Shamy *et al.* 2005; Wisco *et al.* 2008; Dash *et al.* 2023) and putamen

(Matochik *et al.* 2000; Lacreuse *et al.* 2005; Shamy *et al.* 2005; Dash *et al.* 2023), though this was disputed by Alexander *et al.* (2008). Additionally, age-related decreases in grey matter volume have also been noted in the hypothalamus, thalamus (Dash *et al.* 2023) and globus pallidus (Wisco *et al.* 2008). However, Dash and colleagues (2023) actually found increased grey matter volume in the globus pallidus for older macaques, as well as in the hippocampus and amygdala.

Furthermore, Koo *et al.* (2012) found that older macaques had lower cortical thickness than younger macaques in the pre- and post-central gyri, and higher cortical thickness in the anterior cingulate cortex, superior temporal sulcus and temporal pole. Given the limited and mixed results of previous macaque studies, and the overwhelming focus on older macaques, there is a need for further research into the effects of ageing on brain structure in rhesus macaques, particularly during the period of early to mid-adulthood. As such, the second aim of the current project was to assess the impacts of ageing on the brain structure of rhesus macaques during early to mid-adulthood.

1.4.3 The relative benefits and drawbacks of cross-sectional and longitudinal designs for studies of the impacts of ageing on brain structure

As aforementioned, the majority of MRI studies of ageing utilise a cross-sectional design. This is likely due to cross-sectional studies being relatively quick, easy and cost effective to carry out (Caruana *et al.* 2015; Wang and Cheng 2020). However, a cross-sectional design also comes with major drawbacks, such as an inability to determine cause and effect. This is due to cross-sectional studies only capturing information from a single point in time. As a consequence of this, potential causes and effects are measured simultaneously, making it impossible to establish a true cause and effect relationship (Caruana *et al.* 2015; Wang and Cheng 2020). For example, if a cross-sectional study of dementia patients investigated brain structural changes and identified grey matter loss in a specific region, it would not be possible to determine whether the loss was caused by their dementia or whether their dementia was caused by the grey matter loss. Additionally, a cross-sectional study can require a large sample size in order to reach statistical power, due to the noise inherent when looking at between-subject effects, as different subjects not only

exhibit variability in terms of genetics but also in terms of environmental factors they have been exposed to such as diet and stress (Song *et al.* 2021).

In contrast, longitudinal studies can be logistically difficult and both more time consuming and costly than cross-sectional studies (Caruana *et al.* 2015). Longitudinal studies also suffer from difficulty in retaining subjects over the full period of the study, especially if the study is aiming to look at changes over years or decades (Caruana *et al.* 2015). However, the nature of longitudinal studies allows for more realistic investigation of changes over time, as it is capturing information over an extended period rather than at a single point in time. This allows for the order of events to be better established, meaning that cause and effect can be more clearly determined than would be possible with a cross-sectional design (Caruana *et al.* 2015).

Additionally, longitudinal studies also benefit from a focus on within-subject differences, which removes any impact of genes or gene x environment interactions, increasing their statistical power. This inherent increase in statistical power allows longitudinal studies to utilise fewer subjects than cross-sectional studies, fitting with the principle of the '3Rs' (Replacement, Reduction and Refinement) for studies using animal models (Song *et al.* 2021).

A longitudinal design can also eliminate a confounder that can occur in cross-sectional studies known as a cohort effect. A cohort effect is when a difference between groups in a cross-sectional study is misinterpreted as being due to differences in the variable of interest, when it is actually due to a characteristic unique to one of the groups (Song *et al.* 2021). For example, if an ageing study is carried out and one of the groups was born during a stressful period (e.g., wartime or famine) then a result may be misinterpreted as being due to ageing when it is actually due to early life stress. Finally, longitudinal studies can also be benefitted simply by the ability to collect a greater breadth and depth of information than is possible in a cross-sectional study due to the amount of time dedicated to the study.

Given the clear strengths of a longitudinal approach, and the fact that the minority of previous studies have utilised this approach, more longitudinal MRI studies of the impacts of ageing on brain structure are needed. This is especially true given the aforementioned findings of Di Biase *et al.* (2023), which highlighted an underestimation of ageing effects when a cross-sectional approach was utilised as

opposed to a longitudinal approach. However, given how extensively a cross-sectional approach is utilised for MRI studies of ageing it would be useful to be able to directly contrast the findings of a cross-sectional and a longitudinal approach. This would allow for identification of any results when using a cross-sectional approach that are not 'true' effects of ageing but are actually arising erroneously due to the nature of the approach itself and the fact that it focuses on between-subject effects. This project will therefore utilise both cross-sectional and longitudinal approaches in order to carry out the aim of assessing the impacts of ageing, on the brain structure of rhesus macaques, during early to mid-adulthood.

1.5 The Impacts of Early Life Stress on Brain Structure

Early life stress (ELS) can be defined as any event during childhood in which an individual is exposed to physical or psychological stimuli which elicits a stress response. Common forms of ELS include maternal deprivation, neglect (emotional and/or physical) and abuse (emotional, physical and/or sexual) (Smith and Pollak 2020). ELS is known to have both acute effects, that end relatively soon after the event occurs, and chronic effects, lasting through later life.

Studies have shown that ELS in humans is correlated with an increased risk of developing neuropsychiatric disorders, such as depression, anxiety and substance abuse disorders, later in life, as well as an increased risk of cardiovascular and autoimmune diseases (Dube *et al.* 2009; Carr *et al.* 2013; LeMoult *et al.* 2020; Bengtsson *et al.* 2023). Furthermore, the risk of premature mortality is also higher in those who have experienced high levels of early life stress (Johnson *et al.* 2020).

ELS is theorised to have such a large impact due to it altering brain developmental trajectories (Smith and Pollak 2020). Additionally, it is thought that being exposed to ELS may lead to poorer coping mechanisms for stress later in life (McLafferty *et al.* 2019). This impeded ability to cope with future stress following ELS could then contribute to the impacts of stress accumulating over the life course, and this cumulative effect resulting in greater brain structural changes.

Previous studies have identified mechanisms through which early life stress (and stress more generally) may alter brain structure. For example, chronic stress has been associated with both decreases in the formation of new neurons, as well as neuronal loss as a result of apoptosis (Lucassen *et al.* 2001; Simon et al. 2005).

Early-life stress in particular has also been linked to increases in apoptosis, as well as decreases in neurogenesis (Lemaire *et al.* 2000; Catale *et al.* 2021). Additionally, the level of stress-induced apotoptosis appears to vary across brain regions (Lucassen et al. 2001). This suggests that the magnitude of the impact of stress is also different across different brain regions, potentially indicating resilience and vulnerability to stress is region-specific.

As was previously discussed, loss of neurons plays a role in grey matter loss, but may not be the largest contributor (von Bartheld 2018). Dendritic changes, which may play a greater role in grey matter loss or shrinkage, have also been identified as a consequence of stress. For example, significant decreases in dendritic spine density have been noted in association with chronic stress, as well as reductions in the level of dendrite branching (Vyas *et al.* 2002; Shansky et al. 2009; Kassem et al. 2013). Stress-induced changes in the dendrites appear to vary across brain regions, again suggesting that some regions may be more resilient to stress whereas others are more vulnerable (Vyas *et al.* 2002; Shansky *et al.* 2009). Importantly, there is evidence that dendritic changes are most pronounced when chronic stress is experienced during early life (Helmeke *et al.* 2009; Kaul *et al.* 2020).

Notably, these mechanisms are very similar to those linked to age-related changes in brain structure, potentially highlighting both how stress may have a larger effect in some brain regions than others, and how stress and ageing may interact to cause more extensive changes in brain structure.

1.5.1 Early life stress vs. stress during adulthood

Stress during adulthood is any event that exposes an individual to physical or psychological stimuli, which elicits stress during adulthood. As with ELS, stress during adulthood can have both acute and chronic effects, and multiple stressful events in adulthood can have a cumulative impact. Stress during adulthood has also been shown to impact on brain structure, with studies highlighting stress-related decreases in grey matter volume in areas such as the hippocampus (Papagni *et al.* 2011). As with ELS, stress during adulthood has also been linked to the development of psychiatric disorders such as depression and anxiety, as well as physical conditions such as cardiovascular disease (Revollo *et al.* 2011*;* Satyjeet *et al.* 2020).

However, as the stress is occurring later in the life course, it cannot alter developmental trajectories in the way ELS can, meaning that the impacts may not be as long-lasting and/or that the chronic effects may be less sizeable. Additionally, there is less time for the stress to accumulate if it is occurring in adulthood rather than during early life, which could further reduce the size or endurance of the effects. Consequently, it is theorised that the impacts of ELS could be more detrimental in the long term than the impacts of stress occurring during adulthood. The current project therefore focused on ELS.

1.5.2 Human MRI studies of the impacts of early life stress on brain structure

Human MRI studies have investigated the impacts of ELS across children, adolescents, and adults, allowing for the discovery of both acute and chronic effects. First of all, in terms of white matter, reductions with ELS have been observed in the corpus callosum (Paul *et al.* 2008; Teicher *et al.* 2010; McCarthy-Jones *et al.* 2017) and uncinate fasciculus (Eluvathingal *et al.* 2006; McCarthy-Jones *et al.* 2017) for both children and adults, with reductions in the corona radiata also being observed in adults (McCarthy-Jones *et al.* 2017). These studies suggest fairly consistent decreases in white matter volume, with potentially more extensive declines manifesting during adulthood.

For grey matter, a meta-analysis of children, adolescents and adults that had experienced ELS found lower grey matter volume in the inferior frontal gyrus, the orbitofrontal gyrus, the superior temporal gyrus and the middle temporal gyrus across all age groups (Lim *et al.* 2014). This suggests ELS can have impacts that begin in childhood and last across the life course.

A study in children found that those that experienced maltreatment had lower grey matter volume in the medial orbitofrontal cortex and middle temporal gyrus (De Brito *et al.* 2012). This appears to highlight that the relatively acute impacts of ELS predominantly affect regions similar to those thought to be affected earliest by ageing (Good *et al.* 2001, Tisserand *et al.* 2004, Smith *et al.* 2007, Hutton *et al.* 2009, Peelle *et al.* 2012, Farokhian *et al.* 2017; Ramanöel *et al.* 2018).

Research in adolescents can identify somewhat more chronic impacts and can determine whether the impacts seen during childhood persist. Interestingly, adolescents appear to be the group most extensively researched in terms of ELS in

humans, perhaps in order to minimise either the impacts of recall bias or any potential age-related diminishment of effects, as the experience is more recent than it would be for adults. Tyborowska *et al.* (2018) found that adolescents that had experienced ELS showed lower grey matter volume in subcortical regions such as the amygdala, putamen and insula, as well as in the anterior prefrontal cortex. For adolescents and young adults that reported maltreatment during early life, Walsh *et al.* (2014) found decreased grey matter volume only in the cerebellum. This was contrasted by Malhi *et al.* (2023) who found that female adolescents who had experienced emotional trauma during early life first showed increases in grey matter volume during early adolescence, followed by decreases in grey matter volume during late adolescence. These changes were identified across the brain, with clusters in the parahippocampal gyrus, posterior cingulate cortex, prefrontal cortex and other areas of the frontal lobe. Similarly, a meta-analysis of adolescents exposed to childhood maltreatment identified both increases and decreases in grey matter volume, with the increases covering the pre- and post-central gyri, body of the corpus callosum and inferior frontal gyrus, and the decreases localised to the supramarginal gyrus, middle temporal gyrus, rostrum of the corpus callosum and cerebellum (Tymofiyeva *et al.* 2022). Clearly results from adolescent studies are very mixed, possibly due to differences in the severity or number of stressors across studies and/or subjects. As ELS is known to alter developmental trajectories, it is possible that differences in severity or number of stressors could subsequently lead to differing alterations to developmental trajectories, which could then manifest as different patterns of grey matter changes during the crucial developmental period of adolescence.

In terms of the impacts of ELS in human adults, the aforementioned results of Walsh *et al.* (2014) for young adults (decreased grey matter volume only in the cerebellum) were contrasted by Gorka *et al.* (2014), where the left hippocampus and medial prefrontal cortex both showed reduced grey matter volume in young adults that had reported childhood maltreatment. Tomoda *et al.* (2009) found that young women who experienced childhood sexual abuse had lower grey matter volume in visual area 1, within the occipital lobe.

In cortical thickness studies, ELS has been associated with cortical thinning of the frontal regions in children, adolescents and adults (Kelly *et al.* 2013; McLaughlin

et al. 2014; Saleh *et al.* 2017; Busso *et al.* 2017; Bounoua *et al.* 2020). ELS-related cortical thinning in children, adolescents and adults has also been identified in the cingulate cortex (Kelly *et al.* 2013; Ross *et al.* 2020). Additionally, cortical thinning of temporal regions with ELS has been previously reported in children (McLaughlin *et al.* 2014) and adolescents (Busso *et al.* 2017), and cortical thinning of parietal regions with ELS has been previously reported in children (McLaughlin *et al.* 2014) and adults (Saleh *et al.* 2017). For adults alone, there is evidence of cortical thinning with ELS in the insula (Saleh *et al.* 2017) and regions within the occipital lobe (Tomoda *et al.* 2012; Bounoua *et al.* 2020; Rosada *et al.* 2022). As such, it would appear that results of previous cortical thickness studies are somewhat more consistent than those of studies of grey matter volume changes, with cortical thinning after ELS seen across much of the brain, not only relatively acutely (during childhood) but persisting through to adulthood.

Overall, the results of previous human studies of the impacts of early life stress on brain structure are mixed, with studies of the impacts during adulthood being particularly limited. Additionally, human studies often utilise a study design reliant on the retrospective collection of data on ELS, in which participants are asked to remember their experiences during childhood. This approach can introduce recall bias if participants remember incorrectly, confounding the results of the study (Althubaiti 2016). Human studies of ELS can also suffer from a lack of control over all of the potential stressors that participants may experience, as they do not live in a controlled environment. This can mean that the results of a study are impacted by individual differences in the amount or severity of ELS experienced. These issues can be circumvented by studying the impacts of ELS on brain structure during adulthood in laboratory macaques, which live in a controlled environment and can be observed and monitored across the whole life course.

1.5.3 Rhesus macaque MRI studies of the impacts of early life stress on brain structure

Similar to with human studies, rhesus macaque studies have previously identified a clear impact of ELS on white matter, with reduced integrity identified in longitudinal fasciculus, brainstem, medullary lamina, corpus callosum and occipital lobe (Howell *et al.* 2013 and 2019). In terms of grey matter though, results are more

mixed. This is likely due to there being far fewer studies that investigate the impacts of ELS on grey matter in rhesus macaques, than there are studies in humans. In fact, there were no identifiable studies of the impacts of ELS on cortical thickness.

The impacts of ELS on grey matter volume have been previously investigated, but the results are highly inconsistent. Spinelli *et al.* (2009) found that juvenile macaques that experienced ELS in the form of maternal deprivation (removal from mother immediately after birth) showed *higher* grey matter volume in the cerebellum, cingulate cortex and prefrontal cortex. Directly contrasting previous human studies which identified lower grey matter volume in these regions for subjects that experienced ELS (Gorka *et al.* 2014; Walsh *et al.* 2014; Tyborowska *et al.* 2018; Tymofiyeva *et al.* 2022; Malhi *et al.* 2023). Wang *et al.* (2018) also investigated the impacts of maternal deprivation on adolescent rhesus macaques, and further contrasting Spinelli *et al.* (2009), identified lower grey matter volume in visual area 1 of subjects that were maternally deprived. This result parallels the findings of Tomoda *et al.* (2009) in humans.

There is a clear need for further research into how early life stress impacts on grey matter in rhesus macaques, both in terms of grey matter volume as previous studies conflict, and in terms of cortical thickness as this has not been previously investigated. Taken together with the mixed results of previous human studies, and the particularly limited previous research into the impacts of ELS during adulthood, the third aim of the current project was to assess the impacts of early life stress on the brain structure of rhesus macaques, during early to mid-adulthood. This age range was chosen rather than late adulthood as not only is any diminishment of the impacts of ELS with ageing likely to be greater in late adulthood, but also early to mid-adulthood is a period in humans in which the onset of many psychiatric disorders often begins (Leach and Butterworth 2020).

1.6 The Impacts of Stress x Ageing Interactions on Brain Structure

It has been hypothesised that stress may accelerate ageing effects on brain structure, implying that increased stress over the life course may result in age-related changes in brain structure occurring earlier than expected (Chaudhari, Singla and Vaidya 2022). In turn, these earlier brain structural changes may correspond to earlier functional changes and/or earlier onset of age-related disorders such as

dementia. Consequently, determining whether stress does accelerate brain ageing may be essential for the development of interventions for both age-related disorders and the more general impacts of brain ageing. However, though this hypothesis appears to be widely accepted, evidence to support it is actually somewhat limited.

The majority of studies that have considered the hypothesis of stress accelerating ageing effects have investigated stress in relation to processes believed to play a role in biological ageing. For example, chronic stress has been linked to an increase in pro-inflammatory cytokine release (Toft *et al.* 2018), a process shown to be involved in ageing (Fülöp *et al.* 2019). Additionally, oxidative stress and telomere shortening are also thought to play a role in ageing, and both have been linked to psychological stress (Epel *et al.* 2004). Furthermore, studies have also linked early life stress specifically to ageing processes such as mitochondrial dysfunction, telomere shortening and a decline in hippocampal neurogenesis (Correia-Melo *et al.* 2016; Tyrka *et al.* 2016; Ruiz *et al.* 2018).

Recently, Gotlib *et al.* (2021) investigated the impacts of stress (in the form of COVID-19 lockdowns) on cortical thickness, hippocampal and amygdala volume, and brain age in adolescents. This study identified that stress resulted in lower cortical thickness, increased hippocampal and amygdala volume, and increased brain age, implying that there was an acceleration of brain maturation and that this stress resulted in older-appearing brains.

In conclusion, though there are multiple studies indicating that stress appears to alter processes associated with ageing, evidence of how stress and ageing interact to impact on brain structure is more limited. As such, further research is needed into the impacts (if any) of stress x ageing interactions on brain structure. In particular, further insight into how stress during early life may accelerate ageing processes to impact on brain structure could be crucial, given the theory that early life stress may be more detrimental than stress during adulthood. Consequently, the final aim of this project was to assess the impacts (if any) of early life stress x ageing interactions on the brain structure of rhesus macaques, during early to mid-adulthood. The cross-sectional impacts of ageing and early life stress will be compared to determine whether they affect the same brain structures, and a longitudinal approach will be utilised to directly investigate the impacts of early life stress x ageing interactions on brain structure.

1.7 Aims and Hypotheses

To reaffirm, this project had 4 main aims:

1) To design, optimise and implement an analysis pipeline capable of processing structural MRI data from rhesus macaques
2) To assess the impacts of ageing on the brain structure of rhesus macaques, using both a cross-sectional and a longitudinal approach, during early to mid-adulthood
3) To assess the impacts of early life stress on the brain structure of rhesus macaques, using a cross-sectional approach, during early to mid-adulthood
4) To assess the impacts of early life stress x ageing interactions on the brain structure of rhesus macaques, using a longitudinal approach, during early to mid-adulthood

The first aim will be addressed in chapter 3, which details the creation of the AutoMacq pipeline. The second aim will be addressed in chapters 4 and 5, with chapter 4 covering a voxel-based morphometry investigation of the impacts of ageing on grey matter volume, and chapter 5 detailing a surface-based investigation of the impacts of ageing on cortical thickness. Similarly, chapters 6 and 7 will address the third and fourth aims. Chapter 6 covers a voxel-based investigation of the impacts of early life stress and early life stress x ageing interactions on grey matter volume. Chapter 7 then covers a surface-based investigation of the impacts of early life stress and early life stress x ageing interactions on cortical thickness.

Given the previous human and macaque literature (discussed in sections 1.4.1, 1.4.2, 1.5.1 and 1.5.2), the primary hypotheses of this project were as follows:

1) That the impacts of ageing would be linked to significant decreases in grey matter volume and cortical thickness, primarily in regions of the frontal and temporal lobes.
2) That the impacts of early life stress would be related to significant decreases in grey matter volume and cortical thickness, with changes being widespread and seen across every lobe of the brain.
3) That interactions between early life stress and ageing would lead to more extensive declines in grey matter volume and cortical thickness than those observed with either factor alone.

Chapter 2: General Materials and Methods

2.1 Datasets Utilised

Scans from publicly available datasets, as well as those acquired locally and datasets privately shared with the authors, were selected for this project. Data had been acquired on various scanners with various parameters and coil arrangements (see section 2.2). All of the scans though were acquired with a scanner strength of at least 3T in order to set a baseline level of signal strength. For some subjects, T2 data was available alongside the T1 data. Both male and female macaques were included, though scans were available from far more male subjects than female subjects.

Initially, rhesus macaque MRI data from across 9 different sites (N=109) was chosen to be utilised. 3 sites had longitudinal data as well as cross-sectional, and scan-rescan data was available from 1 site. The first of these sites was Newcastle University, UK, where data was collected as part of an ongoing, longitudinal project. Cross-sectional, longitudinal and scan-rescan datasets were available from Newcastle, and there was some overlap in the scans included in the cross-sectional, scan-rescan and longitudinal datasets.

Three other sites privately shared datasets for this project. These datasets came from Deutsches Primatenzentrum (DPZ), Germany, the National Institute on Drug Abuse (NIDA), USA, and the University of Oxford, UK. Both DPZ and NIDA provided longitudinal datasets as well as cross-sectional datasets, whereas only cross-sectional data was available from Oxford. Some scans from DPZ and NIDA were included in both the cross-sectional and longitudinal datasets.

The remaining cross-sectional datasets utilised for this research were from the primate data exchange (PRIME-DE), an open science resource which provides access to macaque MRI datasets from around the world, with varied scan parameters and sample sizes (Milham et al. 2018). The 6 PRIME-DE datasets selected for this research were acquired at: Mount Sinai School of Medicine (MSP and MSS), USA, Stem Cell and Brain Research Institute (SBRI), France, University of California Davis (UC-Davis), USA and University of Western Ontario (UWO), Canada.

Visual quality control of scans was carried out prior to any processing. This resulted in the exclusion of 35 cross-sectional scans, from across 4 of the selected 9 sites (see section 2.6, supplementary figure 1 for examples of excluded scans). The majority of these scans (N=32) were excluded due to a poor signal-to-noise ratio or generally poor image contrast, with 2 further scans being excluded due to prominent hyperintensities, and 1 scan being excluded due to excessive motion artefacts. Notably, the entire UC-Davis dataset (N=19) was excluded at the visual quality control check, due to poor contrast between the grey matter and white matter of the scans (see section 2.6, supplementary figure 1). The exclusion of cross-sectional data from across 4 sites did not result in the exclusion of any subjects from the longitudinal datasets. The visual quality control resulted in the retention of cross-sectional MRI data from 74 subjects, across 8 different sites, and longitudinal MRI data from 16 subjects, across 3 different sites (see table 2).

2.2 Scan Parameters

Table 3 provides a breakdown of the scan parameters for each site, including the scanners and coil arrangements that were utilised. All of the sites, except for Newcastle University, scanned anaesthetised macaques. Anaesthetised scans are the most common for macaque datasets due to it simplifying the scanning process and reducing noise due to body/head movements. However, as the majority of human studies involve awake scanning, scans in awake animals are of great interest, and may be more comparable to the scans acquired in those human studies.

The DPZ dataset consists of subjects scanned using 2 different scanners, each of which were upgraded once during the course of data collection (i.e., there were 4 different sets of scanner parameters for this site). On account of this, the DPZ dataset was actually treated as 4 different scanners/sites during subsequent statistical analyses.

Data Type	Site	Subjects (M/F)	Age Range (in year)	Subjects with T2 data	Awake vs. Anaes.	Scanner Strength
CS	Newcastle	18 (12/6)	5-15	18	Awake	4.7T
CS	DPZ	21 (21/0)	6-11	6	Anaes.	3T
CS	NIDA	6 (6/0)	7-10	0	Anaes.	3T
CS	Oxford	8 (5/3)	5-8	0	Anaes.	3T
CS	MSP	8 (8/0)	3-5	4	Anaes.	3T
CS	MSS	5 (5/0)	5-6	5	Anaes.	3T
CS	SBRI	3 (1/2)	7-14	3	Anaes.	3T
CS	UWO	5 (5/0)	4-8	5	Anaes.	7T
	Total	*74 (63/11)*	*3-15*	*41*		
S-RS	Newcastle	13 (8/5)	5-15	13	Awake	4.7T
L	Newcastle	10 (8/2)	6-15	10	Awake	4.7T
L	DPZ	1 (1/0)	6-8	0	Anaes.	3T
L	NIDA	5 (5/0)	6-10	0	Anaes.	3T
	Total	*16 (14/2)*	*6-15*	*10*		

Table 2: Description of Included Datasets After the Initial Quality Control

CS: cross-sectional datasets, S-RS: scan-rescan dataset and L: longitudinal.

M: male and F: female. Anaes.: anaesthetised.

	Scanner Type	Coils Used	Sequences Used	Voxel Size	TE T1 (T2)	TR T1 (T2)
New-castle	Bruker 4.7T vertical	4 channel parallel imaging coils	MPRAGE, RARE	0.608 x 0.608 x 0.618 mm	3.75ms (14.33ms)	2000ms (12296.7 ms)
DPZ1	Siemens Prisma 3T	Siemens Loop 11cm	MPRAGE	0.5 x 0.5 x 0.5mm	2.96ms	2700ms
DPZ2	Siemens Prisma 3T	Siemens Loop 11cm/7-loop RX	MPRAGE, T2SPACE	0.5 x 0.5 x 0.5mm	2.97ms (500ms)	2700ms
DPZ3	Siemens Magnetom Trio	7-loop RX	MPRAGE	0.65 x 0.651 x 0.651 mm	2.96ms	2700ms
DPZ4	Siemens Magnetom TIM Trio	4-channel, phased-array coil	MPRAGE	0.5 x 0.5 x 0.5mm	2.63ms	2700ms
NIDA	Siemens 3T Allegra	Custom-designed holder/secondary coil (NOVA_16)	MPRAGE	0.6 x 0.598 x 0.598 mm	3.04ms	1680ms
Oxford	3T whole body scanner	4-channel, phased-array, radio-frequency coil w/ local transmission coil	MPRAGE	0.5 x 0.5 x 0.5mm	4.01ms	2500ms
MSP	Philips Achieva 3T	4-channel phased array coil (Windmiller-Kolster Scientific), transmit through body coil	MPRAGE	0.5 x 0.5 x 0.5mm	6.93ms (366ms)	1500ms (2500ms)

MSS	Siemens Skyra 3T	4-channel clamshell coil	MPRAGE	0.5 x 0.5 x 0.5mm	3.02ms (539ms)	2700ms (3200ms)
SBRI	Siemens Prisma 3T	2 x L11 and 1 x L7 Siemens ring coils	T1 MPR 3D, T2 SPACE TRA	0.5 x 0.5 x 0.5mm	3.62s (366ms)	3000ms (3000ms)
UWO	Siemens Magnetom 7T	Custom-made 24-channel phased array receive coil w/ 8-channel transmit coil	MPRAGE	0.5 x 0.5 x 0.5 mm	3.88ms	65000ms

Table 3: Detailed Scan Parameters for Each Site
TE: Echo Time, TR: Repetition Time. *Information requested from collaborators, awaiting response.

2.3 Newcastle University Scan Procedure

Macaques at Newcastle University were scanned using a vertical MRI scanner (Biospec 4.7 Tesla, Bruker Biospin, Ettlingen, Germany), whilst awake and sitting upright in a primate chair. All of the macaques had previously undergone training and acclimatisation to both the primate chair and scanner environment. Positive reinforcement was used for the training, in the form of food rewards. Macaques were head fixed throughout the scans so that head movements could be minimised. During the scans, macaques were shown nature videos and were rewarded with juice, in order to reduce boredom and further minimise body/head movements.

2.4 Husbandry and Ethics

The re-use of MRI data for the current project was approved by the Newcastle University Animal Welfare Ethical Review Board (reference number 1021).

Newcastle- Macaques were pair- or trio-housed in cages approximately 2.1 by 3.0 by 2.4 m and had both auditory and visual contact with other macaques in the facility. On rare occasions macaques may have been transiently single housed for husbandry reasons or due to veterinary concerns. However, single-housing was minimised as much as possible to reduce any potential welfare impacts, and single-

housed subjects still had auditory and visual contact with other macaques. Daily foraging opportunities as well as swings, shelves and other play objects provided the macaques with enrichment.

All procedures were in full compliance with the UK Animal Scientific Procedures Act (1986) and the European Directive on the protection of animals used in research (2010/63/EU). Procedures were carried out under authority of personal and project licences approved by the UK home office. See table 4 for a breakdown of project licences this research came under.

	Licence Numbers	**Licence Holders**
Newcastle	70/7976, PABAD450E; PPL 60/4095, PPL 70/8318, PA2C18B73; PP8119034;	Professor Alexander Thiele; Professor Christopher Petkov; Dr Yukiko Kikuchi

Table 4: Project Licences for the Newcastle University Data

Oxford- All procedures were in full compliance with the UK Animal Scientific Procedures Act (1986) and the European Directive on the protection of animals used in research (2010/63/EU). Procedures were carried out under authority of personal and project licences approved by the UK home office.

DPZ- All procedures were carried out in accordance with institutional guidelines at DPZ, as well as the European Directive on the protection of animals used in research (2010/63/EU) and the relevant German law on animal welfare.

NIDA- All procedures were approved by the Institutional Animal Care and Use Committee at the University of Pittsburgh and conformed with the USPHS Guide for the Care and Use of Laboratory Animals.

PRIME-DE datasets- Ethical approvals for all of the PRIME-DE datasets are provided on the PRIME-DE website in the 'Data Collections' section (https://fcon_1000.projects.nitrc.org/indi/indiPRIME.html).

2.5 Software Utilised

Voxel-based processing of MRI data was carried out using Matlab (R2021a; The MathWorks Inc. 2021) and SPM12 (www.fil.ion.ucl.ac.uk/spm/software/spm12/)

on a Windows PC. Bias correction and surface-based processing was undertaken on a Linux PC. Bias correction was implemented using FSL (Jenkinson *et al.* 2012), ANTs (Avants *et al.* 2009) and the connectome workbench (Marcus *et al.* 2011). Surface-based processing was performed using FreeSurfer (v6.0.0; Fischl 2012). Statistical analyses were carried out using Matlab, SPM12, SurfStat (www.math.mcgill.ca/keith/surfstat/#mixed), R (R Core Team 2021) and Rstudio (RStudio Team 2020).

2.6 Supplementary Materials

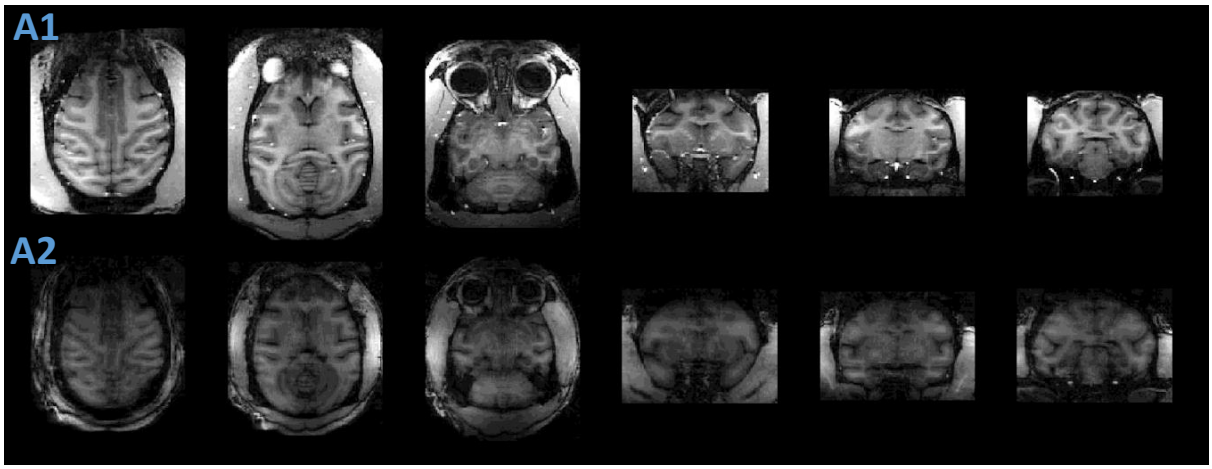

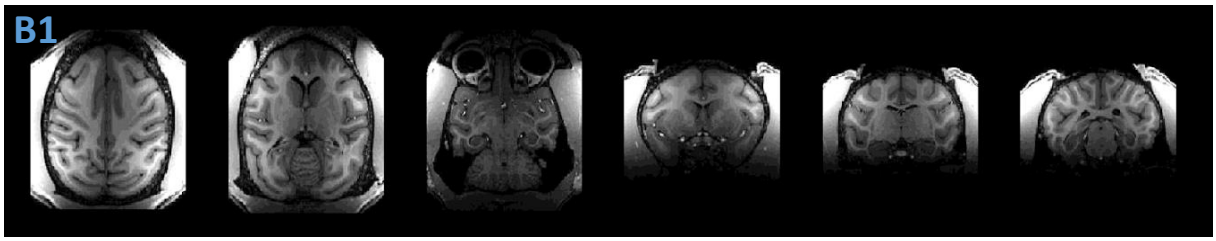

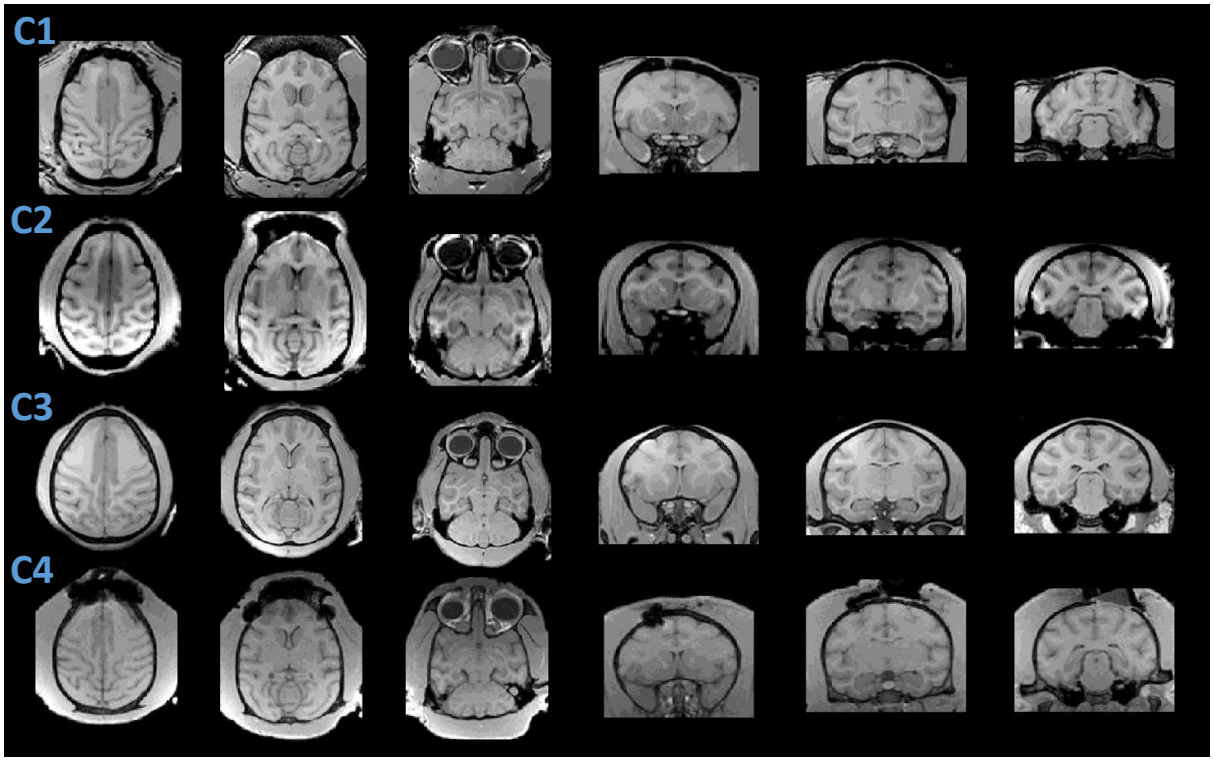

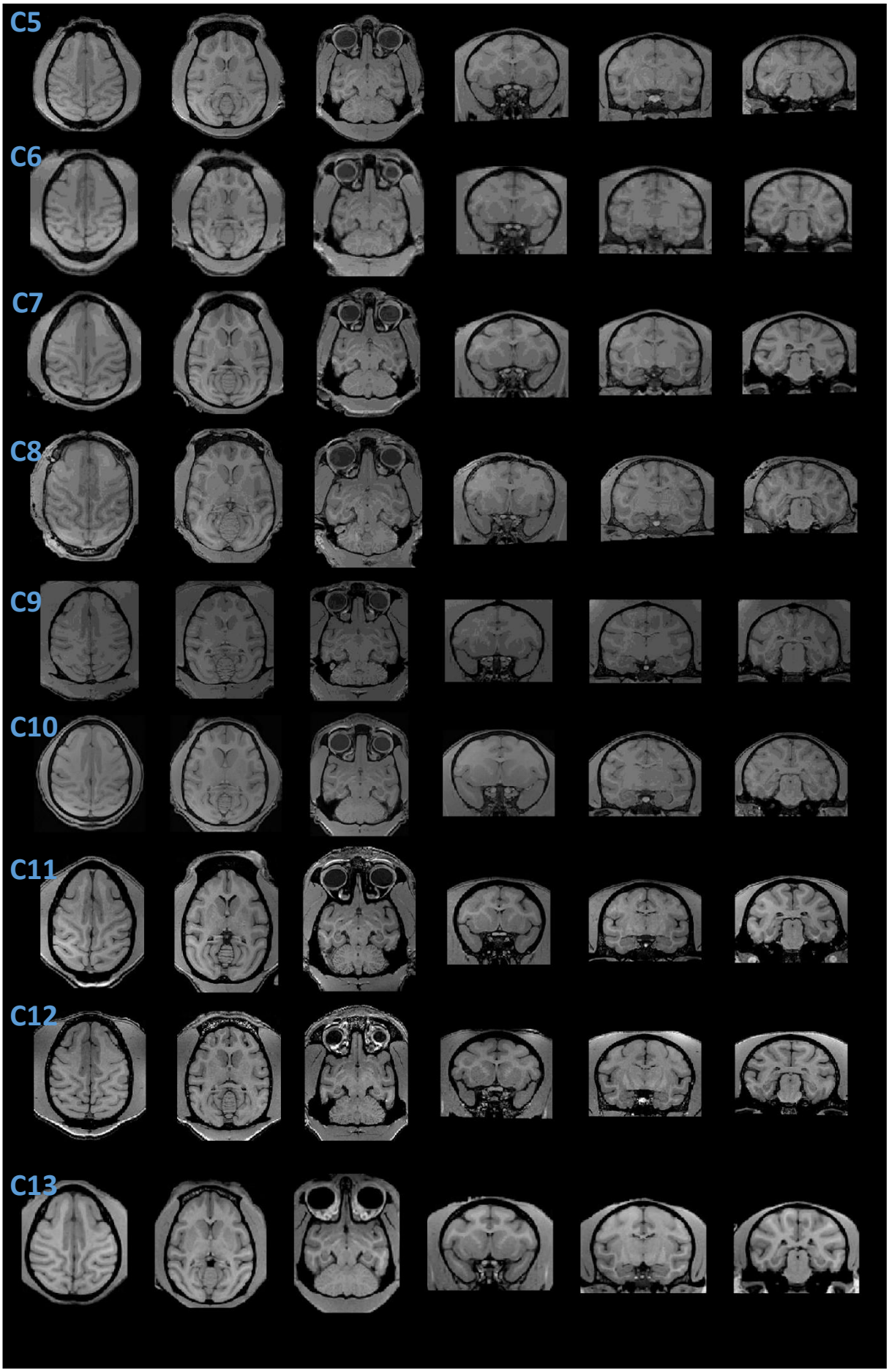
C5
C6
C7
C8
C9
C10
C11
C12
C13

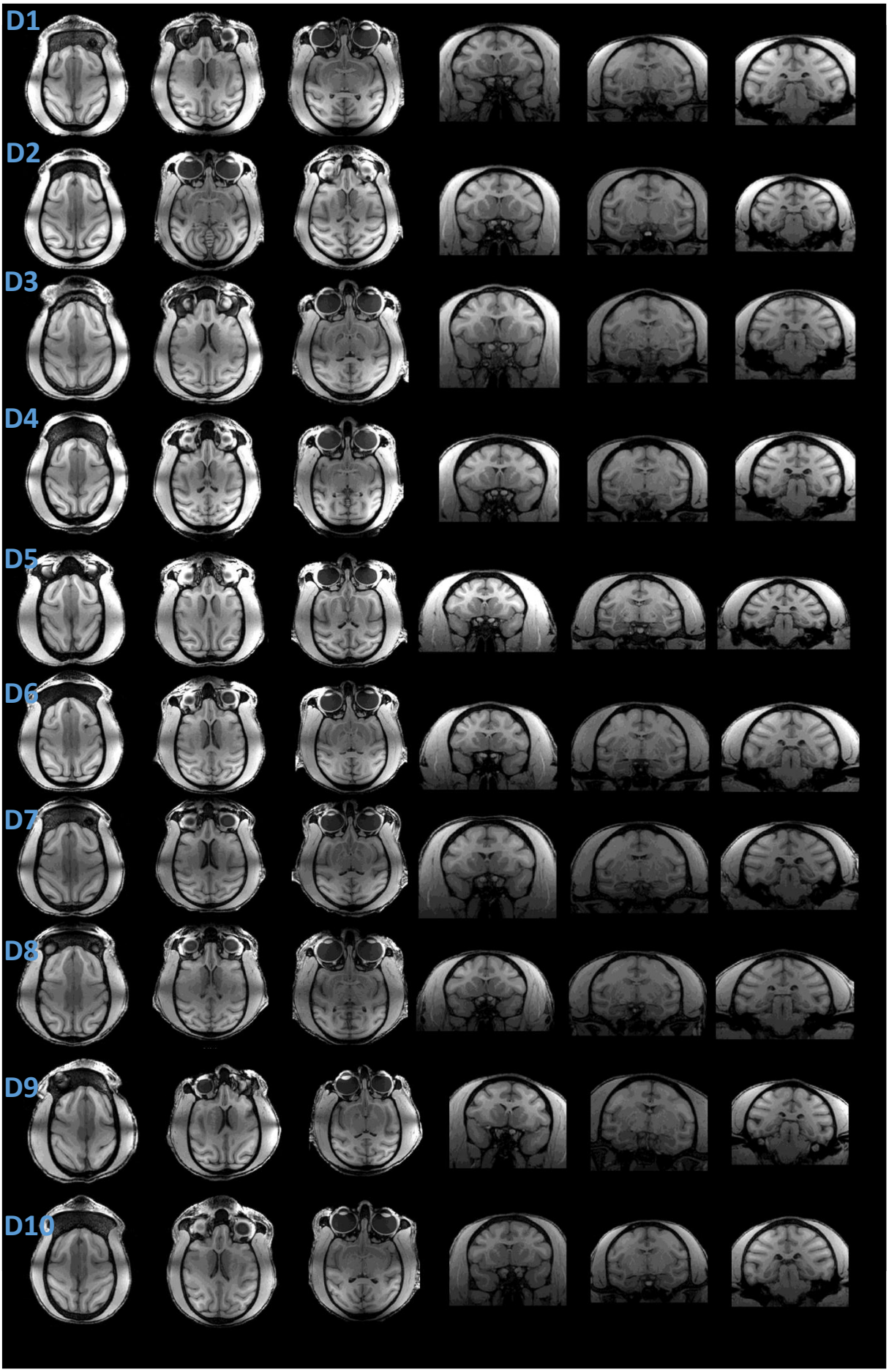
D1
D2
D3
D4
D5
D6
D7
D8
D9
D10

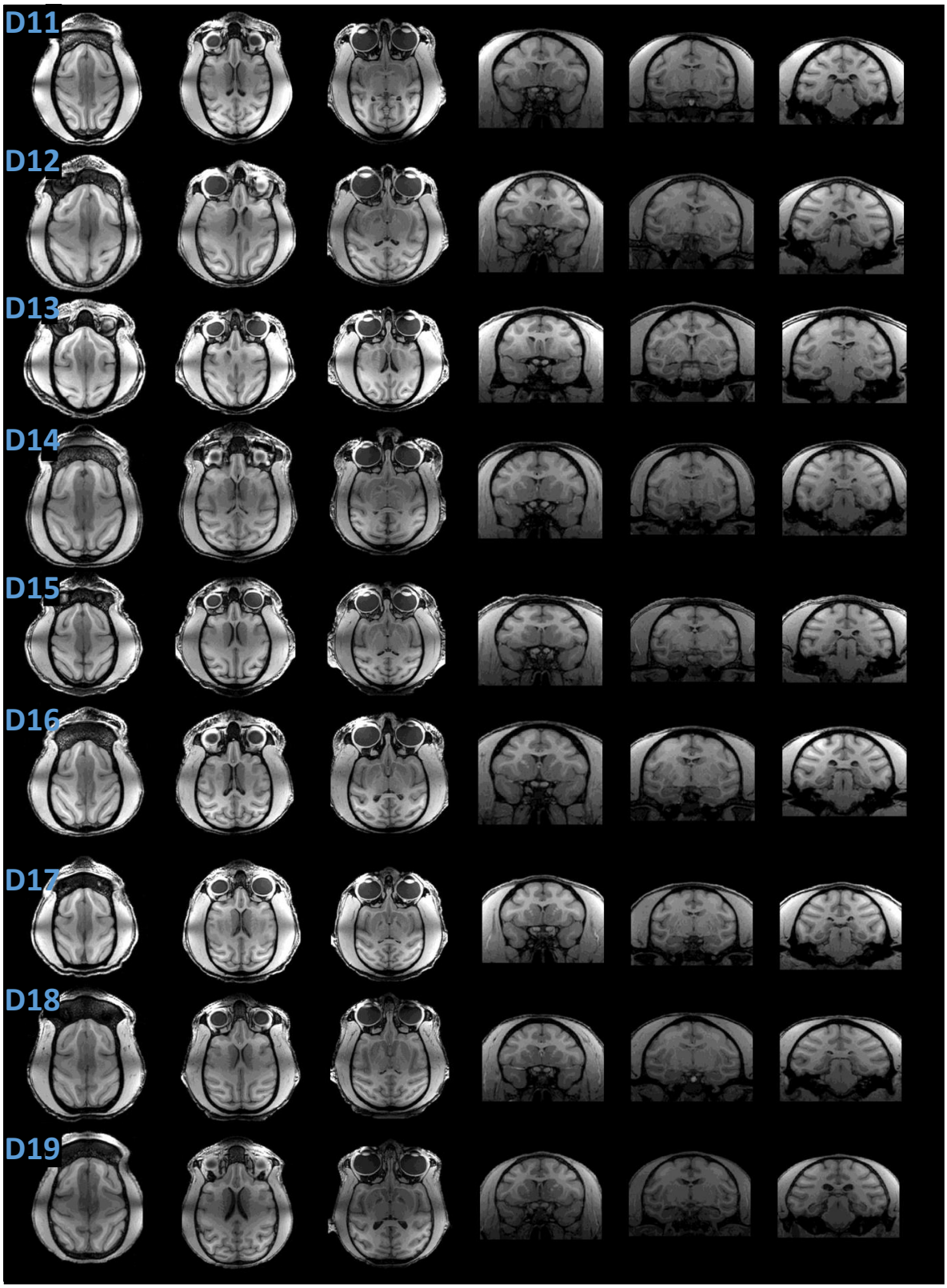

Supplementary Figure 1: Slices from Excluded Scans. 3 horizontal and 3 coronal slices from the scans of every subject excluded due to image quality issues, separated by site (A= Newcastle, B= Oxford, C= DPZ, D= UC-Davis). One subject was excluded due to motion artefacts (A2), 2 subjects were excluded due to prominent hyperintensities (A1 and B1), and the remaining ones (n=32) were excluded due to poor contrast to noise ratio in some parts of the brain.

Chapter 3: Development of AutoMacq: an Automatic Pipeline to Analyse Macaque Structural MRI Data

3.1 Abstract

MRI scanning of rhesus macaques is a growing field due to their evolutionary proximity and similar neuroanatomy to humans. Consequently, there is a need for automatic macaque MRI processing pipelines. AutoMacq is a pipeline capable of processing rhesus macaque MRI data to produce both voxel-based and surface-based metrics. It involves minimal manual intervention and can be carried out without expert knowledge of macaque neuroanatomy. To test the quality of the pipeline, scans from 74 subjects across 8 different sites were processed. Results indicate that over 87% of cross-sectional tissue segmentations and surfaces were of satisfactory quality to not require additional manual correction. Hemispheric comparisons and analyses of scan-rescan data showed strong reliability of the volumetric and surface-based outputs. Finally, to illustrate potential applications of AutoMacq, the change in grey matter volume with ageing was investigated cross-sectionally using subjects aged 3-15 years (corresponding to adolescence until mid-adulthood). The analysis revealed a linear decrease in grey matter volume with age similar to what has been found in humans, reinforcing the value of rhesus macaques as a model of healthy human ageing.

3.2 Introduction

Automatic pipelines are the gold standard in MRI data processing as they avoid biases that could be introduced by manual interventions and allow for standardisation of data processing. Many pipelines have been created to automatically process and analyse human MRI data, with minimal manual intervention from the researcher (https://neuro-jena.github.io/cat/; https://surfer.nmr.mgh.harvard.edu/fswiki/FreeSurferAnalysisPipelineOverview; https://www.nipreps.org/smriprep/; https://www.fil.ion.ucl.ac.uk/spm/software/spm12/; Fischer *et al.* 2012; Glasser *et al.* 2013; Reuter *et al.* 2012). These pipelines can often handle both cross-sectional and longitudinal datasets, and allow for investigation of voxel-based morphometry (VBM) and/or surface-based morphometry (SBM).

Over the last couple of decades, MRI scanning of animal models has become a rapidly growing field (Öz, Tkáč and Ugurbill 2013). The evolutionary proximity of non-human primates (NHPs), such as rhesus macaques, to humans means they are of great comparative and translational interest as animal models. The similarity of NHPs to humans in terms of brain anatomy and cognitive abilities has also meant they are particularly valuable as model animals in neuroscience research (Phillips *et al.* 2014; Roefsema and Treue 2014; Stonebarger *et al.* 2021). Additionally, rhesus macaques are a promising model for ageing research due to their comparable life stages to humans, combined with their accelerated rate of ageing (3-4 times the rate of humans) which can allow for more efficient research (Mattison and Vaughan 2017).

The processing of macaque MRI data comes with unique issues, precluding the use of established human pipelines to process macaque MRI data (Milham et al., 2018; PRIMatE Data Exchange [PRIME-DE] Global Collaboration Workshop and Consortium 2020). Though similar in shape and organisation to the human brain, the macaque brain is around 12-16 times smaller than the human brain (in terms of volume), with specific areas accounting for different proportions of the macaque brain compared to the human brain (Croxson *et al.* 2018). Other differences include differences in the amount of tissue surrounding the brain as well as in tissue contrast, making it more difficult to extract and segment the brain in macaque MRI scans, compared to human scans. Non-standardized surface coil arrangements are common when scanning macaques, and often result in variations in coil coverage and image intensity, which can cause further difficulty in processing macaque MRI data. Differences between sites in terms of equipment and protocols are also common and result in data across sites that varies greatly in terms of quality and scan parameters. As a result of this, a processing method designed for data from one site may not translate to macaque scans from other sites (Milham *et al.* 2018).

Furthermore, motion artefacts can be an additional issue when scanning awake macaques, with the only current way to minimise these artefacts being through training and/or head fixation (PRIMatE Data Exchange [PRIME-DE] Global Collaboration Workshop and Consortium 2020). Even with these methods in place to minimise movement, motion artefacts can still lead to noisier data for awake macaques than those that are anaesthetised, and potentially noisier data than would

be acquired from awake humans who will have a better understanding of the need to remain still during scanning.

Custom processing pipelines tailored to rhesus macaque MRI data are clearly required, and over the last few years such pipelines have been developed (Balbastre *et al.* 2017; Garcia-Saldivar et al. 2021; Lepage et al. 2021). However, these pipelines require manual correction of tissue segmentation and surfaces, which relies on expert knowledge of macaque neuroanatomy. Additionally, the currently available macaque processing pipelines implement surface-based morphometry only, with no clear option to carry out voxel-based morphometry, despite the complementarity of the two approaches (Goto *et al.* 2022). Furthermore, none of these pipelines have been designed with longitudinal data in mind, despite the established benefits of longitudinal research (see chapter 1, section 1.4.3). For MRI studies, pipelines which handle cross-sectional data are not fully leveraging the potential of longitudinal data, as they are optimised to generalise across a cohort, often at the cost of within-individual accuracy. For example, in a longitudinal pipeline, subject-specific templates could be used to improve various steps of the pipeline.

This study therefore aimed to design a processing pipeline for rhesus macaque MRI data that can produce accurate tissue segmentations and surfaces without manual intervention, for both cross-sectional and longitudinal data, and can produce both voxel-based and surface-based metrics.

3.3 Materials and Methods

3.3.1 Datasets

The AutoMacq pipeline was tested using all of the MRI data which passed visual quality control (see chapter 2, table 2). Briefly, this included cross-sectional data from 74 subjects, taken from across 8 sites, a scan-rescan dataset of 13 subjects from Newcastle University, and longitudinal data from 16 subjects, taken from across 3 sites.

The scan-rescan dataset consisted of two scans per subject, acquired within one week, for a subselection of subjects (N = 13). Scan-rescan data was only available from Newcastle University, meaning that all of the data was acquired from awake animals with a scanner strength of 4.7T. Both T1 and T2 data was available

for all of the subjects in this dataset. As was previously mentioned, there was some overlap in the scans included in the cross-sectional and scan-rescan datasets from Newcastle University. However, it should be noted that not all of the scans from the scan-rescan dataset were utilised in the cross-sectional dataset (other scans were chosen for some subjects to better allow for the subsequent investigations of the impacts of ageing- see chapters 4 and 5).

Longitudinal data was available from Newcastle University, NIDA and DPZ. 3 to 13 scans were available for each of the subjects included in the longitudinal datasets (96 scans in total). In order to be utilised for this project the scans for a subject needed to cover a period of at least 18 months, with consecutive scans separated by at least 3 months.

3.3.2 Cross-sectional AutoMacq pipeline

AutoMacq is optimised for the input of both T1 and T2 images, but can process T1 data alone, and utilises freely available software packages. Additionally, any macaque template can be utilised when processing data through AutoMacq. For this study, the population-average 112RM-SL template and its prior maps (McLaren *et al.* 2009) were chosen for testing the pipeline. This template is aligned to the Saleem-Logothetis atlas (Saleem and Logothetis 2012) that provides both high-resolution MRI scans and histological sections to delineate the anatomy of the macaque brain. An Ear Bar Zero (EBZ) coordinate system is employed, meaning that the origin is set to the midpoint of the interaural line (Saleem and Logothetis 2012).

The steps of the AutoMacq pipeline are outlined in figure 5, and each individual step to process cross-sectional data is described in detail below (with step numbers referring to those in Fig. 5). AutoMacq can also process longitudinal structural MRI data from rhesus macaques, and the adaptations required to do so are discussed in section 3.3.3. A detailed walkthrough, scripts and SPM batches for AutoMacq are available at: https://github.com/Nsk97/AutoMacq.git

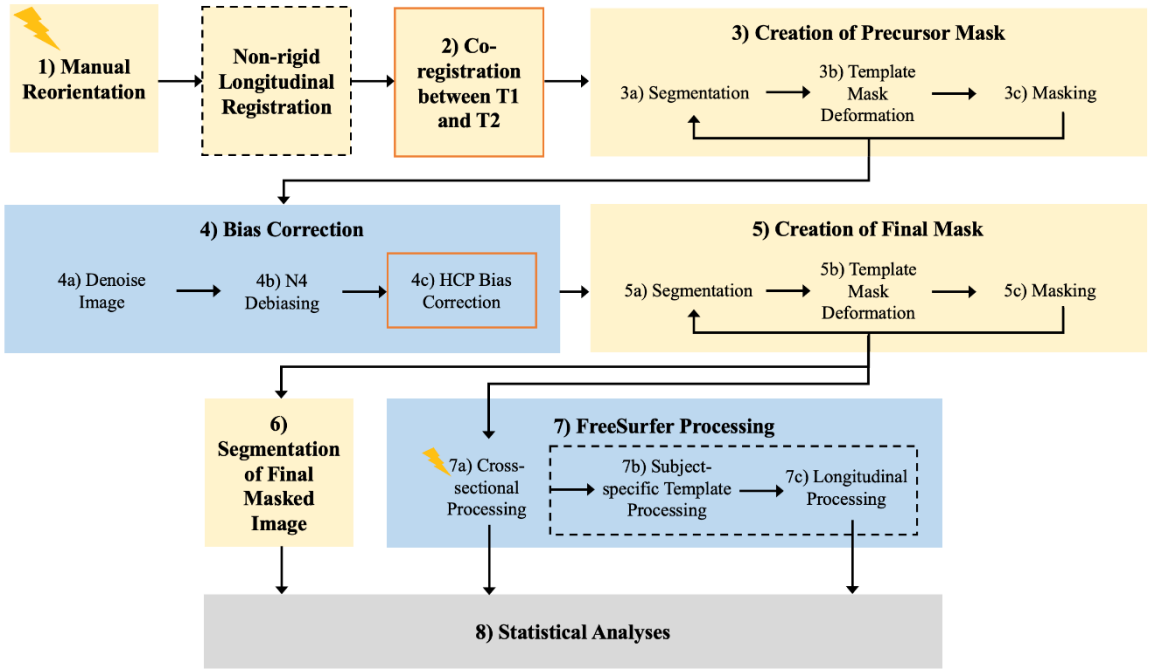

Figure 5: The AutoMacq Pipeline. Yellow boxes represent steps carried out using SPM, blue boxes those carried out in a Linux environment (with ANTs, connectome workbench, FSL and FreeSurfer installed). An orange outline represents a step that is skipped if T2 data are not available, and a dashed black outline a step that would only be carried out for longitudinal data. Lightning bolts indicate a manual intervention.

Step 1: Cropping and manual reorientation

Prior to processing through the AutoMacq pipeline, scans with large fields of view are cropped in FreeSurfer. This cropping minimises empty space and tissue outside of the skull. Cropping the field of view allows for more accurate masking later in the pipeline.

Following this, every T1 and, if available, T2 scan is manually reoriented in SPM. This involves rotating the scans and setting the origin to match the orientation and origin of the atlas. This manual reorientation step is simple and does not require any knowledge of macaque neuroanatomy.

Step 2: Co-registration between T1 and T2

The next step of AutoMacq consists of co-registering the reoriented T1 and T2 scans to ensure that their orientations precisely match. This step is done using the SPM intra-subject co-registration routine, using a rigid-body model and image reslicing (moving the T2 scan to align it with the T1 scan). This step is skipped in the absence of T2 scans.

Steps 3-5: Brain extraction

To obtain accurate tissue segmentation of macaque data, it is helpful to first mask out non-brain tissues, a process called brain extraction or skull stripping. This is done in AutoMacq through 3 steps: (1) the creation of a precursor mask in SPM; (2) bias correction carried out using ANTs, connectome workbench and FSL; and (3) the creation of the final mask in SPM.

Step 3: Creation of precursor mask and initial brain extraction

The precursor mask is an approximate, subject-specific mask that can be utilised for bias correction. A precursor mask in the native space is obtained by first creating a mask of the template (by binarising the sum of the grey matter (GM), white matter (WM) and cerebrospinal fluid (CSF) prior maps), and then deforming the template mask to match the subject-specific scan(s). This deformation between the template space and the native space is calculated using the SPM segmentation routine. This routine combines tissue classification of the subject-specific scans (combining information from T1 and T2 scans to improve the segmentation accuracy), correction of intensity non-uniformity (bias correction) and non-rigid co-registration to the template. The segmentation relies on 4 classes of tissue probability maps: GM, WM, CSF, and non-brain tissues (adding the non-brain tissue class was found to improve the quality of the segmentation). The T1 scan (and coregistered T2 scan, if available) is then masked using this approximate precursor mask.

This process (segmentation, mask deformation and masking) can be repeated several times if necessary to further increase the quality of the subject-specific mask, as long as no brain tissues are masked out. Macaque data differs from human in that images are often acquired using non-standardized arrangements of surface coils (Milham et al., 2018), generating increased variation in image intensity. Using the bias correction developed for human data in SPM, no parameter was found to be good enough to produce accurate subject-specific masks. To increase the quality of the mask, the precursor mask was created using little debiasing (heavy regularisation) in SPM and the main debiasing done outside SPM (please note that the precursor mask needs to be resliced to be used by other software).

Step 4: Bias correction

For the AutoMacq pipeline, the ANTs functions DenoiseImage and N4BiasFieldCorrection are utilised. DenoiseImage removes noise from the scans using a spatially adaptive filter, and N4 debiasing is a variant of non-parametric, non-uniform, normalization (N3) debiasing (Tustison *et al.* 2010). DenoiseImage needs to be applied to the unmasked T1, whereas N4BiasFieldCorrection utilises an unmasked T1 image and the precursor mask as inputs.

To further minimise bias in the images, the program connectome workbench along with the bias correction script from the Human Connectome Pipeline (HCP) can be utilised for subjects with both T1 and T2 scans. This script uses the square root of T1w*T2w in order to correct the bias field, and improvements can be seen when this is used alongside other debiasing steps. The HCP script requires both unmasked and masked T1 images as inputs; the masked T1 is obtained by applying the function fslmaths (from FSL) to the N4 debiasing output.

Step 5: Creation of final mask and brain extraction

A final mask is then created using the same approach described in step 3 but using the debiased scan(s) as input(s) of the segmentation, and a final masked T1 (and T2 if available) is produced which excludes non-brain tissues.

Step 6: Tissue segmentation

A final segmentation of the masked, debiased T1 scan is then performed in SPM. The output files from this segmentation can then be used to calculate the volumes of the grey and white matter (and the cerebrospinal fluid) as well as the local amount (or density) of grey matter in each voxel. These metrics can then be analysed statistically for voxel-based morphometry studies.

Step 7: Surface-based cross-sectional processing

Surface-based processing in AutoMacq utilises custom analysis scripts that adapt the FreeSurfer standard processing stream for human MRI data. For cross-sectional processing, the FreeSurfer stream consists of 3 major stages: autorecon1,

autorecon2 and autorecon3. For cross-sectional processing in AutoMacq, modifications are made to the autorecon1 and autorecon2 stages.

Autorecon1

Autorecon1 begins with computation of the affine transformation from the final masked T1 obtained in step 5 to the MNI305 atlas. This is required as atlas coordinates of different brain areas are needed for several downstream functions. The MNI305 is a human brain atlas, so this automatic computation tends to be extremely inaccurate for macaque data, and there is no simple way to substitute a macaque atlas for the MNI305 atlas. However, macaque MRI data can be successfully processed through FreeSurfer by manual correcting the atlas registration. This is done by matching the size and orientation of the masked T1 to the MNI305. Therefore, this manual step does not rely on any knowledge of macaque neuroanatomy and can be carried out quickly and easily by a non-expert. The rest of the autorecon1 stage includes correction of any remaining non-uniformity or fluctuations in intensity (unchanged FreeSurfer standard step). The final step of skull stripping is skipped since images have already been brain extracted in SPM.

Autorecon2

The autorecon2 stage begins with the segmentation of subcortical structures and the computation of their respective volumes. In AutoMacq, the standard stream is adapted to use the manually corrected atlas registration to initialise the subcortical segmentation. Next, WM is segmented to give a WM volume image (cerebellum and brainstem are excluded), which is then used to create the surfaces encoding the boundary of WM and GM in each hemisphere. These left and right WM surfaces are used as a starting point to generate surfaces encoding the boundary of GM and CSF in each hemisphere (‘pial surfaces’). However, this processing in FreeSurfer alone does not always produce accurate surfaces. Instead of manually correcting the white matter surfaces (WM edits), the WM segmentation file produced by SPM (step 6) can be used to re-run the cortical surface generation. To be recognised correctly in FreeSurfer, the WM segment image is first binarized in SPM (threshold of 0.2).

A custom script was written to recognise this binarized WM volume as WM edits. As the last step of autorecon2, a binary mask of the cortical ribbon is then created.

Autorecon3

The autorecon3 stage carries out the co-registration of the GM and WM surfaces to the spherical atlas (spherical morph), in order to label brain regions for cortical parcellation. The entirety of autorecon3 can be ran unchanged from the standard FreeSurfer stream to acquire global brain metrics, but it is also possible to easily replace the human atlas with a macaque parcellation schema in order to acquire macaque parcellations.

3.3.3 Adaptations to AutoMacq when processing longitudinal data

AutoMacq is intrinsically capable of processing longitudinal MRI datasets from rhesus macaques. The adaptations to the cross-sectional pipeline required to do so are outlined below.

Longitudinal voxel-based processing

The stages to obtain voxel-based metrics for longitudinal datasets using AutoMacq are very similar to those used for cross-sectional data, with one additional step. After all of the scans for a subject have been cropped and reoriented (as described in section 2.3.1), a longitudinal registration step is performed. This includes a rigid-body and a diffeomorphic registration of each T1 scan to a mid-point average image (Ashburner and Ridgway, 2013). If T2 data are available, a longitudinal registration of T2 scans is carried out as well, and the average T2 scan is then coregistered to the average T1 scan. The rest of the voxel-based processing in AutoMacq is carried out in the same way it would be for individual cross-sectional scans but using the average image(s) as input file(s).

Longitudinal surface-based processing

The standard FreeSurfer longitudinal processing stream for human data involves 3 major stages: 1) cross-sectional processing of all timepoints for each subject, 2) creation and processing of an unbiased template for each subject, 3)

Processing of all timepoints for each subject using the unbiased, subject-specific template. The longitudinal processing with AutoMacq therefore starts with the cross-sectional processing of all timepoints, as described in section 2.3. This cross-sectional processing provides a normalised, skull-stripped, atlas-registered T1 scan for every timepoint, which are then used to create a subject-specific template using robust, inverse consistent registration (Reuter et al., 2010). This template is used to help at various stages of the longitudinal re-processing of all time points: for example, skull stripping, Talairach transforms, atlas registration, as well as spherical surface maps and parcellations, are initialized with common information from the within-subject template, significantly increasing reliability and statistical power (Reuter et al., 2012).

The third stage is the actual longitudinal processing of the time points and is unchanged from the standard FreeSurfer longitudinal processing carried out for human MRI data. Briefly, every timepoint is processed again, but the template created in the previous step is used to initialise processing steps involved in the cortical and subcortical segmentation. This should increase the robustness and sensitivity of the overall longitudinal analysis.

3.3.4 Statistics

Whole brain measures of GM, WM and CSF were extracted using SPM for every subject. Hemispheric measures of the same metrics were also extracted in SPM, using a hemisphere mask created through manual editing of the Saleem-Logothetis atlas mask. Whole brain and hemispheric measures of grey matter and white matter surface area, as well as cortical thickness were taken from FreeSurfer for every subject.

For the scan-rescan comparisons, the intraclass correlation coefficient (ICC) was calculated in R, using an absolute-agreement, single-measurement, two-way mixed-effects model. This model was also utilised to calculate the ICC for the analysis of the impact of the manual steps of the AutoMacq pipeline. Pearson correlation analyses were carried out in R (https://www.r-project.org/) for the hemisphere comparisons. This was used rather than ICC for the hemisphere comparisons as ICC accounts for systematic offsets, which could occur biologically between hemispheres.

The change in grey matter volume (GMV) and cortical thickness (CT) with ageing was also investigated in R. Tests for normality and heteroscedasticity were first carried out. A non-linear fit was found to not significantly improve the percentage of variance explained by the model, so a linear model was fitted. Site/scanner was included as a random effect in the model, and total intracranial volume (TIV) was controlled for (fixed effect) in order to account for differences in head size (Whitwell *et al.* 2001).

3.4 Results

3.4.1 VBM outputs

All of the cross-sectional scans processed through AutoMacq (N=74) produced an accurate brainmask for skull stripping (suppl. figure 2 provides examples of these brainmasks).

Figure 6 illustrates a representative example of SPM segmentation outputs (grey matter and white matter tissue outputs) from AutoMacq. For 95.9% of cross-sectional scans (N=71/74) outputs of comparable quality to those in figure 6 were produced. The remaining cross-sectional scans (4.1%, 3/74) had some errors in their grey and white matter segmentation outputs (suppl. figure 3 illustrates these problematic outputs).

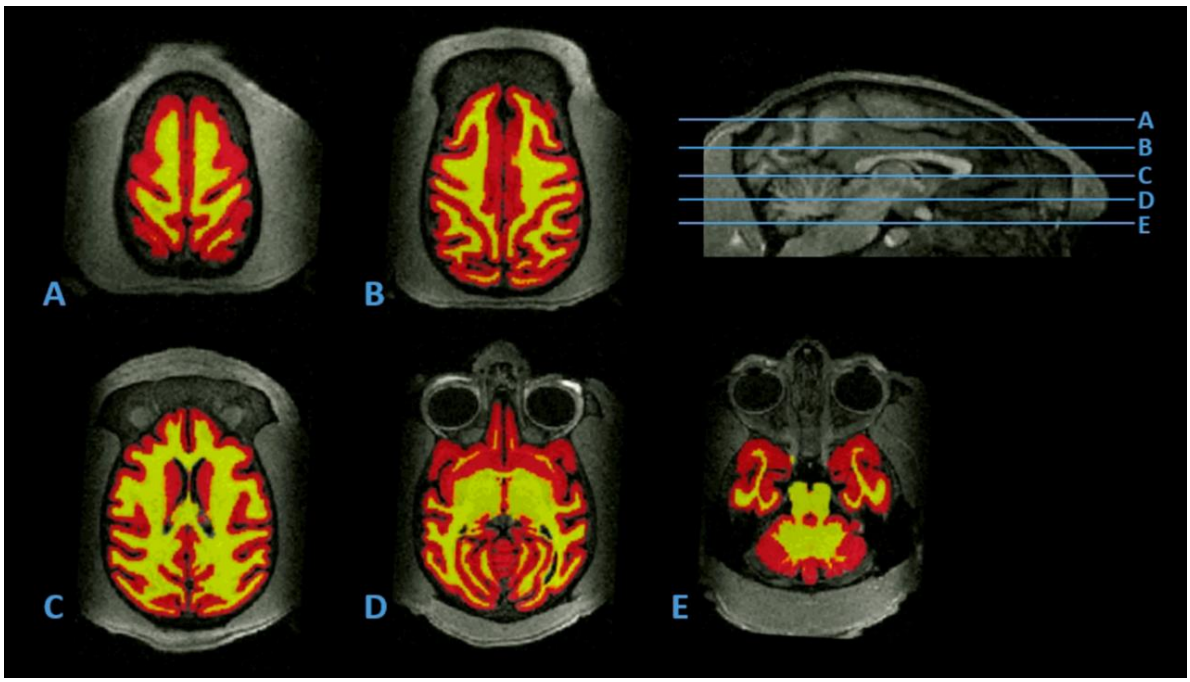

Figure 6: Representative Tissue Volumes Produced by AutoMacq. Horizontal slices of a representative example of GMV (shown in red) and WMV (shown in yellow), produced using the cross-sectional AutoMacq pipeline, displayed on the corresponding T1 scan, and presented alongside a midsagittal image showing where each slice is taken from.

For longitudinal VBM processing in AutoMacq, 87.5% of subjects (14/16) produced SPM segmentation outputs of similar quality to figure 6, and 12.5% of subjects showed some errors in the segmentation of grey and white matter (2/16).

3.4.2 SBM outputs

Figure 7 shows a representative example of FreeSurfer surfaces output from the cross-sectional AutoMacq pipeline, for the same subject for which SPM segmentation outputs were displayed in figure 6. 87.8% of scans (65/74) processed through AutoMacq resulted in surfaces comparable to those shown in figure 7. This was after the WM segmentation file from SPM was used in place of WM edits in FreeSurfer for 60/74 (81.1%) subjects (the other 14 subjects produced good quality surfaces without this step). This improvement of the surface accuracy with this step is illustrated in figure 8. However, even after the incorporation of the WM segmentation file from SPM, 9/74 (12.2%) subjects still showed some errors in their surfaces (see details in suppl. figure 4).

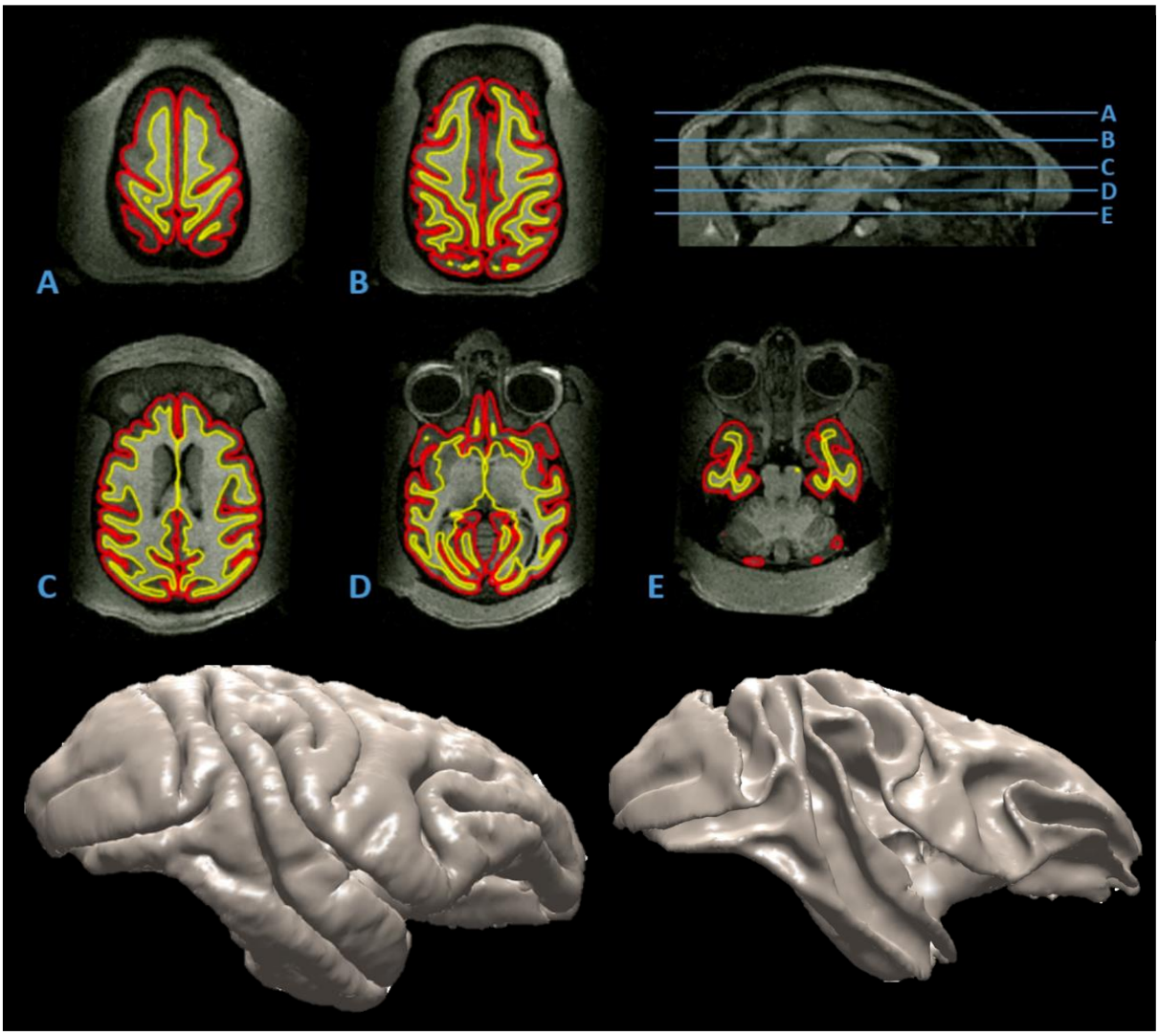

Figure 7: Representative Surfaces Produced by AutoMacq and 3D Models of Those Surfaces. Horizontal slices of a representative example of pial (shown in red) and white matter (shown in yellow) surfaces, produced using the cross-sectional AutoMacq pipeline. A midsagittal image showing where in the brain each slice is taken from, and 3D models of the surfaces are also presented. The cerebellum and brainstem are excluded during FreeSurfer processing.

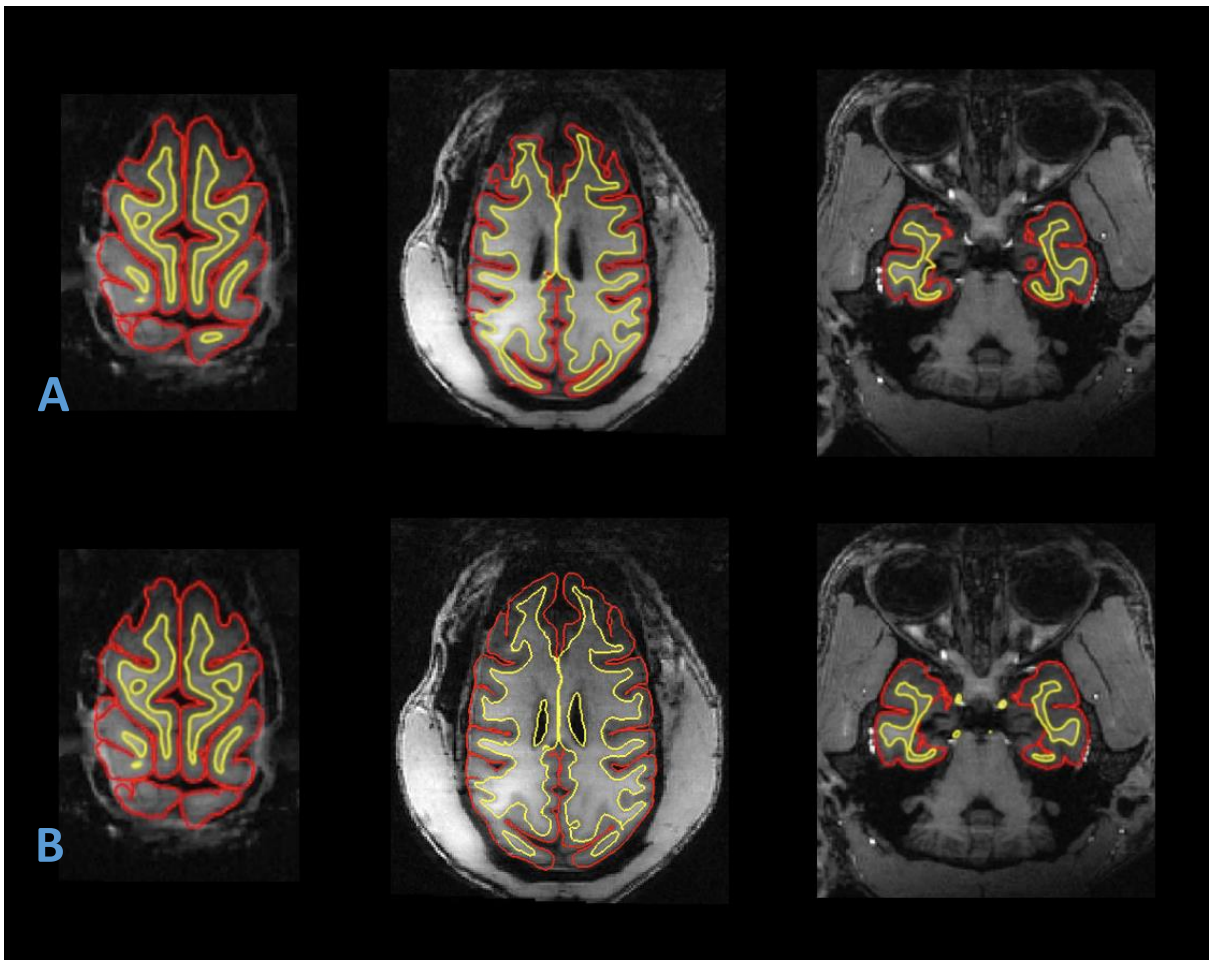

Figure 8: Comparison of Surfaces Produced with AutoMacq, without and with SPM WM. Horizontal slices of examples of pial (shown in red) and white matter (shown in yellow) surfaces, produced for the same subject using the cross-sectional AutoMacq pipeline, without WM from SPM (A) and with WM from SPM (B).

For longitudinal SBM processing in AutoMacq, all 96 of the scans, acquired from 16 subjects, were processed through FreeSurfer. For 59.4% (57/96) of these scans the surfaces produced were comparable to those in figure 7, but 40.6% of scans (39/96) showed some errors in their surfaces. For both the VBM and SBM processing of the longitudinal data, errors were limited to subjects from Newcastle University. However, for some scans the longitudinal processing did result in improved surfaces, compared to those produced through cross-sectional processing (see figure 9).

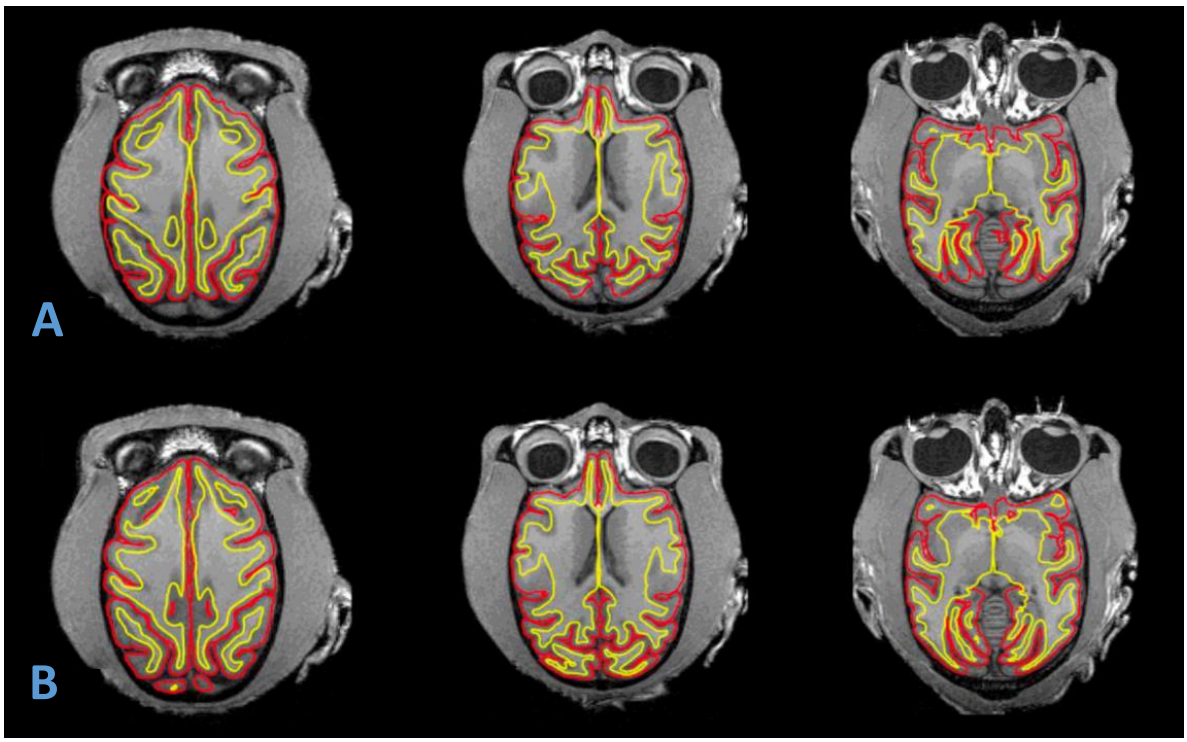

Figure 9: Comparison of Surfaces Produced Using the Cross-sectional vs. Longitudinal AutoMacq Pipeline. Horizontal slices of examples of pial (shown in red) and white matter (shown in yellow) surfaces, produced for the same subject using the cross-sectional AutoMacq pipeline (A) and using the longitudinal AutoMacq pipeline (B)

3.4.3 Hemisphere comparison

To assess the reliability of AutoMacq, various volume-based and surface-based metrics were compared between hemispheres. Considering that hemispheric differences from biological origin are minimal, this analysis allows for quantification of errors mainly due to AutoMacq processing. All of the subjects processed through AutoMacq (including those with errors in their outputs) were included in this analysis. Results indicate strong correlation between hemispheres for all metrics tested (R values between 0.9 and 0.98, Fig. 10).

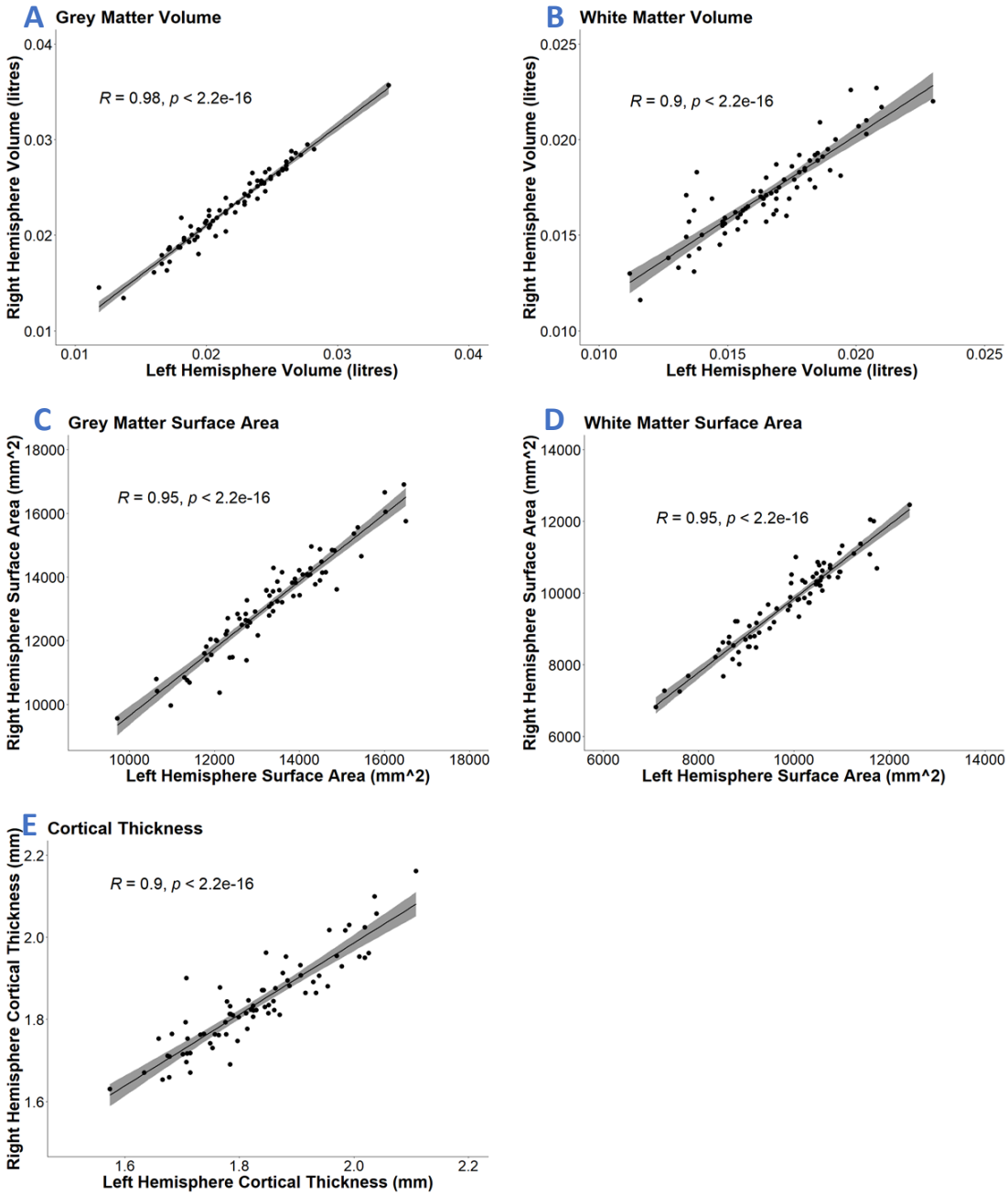

Figure 10: Hemisphere Comparison Graphs. Correlation between left and right hemisphere values for GM volume (A), WM volume (B), GM surface area (C), WM surface area (D) and cortical thickness (E). The linear fit and standard error are plotted, and R and p values are shown on each graph.

3.4.4 Scan-rescan

To further evaluate the reliability of AutoMacq, the scan-rescan dataset was also processed to give both volume-based and surface-based outputs. Over such a short span of time between ‘scan’ and ‘rescan’ (less than 1 week), noticeable structural brain changes are not expected. Rescan data was available for a subset of 13 macaques from the Newcastle University dataset (8 males and 5 females). Results indicate strong correlations across metrics despite a modest sample size and the fact that the animals were scanned while awake (ICC values between 0.6 and 0.95, fig. 11).

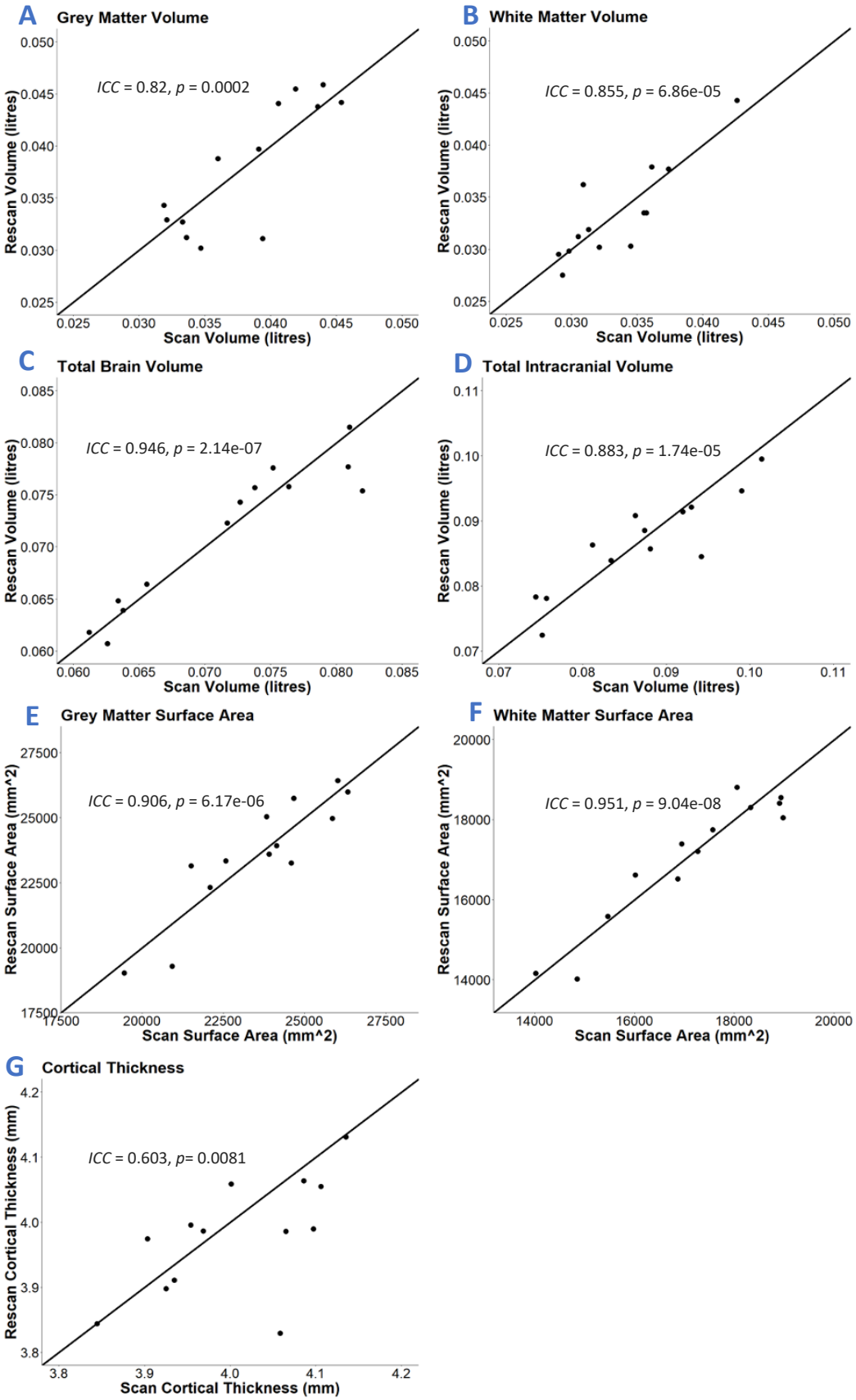

Figure 11: Scan-Rescan Graphs. Graphs of the correlation between the scans and the rescans for GM volume (A), WM volume (B), total brain volume (C), total intracranial volume (D), GM surface area (E), WM surface area (F) and cortical thickness (G). The identity line, ICC value and p value are shown on each graph.

3.4.5 Impact of manual steps

A correlation analysis was carried out in order to assess the impact of the few manual steps of AutoMacq on the outputs of the pipeline. This involved the initial scans for each of the subjects included in the scan-rescan dataset (13 macaques from the Newcastle University dataset; 8 males and 5 females) being reprocessed through the AutoMacq pipeline from the raw data. This was done years after the initial processing in order to create a ‘blind’ approach and avoid any biases in the manual steps. Results indicate very strong correlations across all of the voxel-based metrics, as well as for grey matter surface area and white matter surface area (ICC values between 0.93 and 0.99, fig. 12). The correlation for cortical thickness was much weaker (ICC value of 0.561); however, this was due to two outliers. Removal of these outliers resulted in a strong correlation for cortical thickness as well (ICC value of 0.813).

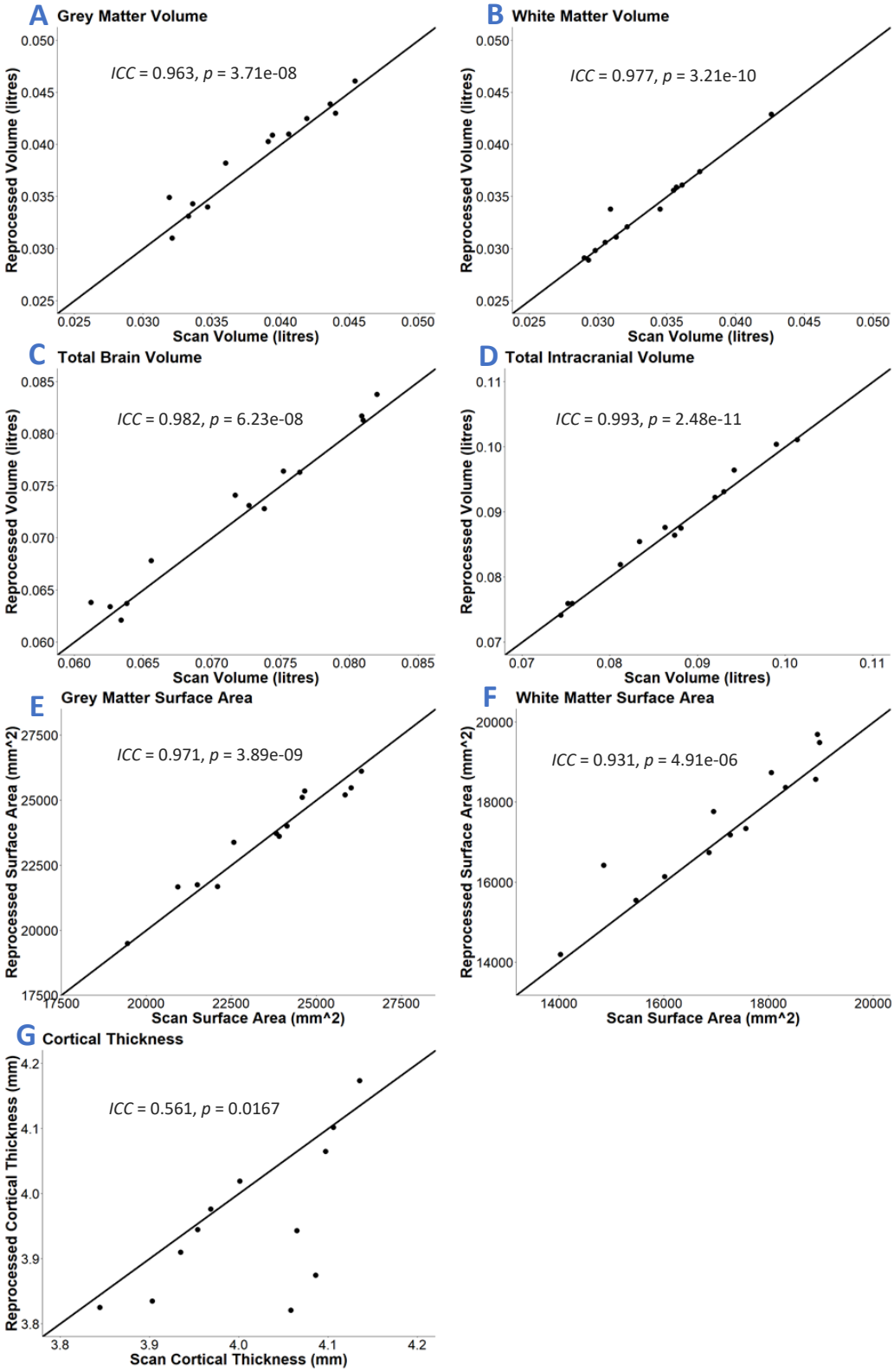

Figure 12: Impact of Manual Steps. Graphs of the correlation between the scans and the reprocessed scans for GM volume (A), WM volume (B), total brain volume (C), total intracranial volume (D), GM surface area (E), WM surface area (F) and cortical thickness (G). The identity line, ICC value and p value are shown on each graph.

3.4.6 Global brain changes with ageing

To demonstrate a possible application of the AutoMacq pipeline, and to confirm the viability of investigating age-related changes in brain structure using the available datasets, the impact of ageing on total grey matter volume, and on average cortical thickness, was tested using the male subjects from the cross-sectional datasets. Female subjects were excluded due to the small sample size, and scans from any site with fewer than 5 male subjects were also excluded so that effect of site could be adequately controlled for in the model. The Oxford dataset was excluded as it lacked variability in terms of age. A significant, linear decrease in total GMV with increasing age (from 3 to 15 years, corresponding to adolescence to mid-adulthood in macaques) was found (β= -0.0013, Std. error= 0.00034, DF= 44, p= 0.0004, fig. 13). However, no significant change in average CT with ageing was identified (β= 0.0075, Std. error= 0.014, DF= 44, p= 0.59, fig. 14).

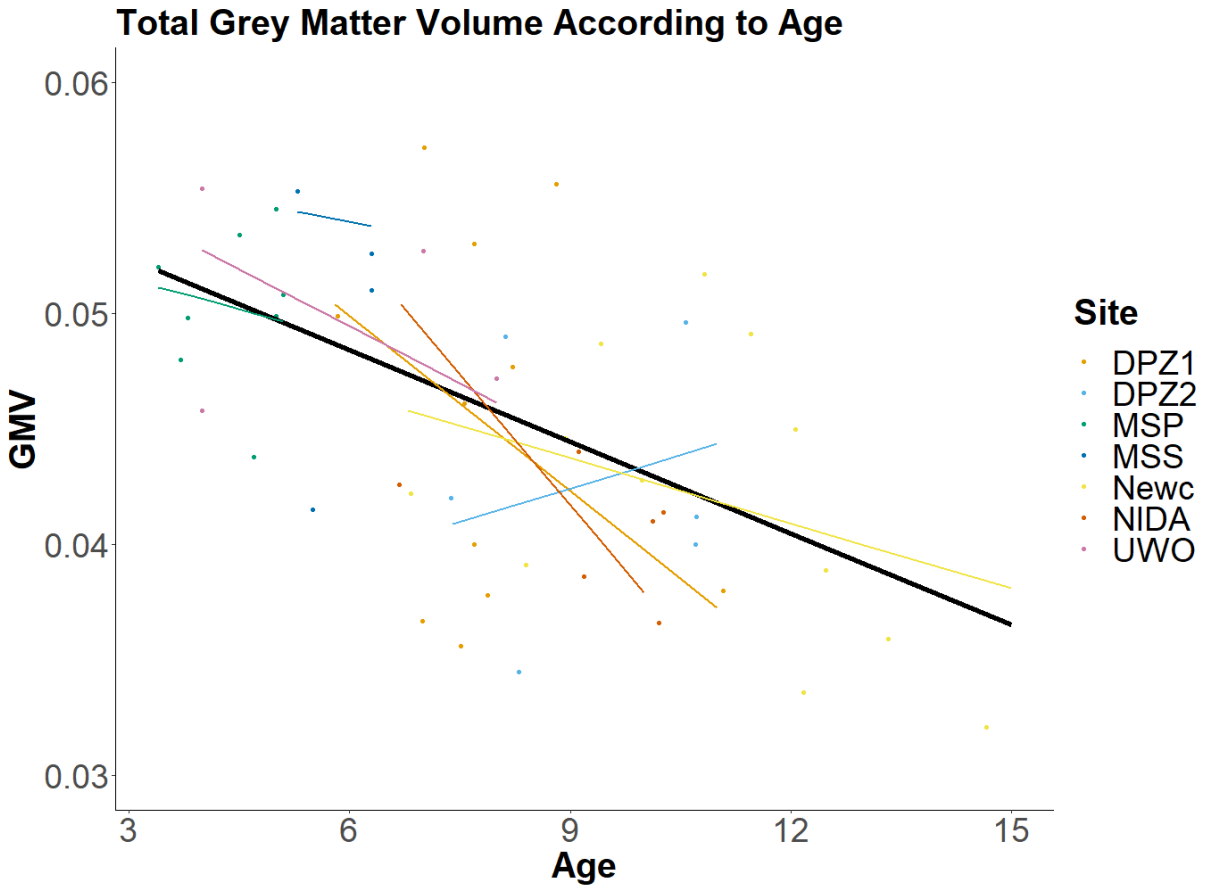

Figure 13: Changes in Total GM Volume According to Ageing. The bold black linear line corresponds to the main effect of age, while controlling for TIV and with site/scanner declared as a random effect. The thin coloured lines correspond to

linear fits of age effect in each site while controlling for TIV. Dots correspond to raw data (unadjusted for TIV).

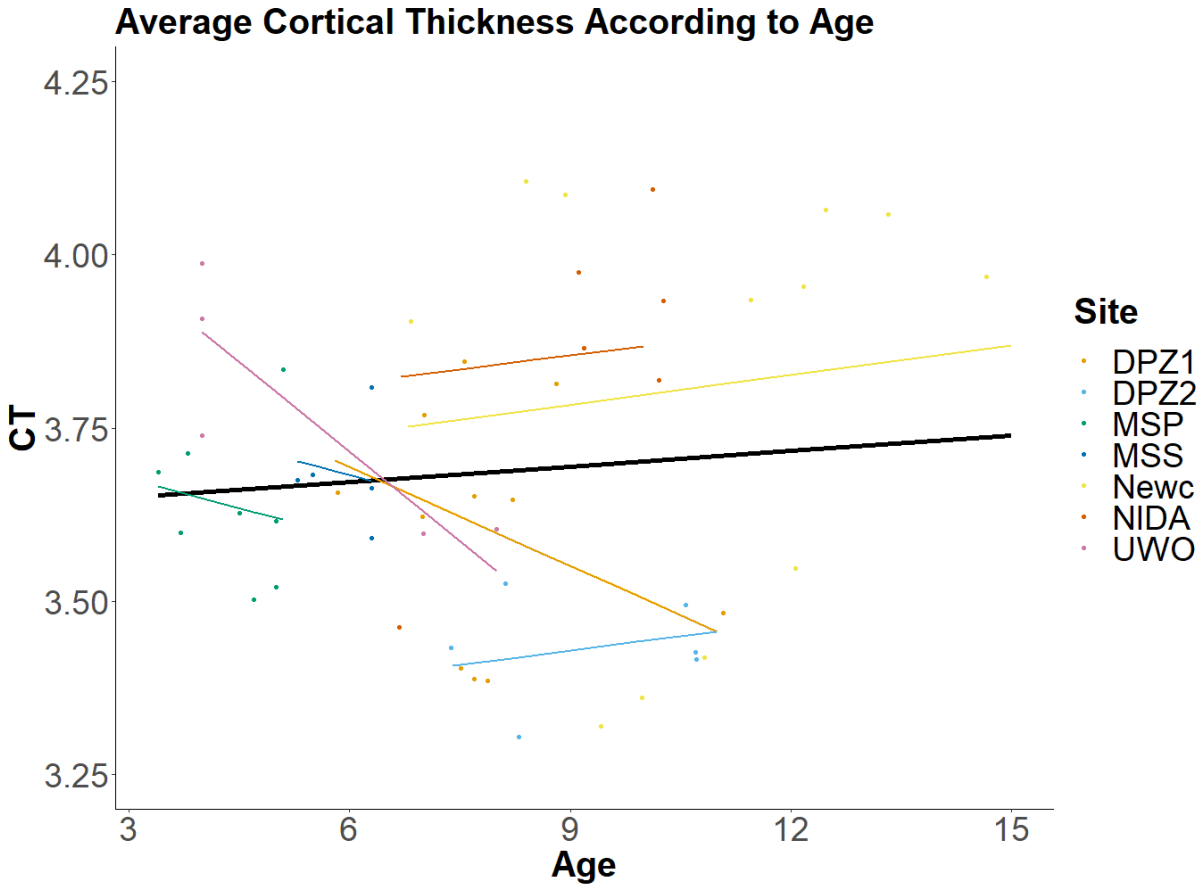

Figure 14: Changes in Average Cortical Thickness According to Ageing. The bold black linear line corresponds to the main effect of age, while controlling for TIV and with site/scanner declared as a random effect. The thin coloured lines correspond to linear fits of age effect in each site while controlling for TIV. Dots correspond to raw data (unadjusted for TIV).

3.5 Discussion

3.5.1 Strengths of AutoMacq

AutoMacq is a robust processing pipeline, capable of successfully processing macaque MRI data with a wide range of quality and scan parameters, with minimal manual intervention. The two manual steps within the pipeline are simple to carry out and do not require any expert knowledge of macaque neuroanatomy. This, coupled with the automation of the rest of pipeline, makes AutoMacq relatively easy to use. Additionally, AutoMacq is unique amongst macaque pipelines in its ability to produce

both voxel-based and surface-based metrics (Balbastre *et al.* 2017; Garcia-Saldivar et al. 2021; Lepage et al. 2021), allowing for more avenues of investigation and comparison with a wider range of previous studies (Goto *et al.* 2022). A further strength of AutoMacq is the use of freely available software packages that anyone can access, as well as the ability to utilise any macaque template when processing data through AutoMacq.

Both T1 scans alone and datasets of T1 and T2 scans were successfully processed through AutoMacq, and 100% of the scans processed through AutoMacq produced an accurate brain mask. This extremely high level of success in terms of brain extraction is better than the one obtained using the FSL bet function (Lepage et al. 2021) and comparable to what can be obtained by more sophisticated deep learning-based approaches (Wang et al., 2021). 95.9% of cross-sectional scans processed through AutoMacq gave good quality volume-based outputs and 87.8% gave good quality surface-based outputs. A good quality output was defined as one not requiring manual correction. The high percentage of good quality outputs produced for cross-sectional data illustrates AutoMacq's accuracy, with fewer errors in the outputs from AutoMacq than those produced when using other pipelines to process data from various sites (Garcia-Saldivar *et al.* 2021; Lepage et al. 2021). This better performance is likely to come from the use of SPM segmentation routine to identify the GM/WM boundary. AutoMacq was able to handle scans with a wide range of scan parameters and quality, including those known to be difficult to process, such as scans acquired in awake subjects (Newcastle University dataset) and scans from subjects that have open skulls due to head implants (Milham et al., 2018; PRIMatE Data Exchange [PRIME-DE] Global Collaboration Workshop and Consortium 2020). The few cross-sectional scans for which AutoMacq produced outputs with errors were not all from one site, indicating that the poorer outputs were not due to an inability to handle specific scanning parameters but likely due to issues specific to the individual scans themselves.

For voxel-based morphometry, AutoMacq had a comparable success rate for cross-sectional and longitudinal datasets, with good quality outputs being produced for 95.9% of cross-sectional scans and 87.5% of longitudinal subjects. This was despite the far larger sample size for the cross-sectional study (74 scans compared to just 16 longitudinal subjects). In terms of surface-based morphometry, the error

rate for AutoMacq was higher with longitudinal data (40.6%) compared to with cross-sectional data (12.2%). It should be noted that almost a third of the subjects with longitudinal data (5/16) were part of the group of subjects which produced surface errors in the cross-sectional study. Because of the way the FreeSurfer longitudinal stream is carried out, errors in the cross-sectional processing of any single timepoint will be transferred to the template, inducing inaccuracies in the re-processing of each timepoint using the subject-specific template, providing a potential explanation for the increase in errors seen with AutoMacq longitudinal processing. Additionally, the longitudinal data available for testing AutoMacq was comprised mainly of subjects from Newcastle University which were both scanned awake and had open skulls due to head implants, making them some of the most difficult to process successfully (Milham et al., 2018; PRIMatE Data Exchange [PRIME-DE] Global Collaboration Workshop and Consortium 2020). Scanning awake macaques is known to increase the noise in images due to motion artifacts, and this reduced image quality may have also contributed to the increased proportion of errors for the longitudinal processing, as errors only occurred for subjects from the Newcastle dataset. For the subjects from other sites, which were scanned whilst anaesthetised, all of their longitudinal data was successfully processed through AutoMacq without errors for either VBM or SBM outputs. The older ages of some of the Newcastle University macaques with longitudinal data, compared to the subjects from other sites with longitudinal data, may also have played a role in the higher error rate. The older subjects tended to have scans covering a longer time period, which may have meant that the later (and possibly earlier) scans were less similar to the subject-specific template, potentially resulting in errors in the longitudinal surface generation.

The present assessment of AutoMacq's quality as a processing pipeline is strengthened by the use of quantitative measures of reliability. The hemisphere comparison resulted in strong correlations for both volume-based and surface-based metrics, despite the fact that problematic volumes and surfaces were not excluded from the analyses. Since only minimal differences from biological origin were expected between hemispheres, this result indicates that AutoMacq produces reliable volume and surface outputs. The reliability of AutoMacq was then further demonstrated by the scan-rescan analysis. This analysis focused on a smaller sample (N=13) from the Newcastle dataset alone. Despite the limited sample size,

good to excellent reliability was observed for all of the volume-based metrics tested and 2 of the 3 surface-based metrics, with the correlation for cortical thickness being weaker but still showing moderate reliability (Koo and Li 2016). This weaker correlation is unsurprising given how much influence sample size has in studies of cortical thickness (Pardoe *et al.* 2013), and the strength of this correlation did increase when the outlier was removed. Also, it is notable that these correlations are fairly strong given the fact that macaques in this subset of data were all scanned whilst awake, and head movements are known to have a major impact on ICC in MRI studies (Hedges *et al.* 2022). Overall, this scan-rescan analysis provides further evidence for the strong reliability of the AutoMacq pipeline, despite the errors present for some scans. In fact, both the hemisphere comparison and scan-rescan analysis resulted in similar correlations to what has been seen for human MRI studies, implying comparable levels of reliability (Carmon *et al.* 2020; Hedges *et al.* 2022).

The impact of the manual steps of the AutoMacq pipeline on the reliability of the outputs was also assessed. This analysis utilised the same sample as the scan-rescan analysis, meaning that the scans included were all from the Newcastle dataset and thus were from awake subjects. As this data was the most difficult to process through the pipeline this should allow for a robust assessment of how differences in carrying out the manual steps of the pipeline may impact on the outputs produced. For all of the voxel-based metrics, and for grey matter surface area and white matter surface area, very strong correlation were identified. This indicates a high level of reliability with minimal impact from the manual steps. It should be noted that though the correlation for cortical thickness was much weaker this was found to be driven by the outputs for two subjects, and with those subjects excluded the correlation was far stronger. Overall, the manual steps appear to have minimal impact on the outputs for the majority of scans, further highlighting the reliability of the outputs of AutoMacq.

A key strength of AutoMacq is the ability to carry out both voxel-based and surface-based morphometry. This is an advantage as it allows for data to be exploited in multiple different ways, and the optional ability to substitute a macaque parcellation schema into the FreeSurfer processing compounds this benefit. Furthermore, the ability to produce both volume-based and surface-based metrics allows for comparison to a wider range of studies, which is particularly important due

to the continued publication of both VBM and SBM human studies, especially in clinical populations (Goto *et al.* 2022). Historically, human cortical VBM analyses have been criticised because they tended to suffer from volumetric projection to a template, particularly due to the highly variable cortical folding pattern between subjects, and SBM has been - in part - developed to avoid these issues (Postelnicu *et al.* 2008; Villalon *et al.* 2011). However, the cortical folding pattern in macaques is much more preserved between subjects (Van Essen *et al.* 2019). Additionally, the probability of problems linked to partial volume effects can be mitigated by the use of high magnetic field strengths, allowing for the acquisition of images at higher spatial resolution, which is fairly common when it comes to non-human primate imaging (Milham *et al.* 2018). We therefore suspect that the potential drawbacks of VBM in human data are less likely to be relevant for macaque analyses, and this could be tested in the future using the AutoMacq pipeline.

Table 5 provides a summary of the strengths of the AutoMacq pipeline compared to other pipelines currently available for the processing of macaque MRI data.

	AutoMacq	PREEMACS (Garcia-Saldivar et al. 2021)	CIVET (Lepage et al. 2021)	Primatologist (Balbastre et al. 2017)
Voxel-based Processing	✓	x	x	x
Surface-based Processing	✓	✓	✓	✓
Automation	Minimal manual intervention	Minimal manual intervention	Minimal manual intervention	Minimal manual intervention
Output Quality	Manual corrections not required for majority of scans	Manual corrections required for many scans	Manual corrections required for many scans	Not discussed
Reliability	High (hemisphere comparison, scan-rescan)	Not quantitatively measured	Not quantitatively measured	Not discussed
Ease of Use	Does not require expert knowledge of neuroanatomy	Knowledge of neuroanatomy may be required	Complex	Complex
Access to Software	Readily available	Readily available	Less Accessible	Less Accessible
Flexibility	Highly flexible- can handle varied scans	Moderate flexibility	Less flexible	Less flexible
Longitudinal Processing	✓	Not discussed	Not discussed	Not discussed

Table 5: Comparison of the strengths of AutoMacq with other pipelines for processing macaque MRI data.

3.5.2 Limitations of AutoMacq

One limitation of AutoMacq is our use of a human atlas for the FreeSurfer processing, as this is what necessitates the manual correction of the atlas registration. The inability to run AutoMacq fully automatically may make processing very large datasets more time consuming, however datasets of hundreds or thousands of macaque MRI scans are currently relatively rare. Additionally, AutoMacq produced good outputs for the vast majority of subjects despite the use of a human atlas. It is possible that substituting in a macaque atlas may result in even fewer errors but given the high success rate, and high level of reliability, already observed this is likely to be unnecessary for most studies (particularly those utilising anaesthetised scans).

3.5.3 Impact of ageing on total grey matter volume

The impact of ageing on total grey matter volume was investigated using 59 male subjects aged between 3 and 15 years, scanned using 8 different scanners, from across 7 different sites. Given macaques age at 4 times the rate of humans during childhood (reaching sexual maturity around 4 and full physical maturity around age 5-6) and 3 times the rate of humans during adulthood (Mattison and Vaughan 2017), the age range tested here can be roughly compared to ages of 12-45 in humans. Therefore, this analysis includes subjects from early adolescence through to mid-adulthood.

A significant linear decrease in grey matter volume was found, indicating that in male rhesus macaques there is a significant decline in grey matter volume prior to reaching mid adulthood. This is a novel finding for this age group and suggests that the age-related decrease in GMV seen in mid/late adulthood in previous studies of macaques (Wisco *et al.* 2008; Chen *et al.* 2013) may actually start earlier in the lifespan. This finding fits with what has been seen in human studies, where a decline in GMV has been seen to occur across adolescence and early adulthood (Bartzokis *et al.* 2001; Lebel *et al.* 2012, Bethlehem *et al.* 2022). This study therefore provides evidence for the translatability of macaque MRI studies, and gives further strength to rhesus macaques as models of healthy human ageing (Phillips *et al.* 2014; Roefsema and Treue 2014; Stonebarger *et al.* 2021).

It should be noted that this study only utilised male subjects, as scans were only available from very few females, meaning it would not have been possible to control for sex. As a consequence of this, the results of this analysis cannot be fully generalised to female rhesus macaques. It is known that female rhesus macaques sexually mature earlier than male macaques, however developmental trajectories have been seen to be similar (Knickmeyer *et al.* 2010). Additionally, human studies have found sex-differences with ageing to be minimal (Podgórski *et al.* 2021; Cui *et al.* 2023). As such, though it is possible that there are sex-differences in the brain ageing of rhesus macaques, this is potentially unlikely.

The impacts of ageing on average cortical thickness were also investigated, but no significant change was identified. This is surprising given that a significant decrease in total grey matter volume was identified, as cortical thickness is thought to be a more sensitive measure for investigating the impacts of ageing (Borgeest *et al.* 2021- preprint; Podgórski *et al.* 2021). However, this lack of a significant change is in line with the results of a previous macaque study of the impacts of ageing on cortical thickness, which did then go on to identify significant regional changes (Koo *et al.* 2012). The lack of a significant change in average cortical thickness could imply that regional changes in cortical thickness, during the age range investigated, may include both significant increases and decreases. Although, the lack of a significant result may also be due to limitations with the sample utilised, and it may be possible to identify significant age-related changes in total cortical thickness with a larger sample size.

3.5.4 Conclusion

AutoMacq offers a processing pipeline for rhesus macaque MRI data that is easy to use and can be completed without expert knowledge of macaque neuroanatomy. AutoMacq can process both cross-sectional and longitudinal data, with a wide range of quality and parameters, from across different sites and scanners, with a high level of success. The pipeline is unique amongst macaque processing pipelines in its ability to generate both surface-based and voxel-based metrics, offering two ways to exploit macaque MRI scans and allowing for easier comparison to a wider range of previous research.

3.6 Supplementary Materials

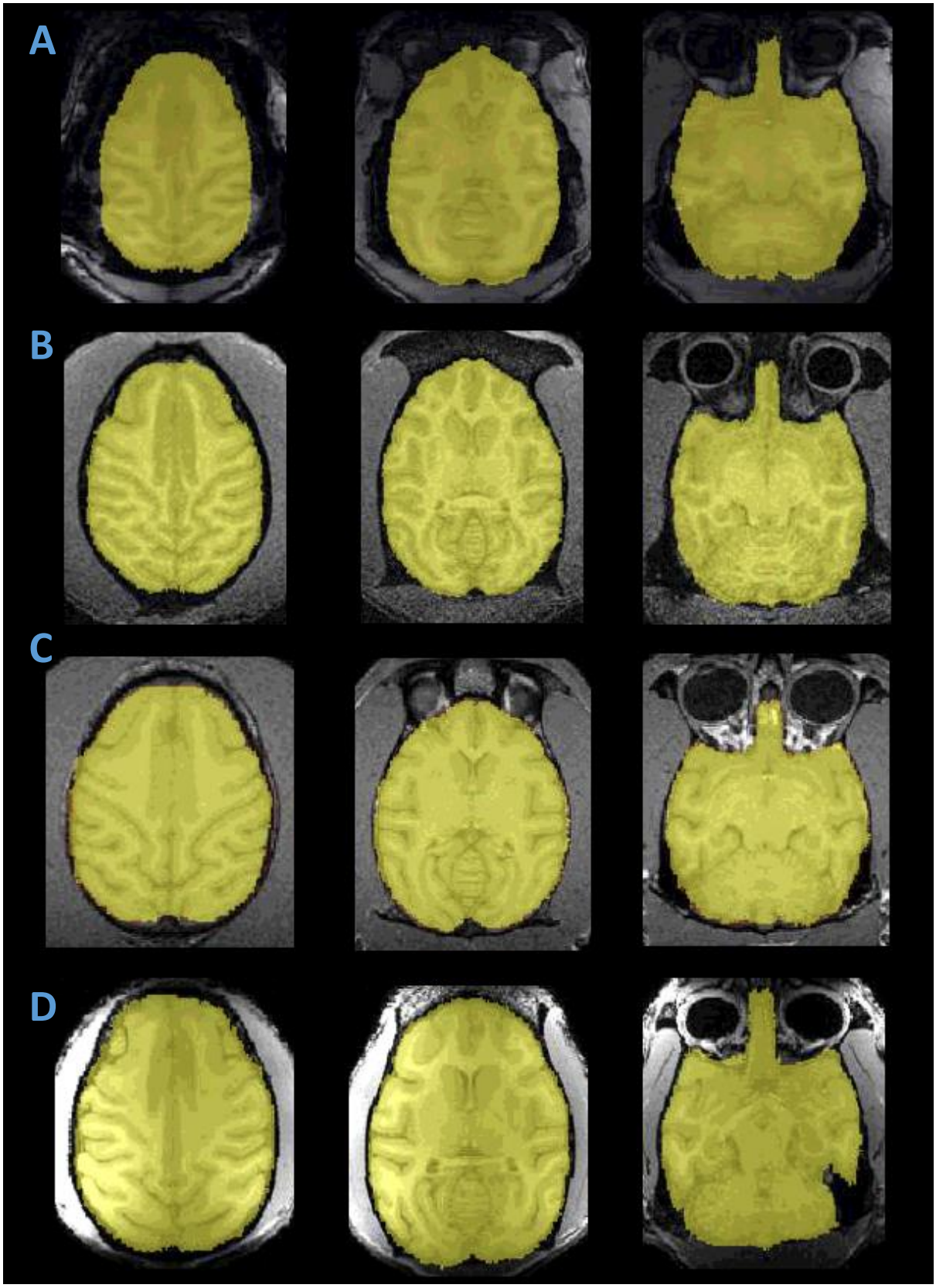

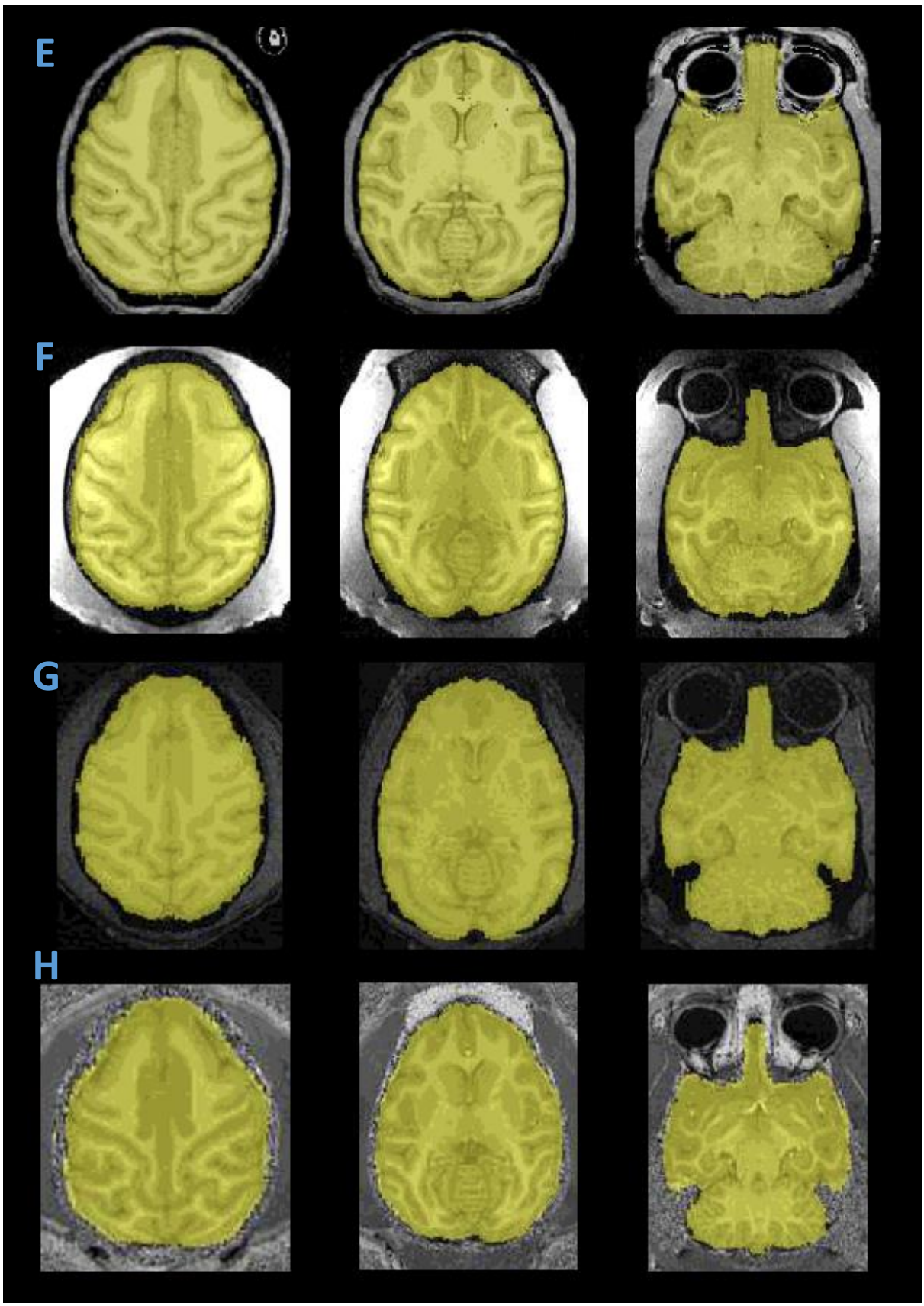

Supplementary Figure 2: Representative Brainmasks Produced by AutoMacq. Masks for one subject from each site are illustrated. A: Newcastle, B: DPZ, C: NIDA, D: Oxford, E: MSP, F: MSS, G: SBRI, H: UWO.

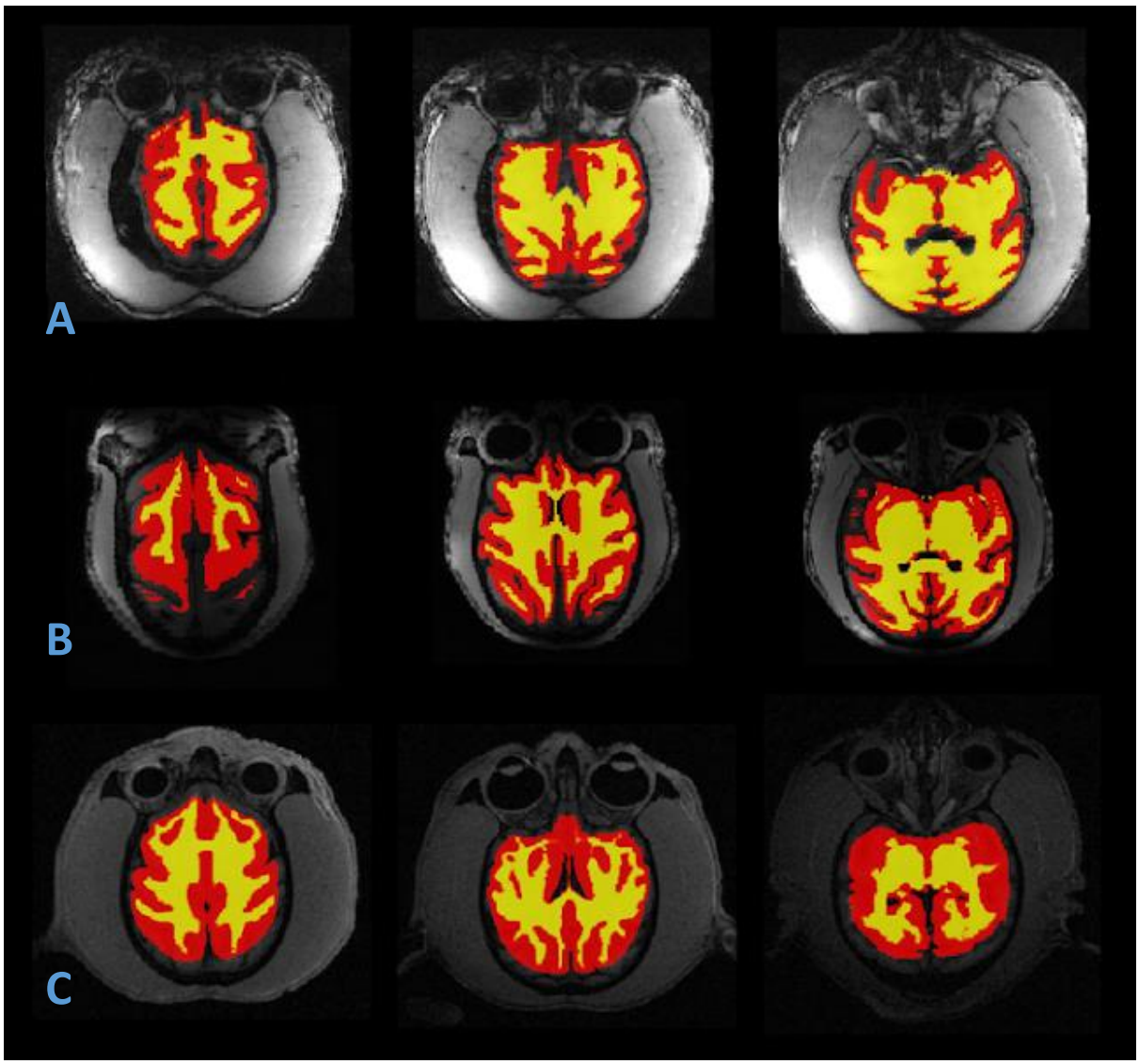

Supplementary Figure 3: Problematic Tissue Volumes Produced by AutoMacq. A: subject from the Newcastle dataset, B: subject from the Oxford dataset, C: subject is from the DPZ dataset.

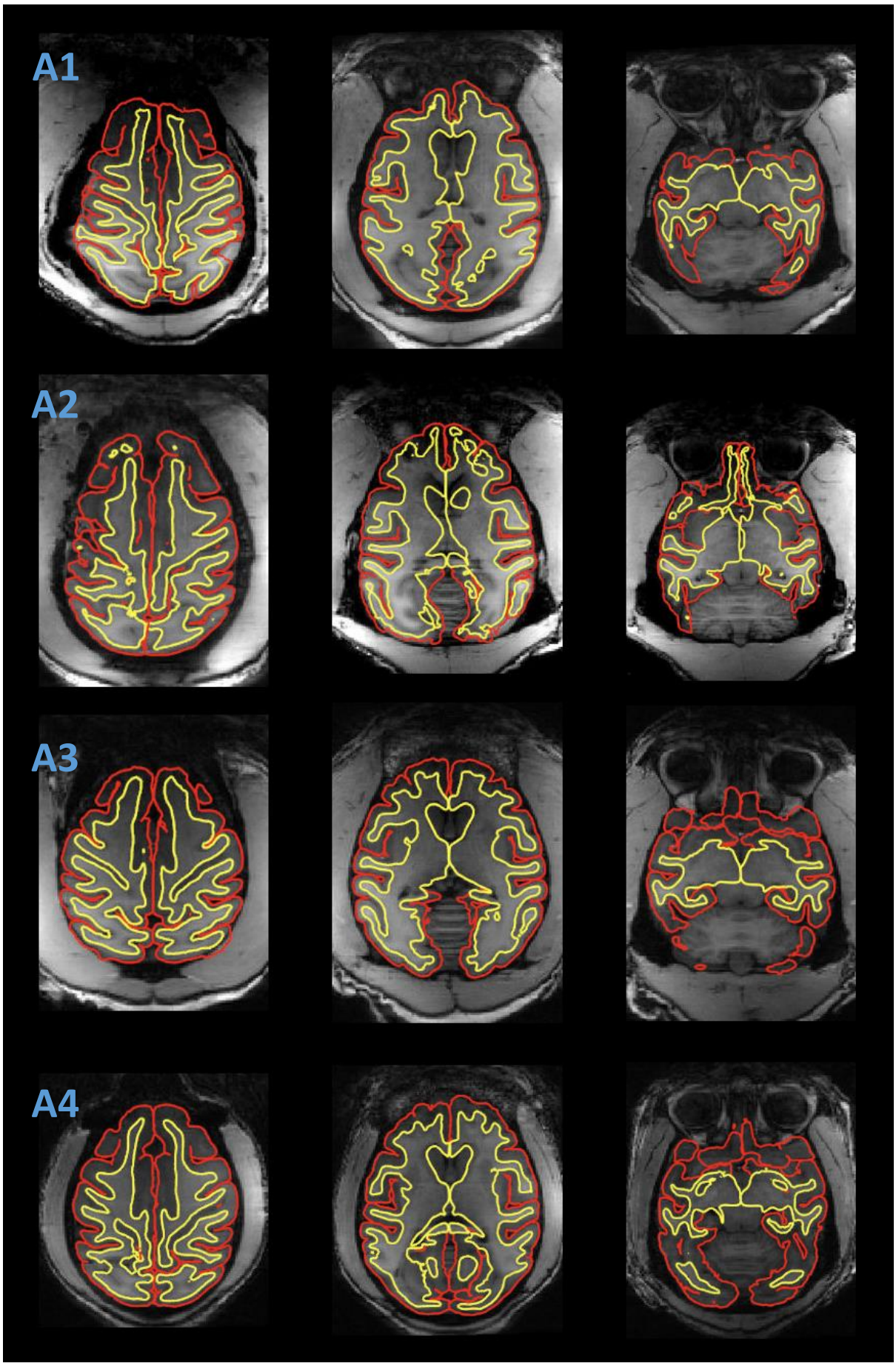
A1
A2
A3
A4

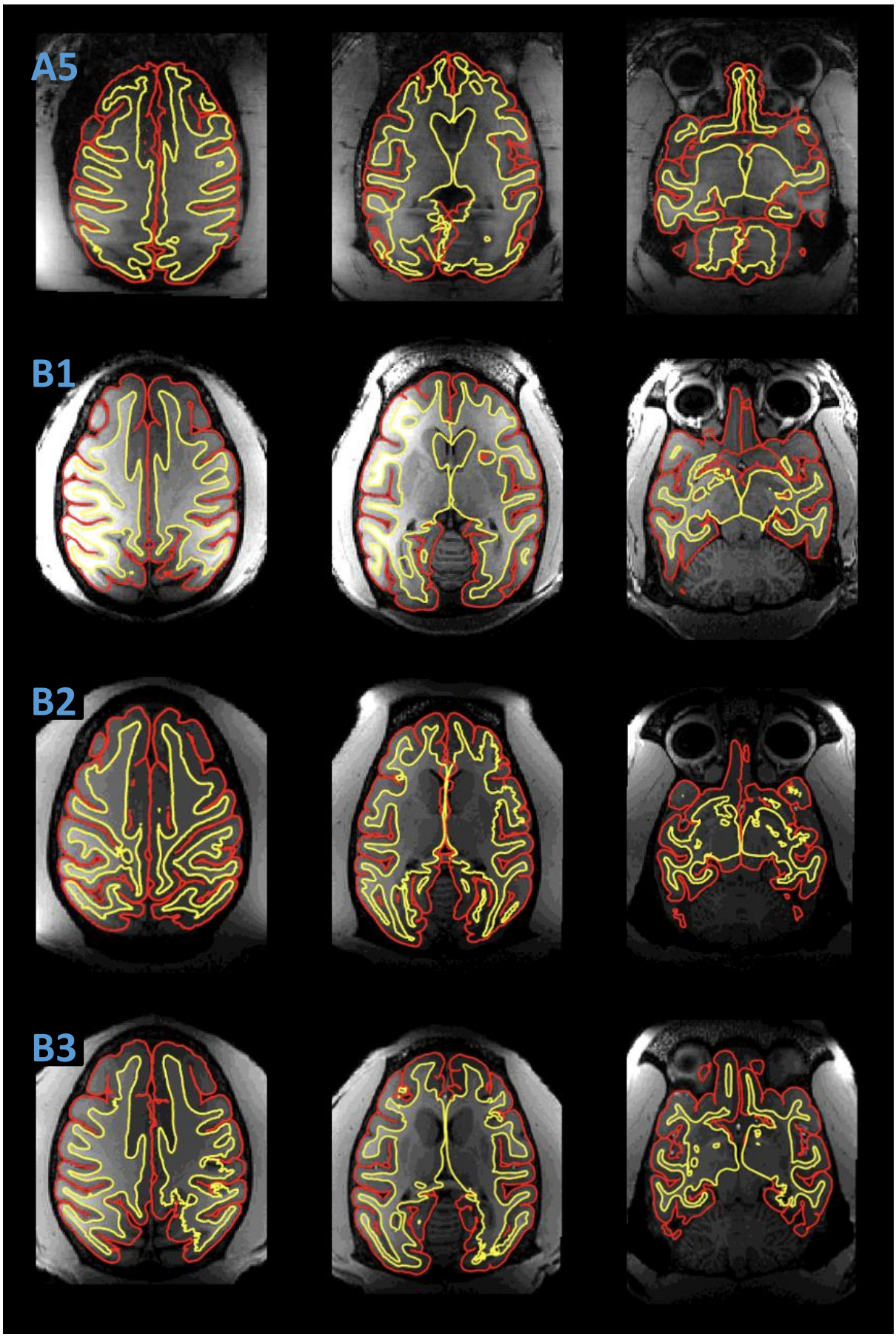
A5
B1
B2
B3

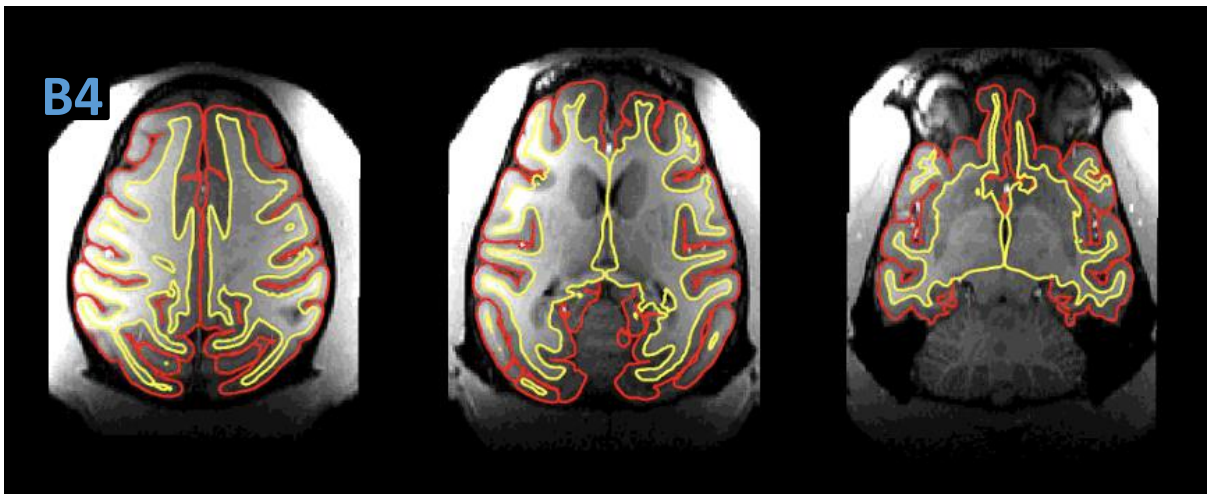

Supplementary Figure 4: Subjects with Problematic Surfaces Produced by AutoMacq. 5 subjects are from the Newcastle dataset (A) and 4 subjects are from the Oxford dataset (B).

Chapter 4: Voxel Based Morphometry Study of the Impacts of Ageing on Brain Structure

4.1 Abstract

The impacts of ageing on grey matter volume in primates during early to mid-adulthood are relatively unknown, with some cross-sectional studies in humans and no studies of this life period in macaques. As such, the current study investigated the impacts of ageing on grey matter volume in rhesus macaques, during early to mid-adulthood, using both a cross-sectional and a longitudinal approach. This investigation was done using cross-sectional data from 63 subjects, taken from across 7 sites, and longitudinal data from 16 subjects, taken from across 3 sites. No significant results were found for the cross-sectional analysis, with this likely being partially explained by the limited sample size. However, the longitudinal analysis detected several regions with significant decreases in grey matter volume with ageing. These decreases occurred between the ages of 5 and 15 and were located primarily in the temporal lobe. Additional significant clusters were identified in the frontal and parietal lobes, as well as in the cerebellum. These findings are novel in that they longitudinally cover early to mid-adulthood in macaques, highlighting that age-related decreases in grey matter volume occur prior to old age. The regions identified as showing decreased grey matter volume in this study broadly correspond to the findings of previous cross-sectional studies of both older macaques and humans. Overall, these results indicate that age-related decreases in grey matter volume occur during early to mid-adulthood in rhesus macaques, with the temporal lobe potentially showing the most extensive, early volumetric decreases with ageing.

4.2 Introduction

Previous human MRI studies have consistently shown decreases in global grey matter volume with ageing. Early studies identified this decrease as being linear (Bartzokis *et al.* 2001, Good *et al.* 2001, Taki *et al.* 2004) but later studies have determined it is more likely to be non-linear (Lebel *et al.* 2012, Mills *et al.* 2016, Vinke *et al.* 2018). Consequently, global grey matter volume is thought to increase in humans during development, then decrease over the rest of the life course, with the relative rate of decline increasing in very old age. However, the exact trajectory of the

age effect is known to vary across regions, and there is generally less agreement amongst voxel-based morphometry studies on when specific regions begin to lose grey matter, as well as the rate of this loss.

A number of previous VBM studies have found that older adults particularly exhibit declines in grey matter volume within the frontal lobe (Good *et al.* 2001, Tisserand *et al.* 2004, Smith *et al.* 2007, Hutton *et al.* 2009, Peelle *et al.* 2012, Farokhian *et al.* 2017; Ramanöel *et al.* 2018). This is often accompanied by decreased grey matter volume in areas of the temporal lobe (Good *et al.* 2001; Tisserand *et al.* 2004, Smith *et al.* 2007, Hutton *et al.* 2009, Peelle *et al.* 2012; Ramanöel *et al.* 2018), though Farokhian *et al.* (2017) did not identify significant age-related decreases in temporal regions. Lower grey matter volume in regions of the parietal lobe have also been reported, though to a lesser extent than both frontal and temporal decreases (Good *et al.* 2001, Smith *et al.* 2007; Ramanöel *et al.* 2018). However, decreases in grey matter volume within the occipital lobe of older adults are even more rarely reported (Tisserand *et al.* 2004; Ramanöel *et al.* 2018), with studies often finding occipital regions to be preserved even in very late adulthood (Farokhian *et al.* 2017). Other regions that have been cited as showing declines in grey matter volume in late adulthood include the insula (Good *et al.* 2001, Hutton *et al.* 2009, Peelle *et al.* 2012, Farokhian *et al.* 2017), the cerebellum (Good *et al.* 2001, Smith *et al.* 2007; Ramanöel *et al.* 2018) and the basal ganglia (Smith *et al.* 2007).

However, ageing effects are known to be greatly influenced by environmental factors, which can be very difficult to control for in human studies, particularly those using a cross-sectional design. The influence of these factors can be reduced by utilising an animal model, as they spend their lives in a highly controlled environment. As was previously discussed, rhesus macaques are particularly useful animal models for studies of the ageing brain due to their comparable life course and neuroanatomy, as well as their accelerated rate of ageing compared to humans (Phillips *et al.* 2014; Roefsema and Treue 2014; Mattison and Vaughan 2017; Stonebarger *et al.* 2021). Additionally, with human studies of ageing it is not possible to control for the fact some subjects may be presymptomatic for age-related neurodegenerative disorders, and therefore are not representative of ‘healthy’ ageing. As rhesus macaques do not develop neurodegenerative disorders, this issue is circumvented by their use as an animal model (Peters and Kemper 2012; Arnsten *et al.* 2019).

Though the impacts of ageing on the macaque brain have been previously studied, there is generally less consensus in terms of the results of these studies than is seen with human research. This lack of consensus is likely the result of brain ageing being less researched in macaques than it is in humans, which is at least somewhat due to the difficulties in processing macaque MRI data (which have been previously discussed in sections 1.3.1 and 3.2). Previous MRI studies of rhesus macaques have found a decrease in total grey matter volume with ageing, but these studies utilised a cross-sectional, manual tracing design to compare young macaques to very old macaques (Andersen *et al.* 1999, Wisco *et al.* 2008). As such, they are not truly capturing ageing effects by just contrasting the brains of old and young macaques, and the subjective nature of the manual tracing design, as well as the cross-sectional approach more generally, may introduce bias.

Though there are particularly few voxel-based morphometry studies of brain ageing in macaques, the studies that do use this methodology have identified broadly similar results to human studies. Alexander *et al.* (2008) cross-sectionally compared the brains of “young” (aged 8-12 years) and “old” (aged 20-28 years) macaques, and found the older macaques showed decreased grey matter volume in regions of the frontal and temporal lobes. Grey matter volume decreases in similar regions were identified with ageing in another group of old macaques (age 19-31) by Colman *et al.* (2009). A more recent cross-sectional macaque study which investigated volumetric changes (though not with voxel-based morphometry), using macaques between the ages of 6 and 31, found that older macaques displayed decreased grey matter volume in the frontal cortex, as well as subcortical regions such as the caudate, putamen, hypothalamus and thalamus. However, they also identified unexpected increases in grey matter volume for older macaques in the hippocampus, amygdala and globus pallidus (Dash *et al.* 2023). As Dash *et al.* (2023) did not utilise voxel-based morphometry it is unclear if the differences between their findings and those of other macaque studies (Alexander *et al.* 2008; Colman *et al.* 2009) are due to methodological differences, such as differences in sensitivity or error-rate.

Crucially the majority of previous studies of age-related changes (in both humans and macaques) focus on either development and adolescence or late adulthood. Relatively few human voxel-based morphometry studies have focused on the period of time in between adolescence and late adulthood, and those which have

utilised a cross-sectional design (Bourisly *et al.* 2015; Su *et al.* 2021). There appear to be no previous voxel-based studies of ageing effects during this life period in macaques. Due to this, ageing trajectories during early to mid-adulthood are even less agreed upon than those in later life. This study therefore aimed to use a VBM approach in order to investigate changes in grey matter volume across early to mid-adulthood in rhesus macaques.

Furthermore, as aforementioned, the vast majority of previous VBM studies of ageing use a cross-sectional approach, likely due to the difficulties associated with longitudinal research (see chapter 1, section 1.4.3). This means that the results may be confounded by both genetic differences between subjects and biases such as the cohort effect, making it unclear which results from these previous studies are 'true' age effects. A longitudinal approach mitigates the impact of these factors, which should allow for clearer identification of 'true' age effects. In fact, Di Biase *et al.* (2023) recently provided evidence for cross-sectional MRI studies underestimating age-related changes when compared with longitudinal analyses. Therefore, a further aim of this study was to carry out both a cross-sectional and a longitudinal approach, in order to compare and contrast the results and better identify which results from previous studies were likely to be 'true' age effects.

4.3 Methods and Materials

4.3.1 Datasets and inclusion criteria

Visual quality control was first carried out, and any scans with artifacts, poor contrast or hyperintensities were excluded. To be included in either the cross-sectional or longitudinal dataset subjects needed to be at least 5 years old, and no older than 16, at the time of scanning, so that the sample would be restricted to early to mid-adulthood. Additionally, for the cross-sectional dataset, sites with less than 3 subjects passing quality control and meeting the age criterion were excluded so that site could be controlled for in the model. Scans from an individual site needed to cover at least 18 months, otherwise the site was excluded due to a lack of age variability. The complete cross-sectional dataset consisted of 55 scans, taken from across 5 sites (see table 6). The DPZ site was further divided into 3 different

scanners for the statistical analyses. 44 out of the 55 subjects included were male, and T2 data was available for 26 of the 55 subjects.

To be included in the longitudinal dataset subjects needed to have at least 3 scans, that covered a minimum of 18 months, with 3 or more months between consecutive scans (the rescan data for the Newcastle subjects, discussed in sections 2.1.2 and 3.4.4, was therefore excluded). The longitudinal dataset subsequently consisted of scans from 16 subjects (14 of which were male) from across 3 sites (table 6). T2 data was available for 10 out of the 16 subjects. The number of scans acquired varied by subject, with the minimum number of scans being 3 and the maximum being 13. The total number of included scans in the full longitudinal sample was 96. Subjects from the Newcastle dataset tended to have more scans than subjects from DPZ and NIDA.

Dataset	**Site**	**Included Subjects (M/F)**	**Age Range (in years)**	**Subjects with T2 data**	**Awake vs. Anaes**	**Scanner Strength**
C	Newcastle	18 (12/6)	6-15	18	Awake	4.7T
C	DPZ	20 (20/0)	6-11	5	Anaes.	3T
C	NIDA	6 (6/0)	7-10	0	Anaes.	3T
C	Oxford	8 (5/3)	5-8	0	Anaes.	3T
C	SBRI	3 (1/2)	7-14	3	Anaes.	3T
C	*Total*	*55 (44/11)*	*5-15*	*26*		
L	Newcastle	10 (8/2)	6-15	10	Awake	4.7T
L	DPZ	1 (1/0)	6-8	0	Anaes.	3T
L	NIDA	5 (5/0)	6-10	0	Anaes.	3T
L	*Total*	*16 (14/2)*	*6-15*	*10*		

Table 6: Description of Subjects Included in the Ageing Analyses.
C: cross-sectional and L: longitudinal. M: Male and F: Female. Anaes.: anaesthetised.

4.3.2 Statistical analyses

Statistics were carried out in SPM12. The total grey matter volume and the local amount of grey matter in each voxel was utilised as input data. For the voxel-based approach, data was smoothed using a 1mm kernel prior to statistical analysis. A two-step approach was utilised for both the cross-sectional data and the longitudinal data, in order to allow for the modelling of a random slope (and random intercept) for each scanner/subject. For the cross-sectional data, the slope of the ageing effect for each *scanner* was first calculated using a multiple-linear regression, with total intracranial volume (TIV) included as a fixed effect (the statistical model utilised was GMV= β1*age + β2*TIV + constant). TIV was included in the model to control for inter-individual differences in head size. A 1-sample T test was then utilised in order to determine whether the mean slope at the group level was significantly different from 0. Significance was thresholded at 0.001 (uncorrected) at the voxel-level, and 0.05 (corrected for multiple comparisons with family wise error [FWE]) at the cluster-level.

For the longitudinal data, the slope of the ageing effect for each *subject* was first calculated, for total GMV and in each voxel, using a simple linear regression (the statistical model utilised was GMV= β1*Age + constant). As with the cross-sectional approach, it was then determined whether the mean slope at the group level was significantly different from 0 using a 1-sample T test. TIV was not included in the model for the longitudinal approach, as intra-individually TIV is fairly constant during the life period investigated and therefore does not need to be controlled for. Significance was thresholded at 0.001 (uncorrected) at the voxel-level, and 0.05 (corrected for multiple comparisons with FWE) at the cluster-level. Due to both cross-sectional and longitudinal scans being available for very few female macaques, statistics were carried out both including and excluding the female subjects. Due to the age range covered it was assumed that linear effects would be observed, however non-linear effects were also tested for posteriorly in significant clusters.

4.4 Results

4.4.1 Longitudinal approach

The impacts of ageing on total grey matter volume were first investigated using the full longitudinal dataset. A significant decrease in total grey matter volume with increasing age was identified (DF= 15, p= 0.0059, figure 15).

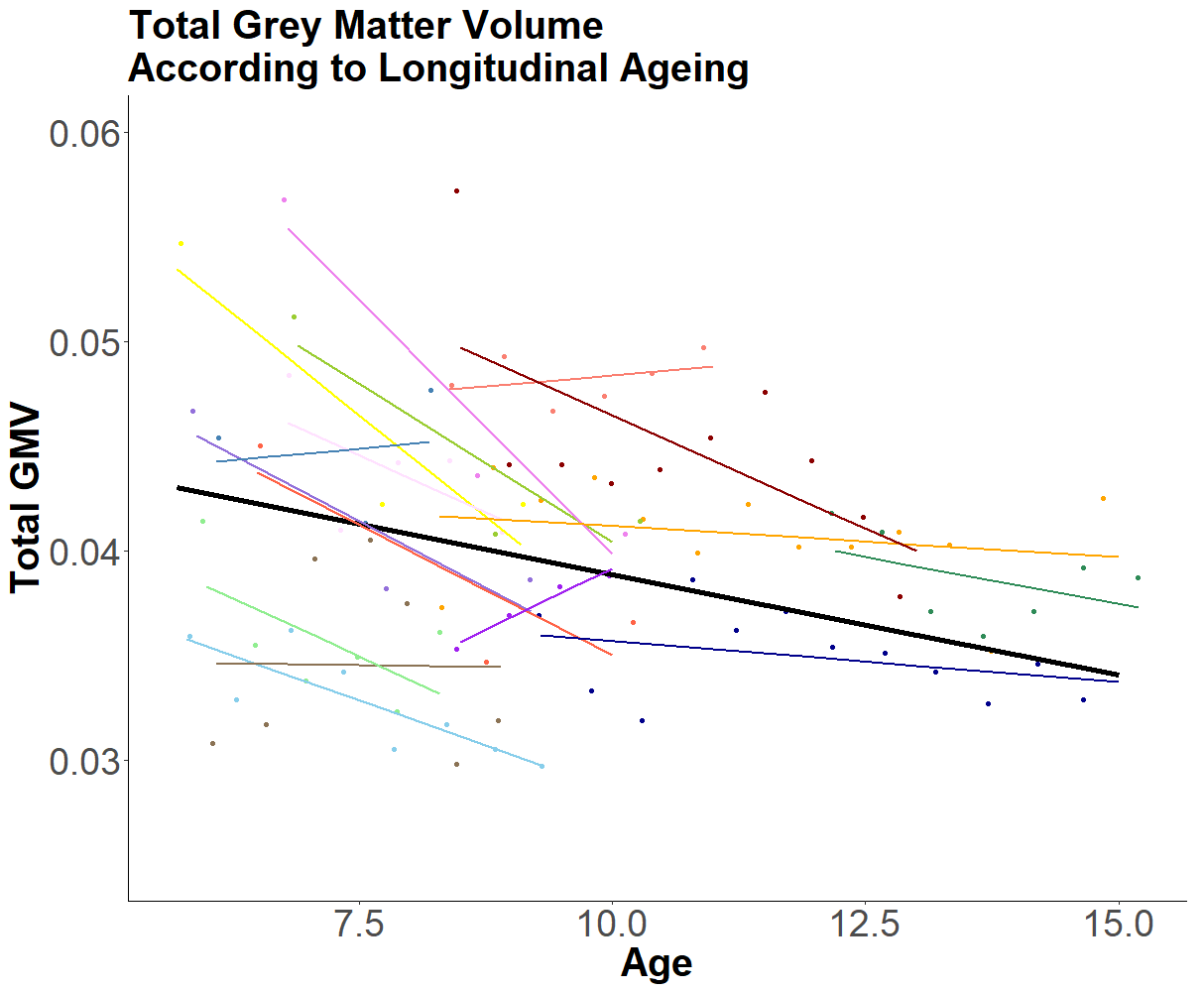

Figure 15: Changes in Total GM Volume According to Longitudinal Ageing. The bold black linear line corresponds to the main effect of age, while controlling for TIV and with subject declared as a random effect. The thin coloured lines correspond to linear fits of the age effect for each subject while controlling for TIV. Dots correspond to raw data (unadjusted for TIV).

The regional longitudinal approach identified a number of brain regions which showed significant grey matter volume decreases with ageing (see table 7). Results

were similar regardless of whether the female subjects were included in or excluded from the sample. As such, the results for the complete sample are presented and discussed below.

Region	Hemisphere	Peak Coordinates	$P_{FWE-corr}$	T
Superior temporal sulcus (dorsal bank)	Right	23.0, 15.5, 5.0	<0.001	9.39
Superior temporal sulcus (dorsal bank)	Left	-20.0, 15.0, 5.5	0.017	4.87
Rostrotemporal region (polar part)	Right	22.0, 24.5, 8.0	<0.001	7.86
Temporal pole	Left	-14.5, 25.5, -3.0	0.014	6.71
Cortical areas 44 and 45	Left	-21.0, 30.5, 17.0	<0.001	6.59
Precentral opercular area	Left	-21.0, 27.0, 11.0	0.021	5.86
Cerebellum	Right	15.0, -8.0, 6.5	0.009	6.55

Table 7: Significant GMV Decreases with Ageing.
Peak Coordinates: Coordinates of the voxel with the highest T value; $P_{FWE-corr}$: Family-wise error corrected probability; T: t statistic.

First of all, there was a significant, bilateral, age-related decrease in the grey matter volume of the superior temporal sulcus, which was specifically localised to the dorsal bank (see figures 16a+b). This was accompanied by a significant cluster in the right superior rostrotemporal region, localised to the polar part (see figures 16c). A final significant cluster in the temporal lobe was localised to the temporal pole of the left hemisphere (see figures 16d). Figure 17 provides plots for the change in grey volume with ageing for each of the 4 significant temporal lobe clusters.

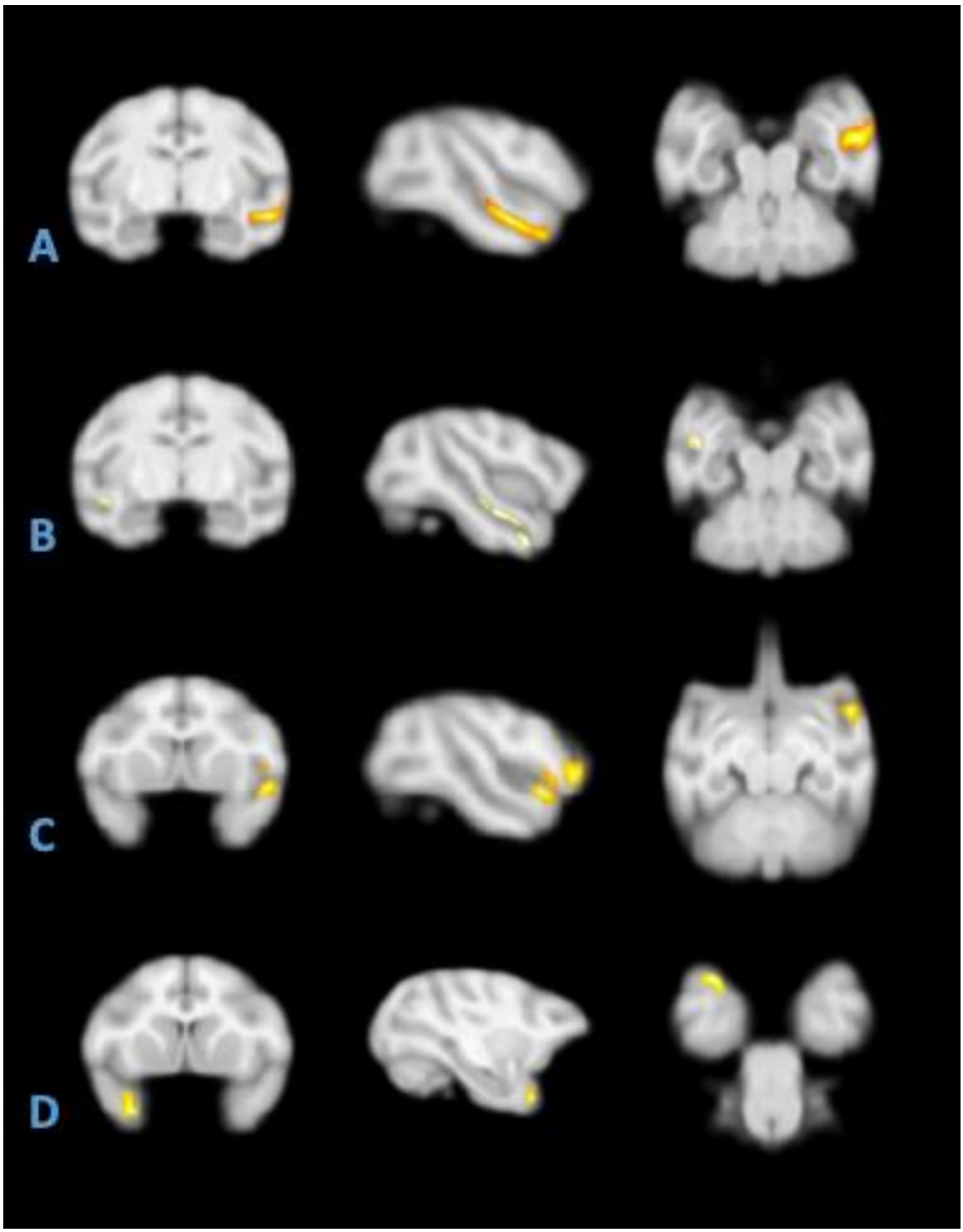

Figure 16: Clusters in the Temporal Lobe Showing a Significant Age-related Decrease in Grey Matter Volume. A: right superior temporal sulcus (dorsal bank), B: left superior temporal sulcus (dorsal bank), C: rostrotemporal region (polar part), D: left temporal pole.

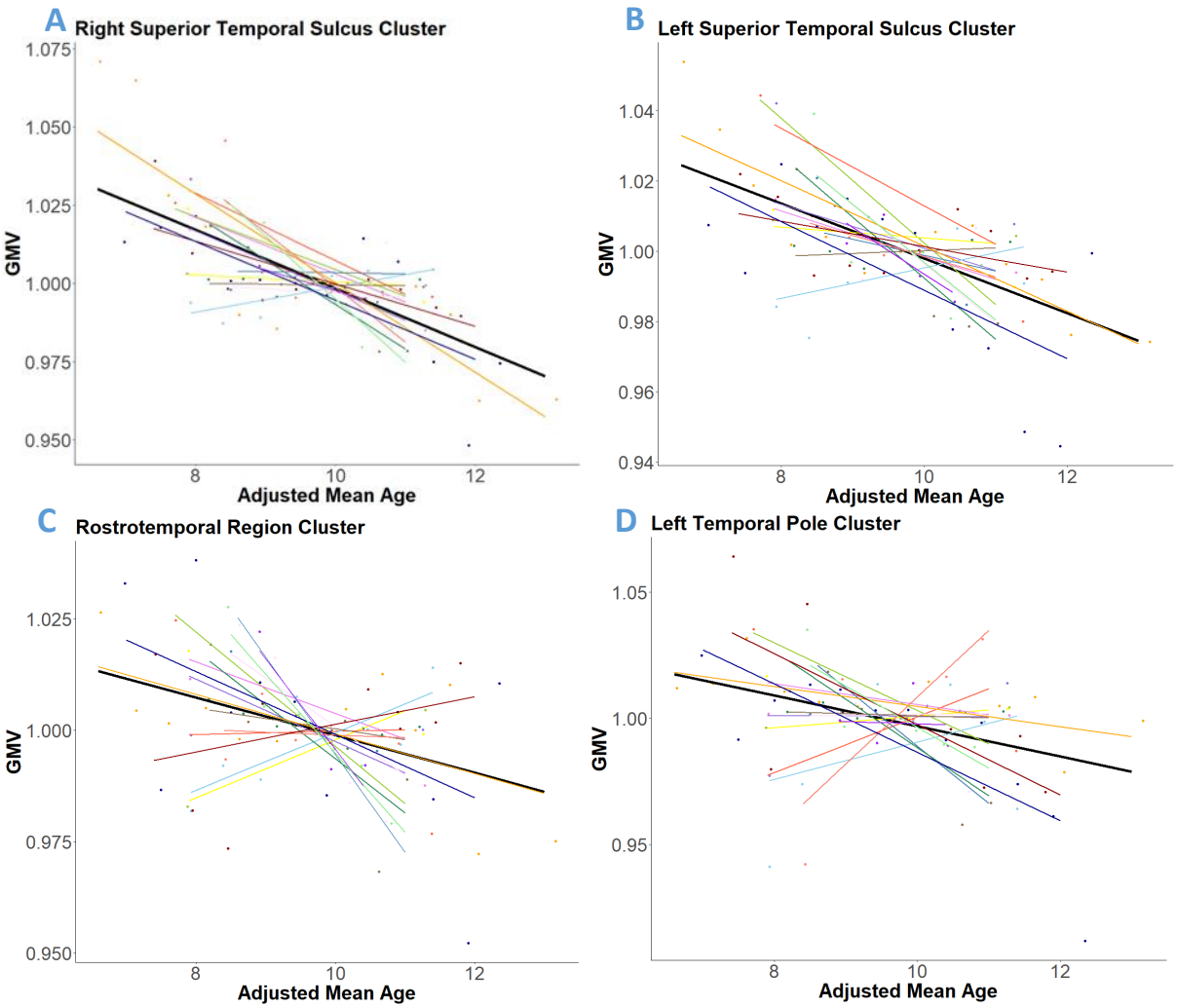

Figure 17: Changes in GM Volume Within Significant Temporal Lobe Clusters According to Ageing. The bold black linear line corresponds to the main effect of age at the group level. The thin coloured lines correspond to linear fits of age effect in each subject. Dots correspond to raw data. A: right superior temporal sulcus (dorsal bank), B: left superior temporal sulcus (dorsal bank), C: rostrotemporal region (polar part), D: left temporal pole.

Two significant clusters in the left frontal lobe also showed a decrease in GMV with ageing. The first of these clusters was localised to cortical areas 44 and 45 (see figures 18a), and the second was localised to the precentral opercular area (see figure 18b). Figure 19 provides plots for the change in grey volume with ageing for both of the significant frontal lobe clusters. Finally, a cluster in the right side of the cerebellum (see figures 20) also showed a significant decrease in GMV with ageing. Figure 21 plots the change in grey matter volume with ageing for this cluster within the cerebellum.

There were no regions showing significant increases in GMV with ageing, though a cluster in visual area 1 (V1; -12.5, -5.5, 19.0) did trend towards significance

(p=0.086, T=5.75; see figure 22). Figure 23 plots the increase in GMV with ageing for this cluster.

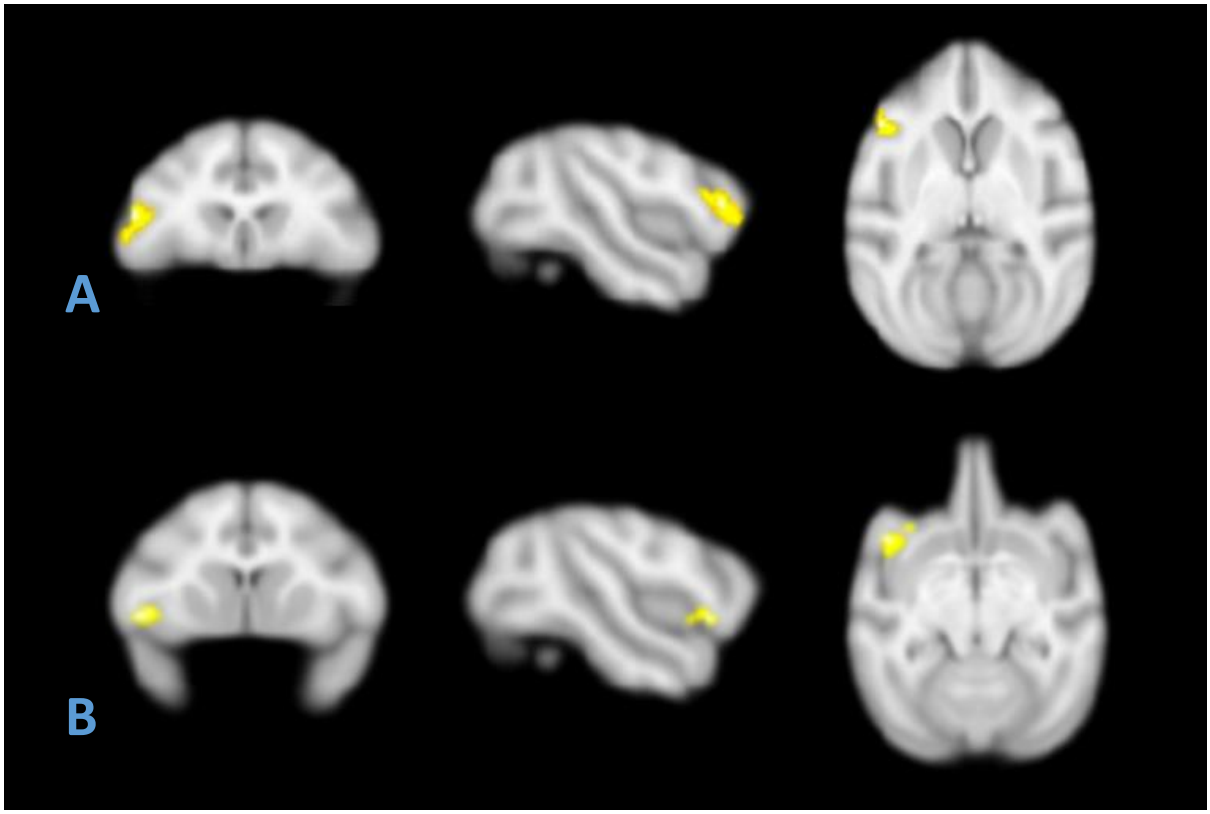

Figure 18: Clusters in the Frontal Lobe Showing a Significant Age-related Decrease in Grey Matter Volume. A: Cortex areas 44 and 45 in the left hemisphere, B: Precentral opercular area.

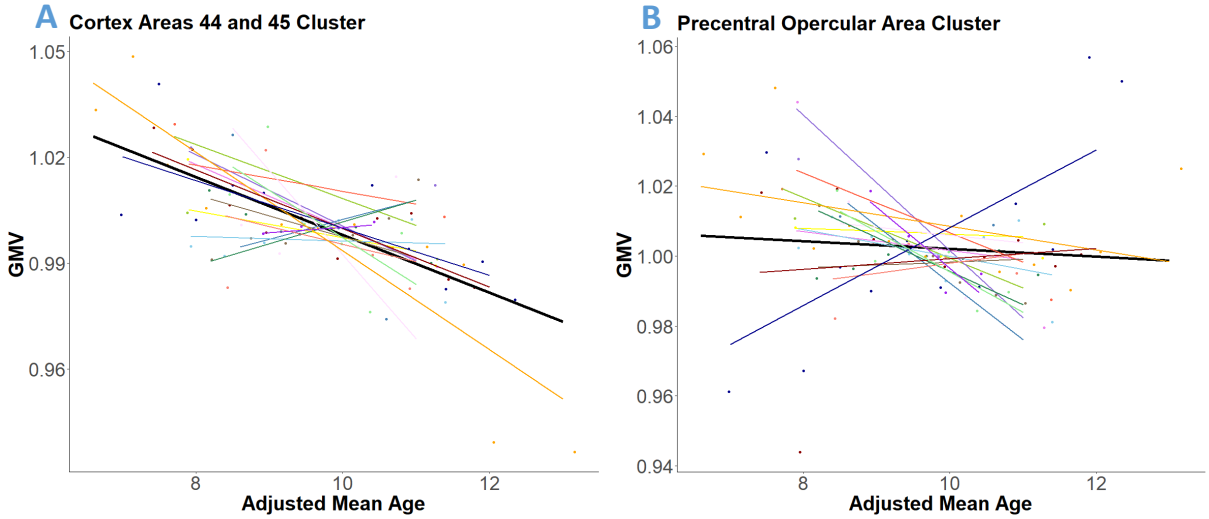

Figure 19: Changes in GM Volume Within Significant Frontal Lobe Clusters According to Ageing. The bold black linear line corresponds to the main effect of age at the group level. The thin coloured lines correspond to linear fits of age effect in each subject. Dots correspond to raw data. A: Cortex areas 44 and 45 in the left hemisphere, B: Precentral opercular area.

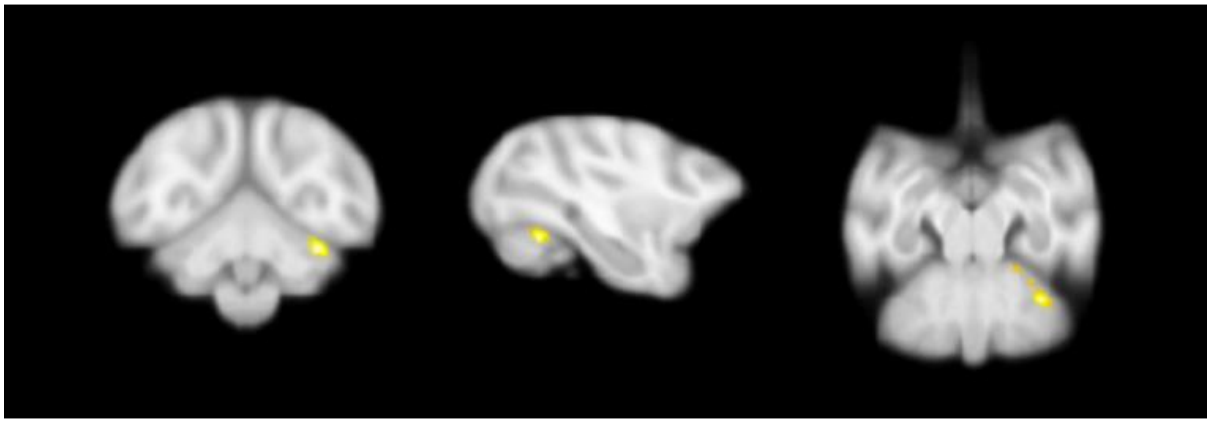

Figure 20: Cluster in the Cerebellum Showing a Significant Age-related Decrease in Grey Matter Volume. Cluster localised to the right cerebellum.

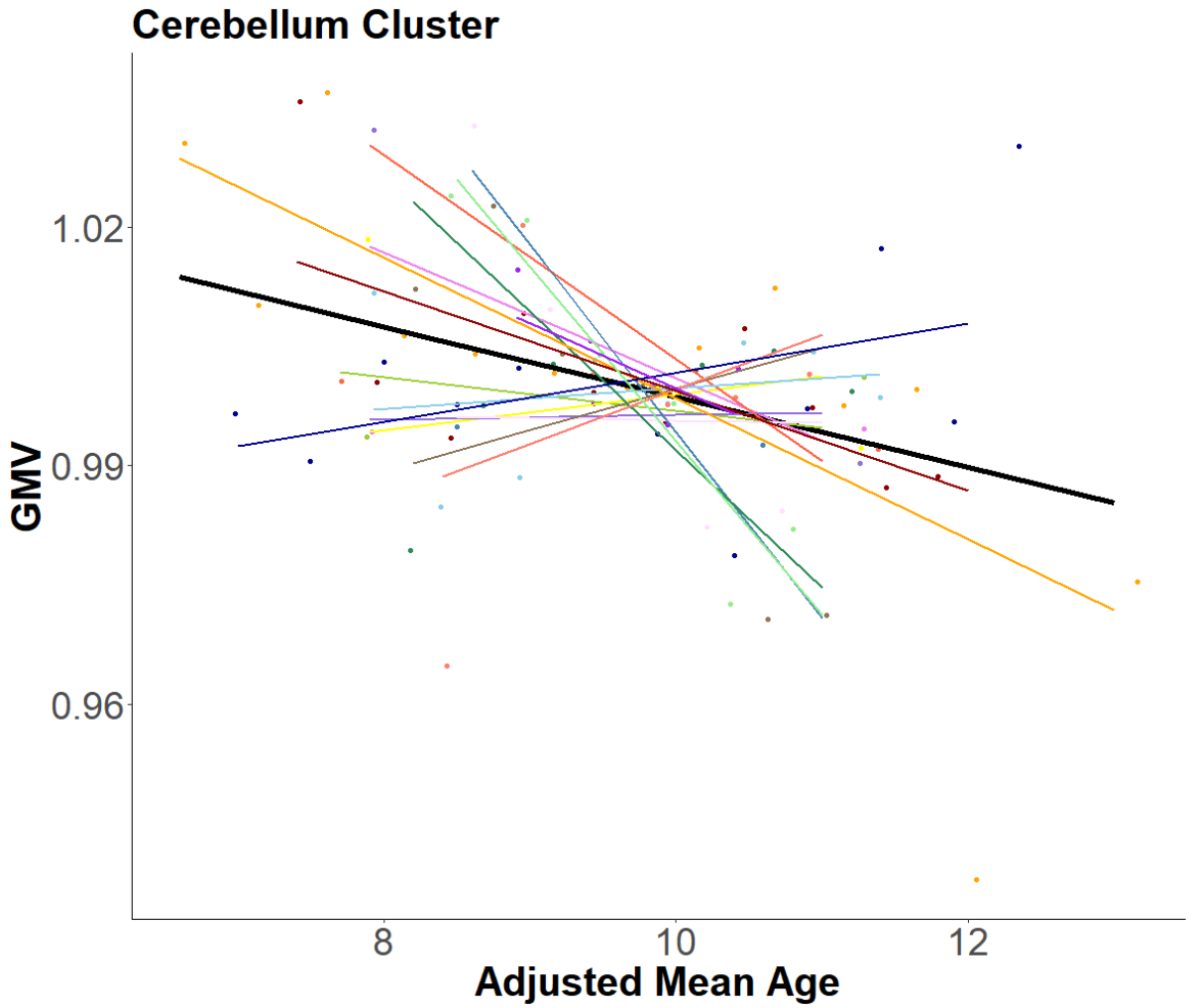

Figure 21: Changes in GM Volume Within the Significant Cerebellum Cluster According to Ageing. The bold black linear line corresponds to the main effect of age at the group level. The thin coloured lines correspond to linear fits of age effect in each subject. Dots correspond to raw data.

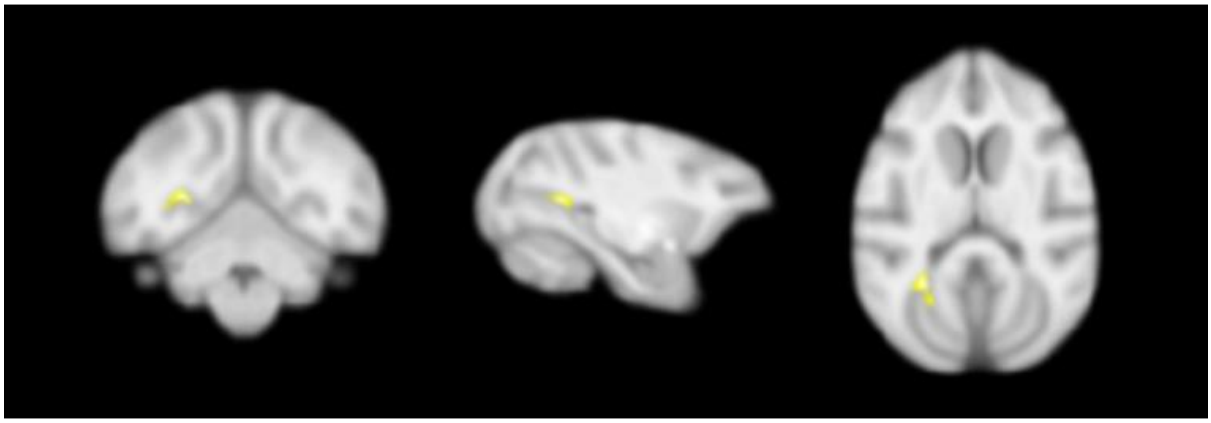

Figure 22: Cluster in the Occipital Lobe that Trended Towards a Significant Age-related Increase in Grey Matter Volume. Localised to visual area 1, within the left hemisphere.

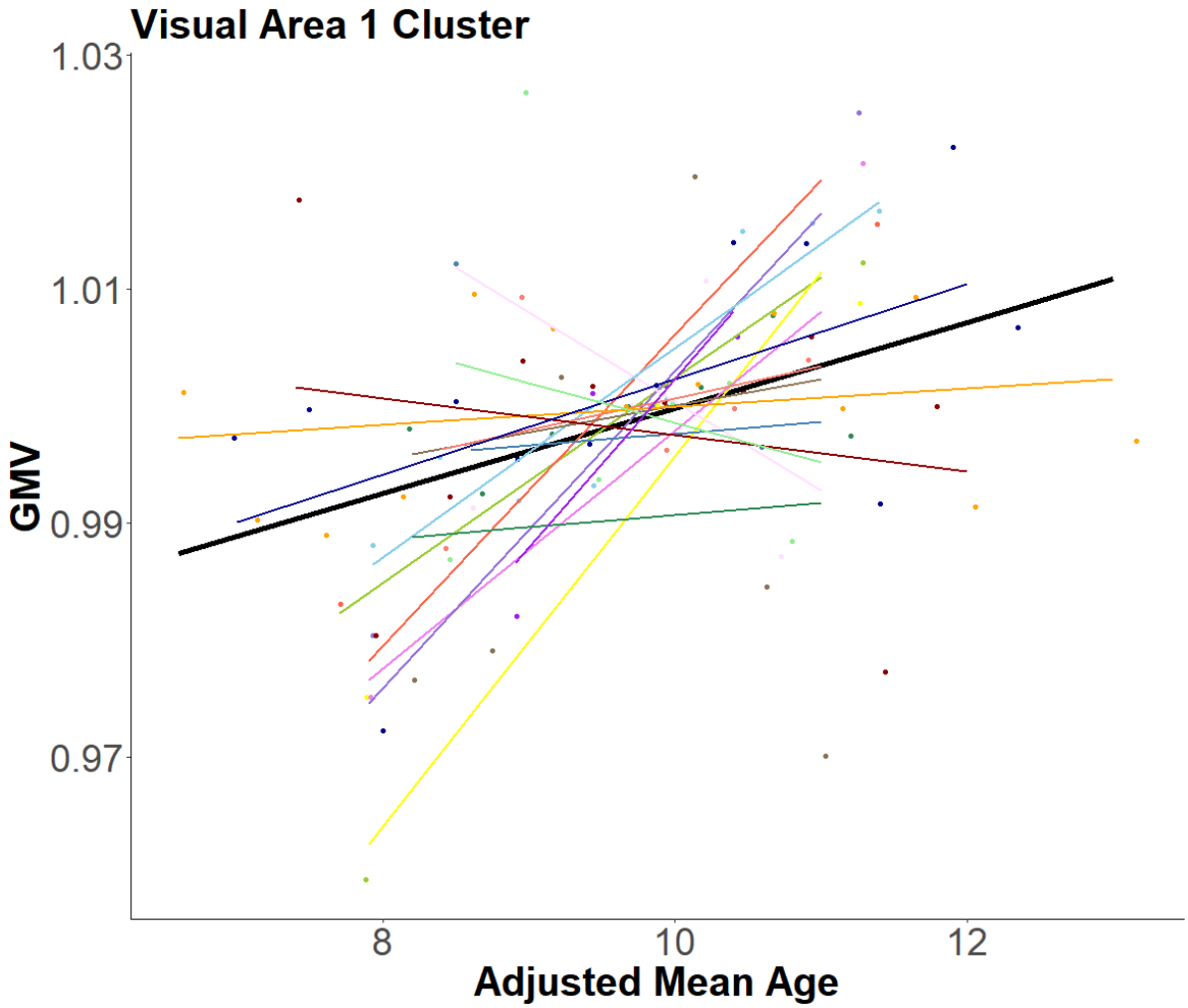

Figure 23: Changes in GM Volume Within the Occipital Lobe Cluster According to Ageing. The bold black linear line corresponds to the main effect of age at the group level. The thin coloured lines correspond to linear fits of age effect in each subject. Dots correspond to raw data.

For all of the discussed clusters, a non-linear analysis did not produce significant results, with the exception of the cluster localised to the precentral opercular area where the p value was 0.0325. If the number of clusters is corrected for with a Bonferoni correction though then this result would no longer be significant. However, this result does warrant further investigation with more data, as the decrease in grey matter volume for this cluster appears to accelerate with ageing.

4.4.2 Cross-sectional approach

A cross-sectional analysis of the impact of ageing on total grey matter volume was presented in chapter 3, section 3.4.6.

The regional cross-sectional approach did not produce any significant results for increases or decreases in grey matter volume with ageing. This was the case regardless of whether female subjects were included in or excluded from the sample. Excluding the SBRI data, as it was limited to scans from only 3 subjects, also produced no significant results.

A follow-up cross-sectional analysis was carried out restricted to the voxels found to be significant in the longitudinal analysis, however there were still no significant results.

Finally, a more liberal one-step statistical approach was carried out in which TIV and scanner were fixed effects (GMV= β1*age + β2*TIV + β3*Scanner + constant), but this was also unable to produce any significant results.

4.5 Discussion

For the purposes of this study the discussion below will be restricted to comparisons of the results to other studies that utilised a voxel-based morphometry approach. A broader discussion of the results of this project in the context of the wider literature will be carried out in the general discussion chapter (see chapter 8).

The results of the longitudinal approach of this study highlight age-related changes in grey matter volume that occur through early to mid-adulthood in rhesus macaques. To our knowledge this is the first study of its kind to identify age-related changes during this life period in rhesus macaques, and the first study in primates in general to investigate age-related changes during early to mid-adulthood using a longitudinal MRI approach. Identifying brain structural changes during early to mid-adulthood is of particular interest as the onset of age-related neurodegenerative

disorders, such as Alzheimer's Disease, can begin during (or, in some cases, prior to) mid-adulthood in humans (Edwards-Lee *et al.* 2005; Vo *et al.* 2020). Accordingly, the period just prior to this onset may be crucial for preventative measures and treatments, as by late adulthood the loss of grey matter may be too extensive. Even in subjects displaying 'healthy' ageing, targeting brain changes during early to mid-adulthood could be useful to slow the onset of age-associated cognitive decline.

In the current study, the strongest result using the longitudinal approach was found for a cluster in the dorsal bank of the superior temporal sulcus, within the right hemisphere. The corresponding cluster in the left hemisphere was also significant (though less strongly), indicating that this decrease in grey matter volume is bilateral. The superior temporal sulcus is involved in a variety of functions, including social cognition and working memory (Berman and Colby 2002; Deen *et al.* 2015). Previous studies have found that with ageing human subjects show a significant decline in both working memory and some aspects of social cognition, such as social perception (Verhaeghen *et al.* 2020; Grainger *et al.* 2023). Alexander *et al.* (2008) also identified a decrease in grey matter volume in the vicinity of the superior temporal sulcus in older macaques. Our results therefore expand this finding in that the decrease actually begins earlier than late adulthood. Additionally, multiple studies have found similar grey matter volume decreases in older humans (Tisserand *et al.* 2004; Smith *et al.* 2007; Hutton *et al.* 2009; Peelle *et al.* 2012; Ramanöel *et al.* 2018), so our results would suggest that these decreases may actually begin earlier in humans as well.

An additional temporal lobe cluster showing a significant age-related decrease in grey matter volume was identified in the polar part of the right rostrotemporal region. The rostrotemporal polar region appears to be part of the auditory cortex, and therefore plays a role in auditory processing (Scott *et al.* 2017). Age-related declines in auditory processing have been previously identified in older humans, and hearing loss is very common during late-adulthood (Murphy *et al.* 2018; Sharma, Lalwani and Golub 2020). Age-related changes specifically in the functionality of the auditory cortex have also been highlighted by human studies (Lalwani *et al.* 2019; Erb, Schmitt and Obleser 2020). However, the current study did not identify significant decreases in grey matter volume in either the primary or secondary auditory cortex, which would be the areas expected to be implicated in hearing loss. It is therefore

unclear why the grey matter decreases of the auditory cortex observed in the current study appear to be limited to the rostrotemporal region.

There was one final significant decrease in grey matter associated with ageing within the temporal lobe, localised to a cluster in the left temporal pole. This region is known to be involved in semantic and episodic memory, with Setton *et al.* (2022) previously identifying that lower grey matter volume in this region for older humans appears to be associated with the age-related memory issues seen in previous human studies (Korkki *et al.* 2020; Verhaeghen *et al.* 2020). Decreases in grey matter volume specifically within the temporal pole have been previously reported in older macaques by Alexander *et al.* (2008). Additionally, decreases in the temporal lobe in general are widely reported with ageing in studies of middle-aged humans (Bourisly *et al.* 2015), older humans (Good *et al.* 2001; Tisserand *et al.* 2004, Smith *et al.* 2007, Hutton *et al.* 2009, Peelle *et al.* 2012; Ramanöel *et al.* 2018) and older macaques (Alexander *et al.* 2008; Colman *et al.* 2009). Perhaps most comparative to the current study is Bourisly *et al.* (2015) which cross-sectionally investigated early to mid-adulthood in humans and identified similar loss of grey matter in areas of the temporal lobe.

Interestingly in the current study, fewer significant clusters were identified in the frontal lobe, compared to the temporal lobe. Only two significant clusters were identified in the frontal lobe, both of which showed decreases in grey matter volume associated with ageing. The first of these clusters was localised to cortical areas 44 and 45 in the left hemisphere. Cortical areas 44 and 45 are commonly referred to as Broca's area and play a key role in speech and fluency in humans, which is also known to be impacted by ageing (Heim, Eickhoff and Amunts 2008; Kühn, Brass and Gallinat 2013; Hoffman, Loginova and Russell 2018). These areas in the macaque brain have been shown to be involved in volitional vocalizations, implying a similar function to the role of these regions in the human brain (Hage and Nieder 2013). The second significant cluster in the frontal lobe was localised to the precentral opercular area, a region which is known to play a role in working memory, another function which declines with ageing (Sakurai *et al.* 2018; Verhaeghen *et al.* 2020). Previous VBM studies of both older humans and older macaques have identified extensive decreases in grey matter volume across the frontal lobe (Alexander *et al.* 2008; Colman *et al.* 2009; Dash *et al.* 2023; Good *et al.* 2001; Tisserand *et al.* 2004, Smith

et al. 2007, Hutton *et al.* 2009, Peelle *et al.* 2012, Farokhian *et al.* 2017; Ramanöel *et al.* 2018).

Finally, there was also a significant age-related GMV decrease in an area of the right cerebellum. Significant decreases in the cerebellum do not appear to have been previously reported in VBM studies of older macaques but have been reported in VBM studies of older humans (Smith *et al.* 2007; Ramanöel *et al.* 2018), and in a VBM study of brain changes during early adulthood in humans (Su *et al.* 2021). Our results suggest that similar decreases in the cerebellum also occur in macaques during early to mid-adulthood, and may have been missed in previous studies either due to a focus on the cerebral cortex or due to their cross-sectional designs.

No significant increases in grey matter volume were identified in the current study, though visual area 1 in the occipital lobe did trend towards significance. This fits with the relative preservation of occipital lobe regions even into late adulthood in humans that has been previously reported by Farokhian *et al.* (2017). Additionally, no significant clusters were identified within the parietal lobe. This fits with previous VBM studies of ageing in macaques, which also failed to identify significant results within the parietal lobe. However, it should be noted that declines in the parietal lobe have been seen in VBM studies of older humans (Good *et al.* 2001; Smith *et al.* 2007; Ramanöel *et al.* 2018), as well as a previous study of early to mid-adulthood in humans (Bourisly *et al.* 2015).

The current study's findings differ from many previous studies, in both humans and macaques, which identified the frontal lobe as the region with the most extensive decreases in grey matter volume with ageing (Alexander *et al.* 2008; Colman *et al.* 2009; Dash *et al.* 2023; Good *et al.* 2001; Tisserand *et al.* 2004, Smith *et al.* 2007, Hutton *et al.* 2009, Peelle *et al.* 2012, Farokhian *et al.* 2017; Ramanöel *et al.* 2018), including in mid-adulthood for humans (Bourisly *et al.* 2015). It is possible that the current study identified relatively fewer results in the frontal lobe due to the use of a longitudinal approach, with the more extensive decline of the frontal lobe noted by previous studies potentially being an artifact of cross-sectional analyses which are confounded by their focus on between-subject comparisons (see Chapter 1, Section 1.4.3). Alternatively, as the sample studied here did not cover the higher ages investigated by previous macaque studies, it is possible that the more extensive loss of grey matter in the frontal lobe that was identified by previous studies actually

occurs later in life. Though one human study has implied that the frontal regions show extensive decreases in grey matter volume during early to mid-adulthood, it utilised a cross-sectional study design and so may not have identified ‘true’ effects of ageing (Bourisly *et al.* 2015).

Surprisingly, the cross-sectional approach in this study did not identify any significant changes in grey matter volume with ageing. The limited sample size for this approach likely contributed to this lack of significance, especially in terms of how many subjects were included from each site, as scanner was controlled for by the two-step approach. Though this approach to controlling for scanner may be conservative it is believed to be the gold standard for this kind of analysis and would allow for results that could be trusted. Given how surprising the lack of any significant results was a number of follow up analyses were carried out, including a more lenient one-step approach, but it was still not possible to identify any significant results. As such, this analysis should be repeated with a larger sample size. The number of scans that were available and could be processed through AutoMacq was reduced from what was initially expected due to the impacts of COVID-19 and the associated lockdowns (see COVID-19 impact statement). The lack of significant results for the cross-sectional approach appears to support the findings of Di Biase *et al.* (2023) that cross-sectional analyses underestimate ageing effects, as the effects in the current study were too small to be significant.

The fact that the longitudinal approach identified potential ageing effects that were significant, and the cross-sectional approach did not, highlights the benefits of a longitudinal study design, both in terms of the inherent increase in power and the reduction in subjects needed. Furthermore, as no significant results were identified using the cross-sectional approach, it was not possible to compare the results of the cross-sectional and longitudinal approaches in order to identify any cross-sectional results which were due to issues inherent in the approach rather than being ‘true’ ageing effects. However, it is likely that the significant results identified using the longitudinal approach were ‘true’ ageing effects, which lends support for results in similar regions found in previous studies of both older macaques and humans.

Overall, this study identified decreases in grey matter volume with ageing in regions similar to those found by previous studies of older rhesus macaques, implying that these changes may actually begin earlier than was previously thought,

whilst also identifying novel declines in other brain regions. The findings of this study broadly correspond to changes identified both by human studies of late adulthood and human studies of early to mid-adulthood, providing support for rhesus macaques as a model of healthy ageing of the human brain. Additionally, as this study utilised a longitudinal design it strengthens the previous cross-sectional studies of both macaques and humans that found similar decreases in grey-matter volume with ageing.

The major limitation of this study was the limited sample size for the cross-sectional approach. The fact subjects were from different sites exacerbated this issue as scanner had to be controlled for by the statistical approach, further reducing the power of the analysis. The more limited variability for some sites in terms of age may also have contributed to the lack of significant results for the cross-sectional approach, as they will have had less of an impact on the statistical analysis than would be expected for the number of included subjects for those sites.

Additionally, a mixed sex sample was utilised for this study, though data was only available from very few females for both the cross-sectional and longitudinal datasets. Statistics were re-run with the females excluded and similar results were produced, however the results of this study are still likely to be less translatable to females than males. Though previous human studies have indicated that any sex differences in the impacts of ageing on grey matter are minimal (Podgórski *et al.* 2021; Cui *et al.* 2023), it is possible that the impacts may differ more prominently between sexes in macaques and so further research is needed.

To conclude, using a longitudinal approach, the current study highlighted a number of brain regions that showed significant decreases in grey matter volume from early to mid-adulthood in rhesus macaques. This is the first study to investigate this age period in rhesus macaques, and the first study in primates in general to investigate this age period using a longitudinal approach. Understanding brain changes during early to mid-adulthood may be crucial for identifying targets to slow the onset of age-associated cognitive decline.

Chapter 5: Surface Based Analyses of the Impacts of Ageing on Brain Structure

5.1 Abstract

Surface-based morphometry research of changes in cortical thickness with ageing in rhesus macaques is very limited, with no studies investigating changes during early to mid-adulthood. Accordingly, the current study aimed to investigate how ageing during early to mid-adulthood affects cortical thickness in rhesus macaques, using both a cross-sectional and a longitudinal approach. Significant decreases in cortical thickness were identified across the brain using both approaches, with the most extensive decreases being localised to the frontal and temporal lobes. These findings differ from a previous cross-sectional study in older macaques but parallel results of human studies. This indicates that similar age-related changes in cortical thickness occur in both macaques and humans, with the novel finding that changes occur prior to old age, during the period of early to mid-adulthood.

5.2 Introduction

As discussed in chapter 4, we were unable to detect age-related changes in grey matter volume using a cross-sectional approach. However, volumetric measurements may not be particularly sensitive as they are composite measures comprising both surface area and cortical thickness (Storsve *et al.* 2014). Borgeest *et al.* (2021- preprint) demonstrated that cortical thickness is the metric most sensitive to age-related changes, whereas surface area is more sensitive to changes related to cognition. This higher sensitivity of cortical thickness to age-related changes was corroborated by Podgórski *et al.* (2021). Hence, the current study focuses on the impacts of ageing on cortical thickness. Cortical thickness is a measurement of the relative thinning of the cortex, either on a global or region-specific level.

In terms of the impacts of ageing on whole-brain cortical thickness, previous human studies have consistently found a significant, nonlinear decrease from childhood onwards (Lemaitre *et al.* 2012; Long *et al.* 2012; Fjell *et al.* 2015; Proskovec *et al.* 2020). As with the voxel-based morphometry studies discussed in chapter 4, there is strong evidence from previous SBM studies for prominent age

effects on the cortical thickness of areas within the frontal lobe (Fjell *et al.* 2009; Hogstrom *et al.* 2012; Lemaitre *et al.* 2012; Hurtz *et al.* 2014; Storsve *et al.* 2014; Fjell *et al.* 2015; Proskovec *et al.* 2020; Podgórski *et al.* 2021). However, results for other brain regions are less consistent. Fjell *et al.* (2009) utilised an adult sample covering the ages of 18 to 93, and found a strong age-related decrease in cortical thickness for the superior temporal lobe, as well as age-related decreases in regions within the medial temporal, parietal and occipital lobes. Similarly, Hurtz *et al.* (2014) identified widespread cortical thinning with ageing from mid to late adulthood (51 to 79 years), covering regions in the temporal, parietal and occipital lobes, and Storsve *et al* (2014) found pronounced cortical thinning with ageing (using a sample aged 20 to 87 years) in the temporal, parietal and posterior cingulate cortices. In contrast, Lemaitre *et al.* (2012) found the occipital cortex and medial temporal lobe to be relatively preserved with ageing (using a sample aged 18 to 87 years), and Long *et al.* (2012) identified cortical thinning primarily in the parietal and insula regions (with a sample of 18 to 94 year olds).

Though Fjell *et al.* (2009) did not identify any age-related increases in cortical thickness they did identify areas of preservation, localised to the anterior cingulate cortex, the precuneus, the paracentral gyrus, parahippocampal gyrus, entorhinal gyrus and inferior temporal gyrus. Similarly, Fjell *et al.* (2015) found that cortical thickness correlated negatively with ageing in every brain region except for the anterior cingulate cortex, for a sample of 4 to 89 year olds. Both Hurtz *et al.* (2014) and Storsve *et al.* (2014) also observed no significant change in the cortical thickness of the entorhinal cortex with ageing, with Storsve *et al.* (2014) additionally finding no change in the medial occipital lobe and a relatively weak decrease in the medial temporal lobe. However, Hurtz *et al.* (2014) and Storsve *et al.* (2014) did identify age-related declines in cortical thickness within the precuneus, unlike Fjell *et al.* (2009). More recently, Proskovec *et al.* (2020) utilised a sample with an age range of 22 to 72 years, and identified decreases in cortical thickness with ageing localised to the superior temporal lobe, inferior parietal lobe, medial occipital lobe and primary motor and somatosensory cortices. These findings were then corroborated by Podgórski *et al.* (2021) which identified age-related decreases in cortical thickness across very similar regions, in a sample of 38 to 80 year olds.

Unlike the VBM studies discussed in chapter 4, a number of the studies of the impacts of ageing on cortical thickness in humans do utilise a longitudinal design. However, these studies only cover a few years of each subject's life (Storsve *et al.* 2014; Fjell *et al.* 2014; Fjell *et al.* 2015; Borgeest *et al.* 2021). Therefore, cohort effects cannot truly be eliminated, and neither can sampling biases (Fjell *et al.* 2014). By utilising rhesus macaques as an animal model, it is possible to longitudinally investigate the equivalent of a longer life period over a short amount of time, due to their accelerated rate of ageing. This should allow for cohort effects and sampling biases to be more thoroughly mitigated.

However, the impacts of ageing on cortical thickness in rhesus macaques has so far been investigated far less than they have in humans. In fact, only one study appears to have investigated changes in cortical thickness with ageing in rhesus macaques, using surface-based morphometry. Koo *et al.* (2012) utilised a cross-sectional approach to investigate differences in cortical thickness between macaques aged 6-15 years (corresponding to early to mid-adulthood) and macaques aged 18-27 years (corresponding to late adulthood). Though they did not find a significant difference in whole brain cortical thickness between "young" and "old" macaques, both significant increases and decreases were identified for different regions across the brain. Similar to what has been found by some human studies, significant decreases in cortical thickness were localised to the precentral and postcentral gyri (Podgorski *et al.* 2021). However, they also identified significant increases in cortical thickness with ageing for the superior temporal sulcus, the temporal pole and the anterior cingulate cortex, in contrast to results from human SBM studies (though Fjell *et al.* [2009 and 2015] did find a somewhat similar trajectory for the anterior cingulate cortex). Given these contrasting and limited results, and the lack of longitudinal macaque studies, there is a clear need for further research into the impacts of ageing on cortical thickness in rhesus macaques.

Additionally, as with the voxel-based morphometry studies discussed in chapter 4, the majority of surface-based morphometry studies (in both humans and macaques) investigate brain changes in late adulthood. Consequently, cortical thickness changes during early to mid-adulthood are far less understood than those in late adulthood for both macaques and humans. This study therefore aimed to determine how cortical thickness changes with ageing across early to mid-adulthood

in rhesus macaques. Both a cross-sectional and a longitudinal approach were undertaken, in order to allow for a clearer picture of age-effects in macaques to be formed. Additionally, the use of both approaches will make it possible to assess whether the use of a cross-sectional approach (as has been used by the majority of previous studies) results in either an underestimation of age effects, as has been highlighted by Di Biase *et al.* (2023), or in artefactual results rather than results representing 'true' ageing effects.

5.3 Methods and Materials

5.3.1 Datasets and inclusion criteria

The surface-based analyses of this study utilised the same datasets as those used for the voxel-based analyses (see chapter 4, table 6). The cross-sectional sample consisted of 55 scans (44 from males, 11 from females), from across 5 sites and 7 scanners. The longitudinal sample consisted of scans from 16 subjects (14 males, 2 females) from across 3 sites/scanners. For both samples, inclusion criteria involved passing visual quality control and being at least 5 years old, but no older than 16 years old. For the cross-sectional dataset, at least 3 subjects per site were required, with the oldest subject being at least 18 months older than the youngest subject at the time of scanning. For the longitudinal dataset, at least 3 scans, covering at least 18 months, with a minimum of 3 months between consecutive scans, were required for a subject to be included.

5.3.2 Statistical analyses

Analyses were first carried out utilising average cortical thickness as the input data. Following this, for the surface based approach, statistics were carried out on data smoothed with a 1mm kernel in Matlab, using the Surfstat toolbox (www.math.mcgill.ca/keith/surfstat/). The input data for these analyses was the cortical thickness (CT) of each vertex.

Mixed effects models and linear regressions were utilised for both the cross-sectional and the longitudinal approaches. For the cross-sectional approach age and total intracranial volume were included in the models as fixed effects, whilst scanner was included as a random effect (model utilised: $CT = \beta1*Age + \beta2*TIV +$

random(scanner) + constant). For the longitudinal approach mean-centred age was included as a fixed effect and subject was included as a random effect (model utilised: CT= β1*mean-centred age + random(subject) + constant). Significance of the age effect was thresholded at 0.05 (corrected for multiple comparisons with family wise error [FWE]) at the cluster-level for both approaches. Statistics were carried out both including and excluding the female subjects.

5.4 Results

5.4.1 Longitudinal approach

The impacts of ageing on average cortical thickness were first investigated using the full longitudinal dataset. Though there was a trend towards a decrease in average cortical thickness with increasing age, this was not significant (DF= 15, p= 0.079, figure 24).

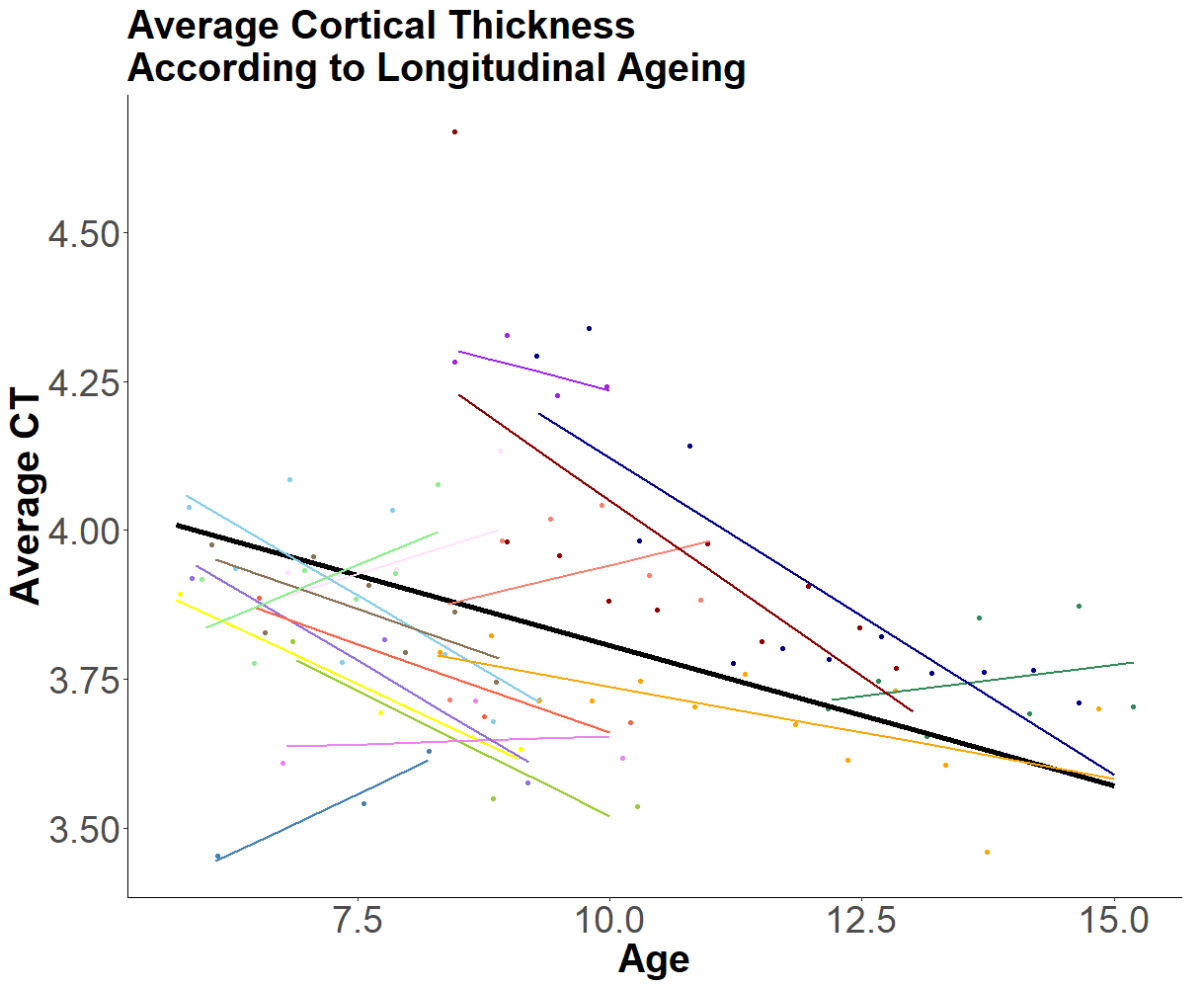

Figure 24: Changes in Average Cortical Thickness According to Longitudinal Ageing. The bold black linear line corresponds to the main effect of age, while controlling for TIV and with subject declared as a random effect. The thin coloured lines correspond to linear fits of the age effect for each subject while controlling for TIV. Dots correspond to raw data (unadjusted for TIV).

In terms of the regional analyses, Figure 25 shows the areas with significant decreases in cortical thickness with ageing. Results for each hemisphere were similar, though the left hemisphere showed the most significant clusters. Results were similar when female subjects were excluded.

Significant clusters were identified across the brain, with the temporal and parietal lobes showing the most extensive regions of cortical thinning. For the temporal lobe, areas showing significant cortical thinning were particularly concentrated around the superior temporal sulcus and within the superior temporal lobe, with noticeably more clusters in the left hemisphere.

For the parietal lobe, significant clusters were widespread, with multiple large clusters in somatosensory areas 1 and 2, as well as visual areas 4 and 7. Significant cortical thinning within the parietal lobe was also present for clusters localised to the precuneus, and the postcentral gyrus.

Significant cortical thinning of the frontal lobe was less extensive, though clusters were present within the precentral gyrus, precentral opercular area and the premotor cortex.

Finally, the occipital lobes appeared to be relatively preserved with ageing, with relatively small clusters showing significant cortical thinning in visual areas 1 and 2.

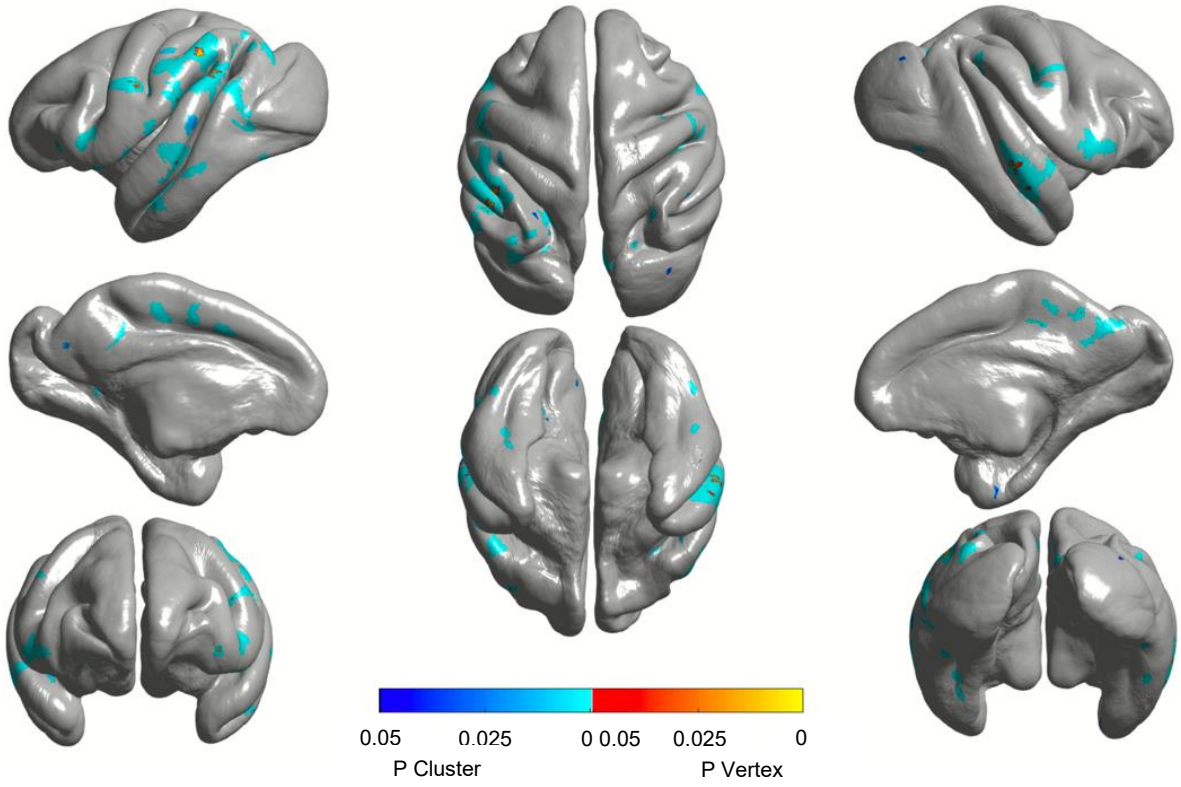

Figure 25: Significant Longitudinal Decreases in Cortical Thickness, Associated with Ageing. 3D surface map showing regions with significant age-related cortical thinning, identified using the longitudinal approach.

When female subjects were excluded, significant clusters only remained in visual area 4 and somatosensory areas 1 and 2, as well as in the vicinity of the superior temporal sulcus (see figure 26).

There were no clusters showing a significant increase in cortical thickness with ageing, regardless of whether female subjects were included or excluded.

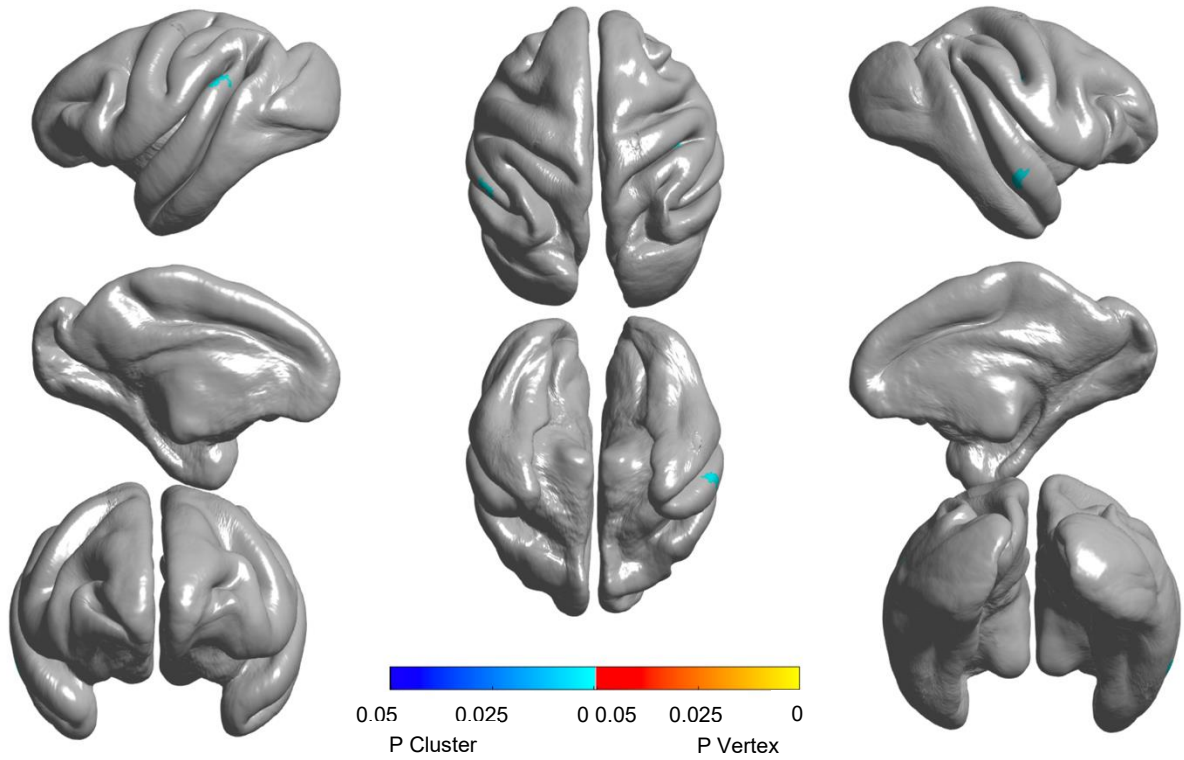

Figure 26: Significant Longitudinal Decreases in Cortical Thickness with Female Subjects Excluded, Associated with Ageing. 3D surface map showing regions with significant age-related cortical thinning, identified using the longitudinal approach with female subjects excluded from the sample.

5.4.2 Cross-sectional approach

Cross-sectional analyses of the impacts of ageing on average cortical thickness were presented in chapter 3, section 3.4.6.

For the regional approach, clusters exhibiting significant decreases in cortical thickness with ageing are shown in figure 27. The majority of clusters were within the frontal lobe, with bilateral clusters in the dorsal subdivision of brain area 46, a cluster localised to the right medial prefrontal cortex and a cluster within the left dorsolateral prefrontal cortex. There were also two significant clusters in the parietal lobe, localised to the medial parietal cortex and somatosensory area 3. A final significant cluster was localised to visual area 1, within the occipital lobe. Results were similar with female subjects excluded.

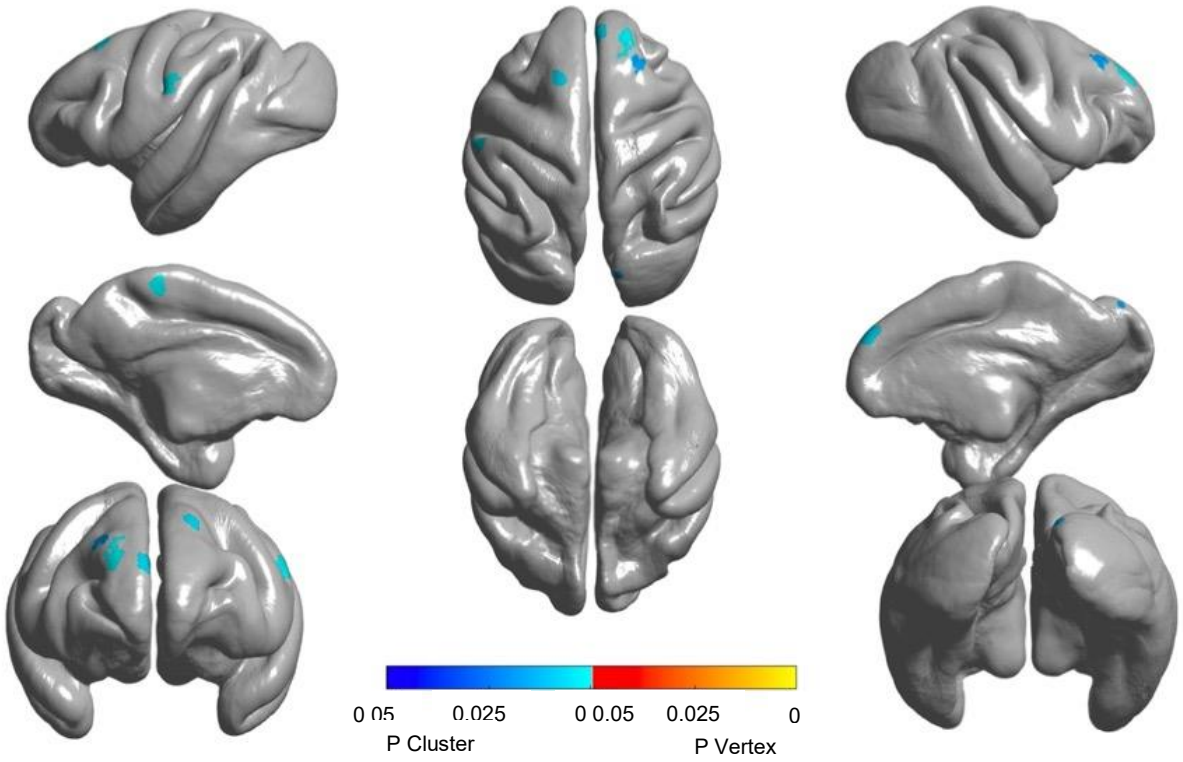

Figure 27: Significant Cross-sectional Decreases in Cortical Thickness, Associated with Ageing. 3D surface map showing regions with significant age-related cortical thinning, identified using the cross-sectional approach.

In terms of significant increases in cortical thickness with ageing, only one cluster was identified using the cross-sectional approach. This cluster was localised to the insula and was present no matter whether female subjects were included in or excluded from the sample (see figure 28).

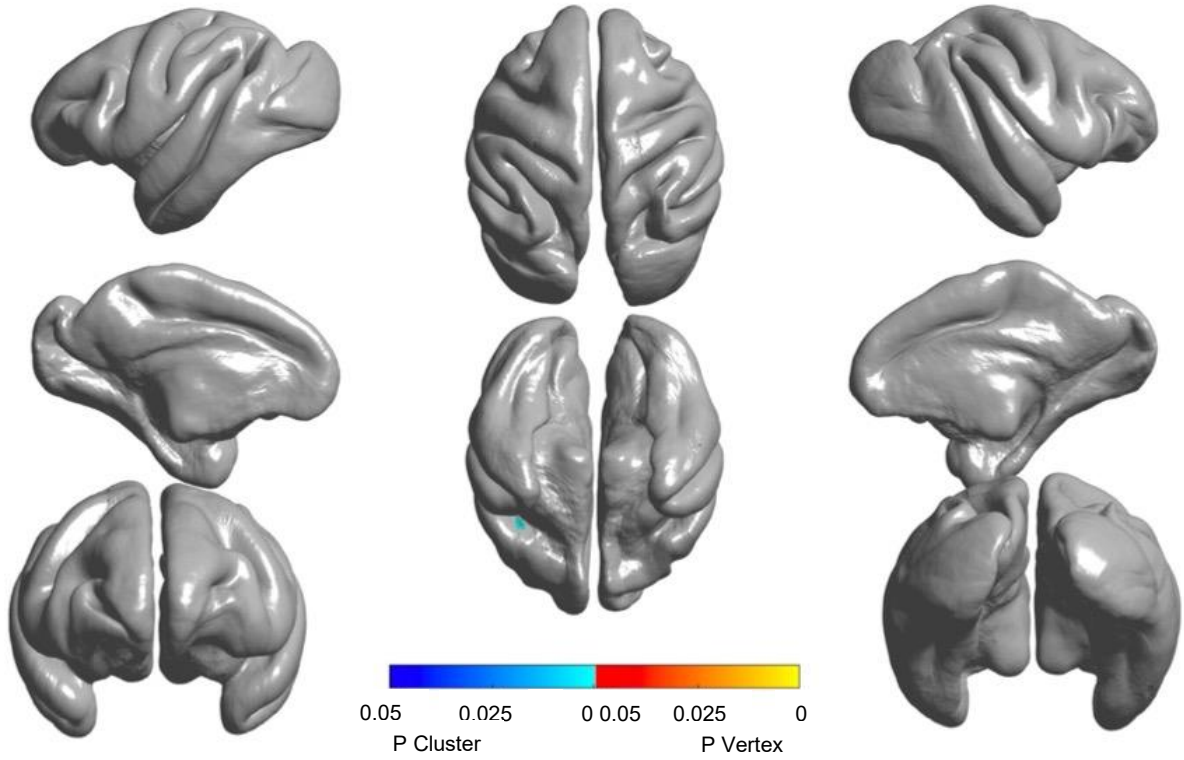

Figure 28: Significant Cross-sectional Increases in Cortical Thickness, Associated with Ageing. 3D surface map showing regions with significant age-related cortical thickening, identified using the cross-sectional approach.

5.5 Discussion

The discussion below is restricted to comparison of the results to other studies that utilised a surface-based morphometry approach, as well as a brief comparison of the voxel-based and surface-based results of this project. A more in-depth comparison of the voxel-based and surface-based results, as well as a broader discussion of the results in the context of the wider literature, will be carried out in the general discussion chapter (see chapter 8).

Table 8 presents a comparison of the longitudinal voxel-based and longitudinal surface-based results for the impacts of ageing. Notably, agreement was identified in terms of age-related decreases in regions surrounding the superior temporal sulcus, and in the precentral opercular area. Though results were generally similar between the two approaches for the temporal and frontal lobes, the surface-based approach identified extensive declines in the parietal lobe (as well as less extensive declines in the occipital lobe) which were not observed with the voxel-based approach. This could indicate that a surface-based approach is more sensitive than a voxel-based approach.

Region	Voxel-based approach	Surface-based approach
Precentral Opercular Area	↓	↓
Cortical Areas 44 and 45	↓	-
Precentral Gyrus	-	↓
Premotor Cortex	-	↓
Superior temporal sulcus	↓	↓
Rostrotemporal regions	↓	-
Temporal Pole	↓	-
Somatosensory area 1	-	↓
Somatosensory area 2	-	↓
Visual area 4	-	↓
Visual area 7	-	↓
Precuneus	-	↓
Post-central gyrus	-	↓
Visual area 1	-	↓
Visual area 2	-	↓
Cerebellum	↓	x

Table 8: Regions showing significant changes associated with ageing. A down arrow represents significant decreases, while a dash represents no significant change. For the surface-based approach it was not possible to investigate changes in the cerebellum.

With the surface-based approach, no significant change in average cortical thickness was identified using either a cross-sectional or a longitudinal approach. This may be due to the limited sample size, or it may be an indication that changes in cortical thickness across the brain are highly varied during this period of ageing. Regardless, these average cortical thickness analyses should be replicated with a larger sample size in order to confirm whether ageing does impact on average cortical thickness.

In terms of regional results, significant decreases in cortical thickness with ageing were found across the brain for both the cross-sectional and the longitudinal approach, though the exact regions differed between approaches. Only the longitudinal approach identified significant decreases in the cortical thickness of the precentral and postcentral gyri, meaning the cortical thinning identified by Koo *et al.* (2012) was replicated by the longitudinal approach but not the cross-sectional

approach. This may highlight the strengths of a longitudinal approach and provide some evidence for the conclusion of Di Biase *et al.* (2023) that a cross-sectional approach may underestimate the impacts of ageing.

Cortical thinning of the parietal lobe with ageing appeared the most extensive with the longitudinal approach. In particular, somatosensory areas 1 and 2, as well as visual areas 4 and 7, had substantial clusters of significant cortical thinning. These findings imply notable age-related decreases in cortical thickness for areas involved in sensory perception. After the frontal lobe, the parietal lobe is perhaps the most consistently identified as showing cortical thinning with ageing in humans, with the somatosensory regions being highlighted as particularly vulnerable (Fjell *et al.* 2009; Hogstrom *et al.* 2012; Lemaitre *et al.* 2012; Hurtz *et al.* 2014; Storsve *et al.* 2014; Fjell *et al.* 2015; Proskovec *et al.* 2020; Podgórski *et al.* 2021). These findings may provide an explanation for the well-established, age-related degeneration of senses, such as vision (Cavazzana *et al.* 2018). Our result of extensive decreases in these somatosensory regions by mid-adulthood in macaques then potentially implies that these changes may also begin earlier than late adulthood in humans. Significant cortical thinning within the parietal lobe was also present for clusters localised to the precuneus. The precuneus is thought to be closely associated with the posterior cingulate cortex, and therefore plays a similar role in memory retrieval and is also involved in the default mode network (Maddock, Garrett and Buonocore 2001; Bernard *et al.* 2015). Fjell *et al.* (2009) previously identified relative preservation of the cortical thickness of the precuneus with ageing in humans, though both Hurtz *et al.* (2014) and Storsve *et al.* (2014) did find significant cortical thinning of the precuneus with ageing in humans.

The temporal lobe also showed widespread age-related cortical thinning with the longitudinal approach. In particular, clusters were concentrated around the superior temporal sulcus, a region that plays a role in functions known to decline with ageing, such as social perception and working memory (Berman and Colby 2002; Deen *et al.* 2015; Verhaeghen *et al.* 2020; Grainger *et al.* 2023). Storsve *et al* (2014) and Proskovec *et al.* 2020 both previously identified cortical thinning with ageing in the vicinity of the superior temporal sulcus in older humans. Additionally, cortical thinning of the temporal lobe more generally has been identified by a number of previous human studies (Fjell *et al.* 2009; Hurtz *et al.* 2014; Storsve *et al.* 2014; Fjell

et al. 2015; Proskovec *et al.* 2020; Podgórski *et al.* 2021). However, Lemaitre *et al.* (2012) found evidence of preservation of the cortical thickness of the temporal lobe with ageing in older humans, and Koo *et al.* (2012) actually found increased cortical thickness in regions of the temporal lobe for older macaques. Both of these studies though utilised a cross-sectional approach and compared a group of older individuals with a group of younger individuals, with the age range of the current study being captured by the younger group utilised by Koo *et al.* (2012). As such, it is possible that the difference in results for the temporal lobe highlights a non-linear ageing trajectory in macaques, with thinning during early to mid-adulthood and then stability or thickening later in life. This could also provide some explanation for the somewhat mixed results for the temporal lobe in human studies.

With the longitudinal approach the majority of clusters showing significant cortical thinning in the frontal lobe were localised to regions F4 and F5, within the premotor cortex. The premotor cortex is known to be involved in the planning and organisation of movements (Svoboda and Li 2018), and Poirier *et al.* (2020) is one study demonstrating the decline in planning and organisation of movements with ageing. Significant cortical thinning was also observed within the precentral opercular area, a region known to be involved in working memory (Sakurai *et al.* 2018), which is well documented as declining with advancing age in humans (Verhaeghen *et al.* 2020). Notably, the frontal brain areas identified by the longitudinal approach are similar to the areas thought to be sensitive to age-related cortical thinning in older humans (Fjell *et al.* 2009; Hogstrom *et al.* 2012; Lemaitre *et al.* 2012; Hurtz *et al.* 2014; Storsve *et al.* 2014; Fjell *et al.* 2015; Proskovec *et al.* 2020; Podgórski *et al.* 2021).

The occipital lobe was the most preserved in the current study, paralleling the findings of Lemaitre *et al.* (2012) and Storsve *et al.* (2014) in humans. With the longitudinal approach, significant cortical thinning was present only for small clusters, localised to visual areas 1 and 2. Both of these regions play a key role in visual processing, and human studies have previously identified thinning in these regions with ageing (Hurtz *et al.* 2014; Proskovec *et al.* 2020). This finding further supports the previously discussed hypothesis of sensitivity of somatosensory regions, particularly those related to the visual system, to ageing.

With the cross-sectional approach, the most extensive age-related cortical thinning was identified in the frontal lobe. Four large, distinct clusters showing significant age-related cortical thinning were identified within the frontal lobe, localised to areas shown to play a role in working memory and attention. It is well-established that these functions are impacted detrimentally by ageing (Sakai, Rowe and Passingham 2002; Barbey, Koenigs and Grafman 2013; Smith *et al.* 2018; Verhaeghen *et al.* 2020). With the frontal regions showing the most prominent thinning with the cross-sectional approach but not with the longitudinal approach, the findings of the cross-sectional approach may somewhat more closely parallel those of previous human studies (Fjell *et al.* 2009; Hogstrom *et al.* 2012; Lemaitre *et al.* 2012; Hurtz *et al.* 2014; Storsve *et al.* 2014; Fjell *et al.* 2015; Proskovec *et al.* 2020; Podgórski *et al.* 2021). This may be due to the majority of these prior studies also using a cross-sectional study design, potentially providing evidence for this more extensive thinning of frontal regions being due to the focus of a cross-sectional approach on between-subject effects rather than reflecting 'true' ageing effects.

No significant age-related changes in cortical thickness were identified in any regions within the temporal lobe, when utilising the cross-sectional approach. Though some previous human studies also found relative preservation within some regions such as the medial temporal lobe (Lemaitre *et al.* 2012; Long *et al.* 2012), many more did identify significant cortical thinning in the temporal lobe, in line with the findings of the longitudinal approach in the current study (Fjell *et al.* 2009; Hurtz *et al.* 2014; Storsve *et al.* 2014; Fjell *et al.* 2015; Proskovec *et al.* 2020; Podgórski *et al.* 2021). The lack of any significant changes in cortical thickness for temporal regions using the cross-sectional approach again highlights the potential underestimation of this approach, previously identified by Di Biase *et al.* (2023).

The cross-sectional approach also identified significant age-related cortical thinning in areas of the parietal lobe, with two significant clusters localised to the medial parietal cortex and somatosensory area 3. The cortical thinning of the medial parietal cortex may be particularly relevant as this region is a key component of the default mode network and has a role in cognitive functions known to be adversely affected by ageing, such as memory recall (Andrews-Hanna *et al.* 2010; Korkki *et al.* 2020; Bainbridge and Baker 2022).

As with the longitudinal approach, only one cluster in the occipital lobe, localised to visual area 1, showing significant cortical thinning with ageing was identified by the cross-sectional approach. As was previously discussed, this fits with the findings of Hurtz *et al.* (2014) and Proskovec *et al.* (2020) in older humans.

Finally, the cross-sectional approach identified significant cortical *thickening* with ageing in one cluster, localised to the insula. This contrasts with the results of Long *et al.* (2012), who found significant cortical *thinning* of the insula in older humans, and with the results of the longitudinal approach of the current study, which also identified significant bilateral cortical thinning in the insula. Though the contrast with Long *et al.* (2012) could be due to the different age-ranges investigated as the current study focused on young to mid-adulthood, whilst Long *et al.* (2012) included human subjects aged 18-94, this would not explain the contrast to the longitudinal approach of the current study. As a consequence, it is likely the significant increase in the cortical thickness of the insula is erroneous and the result of some aspect of the cross-sectional approach, rather than being a 'true' age effect.

Crucially, the current study did not identify increases in cortical thickness in any of the regions highlighted as showing age-related increases in cortical thickness by Koo *et al.* (2012). Thus, though the cortical thinning identified by Koo *et al.* (2012) in older macaques was replicated by the longitudinal approach of the current study, the increases in cortical thickness highlighted by this previous macaque SBM study of ageing were not replicated. This may indicate that these increases in cortical thickness were due to the macaques studied by Koo and colleagues being older than those in the current study, or that they were erroneous due to the cross-sectional methodology employed in Koo *et al.* (2012).

For the cross-sectional approach of the current study, similar results were found whether female subjects were included in or excluded from the sample. When female subjects were excluded from the longitudinal approach significant clusters only remained within visual area 4, somatosensory areas 1 and 2 and the bank of the superior temporal sulcus. The results were therefore in regions previously identified when female subjects were included in the longitudinal sample, though some regions were no longer significant with the female subjects excluded. This may have been due to the cortical thinning in some regions being driven primarily by the female subjects. However, it is perhaps more likely to be due to a reduction in sample size,

given that very similar changes in cortical thickness with ageing for both sexes have been identified in humans by previous studies such as Podgórski *et al.* (2021). However, given how few female subjects were included in the current study, the results may only be translatable to male rhesus macaques. Sex differences in the impacts of ageing on cortical thickness have not been previously studied in rhesus macaques, so further research is needed to determine if the results of this study would have been different if more females had been included.

The major limitation of the current study was the relatively small sample size, particularly for the cross-sectional approach (given the inclusion of scanner in the statistical model). This likely contributed to the cross-sectional approach identifying far fewer regions of significance than the longitudinal approach, though this may also have just been due to inherent underestimation when using a cross-sectional approach (Di Biase *et al.* 2023).

To conclude, the current study identified widespread cortical thinning from young to mid-adulthood in rhesus macaques, using both a cross-sectional and a longitudinal approach. The longitudinal approach identified more widespread decreases in cortical thickness, with significant clusters in all four major lobes of the brain. The results of the two approaches were similar in some regions such as those in the parietal and occipital lobe. However, the cross-sectional approach showed relatively more prominent thinning of the frontal lobe, whilst lacking any significant thinning within the temporal lobe. In contrast, thinning of the frontal lobe appeared to be somewhat less prominent for the longitudinal approach, but thinning within the temporal lobe was extensive. The findings of the current study are novel due to the age range investigated and the use of a longitudinal approach. Though the results broadly align with the findings of previous human SBM studies, they only correspond to cortical thinning results of a previous SBM study that investigated cortical thickness in older macaques, not the cortical thickening results of that study. This perhaps suggests the presence of non-linear ageing trajectories. Overall, there is clear evidence of age-related cortical thinning across the brain, occurring during early to mid-adulthood, in rhesus macaques.

Chapter 6: Voxel Based Morphometry Study of the Impacts of Early Life Stress on Brain Structure

6.1 Abstract

Human voxel-based morphometry studies have previously identified both increased and decreased regional grey matter volumes in subjects who have experienced early life stress (ELS). However, many human studies utilise a cross-sectional design and can suffer from recall bias due to relying on participants recollection of events during childhood. Additionally, human studies in general can be confounded by a lack of control over the stressors experienced and difficulty in excluding subjects with subclinical psychiatric illnesses. These issues can be circumvented through the use of model animals, such as rhesus macaques. This study aimed to investigate the impacts of early life stress on grey matter volume in rhesus macaques, using weaning age, as defined as definitive separation from the mother, as an early life stressor. This was investigated using a cross-sectional design, and a voxel-based morphometry approach. No significant results were found using the cross-sectional approach, likely due to the limited sample size leading to a lack of power. The interaction between weaning age and ageing was also investigated using a longitudinal approach. A significant interaction between weaning age and ageing was identified for a cluster localised to visual area 2, a region previously found to show decreased grey matter volume with ELS in humans and macaques. However, in the current study macaques with earlier weaning ages showed greater increases in the grey matter volume of visual area 2. This result was unexpected and warrants further investigation.

6.2 Introduction

Early-life stress (ELS) can be defined as a natural response to real or perceived threats during childhood. Stressful events during childhood are thought to have a greater impact on the brain than those during adulthood as they may alter developmental trajectories (Smith and Pollak 2020). Studies have found that ELS can cause permanent changes in the hypothalamic-pituitary-adrenal axis, the system which controls the release of stress hormones, as well as in the immune system (Juruena *et al.* 2021; Chen *et al.* 2021). Subsequently, ELS is a major risk factor for

the development of physical diseases such as cardiovascular disease and autoimmune diseases, as well as psychiatric disorders such as anxiety and depression, later in life (Dube *et al.* 2009; Carr *et al.* 2013; LeMoult *et al.* 2020; Bengtsson *et al.* 2023).

Previous voxel-based morphometry studies have identified diverse changes in grey matter volume in humans who have experienced early life stress. Multiple studies have focused on investigating hippocampal volume and have identified smaller volumes in: adolescents exposed to early life adversity (Rao *et al.* 2010), adults with difficulties processing emotions that experienced early life stress (Aust *et al.* 2014) and children that had been physically abused or that were from a low socioeconomic status household (Hanson *et al.* 2015). However, results are relatively less consistent for studies that have utilised a whole brain approach. The acute effects of ELS in children were investigated by De Brito *et al.* (2012) who found that children who had experienced maltreatment had reduced grey matter volume in the medial orbitofrontal cortex and middle temporal gyrus. Walsh *et al.* (2014) then found reduced grey matter volume only in the cerebellum in adolescents and young adults that experienced self-reported childhood maltreatment. In contrast, Gorka et al. (2014) identified grey matter volume reductions in the medial prefrontal cortex and left hippocampus of young adults that self-reported childhood maltreatment. Similarly, Tyborowska et al (2018) found reduced grey matter volume in the anterior prefrontal cortex, as well as in the amygdala, putamen and insula, for adolescent subjects that had negative personal life events during early childhood. Additionally, a voxel-based meta-analysis that included children, adolescents, and young adults, found that those that experienced childhood maltreatment (and were unmedicated) displayed significantly smaller grey matter volumes in the left inferior frontal gyrus, the right orbitofrontal gyrus and the superior and middle temporal gyri (Lim *et al.* 2014).

The impacts of early life stress during early to mid-adulthood were investigated by Dannlowski *et al.* (2012), which identified reductions in grey matter volume associated with high scores on a childhood trauma questionnaire. These reductions were localised to anterior cingulate gyrus, insula, caudate, orbitofrontal cortex and the hippocampus. Baker *et al.* (2013) then specifically investigated volume changes in very similar brain regions to those Dannlowski and colleagues

(2012) identified volume reductions in, though they included the amygdala in place of the orbitofrontal cortex. Baker *et al.* (2013) utilised a sample aged 8-79 years, and separated early life stress into 2 classifications: ELS during early childhood (1 month-7 years) and ELS during late childhood (8 years-17 years). This study identified reduced grey matter volume of the anterior cingulate and insula (but not the other regions investigated) only with ELS during late childhood.

More recently, another meta-analysis (Tymofiyeva *et al.* 2022), which focused on adolescents, found that those exposed to childhood maltreatment actually had increased grey matter volume in the left precentral gyrus, including part of left inferior frontal gyrus, left body of corpus callosum and left postcentral gyrus. Alongside this, they identified decreased volume in the cerebellum, middle temporal gyrus, rostrum of the corpus callosum and the supramarginal gyrus. Malhi et al 2023 later utilised female adolescents who had experienced emotional trauma during childhood and found changes across the brain, with increased grey matter occurring in early adolescence followed by decreased grey matter in late adolescence, for subjects with high levels of ELS compared to those with low levels of ELS. This implies that the effects of early life stress interact with those of ageing/development, resulting in non-linear changes in grey matter volume even just over the course of adolescence. These changes were observed primarily in the posterior cingulate cortex, parahippocampal gyrus, prefrontal cortex and other frontal regions.

Clearly results of previous human studies are fairly mixed, with varied regions being implicated as being sensitive to early life stress. Additionally, human ELS research is often limited to cross-sectional, retrospective studies, in which participants are asked about their experiences during childhood to determine whether they experienced any ELS. This approach comes with a number of issues, one of which being the potential for recall bias, where a participant forgetting or misremembering past events leads to them being misclassified, confounding the results of the study (Althubaiti 2016). Also, as participants will likely have experienced a range of potentially stressful early life events, as well as events which may ameliorate this stress, it can be difficult to identify human subjects who have experienced similar types and/or amounts of early life stress. Furthermore, with human studies it can be difficult to investigate early life stress without unintentionally including subjects who either currently have an underlying psychiatric illness or will

go on to develop one later in life. Accordingly, human studies of early life stress may not always be applicable to 'healthy' individuals who have experienced early life stress but will not go on to develop a psychiatric illness. Utilising animal models who have been raised and lived in a controlled environment can reduce the impact of these factors.

Captive rhesus macaques are a particularly useful animal model for investigating early life stress as they not only live in a controlled environment where significant life events can be identified as they happen, but they also display similar social behaviours to those carried out by humans (Meyer and Hamel 2014). Consequently, they may deal with stress in similar ways to humans (Wooddell *et al.* 2017). Additionally, they have the same stress hormone system as humans and, though they can display depression- and anxiety-like behaviours, they likely cannot develop full psychiatric disorders, allowing for investigation of the impacts of early life stress in 'healthy' subjects (Koch *et al.* 2014; Ausderau *et al.* 2023). Furthermore, the accelerated rate of ageing of rhesus macaques (compared to humans) allows for easier investigation of any chronic effects of early life stress (Mattison and Vaughan 2017).

However, as with ageing, the impacts of early life stress on grey matter volume have not been the focus of many previous macaque studies. One potentially stressful early life event, that is common to the vast majority of captive macaques, is early weaning. Weaning can be defined as permanent separation of a young macaque from their mother. Previous studies have found that being weaned early can lead to alterations in behaviour, physiology, and the immune system (Prescott *et al.* 2012). The impacts of early weaning on brain structure have been previously investigated by only a couple of studies, both of which have focused on immediate weaning after birth (i.e., maternal deprivation). Using manual tracing, Spinelli *et al.* (2009) investigated the impacts of maternal deprivation on grey matter volume in the cerebellum, cingulate cortex, hippocampus, prefrontal cortex and corpus callosum. Though they hypothesised that subjects that underwent maternal deprivation would have smaller grey matter volumes in these areas, they actually found increased grey matter volume in all of the areas investigated, except for the hippocampus and corpus callosum where they found no significant differences. More recently, Wang *et al.* (2018) used voxel-based morphometry to investigate the impacts of maternal

deprivation on grey matter volume. In macaques that had experienced maternal deprivation they identified a significant decrease in grey matter volume in visual area 1. Visual area 1 has previously been implicated in early life stress in humans, with Tomoda *et al.* (2009) finding a similar reduction in grey matter volume in young women that experienced childhood sexual abuse.

Given how different the results of these previous studies are, and the lack of other studies on weaning later than birth, it essentially remains relatively unclear how early weaning impacts on grey matter volume in rhesus macaques. As such, the current study aimed to investigate how weaning age affects grey matter volume in rhesus macaques.

Additionally, though there is a general consensus that a weaning age below 6 months is likely to be stressful, and a recent review recommended a minimum weaning age of 10-14 months, there is no agreement on at what age weaning is no longer stressful (Prescott *et al.* 2012). Therefore, this study also aimed to determine whether at a certain age weaning no longer impacts on grey matter volume, and therefore is likely to no longer be particularly stressful.

It is also possible that weaning has a different impact on males compared to females, as in the wild males will leave their maternal group at around the age of 4 or 5, whereas females will usually remain in their maternal group for the entirety of their lives (Prescott *et al.* 2012). Therefore, it would be logical for weaning to be more stressful for females, and so the age at which weaning is no longer stressful (or at least no longer stressful to the point of inducing long-term changes in grey matter volume) may be later in female macaques. A further aim of this study was consequently to investigate potential sex differences in the impacts of weaning age on brain structure.

Finally, as there is growing evidence that stress may accelerate ageing processes (Gotlib *et al.* 2021), a longitudinal approach will be utilised in this study to investigate the interaction between weaning age and ageing.

6.3 Methods and Materials

6.3.1 Datasets and inclusion criteria

Any scans with artifacts, poor contrast or hyperintensities were excluded during initial visual quality control. As with the ageing study, the sample was restricted to early to mid-adulthood by only including subjects above the age of 5 years and below the age of 16 years. For some subjects, data on weaning age was unavailable, so they were also excluded from this study (for example, the weaning age was unknown for all of the subjects from the PRIME-DE datasets and the NIDA dataset). For the cross-sectional analyses, at least 3 subjects per site were required so that site/scanner could be controlled for in the model. Sites with less than 3 subjects passing quality control and meeting the inclusion criteria were excluded. The final cross-sectional datasets for this study comprised 32 subjects, 24 of which were male, from 3 sites (table 9). T2 data was available for 15 of the 32 subjects.

Weaning age information was only available for subjects with longitudinal data from Newcastle University. To be included in the longitudinal dataset subjects needed at least 3 scans, covering a minimum of 18 months, with at least 3 months between consecutive scans. Scans from 10 subjects were included in the longitudinal dataset, 8 of which were male (table 9). T2 data was available for all of the subjects included in the longitudinal sample.

A further cross-sectional analysis was also carried out using one scan from each of the subjects in the longitudinal dataset who had a scan around the age of 8.4 years (N=8; 6 male and 2 female macaques). This was done to create an age-matched dataset, essentially removing the effect of age from the model (table 9). It was not possible to add any additional subjects into this dataset without greatly expanding the age range.

Dataset	Site	Included Subjects (M/F)	Weaning age (in months)	Age (in years)	Subj. with T2 data	Awake vs. Anaes.	Scanner Strength
C	New-castle	18 (12/6)	6-34	6-15	18	Awake	4.7T
C	DPZ	7 (7/0)	23-47	7-11	3	Anaes.	3T
C	Oxford	7 (5/2)	13-30	5-8	0	Anaes.	3T
C	*Total*	*32 (24/8)*	*6-47*	*5-15*	*15*		
AM	New-castle	8 (6/2)	9-34	8.3-8.5	8	Awake	4.7T
L	New-castle	10 (8/2)	6-34	6-15	10	Awake	4.7T

Table 9: Description of Subjects Included in Early Life Stress Analyses
C: cross-sectional, AM: age matched and L: longitudinal. M: male and F: female. Anaes.: anaesthetised.

6.3.2 Statistical analyses

Total grey matter volume and the local amount of grey matter in each voxel were utilised as input data. For the voxel-based approach, data was smoothed using a 1mm kernel prior to statistical analysis. For each of the cross-sectional analyses, multiple-linear regressions were carried out, with weaning age and total intracranial volume included as fixed effects in both analyses. Age and scanner were also included as covariates when the full cross-sectional sample was analysed (this was not necessary for the age-matched sample as they all had the same age and scanner), with age as a fixed effect and scanner as a random effect. The final statistical models for the analyses of the full cross-sectional sample and the age-matched sample were GMV= β1*weaning age + β2*age + β3*TIV + random(scanner) + constant and GMV= β1*weaning age + β2*TIV + constant, respectively. Significance was thresholded at 0.001 (uncorrected) at the voxel-level, and 0.05 (corrected for multiple comparisons with FWE) at the cluster-level, for both regional cross-sectional analyses. It was not possible to carry out a two-step approach, similar to those used in chapter 4, for the cross-sectional analyses with all variables included due to limitations in terms of the number of subjects per site. An alternate two-step approach was carried out with age excluded, as was a version of the above one-step approach with age excluded.

The longitudinal approach, for both the analysis of total grey matter volume and local grey matter volumes, utilised a two-step approach. The first step involved

calculating the slope of the ageing effect for each subject, using a simple linear regression, with age as a fixed effect (the statistical model was GMV= β1*age + constant). The second step then utilised a simple linear regression in order to determine if the slope of the age effect changes based on weaning age (the statistical model of the second step was slope= β1*weaning age + constant). For the local grey matter analyses, significance was thresholded at 0.001 (uncorrected) at the voxel-level, and 0.05 (corrected for multiple comparisons with FWE) at the cluster-level. As the majority of subjects in both the cross-sectional and longitudinal samples were male, the statistics were carried out including and excluding the female subjects.

6.4 Results

6.4.1 Cross-sectional approach- impacts of weaning age

The impacts of weaning age on total grey matter volume were first investigated for the cross-sectional dataset. No significant effect of weaning age on total grey matter volume was identified (β= -0.00094, Std. error= 0.0012, DF= 23, p= 0.44, figure 29). This analysis was repeated with the age-matched dataset (and age removed from the model), but again no significant effect of weaning age on total grey matter volume was identified (β= -0.0025, Std. error= 0.004, DF= 5, p= 0.55).

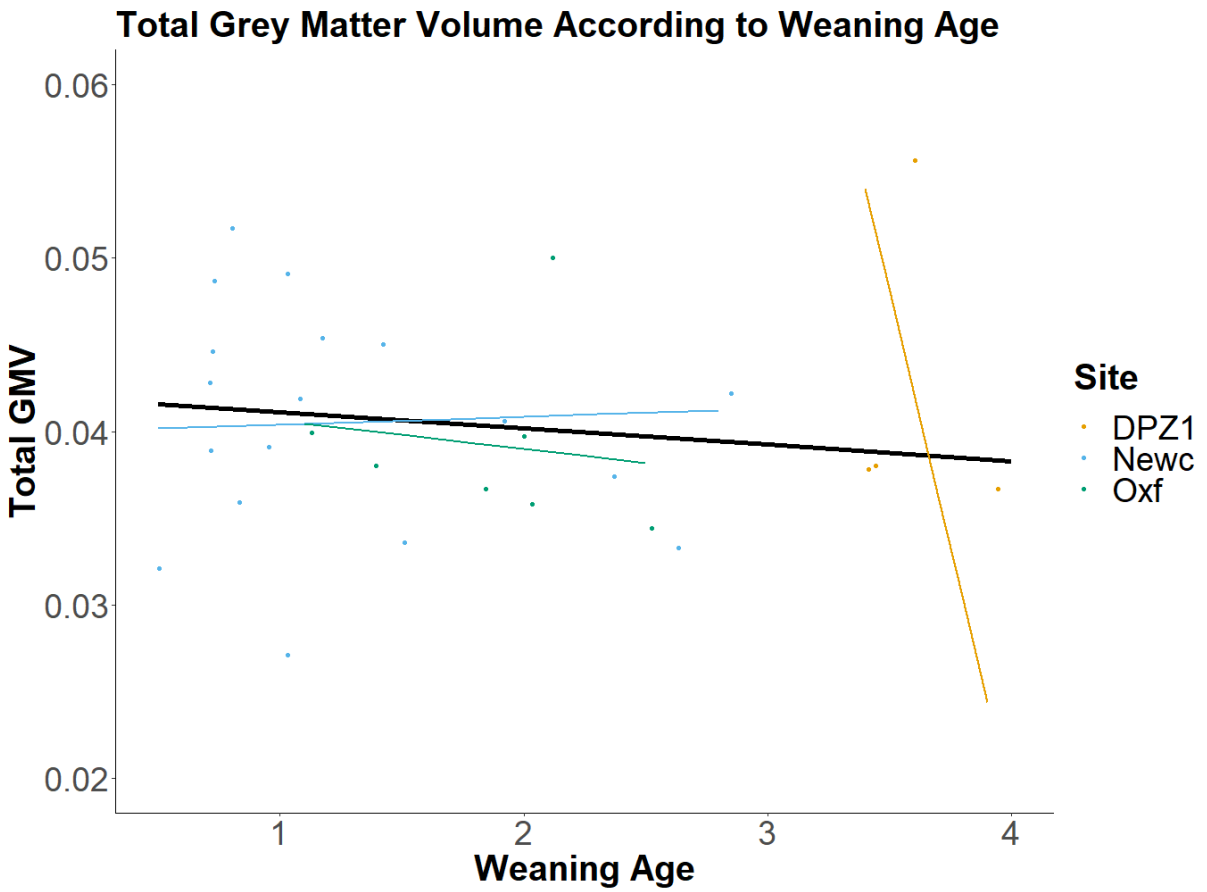

Figure 29: Changes in Total GM Volume According to Weaning Age. The bold black linear line corresponds to the main effect of weaning age, while controlling for TIV and with site/scanner declared as a random effect. The thin coloured lines correspond to linear fits of weaning age effect in each site while controlling for TIV. Dots correspond to raw data (unadjusted for TIV).

The regional cross-sectional approach was initially restricted to investigate the hypothesis that early weaning would be associated with decreases in grey matter volume. No significant results were obtained, either for the full cross-sectional sample or for the age-matched sample. This was regardless of whether female subjects were included in or excluded from the samples.

A statistical model with the weaning age converted from a continuous variable into a categorical variable of 'above or below 12 months' also produced no significant results, using either sample. Additionally, no significant results were identified using either a one-step or a two-step approach with the variable of age removed.

6.4.2 Longitudinal approach- impacts of weaning age x ageing interactions

No significant results were identified for an analysis of the impacts of weaning age and ageing interactions on total grey matter volume (β= -0.00058, Std. error= 0.00073, DF= 8, p= 0.45).

With the regional longitudinal investigation of weaning age and ageing interactions, one significant result was identified when weaning age was encoded as a continuous variable. The significant interaction was present for a cluster within the left occipital lobe, localised to visual area 2 (see figure 30). The interaction was significant both when the female subjects were included ($P_{FWE\text{-}corr}$= 0.028, T= 8.02; -6.0, -14.5, 35.0) and when they were excluded ($P_{FWE\text{-}corr}$= 0.032, T= 8.21; -5.5, 15.0, 35.0). Converting weaning age to a categorical variable though led to no significant results.

The ageing effect within this significant cluster was plotted for each subject in order to determine the direction of the impact of the interaction between weaning age and ageing on grey matter volume (figure 31). Surprisingly, an earlier weaning age appeared to correlate with a greater age-related *increase* in grey matter volume within this cluster. As a consequence of this, the cross-sectional approach was re-analysed in order to determine whether there were any significant *increases* in grey matter volume associated with earlier weaning. However, no significant results were identified.

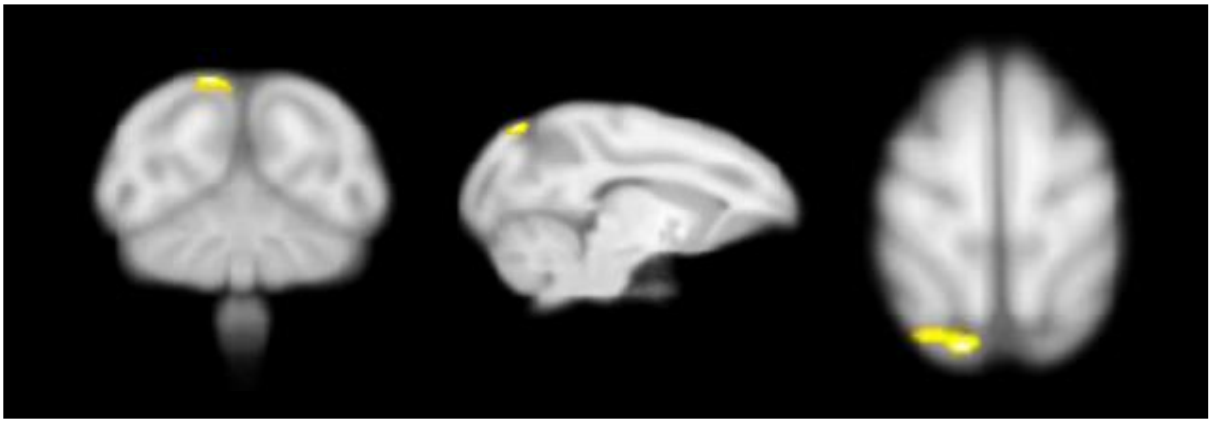

Figure 30: Cluster in the Occipital Lobe Showing a Significant Change in Grey Matter Volume, Associated with an Interaction Between Weaning Age and Ageing. Localised to the left visual area 2.

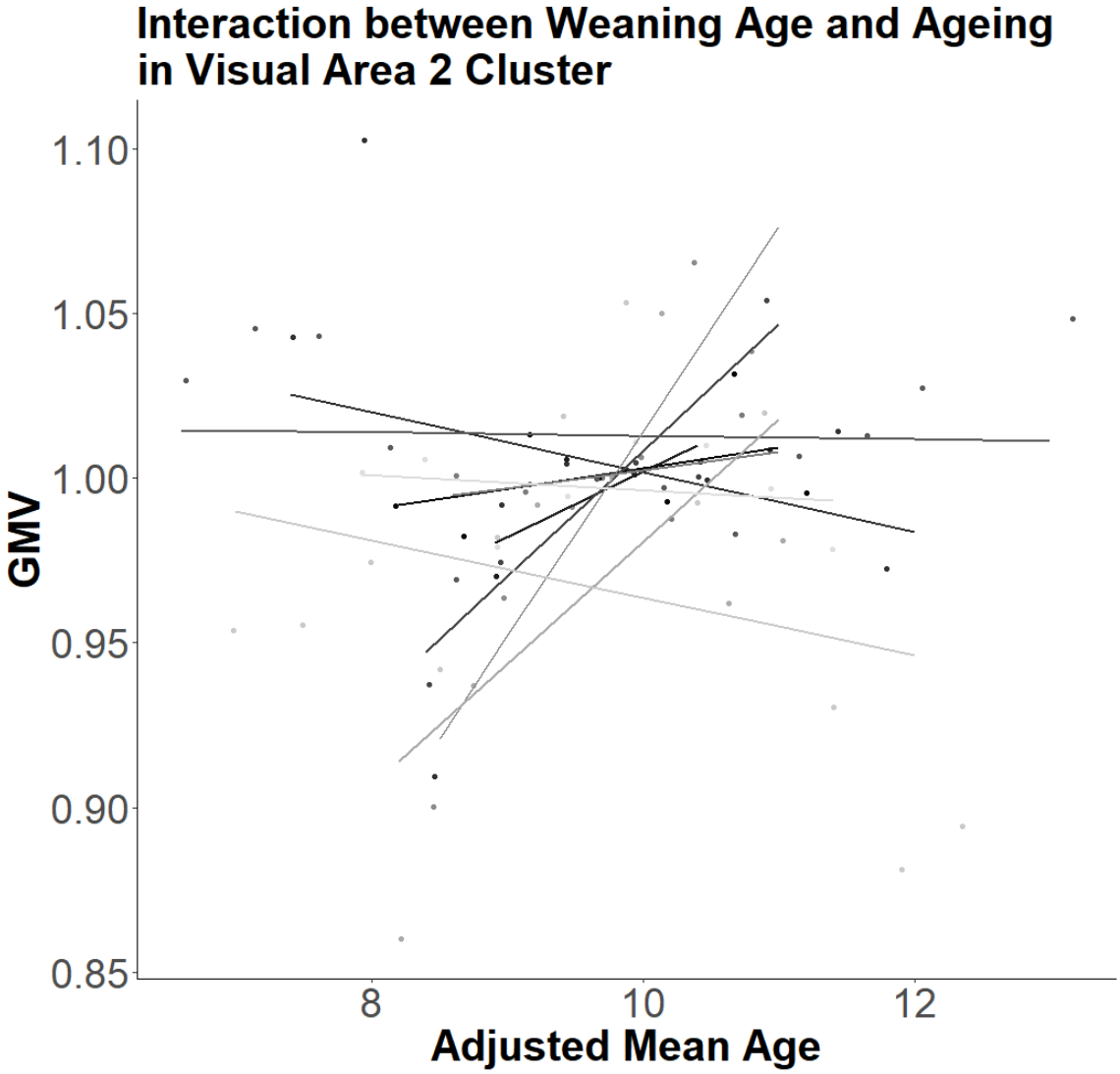

Figure 31: Changes in GM Volume Within a Significant Occipital Lobe Cluster According to the Interaction Between Weaning Age and Ageing. Each line corresponds to the linear fit of the age effect in each subject. Dots correspond to raw data. Lines and dots are colour coded in greyscale, with darker lines representing an earlier weaning age.

6.5 Discussion

As no significant results were produced for the cross-sectional approach it was not possible to investigate changes in grey matter volume associated with early weaning, and therefore the first aim of this study could not be met. As with the ageing VBM study, this lack of significant results can likely be at least partially explained by the limited sample size. Due to the COVID-19 pandemic and subsequent lockdowns it was not possible to collect data from as many subjects as was initially planned (see COVID impact statement). This was a particular issue for the study of early life stress as the PRIME-DE datasets do not provide weaning age information, and the weaning

ages of the macaques in the NIDA dataset were unknown. This resulted in a much smaller sample size for this study than the studies of ageing discussed in chapters 4 and 5. The inclusion of scanner in the model may have further limited the power of the analysis, but given the vastly differing scan parameters and image quality across scanners this inclusion was necessary. Additionally, the relatively limited variability in weaning age may have contributed to the inability to find significant results. The majority of subjects were weaned after 12 months and many were weaned after 24 months, with all of the subjects who were weaned before 12 months coming from Newcastle University.

The impacts of weaning age on grey matter volume were also investigated cross-sectionally using an age-matched dataset. This dataset had fewer subjects than the full cross-sectional dataset, but as age and scanner did not need to be controlled for in the model it was hoped that this analysis would be powerful enough to detect significant results. However, no significant results were detected, again likely due to the limited sample size. Repetition of this particular analysis with a larger sample would be of great interest as it should allow for the impacts of weaning age, and by proxy early life stress, on grey matter volume to be elucidated without them being obscured by the effects of ageing or weaning age and ageing interactions. Acquiring a large enough sample for this analysis to detect significant results though may prove to be difficult, as it would require the weaning ages to not only to be known but also to be fairly varied, and for all of the subjects to have been the same age at the time the scans were acquired.

The analyses with both cross-sectional datasets were repeated with weaning age converted to a categorical variable, with the cut off set at 12 months. This age was chosen as Prescott *et al.* (2012) had previously recommended that macaques should be weaned between the ages of 10 and 14 months. However, no significant results were identified, and this was also likely due to a combination of the limited sample size and the fact that relatively few subjects had a weaning age below 12 months. Further research is therefore needed with a larger sample size in order to elucidate the impacts of weaning age on grey matter volume in macaques, and in particular at what age does weaning no longer have an impact on brain structure.

However, it is also possible that no significant results would have been detected, when weaning was encoded as a categorical variable, even with a larger

sample size. Potentially, when macaques are weaned later than 6 months, any impacts of the stress caused by this event on their grey matter volume may either be: 1) transitory, and so no longer detectable during adulthood, and/or 2) of too small a magnitude to be detectable during adulthood, when other factors such as ageing have had a larger impact on the brain structure. This would explain why Spinelli *et al.* (2009) and Wang *et al.* (2018) both identified grey matter volume changes in their studies, as not only did they utilise subjects that were weaned immediately after birth (which would likely be the most stressful time to be weaned) but they investigated changes prior to adulthood. Future research should therefore investigate the impacts of different weaning ages using subjects that have not yet reached adulthood, as it was not possible in the current study to investigate the aim of whether at a certain age weaning no longer impacts on grey matter volume. These subjects could then be followed through adulthood to identify whether the impacts of weaning are transitory and/or whether they are masked later in life by the impacts of other factors such as ageing.

The longitudinal approach in this study could not directly investigate changes associated with weaning age, but instead was utilised to determine whether there were significant changes in grey matter volume associated with an interaction between weaning age and ageing. No significant impact on total grey matter volume was identified, but one significant cluster was identified. This significant cluster was located in visual area 2 (V2), within the occipital lobe. This indicates that weaning age modulates ageing processes. Though it was hypothesised that subjects weaned earlier would show greater grey matter volume decreases than those weaned later, they actually displayed a greater age-related *increase* in V2 grey matter volume. No previous studies have indicated that early weaning or early life stress (or an interaction between either of these factors and ageing) are associated with increased grey matter in visual area 2. However, both Wang *et al.* (2018) and Tomoda *et al.* (2009) have identified *decreases* in the grey matter volume of the nearby visual area 1 with early life stress, in macaques and humans respectively. Our finding of earlier weaning being associated with greater age-related increases in grey matter volume within V2 is therefore highly unexpected. It is possible that this result indicates non-linear effects of ageing or weaning age and ageing interactions, as the macaques in the current study were older than those included in previous macaque studies of the

impacts of early weaning on grey matter volume (though when tested statistically, there was no significant evidence of non-linear effects of ageing for this cluster in the current study). It also cannot be ruled out that the impacts of weaning itself are non-linear, with potentially both neurodegenerative and neuroprotective impacts resulting from weaning at different ages. Ultimately, this result requires further investigation with a larger sample size.

When weaning age was converted to a categorical variable no significant results were found using the longitudinal approach, potentially indicating that the significant interaction between weaning age and ageing was not driven exclusively by the subjects weaned before 12 months. This could perhaps be an indication that even weaning after 12 months affects the ageing brain. This would not be surprising, as in the wild male macaques do not tend to leave their maternal group until around the age of 4 or 5, and female macaques usually remain in their maternal group for the whole of their lives (Prescott *et al.* 2012). Unlike the cross-sectional samples, the longitudinal dataset has a fairly even split between subjects weaned before 12 months and subjects weaned after, with a ratio of 6 to 4 subjects. It therefore at first appears unlikely that an unevenness of groups contributed to the lack of significant results when weaning age was encoded as a categorical variable. However, it should be noted that both of the female subjects were included in the group weaned after 12 months, so in terms of male subjects the ratio is actually 6 to 2. If the hypothesis that early weaning has a greater impact on female macaques than males is true, then this may then have confounded the analysis and played a role in the lack of significant results.

Furthermore, because data was only available for very few female macaques (both cross-sectionally and longitudinally) it was not possible to compare the impacts of weaning age, or weaning age and ageing interactions, on males and females in this study. Therefore, future research is needed to determine if there is a sex difference in the impacts of both weaning age, and weaning age and ageing interactions, on grey matter volume.

In conclusion, using a longitudinal approach the current study identified greater grey matter volume expansion associated with earlier weaning age, localised to visual area 2, within the occipital lobe. This finding is both novel and unexpected, and therefore requires further research with a larger sample size.

Chapter 7: Surface Based Analyses of the Impacts of Early Life Stress on Brain Structure

7.1 Abstract

The impacts of early life stress on cortical thickness in rhesus macaques have not been previously investigated. One potential source of stress during early life, which is common amongst captive macaques, is early weaning. In the wild, male macaques tend to leave their maternal group around the age of 4 or 5 years, whereas female macaques often spend their whole lives in their maternal group. The current study utilised macaques during early to mid-adulthood, which had been weaned between the ages of 6 and 47 months. For subjects weaned before 12 months, significantly lower cortical thickness was identified in regions of both the temporal and occipital lobes. These results are similar to those previously identified in human adults, though there was a notable lack of significant results in the frontal lobe. The current study also utilised a longitudinal approach, which allowed for investigation of the interaction between weaning age and within-subject ageing effects. Significant results were identified in regions of the parietal and occipital lobes, with subjects that were weaned earlier showing decreases in cortical thickness with ageing in these regions. All of the findings of this study are novel, as no prior studies have investigated how early life stress affects cortical thickness in rhesus macaques. Importantly though, the results were in similar regions to those identified by previous human studies of the impacts of early life stress on cortical thickness, giving strength to the use of rhesus macaques as model animals.

7.2 Introduction

It is well established that early life stress is associated with changes in brain structure and, though our voxel-based morphometry study was unable to find any significant results (see chapter 6), previous studies did identify volumetric changes connected to early life stress (Spinelli *et al.* 2009; Tomoda *et al.* 2009; De Brito *et al.* 2012; Gorka *et al.* 2014; Lim *et al.* 2014; Walsh *et al.* 2014; Tyborowska *et al.* 2018; Wang *et al.* 2018; Tymofiyeva *et al.* 2022; Malhi *et al.* 2023). However, tissue volumes are composite measures comprising both thickness and surface area, and so may lack sensitivity (Storsve *et al.* 2014). By investigating cortical thickness or

surface area individually it may be possible to better elucidate subtle impacts of early life stress on brain structure. The present study therefore focused on the impacts of early life stress on cortical thickness, measured using a surface-based morphometry approach.

In human surface-based morphometry studies, one of the most consistent findings is that early life stress is associated with reduced cortical thickness in the orbitofrontal cortex. This has been reported in children, adolescents and adults (Kelly *et al*. 2013; McLaughlin *et al.* 2014; Monninger *et al.* 2020; Kautz *et al.* 2021). The prefrontal and frontal regions more generally are also widely implicated as being thinner in those that have experienced early life stress, across children, adolescents and adults (Kelly *et al.* 2013; McLaughlin *et al.* 2014; Saleh *et al.* 2017; Busso *et al.* 2017; Bounoua *et al.* 2020).

McLaughlin *et al.* (2014) also found that children that had experienced early life stress, in the form of institutionalisation, had decreased cortical thickness in both temporal and parietal brain regions. Saleh *et al.* (2017) then identified decreased cortical thickness in areas of the parietal lobe of adults who experienced early life stress, and Busso *et al.* (2017) found decreased cortical thickness in areas of the temporal lobe for adolescents that had experienced childhood abuse.

Tomoda *et al.* (2012), Bounoua *et al.* (2020) and Rosada *et al.* (2022) all found evidence of reduced cortical thickness in regions within the occipital lobe for adults that had experienced early life stress, with Tomoda *et al.* (2012) and Rosada *et al.* (2022) particularly highlighting lower cortical thickness in the lingual gyrus. Other regions reported as showing cortical thinning in relation to early life stress include the cingulate cortex (Kelly *et al.* 2013- in children; Ross *et al.* 2021- in adolescents and adults) and the insula (Saleh *et al.* 2017- in adults). Results of human studies are therefore somewhat mixed but imply that widespread cortical thinning may be present in those that experience early life stress.

However, investigating early life stress in humans comes with a number of issues which could confound the results of the studies. First of all, it is difficult to investigate early life stress in humans without including subjects who have psychiatric disorders (either diagnosed or underlying) such as post-traumatic stress disorder or depression. These subjects may have brain structural differences that are connected to their disorder rather than being a result of early life stress, which can

then obfuscate the true impacts of early life stress. Additionally, it is near impossible to control for all potential stressors (and anti-stressors) in humans, meaning that other factors unrelated to early life stress may cause brain structural changes that are then misinterpreted as being due to early life stress. Finally, the use of a cross-sectional, retrospective study design, which is common to many human studies, can introduce recall bias (Althubaiti 2016). This study design means that whether someone experienced early life stress, and the severity and type of this stress, is determined later in life through simply asking the subjects about their early life experiences. If the subjects then misremember or forget experiences, that would be relevant to the study, they may be misclassified in terms of early life stress, confounding the final results. These issues can be avoided through the use of animal models, such as rhesus macaques.

As macaques can only show depression- and anxiety-like behaviours rather than developing full psychiatric conditions, such as post-traumatic stress disorder or depression, there is minimal concern of the results being confounded by brain changes resulting from underlying or diagnosed disorders (Ausderau *et al.* 2023). Additionally, macaques utilised in research live in a highly controlled environment, allowing for easier identification of any potential stressors (or antistressors), allowing for factors unrelated to early life stress to be identified and either avoided or statistically controlled for. Also, as has been previously discussed, longitudinal research is more efficient in macaques and, even for cross-sectional studies of early life stress, captive macaques are usually monitored throughout their life course, allowing for objective identification of any early life stress as opposed to subjective, retrospective recall.

Prior to the current study, no previous surface-based morphometry research on the effects of early life stress on cortical thickness in rhesus macaques could be identified, so the impacts are currently unknown. Hence, there is a clear need for research into the impacts of early life stress on cortical thickness in rhesus macaques, and one potential cause of early life stress is premature weaning. As discussed in chapter 6, early weaning is thought to be a source of stress as it has been shown to lead to alterations in behaviour, physiology and the immune system (Prescott *et al.* 2012). Furthermore, studies which investigated subjects weaned immediately after birth have found distinct volumetric losses in different brain regions

(Spinelli *et al.* 2009; Wang *et al.* 2018). This study aimed to identify how being weaned early affects cortical thickness in rhesus macaques, with a focus on the period of young to mid-adulthood, as this is the life period in humans when many psychiatric disorders will commonly manifest (Leach and Butterworth 2020). It is possible that the inclusion of subjects of different ages in the sample will affect the results, so the analysis will also be undertaken using an age-matched dataset. A longitudinal analysis in order to elucidate any weaning age x ageing interactions will also be carried out.

7.3 Methods and Materials

7.3.1 Datasets and inclusion criteria

The same datasets as were used for the VBM study of the impacts of early life stress were utilised for the surface-based analyses (see chapter 6 table 9). Briefly, inclusion criteria consisted of: 1) being at least 5 years of age but below 16 years of age, 2) weaning age data being available, 3) passing visual quality control, and 4) having at least 3 subjects per site for cross-sectional data or at least 3 scans per subject for longitudinal data (covering minimum of 18 months, with 3 or more months between scans). Scans from 32 subjects (24 of which were male), across 3 sites, were included in the final cross-sectional sample. The longitudinal sample consisted of 10 subjects (8 of which were male) from the Newcastle University dataset. An age-matched cross-sectional dataset was also utilised, which included scans from 8 subjects (6 of which were male) from the longitudinal sample, taken when they were around 8.4 years old.

7.3.2 Statistical analyses

Analyses were first carried out utilising average cortical thickness as the input data. Following this, the Matlab toolbox Surfstat was used to carry out the statistical analyses, on data smoothed with a 1mm kernel. The cortical thickness (CT) of each vertex was utilised as input data for these analyses. Both the cross-sectional and the longitudinal approaches utilised general linear models. For the cross-sectional approach with the full sample, weaning age, age and total intracranial volume were included in the model as fixed effects, whilst scanner was included as a random

effect (statistical model: CT= β1*weaning age + β2*age + β3*TIV + random(scanner) + constant). With the age-matched cross-sectional dataset, weaning age and total intracranial volume were included as fixed effects (age and scanner did not need to be included in the model as they were unchanged across subjects; statistical model: CT= β1*weaning age + β2*TIV + constant). For the longitudinal approach weaning age and mean-centred age were included as fixed effects, and subject was included as a random effect (statistical model: CT= β1*weaning age + β2*mean-centred age + β3*(weaning age*mean-centred age) + random(subject) + constant). For all of the analyses significance was thresholded at 0.05 (corrected for multiple comparisons with family wise error [FWE]) at the cluster-level. As very few subjects in either the cross-sectional or the longitudinal samples were female, statistics were carried out both including and excluding the female subjects.

7.4 Results

7.4.1 Cross-sectional approach- impacts of weaning age

The impacts of weaning age on average cortical thickness were first investigated for the cross-sectional dataset. No significant effect of weaning age on average cortical thickness was identified (β= -0.05, Std. error= 0.06, DF= 23, p= 0.40, figure 32). This analysis was repeated with the age-matched dataset (and age removed from the model), but again no significant effect of weaning age on total grey matter volume was identified (β= -0.20, Std. error= 0.14, DF= 5, P= 0.21).

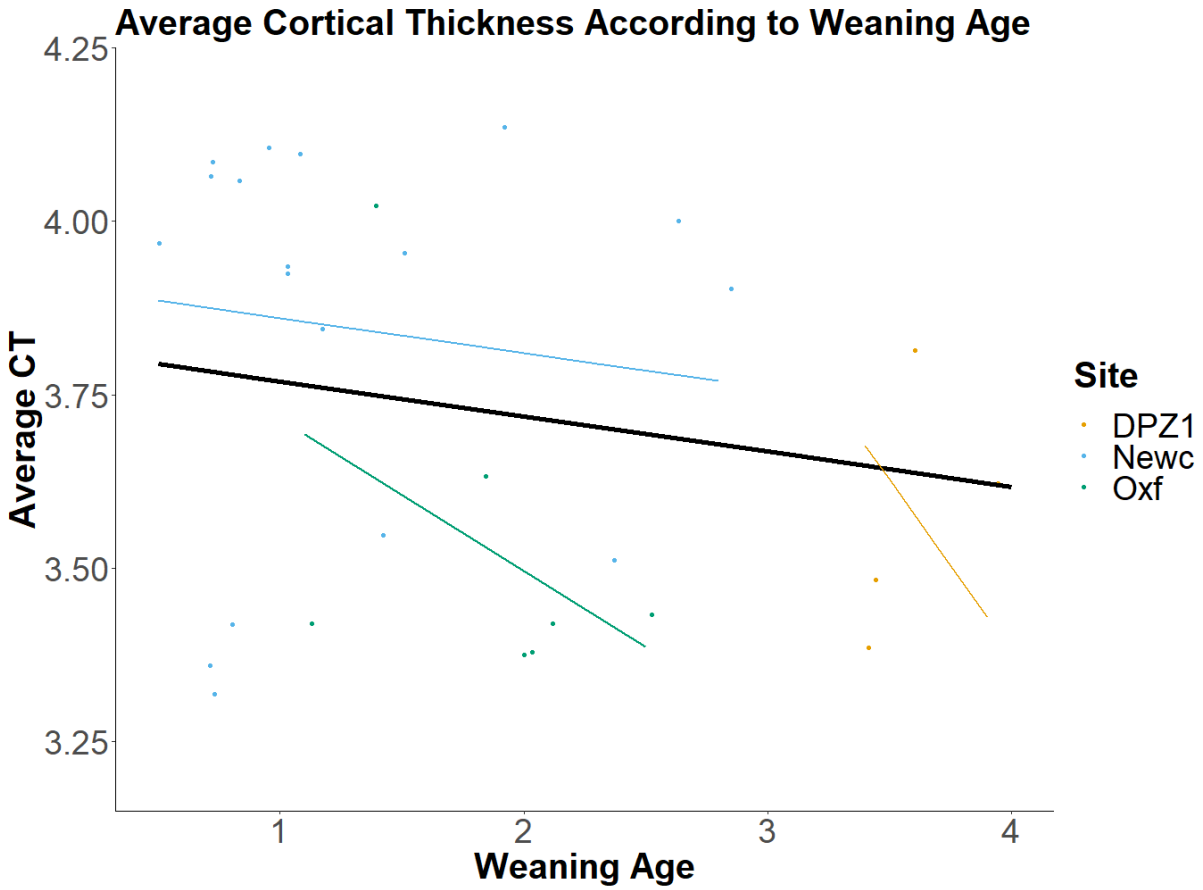

Figure 32: Changes in Average Cortical Thickness According to Weaning Age. The bold black linear line corresponds to the main effect of weaning age, while controlling for TIV and with site/scanner declared as a random effect. The thin coloured lines correspond to linear fits of weaning age effect in each site while controlling for TIV. Dots correspond to raw data (unadjusted for TIV).

Due to the results of the longitudinal VBM approach (see Chapter 6, section 6.4.2) both potential decreases and potential increases in cortical thickness associated with weaning age were investigated. No significant results were identified using the cross-sectional approach with weaning age encoded as a continuous variable. This was the case for both the full cross-sectional sample and the age-matched dataset. Excluding the female subjects also did not lead to any significant results for either of these cross-sectional analyses.

However, when weaning age was converted to a categorical variable ('weaned before or after 12 months of age') there were significant results for both the full cross-sectional sample and the age-matched dataset. For the full cross-sectional sample, there were 3 clusters in the right hemisphere and 2 in the left hemisphere where

cortical thickness was significantly lower for subjects with a weaning age below 12 months. (see figure 33). The right hemisphere clusters were localised to the isthmus of the cingulate cortex (2 clusters) and visual area 2. The left hemisphere clusters were localised to the parahippocampal gyrus and visual area 2.

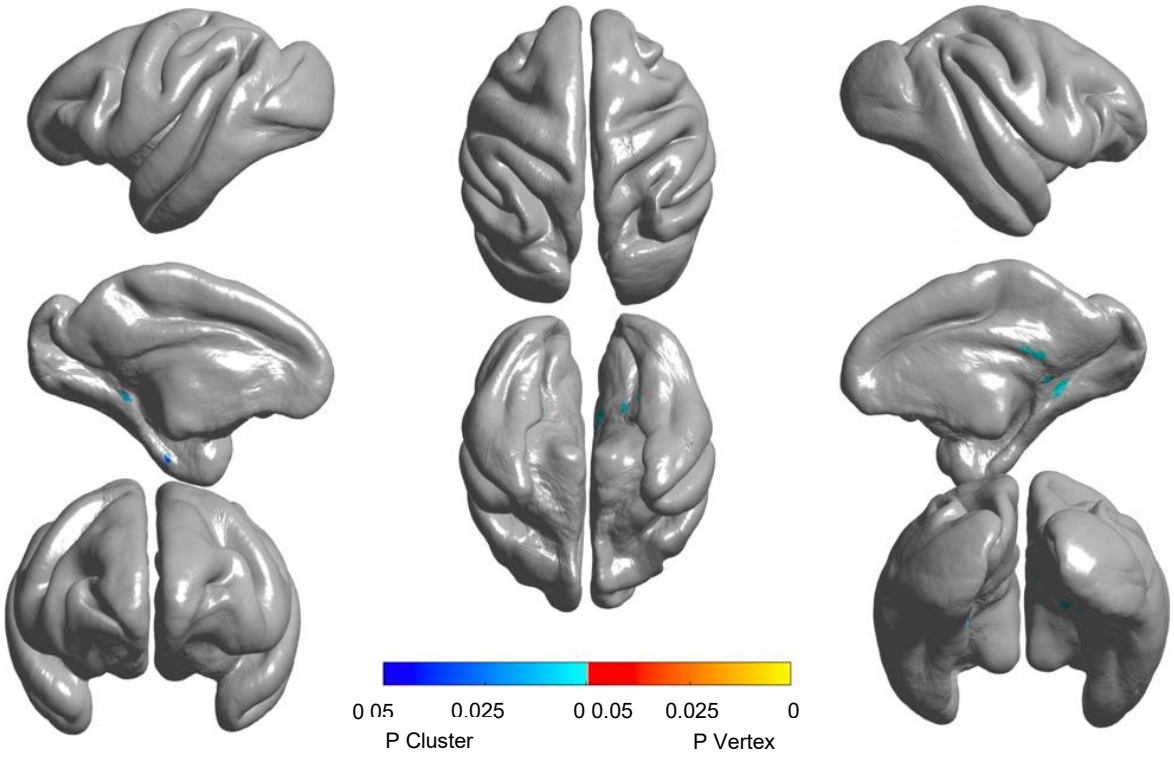

Figure 33: Significant Cross-sectional Decreases in Cortical Thickness, Associated with Early Weaning. 3D surface map showing regions where subjects weaned before 12 months had significantly lower cortical thickness, identified using the full cross-sectional dataset.

However, when the female subjects were excluded, these clusters were no longer significant, but two clusters towards the back of the brain were weakly significant (see figure 34). One of these clusters was localised to left visual area 2 and the other to dorsal visual area 4.

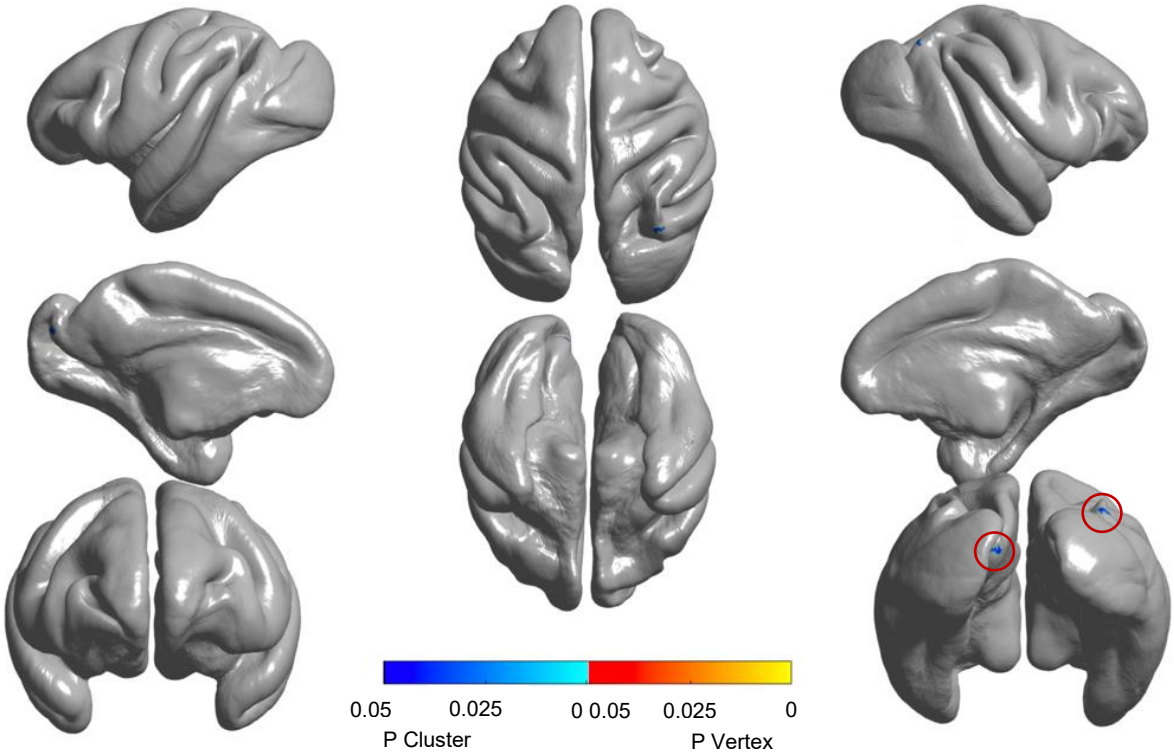

Figure 34: Significant Cross-sectional Decreases in Cortical Thickness with Female Subjects Excluded, Associated with Early Weaning. 3D surface map showing regions where subjects weaned before 12 months had significantly lower cortical thickness, when females were excluded from the full cross-sectional dataset.

With the full cross-sectional dataset there were also 3 clusters where cortical thickness was significantly higher for subjects weaned before 12 months (see figure 35). These clusters were localised to brain region TEO (2 clusters) and the dorsal subdivision of brain area 46.

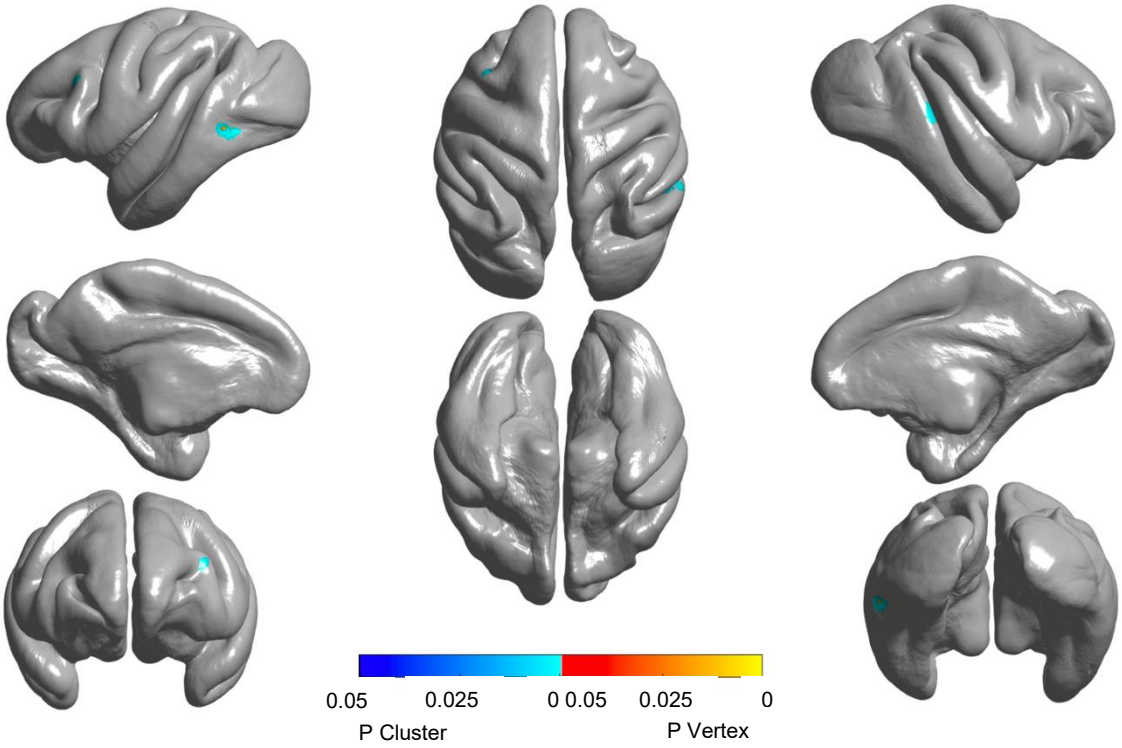

Figure 35: Significant Cross-sectional Increases in Cortical Thickness, Associated with Early Weaning. 3D surface map showing regions where subjects weaned before 12 months had significantly *greater* cortical thickness, identified using the full cross-sectional dataset.

When female subjects were excluded one cluster within brain region TEO was the only one of the aforementioned 3 clusters still to be significant. Additionally, there were two further clusters where cortical thickness was significantly higher for subjects weaned before 12 months, localised to the ventral part of visual area 4 and within the orbito-medial prefrontal area (see figure 36).

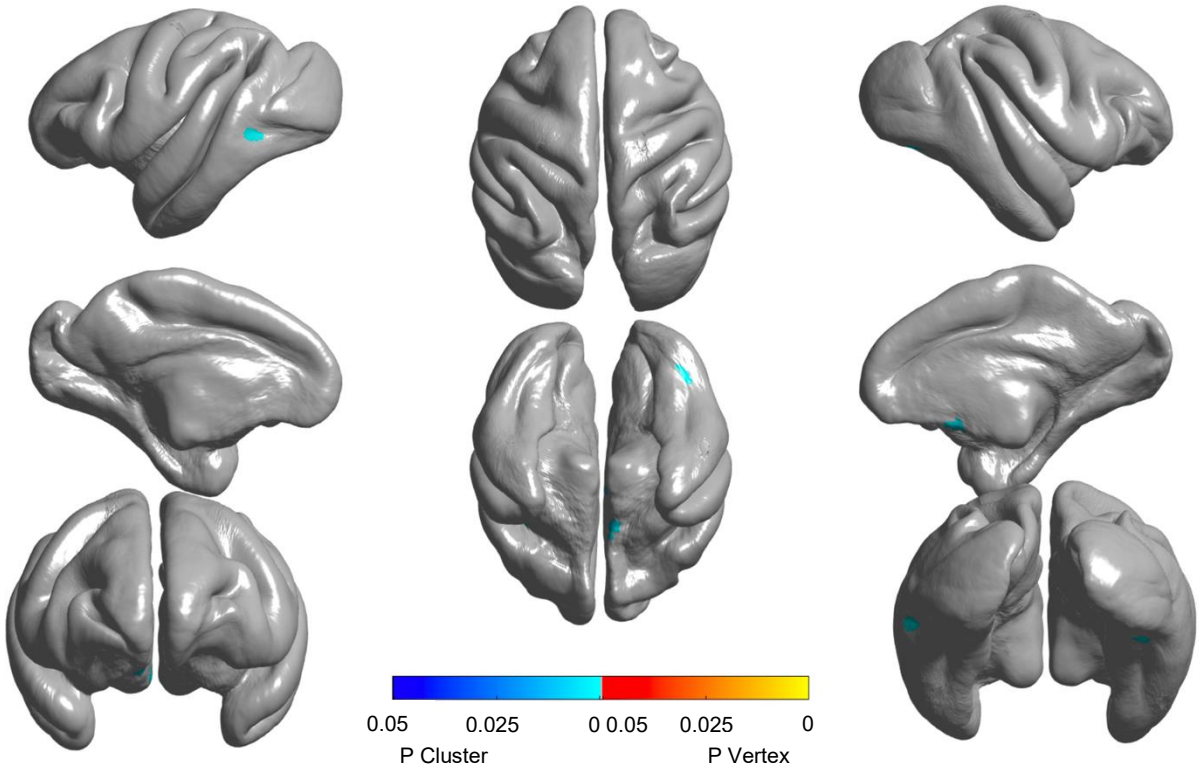

Figure 36: Significant Cross-sectional Increases in Cortical Thickness with Female Subjects Excluded, Associated with Early Weaning. 3D surface map showing regions where subjects weaned before 12 months had significantly *greater* cortical thickness, when females were excluded from the full cross-sectional dataset.

For the age-matched dataset, there was also a cluster showing significantly lower cortical thickness for subjects with a weaning age below 12 months. For this dataset the cluster was localised to temporal area TE, within the left temporal lobe (see figure 37). There were no clusters showing significantly higher cortical thickness for subjects with a weaning age below 12 months. When the female subjects were excluded, there were no significant results, likely due to only one male in this dataset having a higher weaning age than 12 months.

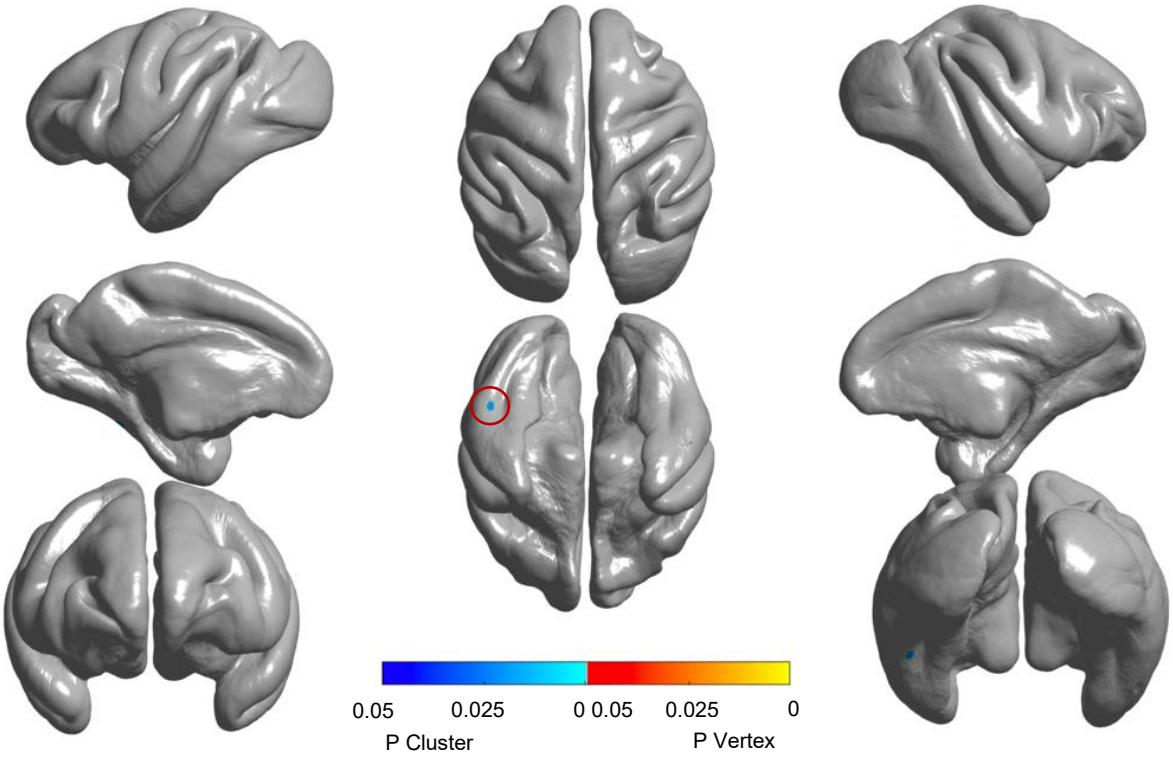

Figure 37: Significant Age-matched Differences in Cortical Thickness, Associated with Early Weaning. 3D surface map showing regions where subjects weaned before 12 months had significantly lower cortical thickness, identified using the age-matched dataset.

7.4.2 Longitudinal approach- impacts of weaning age x ageing interactions

An initial investigation of the impacts of weaning age and ageing interactions on average cortical thickness did not identify any significant change (β= -0.045, Std. error= 0.033, DF= 8, p= 0.21).

For the investigation of weaning age and ageing interactions using a regional longitudinal approach, subjects with a lower weaning age showed significant decreases in cortical thickness with ageing in four clusters (see figure 38). This included a bilateral cluster in visual area 1, a cluster localised to the left dorsal visual area 4, and a cluster within the left ventral subdivision of brain area 46.

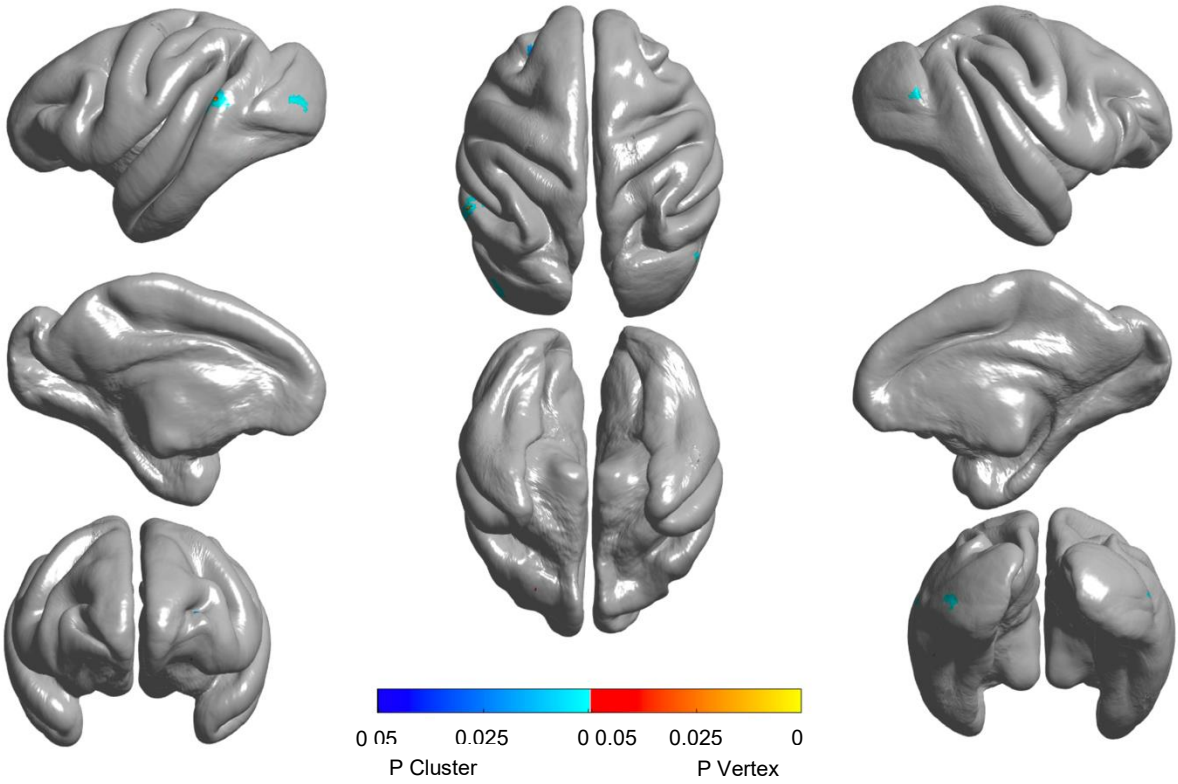

Figure 38: Significant Weaning Age x Ageing Interactions for the Full Longitudinal Dataset. 3D surface map showing regions where significant weaning x ageing interactions were identified, using the full longitudinal dataset.

All four clusters remained significant when female subjects were excluded from the longitudinal analysis of weaning age and ageing interactions, however there were also additional significant clusters in the vicinity of visual area 2, as well as a cluster within the midcingulate cortex (see figure 39).

These clusters were no longer significant when weaning age was encoded as a categorical variable, regardless of whether female subjects were included or excluded.

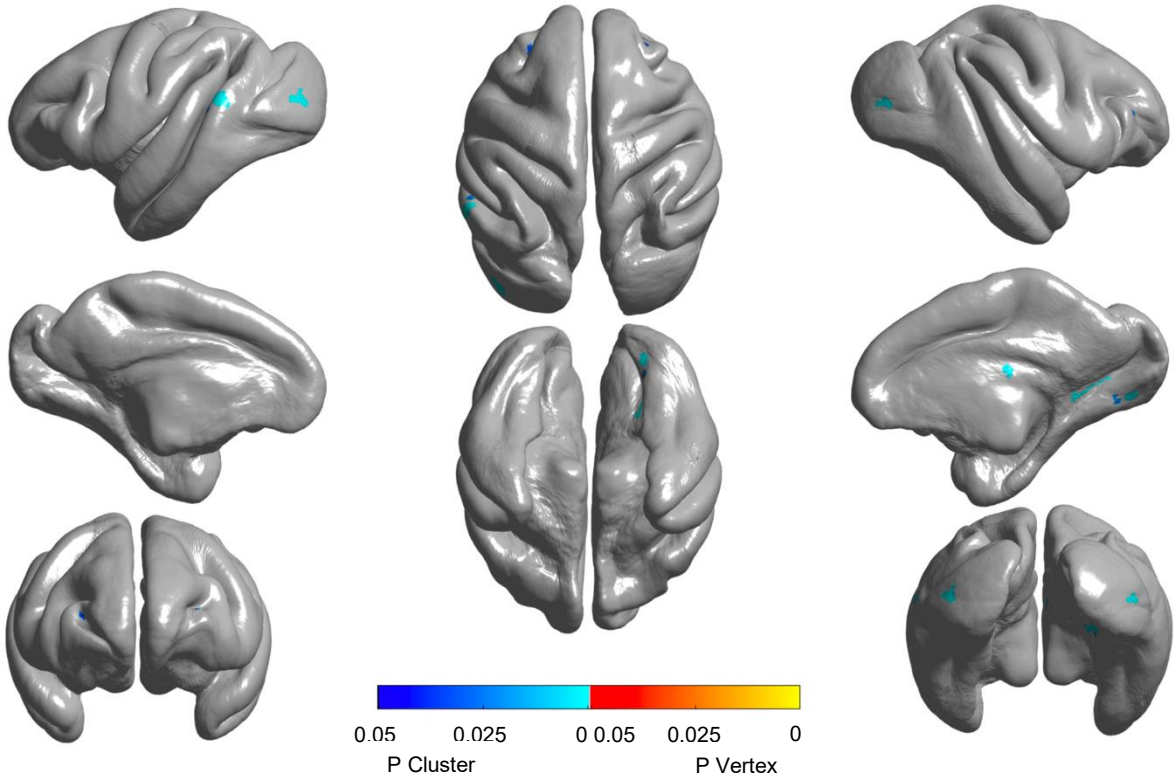

Figure 39: Significant Longitudinal Weaning Age x Ageing Interactions with Female Subjects Excluded. 3D surface map showing regions where significant weaning x ageing interactions were identified, using the longitudinal dataset with female subjects excluded.

7.5 Discussion

As with the voxel-based morphometry study of weaning age, the limited sample size likely contributed to the lack of significant results when weaning age was studied cross-sectionally as a continuous variable. However, with the surface-based morphometry approach, there were significant results when weaning age was treated as a categorical variable. With the full cross-sectional dataset, subjects with a weaning age before 12 months had significantly lower cortical thickness across multiple brain regions, primarily in the occipital lobe. A bilateral cluster was identified in visual area 2, a key region in the visual cortex, crucial to visual processing (Freeman *et al.* 2014). Tomoda *et al.* (2012) previously reported cortical thinning in this region for human adults who witnessed domestic violence during childhood.

There were also two clusters in the isthmus of the cingulate cortex. The cingulate cortex in general has been shown to be involved in a wide array of functions. Most relevantly for studies of stress, it appears to have a role in emotions (Stevens, Hurley and Taber 2011). In human studies, Kelly *et al.* (2013) identified reduced cortical thickness in the anterior cingulate cortex of children who had

experienced early life stress, and Ross *et al.* (2021) found a similar result in the middle cingulate cortex for adolescents and adults who had experienced early life stress.

Finally, there was also a cluster in the left parahippocampal gyrus, which is part of the medial temporal lobe and known to have a major role in encoding and retrieving episodic memories (Zola-Morgan *et al.* 1989; Diana, Yonelinas and Ranganath 2010). A multitude of studies have shown that episodic memories appear to be affected by stress (Shields *et al.* 2017). Cortical thinning of the parahippocampal gyrus with early life stress has been previously reported in human adolescents (Busso *et al.* 2017). The results for the full cross-sectional sample therefore parallel previous human studies, expanding their findings to cover the period of early to mid-adulthood. Additionally, the fact that significant changes in cortical thickness were identified at all, when no significant changes in volume could be identified using a cross-sectional approach (see chapter 6), supports the concept of cortical thickness being a more sensitive measure than grey matter volume.

Notably, when the female subjects were excluded from the cross-sectional dataset, the previously discussed clusters were no longer significant. Another cluster in visual area 2 was weakly significant, however it was not near to the bilateral cluster observed with the full dataset. There was also a (weakly) significant cluster within visual area 4, another region in the visual cortex, which interacts with visual area 2 (Fang *et al.* 2022). The difference in results is likely partially due to the relatively small sample size, though sex differences may also have played a role. Importantly, it should be noted that though the clusters differ when females are excluded, the brain regions showing significance are still broadly similar, as they cover areas of the visual cortex within the occipital lobe.

However, there were also clusters for which subjects with a weaning age before 12 months had significantly *higher* cortical thickness. These clusters were within the temporal and occipital lobes and differed slightly depending on whether female subjects were included or excluded from the sample. These significant increases were relatively unexpected as we hypothesised that earlier weaning would be associated with decreases in cortical thickness, as there is strong evidence for early life stress being associated with decreases in cortical thickness in humans. Notably many previous human studies which have highlighted the occipital lobe in

particular as displaying widespread decreases in cortical thickness associated with early life stress, conflicting with our finding of significantly higher cortical thickness in some regions (Tomoda *et al.* 2012; Bounoua *et al.* 2020; Rosada *et al.* 2022). Further studies of the impacts of early weaning on cortical thickness in rhesus macaques are clearly needed in order to clarify and explain these findings.

When the age-matched dataset was utilised, with weaning age as a categorical variable, there was one cluster where subjects with a weaning age before 12 months had significantly lower cortical thickness. This cluster was localised to temporal area TE, in the left inferior temporal lobe, another brain area associated with visual processing (Kravitz *et al.* 2013). Busso *et al.* (2017) also found significantly lower cortical thickness in this region for human adolescents that had experienced early life stress. Exclusion of the female subjects from the age-matched dataset resulted in this cluster no longer being significant, likely due to the further limiting of the sample size. For the age-matched dataset there were no clusters where subjects weaned before 12 months displayed significantly higher cortical thickness. As the subjects in this dataset were age-matched to be approximately 8.4 years old, the results of this analysis suggest that early weaning, and therefore early life stress, may be most strongly associated with cortical thickness changes in the temporal lobe during early adulthood. Taken together with the results for the full cross-sectional dataset, this perhaps implies that early life stress may be associated with cortical thickness changes in the temporal lobe first during early adulthood, followed by the occipital lobe as the macaques age through to mid-adulthood. This could potentially explain why human studies have previously reported cortical thickness reductions in the temporal lobes of children and adolescents that experienced early life stress (McLaughlin *et al.* 2014; Busso *et al.* 2017), whilst reductions in the occipital lobe are more widely reported in adults that experienced early life stress (Tomoda *et al.* 2012; Bounoua *et al.* 2020; Rosada *et al.* 2022). Additionally, the findings with both the age-matched dataset and the full cross-sectional dataset appear to indicate a particular vulnerability of regions involved in visual processing to the impacts of early life stress (in the form of earlier weaning). This correlates with and expands the findings of our voxel-based morphometry study of the impacts of early weaning, which identified an age-related decrease in the grey matter volume of visual area 2 for subjects weaned earlier. This vulnerability of the

visual system to early life stress has been recently confirmed and expanded on in a study utilising mice (Poplawski *et al.* 2023- preprint).

The longitudinal analysis in this study allowed for the investigation of how weaning age and ageing interactions relate to changes in cortical thickness, during early to mid-adulthood in rhesus macaques. Though the interaction between weaning age and mean-centred age did not have a significant impact on average cortical thickness, significant changes in the cortical thickness of a number of brain regions was identified, giving support for early weaning modulating the impacts of ageing on brain structure. When treating weaning age as a continuous variable, two significant clusters were identified in the occipital lobe, one significant cluster was identified in the parietal lobe and one significant cluster was identified in the frontal lobe. The occipital lobe clusters were localised to bilateral visual area 1 and the parietal lobe cluster was localised to the dorsal part of visual area 4, providing further evidence for a vulnerability of the visual system to early life stress. Additionally, these results could be an indication that the cortical thinning of areas of the visual cortex identified by the cross-sectional approach of the current study were influenced by ageing, providing a potential explanation for why the age-matched dataset did not identify significant results in the same regions.

The frontal lobe cluster identified by the longitudinal approach was localised to brain area 46, which is part of the dorsolateral prefrontal cortex. Previous studies in human children have identified cortical thinning of brain area 46, and the dorsolateral prefrontal cortex more generally, as being associated with early life stress (Kelly *et al.* 2013; McLaughlin *et al.* 2014). It is notable that this was the only significant frontal lobe cluster identified by the current study, with no frontal lobe regions being identified by the cross-sectional approach as showing cortical thinning associated with early weaning. This contrasts with how frequently cortical thinning of frontal lobe regions has been highlighted by human studies of the impacts of early life stress on cortical thickness (Kelly *et al.* 2013; McLaughlin *et al.* 2014; Saleh *et al.* 2017; Busso *et al.* 2017; Bounoua *et al.* 2020). Given that we previously detected results in the frontal lobe using both a cross-sectional and a longitudinal approach for the impacts of ageing on cortical thickness (see chapter 5), it is unlikely that the limited frontal lobe results in the current study are due to errors in the surfaces utilised. It is possible that the limited frontal lobe results are due to the age group used, however

human studies have found more extensive changes in frontal regions across children, adolescents and adults (Kelly *et al.* 2013; McLaughlin *et al.* 2014; Saleh *et al.* 2017; Busso *et al.* 2017; Bounoua *et al.* 2020). There could be a species-specific difference in terms of the vulnerability of the frontal lobe to early life stress, but this is difficult to determine due to the lack of other macaque studies, and would contrast with the similar vulnerability of frontal regions in macaques and humans to other factors such as ageing. One other potential explanation would be that different forms of early life stress may result in different impacts on brain structure, and so early weaning may simply not be a stressor that causes extensive grey matter changes in the frontal lobe. Further research is clearly needed to elucidate the true reason for the differing results in the frontal lobe for the current study and previous studies in humans.

When female subjects were excluded from the longitudinal dataset the aforementioned clusters remained significant, but there were also two further significant clusters, localised to visual area 2 and the midcingulate cortex. It is unclear why the exclusion of female subjects would lead to the addition of these significant clusters, but sex-differences in the impacts of weaning age and ageing interactions cannot be ruled out. Notably, this finding contrasts with the significant increase in the grey matter volume of visual area 2, associated with a weaning age and ageing interaction, which was observed using a voxel-based approach. It is unclear why these conflicting results were present. However, given that significant decreases in the cortical thickness of visual area 2 have previously been identified in humans that have experienced early life stress, the surface-based result for this region may be more reliable (Tomoda *et al.* 2012). As such, the identification of cortical thinning associated with a weaning age and ageing interaction within visual area 2 provides support for the findings of the cross-sectional surface-based approach, and for those of Tomoda *et al.* (2012), whilst also indicating that those results may be influenced by ageing. Additionally, this significant longitudinal results gives further evidence for the vulnerability of brain regions involved in visual processing to the impacts of early weaning and weaning age x ageing interactions. The significant cortical thinning of the midcingulate cortex is similar to the thinning of the isthmus of the cingulate cortex observed with the cross-sectional approach. As was previously discussed, the cingulate cortex plays a role in emotions and thinning

of the midcingulate cortex specifically has been previously observed in a study of adolescent and adult humans that had experienced early life stress (Ross *et al.* 2021).

Given the limited sample size of the current study, future studies should utilise a larger sample, with a more even proportion of male and female subjects. This should allow for any sex differences to be accurately identified. Additionally, these studies could aim to investigate a wider range of weaning ages, in order to determine whether there is an age at which weaning no longer has lasting impacts on cortical thickness.

To conclude, the current study found clear evidence of early weaning impacting on cortical thickness in rhesus macaques during young to mid adulthood. Subjects weaned before 12 months showed both significantly lower and higher cortical thickness than those weaned after 12 months, in different regions of both the temporal and occipital lobes. These results are relatively in line with what has previously been reported in human studies, though the lack of significant findings in the frontal lobe, and the presence of significantly higher cortical thickness in some regions of the temporal and occipital lobes, are notable differences. The longitudinal analysis of the current study also found a significant weaning x ageing effect, specifically in regions of the parietal and occipital lobes. Notably, for both the cross-sectional and longitudinal analyses, the majority of significant results were in regions involved in visual processing, suggesting a potential vulnerability of this system to early life stress. This is the first study to investigate the impacts of early weaning, and early life stress in general, on cortical thickness in rhesus macaques.

Chapter 8: General Discussion and Conclusions

8.1 Aim 1: Creation of the AutoMacq Processing Pipeline

The first aim of this project was to design, optimise and implement an analysis pipeline capable of processing structural MRI data from rhesus macaques. This aim was successfully met through the creation and optimisation of AutoMacq, an analysis pipeline capable of processing both cross-sectional and longitudinal datasets of macaque MRI data, with minimal manual intervention. AutoMacq utilises freely available software packages and can produce both voxel-based and surface-based metrics, making it accessible and novel amongst NHP processing pipelines.

Cross-sectional scans from 74 subjects and longitudinal datasets from 17 subjects were processed through AutoMacq. Scans were taken from across 7 sites with a wide range of scan protocols and parameters, and included subjects that were awake and subjects with open skulls (both of which are known to be problematic). AutoMacq produced accurate brainmasks for all of the scans processed through it, a comparable rate of success to what has been seen with more sophisticated deep-learning based approaches (Wang *et al.* 2021). Output error rates with AutoMacq were also notably low for cross-sectional data, with a slightly higher error rate for surface-based morphometry, compared to voxel-based morphometry. This difference may be partially explained by errors in surfaces being easier to visually identify than errors in voxel-based tissue segmentations, potentially resulting in some underestimation of voxel-based errors and/or some overestimation of surface-based errors. Regardless, for the cross-sectional data processed in the current project the error rate was low. This low error rate indicates that AutoMacq outperforms other pipelines when processing cross-sectional macaque MRI data, taken from across multiple sites (Garcia-Saldivar *et al.* 2021; Lepage *et al.* 2021).

However, output errors were more widespread when processing longitudinal data through AutoMacq, particularly in terms of surface-based outputs. These errors were often towards the front of the brain, and may have contributed to the identification of fewer results in the frontal regions than was expected for the ageing and weaning age studies (see sections 8.2 and 8.3). This higher error rate was likely the result of a number of factors.

Firstly, the nature of longitudinal processing in FreeSurfer means that any errors in the initial cross-sectional processing of some timepoints can be transmitted via the template to all of the timepoints during longitudinal processing. For the longitudinal processing of human data, it is recommended that manual corrections be carried out at the template stage and/or the cross-sectional processing stage in order to avoid this. With the current project we wanted to assess the success rate for macaque data without major manual corrections, and attempted to use the SPM tissue segmentations in place of manual corrections in FreeSurfer. This was successful in the vast majority of cases for the cross-sectional datasets but success for the longitudinal datasets was more limited. This highlights another factor potentially contributing to the lower success rate with longitudinal data though, the composition of the longitudinal datasets tested.

Longitudinal data was only available from relatively few sites, which resulted in the longitudinal sample being heavily weighted towards macaques from Newcastle University. The subjects from the Newcastle dataset were all scanned whilst awake, which can result in motion artifacts and a poorer signal to noise ratio. Additionally, the Newcastle scans utilised a coil set up that was not standardised between scans, and so the coils may have been in slightly different positions for each acquisition. Crucially, it is apparent visually that the scans from the Newcastle dataset often had particularly poor contrast towards the front of the brain, which matches where errors most commonly occurred in both the surfaces produced and the voxel-based segmentation outputs.

However, previous pipelines designed to process macaque MRI data have not discussed processing longitudinal data, and so it is not possible to compare the error rate for longitudinal data processed through AutoMacq with that of previously designed pipelines. Despite the errors in some of the outputs from AutoMacq though we subsequently demonstrated that the pipeline was highly reliable using both hemisphere and scan-rescan comparisons. This implies that even though some of the scans had errors, outputs were consistent both across hemispheres and between scan and rescan. Consequently, the errors observed are more likely to be due to issues with the quality of the individual scans than methodological issues coming from the pipeline itself.

8.2 Aim 2: Investigation of the Impacts of Ageing on Brain Structure During Early to Mid-adulthood

The second aim of this project was to assess the impacts of ageing on the brain structure of rhesus macaques, using both a cross-sectional and a longitudinal approach, during early to mid-adulthood. This aim was also successfully met, with investigations of changes in both grey matter volume and cortical thickness with ageing.

Initial investigations of total grey matter volume, utilising both the cross-sectional and longitudinal datasets, identified a significant decrease with ageing through adolescence to mid-adulthood. This decrease was found to be linear, though the sample only included a few subjects that were adolescents. As a consequence of this, it is possible that with a larger sample a non-linear trajectory would be identified, with different rates of decline for adolescence to early adulthood and early to mid-adulthood. This is likely to be the case, as many previous studies of ageing in humans have found evidence of a non-linear decrease in total grey matter volume over the life course (Lebel *et al.* 2012; Mills *et al.* 2016; Vinke *et al.* 2018). Notably, no significant decrease with ageing in average cortical thickness was identified, regardless of whether a cross-sectional or longitudinal approach was utilised. This lack of a significant result was unexpected, and merits further investigation with a larger sample size. Though it should be noted that it is in line with the results of Koo *et al.* (2012).

For subsequent analyses, the sample was restricted to only cover early to mid-adulthood. This was done not only because there were not enough adolescent subjects to accurately determine the impacts of ageing during this life period, but also because the period of early to mid-adulthood is rarely studied. This is despite the fact that early to mid-adulthood is potentially a crucial period both for age-related neurodegenerative disorders and cognitive decline, as well as for psychiatric conditions such as depression and anxiety (Edwards-Lee *et al.* 2005; Vo *et al.* 2020; Aartsen *et al.* 2002; Rönnlund *et al.* 2005; Leach and Butterworth 2020).

Region-specific changes in brain structure with ageing were investigated, both cross-sectionally and longitudinally, in terms of grey matter volume and cortical thickness. Cross-sectionally, the only results identified were in terms cortical thickness, with the majority of clusters showing age-related cortical thinning localised

to areas of the frontal lobe. This fits with the majority of previous human studies which identified prominent cortical thinning in regions of the frontal lobe (Fjell *et al.* 2009; Hogstrom *et al.* 2012; Lemaitre *et al.* 2012; Hurtz *et al.* 2014; Storsve *et al.* 2014; Fjell *et al.* 2015; Proskovec *et al.* 2020; Podgórski *et al.* 2021), though those studies focused on late adulthood. Further clusters of age-related cortical thinning were then also significant in the parietal lobe, as well as visual area 1 in the occipital lobe. Previous human studies have consistently identified cortical thinning of parietal regions during late adulthood (Fjell *et al.* 2009; Hogstrom *et al.* 2012; Lemaitre *et al.* 2012; Hurtz *et al.* 2014; Storsve *et al.* 2014; Fjell *et al.* 2015; Proskovec *et al.* 2020; Podgórski *et al.* 2021), and both Hurtz *et al.* (2017) and Proskovec *et al.* (2020) identified age-related cortical thinning of visual area 1 in human subjects (again during late adulthood). Notably, visual area 1 was the only brain region where the current study identified a decrease in cortical thickness using both a cross-sectional and a longitudinal approach.

With a longitudinal approach, decreases in grey matter volume with ageing were found primarily in areas of the temporal lobe, with further decreases in the frontal lobe, as well as the cerebellum. In terms of cortical thickness, with a longitudinal approach, more extensive decreases were identified, though they covered broadly similar regions to those where grey matter volume decreases were observed, with the addition of parietal lobe clusters. In particular, both the longitudinal study of grey matter volume and the longitudinal study of cortical thickness highlighted age-related decreases in regions around the superior temporal sulcus, and within the precentral opercular area. Previous studies in humans during late adulthood have also identified age-related decreases in both grey matter volume and cortical thickness in regions surrounding the superior temporal sulcus (Tisserand *et al.* 2004; Smith *et al.* 2007; Hutton *et al.* 2009; Fjell *et al.* 2009; Peelle *et al.* 2012; Hurtz *et al.* 2014; Storsve *et al.* 2014; Fjell *et al.* 2015; Ramanöel *et al.* 2018; Proskovec *et al.* 2020; Podgórski *et al.* 2021), with Alexander *et al.* (2008) also finding similar decreases in grey matter volume in macaques during late adulthood. Similarly, age-related decreases in the cortical thickness and grey matter volume of the precentral opercular area have been highlighted by previous studies in humans during late adulthood (Peelle *et al.* 2012; Lemaitre *et al.* 2012; Storsve *et al.* 2014; Podgórski *et al.* 2021). In fact, all of the significant results of both longitudinal

investigations broadly correspond to regions previously identified as showing age-related declines in studies of humans during late adulthood (Good *et al.* 2001; Tisserand *et al.* 2004; Smith *et al.* 2007; Fjell *et al.* 2009; Hutton *et al.* 2009; Hogstrom *et al.* 2012; Lemaitre *et al.* 2012; Long *et al.* 2012; Peelle *et al.* 2012; Hurtz *et al.* 2014; Storsve *et al.* 2014; Fjell *et al.* 2015; Ramanöel *et al.* 2018; Proskovec *et al.* 2020; Podgórski *et al.* 2021), older macaques (Alexander *et al.* 2008; Colman *et al.* 2009), and mid-adulthood (Bourisly *et al.* 2015).

However, age-related decreases in the parietal lobe were only identified longitudinally in terms of cortical thickness, and the frontal lobe showed somewhat more extensive age-related decreases in thickness than were seen longitudinally for grey matter volume. This could imply a greater sensitivity of cortical thickness to the impacts of ageing on brain structure, as was previously indicated by Borgeest *et al.* (2021- preprint) and Podgórski *et al.* (2021). Neither the voxel-based or the surface-based approach of the current study identified any significant increases associated with ageing. Though the longitudinal investigation of grey matter volume changes with ageing identified a trend towards an increase in visual area 1, both the cross-sectional and longitudinal studies of cortical thickness changes with ageing identified a significant decrease in this region. Both Hurtz *et al.* (2017) and Proskovec *et al.* (2020) also identified age-related decreases in cortical thickness in visual area 1, giving strength to the finding of significant decreases identified in the current project. Table 10 provides a summary of the areas of agreement and disagreement between the results of the current study and those of the previous ageing studies discussed.

Region	Current Study	Previous Studies
Precentral Opercular Area	↓GMV^{L}, ↓CT^{L}	↓CT^{CS} (Humans- [18])
Cortical Areas 44 and 45	↓GMV^{L}	↓CT^{CS} (Humans- [18])
Precentral Gyrus	↓CT^{L}	↓GMV^{CS} (Humans- [1]), -CT^{CS} (Humans- [5]), ↓$CT^{CS,L}$ (Macaques- [8]; Humans- [7,9,13,14,18])
Premotor Cortex	↓CT^{L}	↓$CT^{CS,L}$ (Humans- [12,15])
Superior temporal sulcus	↓GMV^{L}, ↓CT^{L}	↓GMV^{CS} (Macaques- [4]; Humans- [2,3,6,11,14,16]), ↓$CT^{CS,L}$ (Humans- [5,13,17])
Rostrotemporal regions	↓GMV^{L}	↓GMV^{CS} (Humans- [6])
Temporal Pole	↓GMV^{L}	↓GMV^{CS} (Macaques- [4]), ↓CT^{L} (Humans- [13,15])
Somatosensory area 1	↓CT^{L}	↓CT^{CS} (Humans- [12,17])
Somatosensory area 2	↓CT^{L}	↓CT^{CS} (Humans- [12])
Visual area 4	↓CT^{L}	↑CT^{CS} (Macaques- [8])
Visual area 7	↓CT^{L}	-
Precuneus	↓CT^{L}	-CT^{CS} (Humans- [5]), ↓$CT^{CS,L}$ (Humans- [9,12,13,14,18])
Post-central gyrus	↓CT^{L}	↓GMV^{CS} (Humans- [1,6,16]), -CT^{CS} (Humans- [5]), ↓CT^{CS} (Humans- [18])
Visual area 1	↓$CT^{CS,L}$	↓CT^{CS} (Humans- [12,17]), ↑CT^{CS} (Macaques- [8])
Visual area 2	↓CT^{L}	↓CT^{CS} (Humans- [12,17])
Cerebellum	↓GMV^{L}	↓GMV^{CS} (Humans- [1,3,16,19]),

		↑GMV^{CS} (Macaques- [4])
Brain Area 46	↓CT^{CS}	↓CT^{CS} (Humans- [9,18])
Medial Prefrontal Cortex	↓CT^{CS}	↓CT^{CS,L} (Humans- [5,15])
Dorsolateral Prefrontal Cortex	↓CT^{CS}	↓GMV^{CS} (Macaques- [4,20]), ↓CT^{CS,L} (Humans- [5,15])
Medial Parietal Cortex	↓CT^{CS}	-
Somatosensory Area 3	↓CT^{CS}	↓CT^{CS} (Humans- [12])
Insula	↑CT^{CS}	↓GMV^{CS} (Humans- [1,6,16]), ↓CT^{CS,L} (Humans- [10,13,14,18])

Table 10: Region-specific agreement and disagreement between the current study and previous ageing studies. A down arrow represents significant decreases, an up arrow represents a significant increase, and a dash represents no significant change. CT= cortical thickness, GMV= grey matter volume, ^{CS}= cross-sectional study, ^{L}= longitudinal study. 1= Good *et al.* 2001, 2= Tisserand *et al.* 2004, 3= Smith *et al.* 2007, 4= Alexander *et al.* 2008, 5= Fjell *et al.* 2009, 6= Hutton *et al.* 2009, 7= Hogstrom *et al.* 2012, 8= Koo *et al.* 2012, 9= Lemaitre *et al.* 2012, 10= Long *et al.* 2012, 11= Peelle *et al.* 2012, 12= Hurtz *et al.* 2014, 13= Storsve *et al.* 2014, 14= Bourisly *et al.* 2015, 15= Fjell *et al.* 2015, 16= Ramanöel *et al.* 2018, 17= Proskovec *et al.* 2020, 18= Podgórski *et al.* 2021, 19= Su *et al.* 2021, 20= Dash *et al.* 2023.

Taken together, these results show that the impacts of ageing are widespread and predominantly affect the frontal, temporal and parietal lobes during early to mid-adulthood. This is the first study to investigate the impacts of ageing on brain structure during the period of early to mid-adulthood in rhesus macaques. As such, the findings of the current study are novel in their implication that age-related grey matter loss in these regions occurs earlier than has been previously identified in cross-sectional macaque studies which utilised subjects during late adulthood (Alexander *et al.* 2008; Colman *et al.* 2009; Dash *et al.* 2023). They also support the findings of previous cross-sectional human studies covering this life period (Bourisly *et al.* 2015; Su *et al.* 2021), and imply that many of the age-related declines noted by

previous studies of humans during late adulthood likely begin earlier in the life course, with notable changes from at least early adulthood onwards. The similar findings of the current study and previous human studies also gives evidence for the strengths of rhesus macaques as models of healthy ageing.

8.3 Aims 3 and 4: Investigation of the Impacts of Early Weaning, and Weaning x Ageing Interactions, on Brain Structure During Early to Mid-adulthood

The final two aims of this project were to assess the impacts of early life stress, and the impacts of early life stress x ageing interactions, on the brain structure of rhesus macaques, during early to mid-adulthood. This aim was also met, through the use of early weaning as a form of early life stress.

Early weaning has previously been identified as a stressful experience during early life for macaques, and it is a common experience amongst many captive macaque populations (Prescott *et al.* 2012). Initial cross-sectional investigations of the impacts of early weaning on total grey matter volume and average cortical thickness identified no significant changes. This is perhaps unsurprising given that previous studies have primarily highlighted localised impacts of early life stress on brain structure as opposed to global changes. As such, a regional cross-sectional approach was utilised to investigate the impacts of weaning age on both grey matter volume and cortical thickness, using both a mixed age population and an age-matched sample. However, when weaning age was encoded as a continuous variable there were no significant differences in either grey matter volume or cortical thickness. Encoding weaning as a categorical variable did lead to significant results for cortical thickness, but not for grey matter volume. This could be an indication that cortical thickness is a more sensitive measure than grey matter volume for changes in brain structure associated with early life stress, similar to how it has been found to be more sensitive to age-related changes (Borgeest *et al.* 2021 [preprint]; Podgórski *et al.* 2021). For the full cross-sectional sample, subjects weaned before 12 months had lower cortical thickness in the cingulate cortex, as well as visual area 2 and the parahippocampal gyrus. Human studies have previously identified cortical thinning of the cingulate cortex in children, adolescents and adults that have experienced early life stress (Kelly *et al.* 2013; Ross *et al.* 2021). Additionally, Tomoda *et al.* (2012) previously identified cortical thinning of visual area 2, and Busso *et al.* (2017)

identified cortical thinning of the parahippocampal gyrus, in humans (adults and adolescents respectively) that have experienced early life stress. However, subjects weaned before 12 months also had higher cortical thickness in brain region TEO and the dorsal subdivision of brain area 46, an unexpected result which is not in line with human studies of early life stress.

When female subjects were excluded from the cross-sectional sample clusters showing significantly lower cortical thickness associated with being weaned before 12 months were localised to visual areas 2 and 4. This result again fits with the findings of Tomoda *et al.* (2012) in humans that have experienced early life stress. However, unexpected clusters where subjects weaned before 12 months had higher cortical thickness were again present within the temporal and occipital lobes, suggesting that though early weaning may primarily affect these two lobes it has varying impacts across the brain structures within them.

With the age-matched cross-sectional dataset, the only area showing a significant result (lower cortical thickness for subjects weaned before 12 months) was within the temporal lobe, and did not match any of the regions identified with the full cross-sectional sample, but was in a region previously found to exhibit lower cortical thickness in adolescents that had experienced early life stress (Busso *et al.* 2017). The difference in the results between the full cross-sectional sample and the age-matched dataset implies that the impacts of weaning age and ageing interact to affect different brain regions.

The interactions between weaning age (and in turn early life stress) and ageing were then specifically investigated using a longitudinal approach. No significant impact of the interaction between weaning age and ageing on total grey matter volume, or on average cortical thickness, was identified in the current study. This is unsurprising given the lack of significant results for the impacts of weaning age alone on total grey matter volume and average cortical thickness, but does warrant further investigation with a larger sample size. In terms of regional grey matter volume, the only significant cluster identified was localised to visual area 2. Surprisingly, for this significant cluster, subjects weaned earlier showed a greater increase in grey matter volume with ageing. This contrasts with the aforementioned result for the full cross-sectional sample in terms of cortical thickness, and the findings of Tomoda *et al.* (2012) in humans.

Significant interactions between weaning age and ageing were observed for cortical thickness in areas of the parietal, occipital and frontal lobes, with subjects with a lower weaning age showing decreases in cortical thickness with ageing. Notably, clusters in both visual area 2 and visual area 4 were significant for this investigation. This further contrasts the previously discussed finding of age-related increases in the grey matter volume of visual area 2 in those weaned earlier, but provides further support for the cross-sectional finding of lower cortical thickness in visual area 2 and visual area 4 (in those weaned before 12 months) being due to weaning age x ageing interactions. A summary of the areas of agreement and disagreement between the results of the current study and those of the previous early life stress studies discussed is provided in table 11.

Region	Current Study	Previous Studies
Visual Area 4	↓$CT^{CS, L}$ (dorsal), ↑CT^{CS} (ventral)	-
Visual Area 2	↓$CT^{CS, L}$, ↑GMV^{L}	↓GMV^{CS} (Humans- [1]), ↓CT^{CS} (Humans- [2])
Visual Area 1	↓CT^{L}	↓GMV^{CS} (Macaques- [6]; Humans- [1])
Cingulate Cortex	↓$CT^{CS, L}$	↓CT^{CS} (Humans- [3,7])
Parahippocampal Gyrus	↓CT^{CS}	↓CT^{CS} (Humans- [5])
TEO	↑CT^{CS}	-
Brain Area 46	↑CT^{CS} (dorsal), ↓CT^{L} (ventral)	↓CT^{CS} (Humans- [3,4])
Orbito-medial Prefrontal Area	↑CT^{CS}	↓CT^{CS} (Humans- [5])
Temporal Area TE	↓CT^{CS}	↓CT^{CS} (Humans-[5])

Table 11: Region-specific agreement and disagreement between the current study and previous early life stress studies. A down arrow represents significant decreases, an up arrow represents a significant increase, and a dash represents no significant change. CT= cortical thickness, GMV= grey matter volume, ^{CS}= cross-sectional study, ^{L}= longitudinal study. For some regions results are specific to the doral or ventral portions, this is indicated in brackets after the result. 1= Tomoda et al. 2009, 2= Tomoda et al. 2012, 3= Kelly et al. 2013, 4= McLaughlin et al. 2014, 5= Busso et al. 2017, 6= Wang et al. 2018, 7= Ross et al. 2021.

Taken together the results of this project demonstrate that early life stress, in the form of early weaning, has impacts on brain structure that persist through early and mid-adulthood in rhesus macaques. These impacts involve interactions with ageing effects, and appear to affect the occipital lobe most prominently. Though when the effects of ageing were minimised through the use of an age-matched dataset only the temporal lobe showed a significant impact of early weaning. Notably, many of the brain regions that were affected by early weaning, and/or weaning age x

ageing interactions, play a role in visual processing, suggesting a particular vulnerability of this system to early life stress. This vulnerability has also been recently identified in a study of early life stress in mice (Poplawski *et al.* 2023-preprint). However, further research is needed into the impacts of early weaning, and the interaction between early weaning and ageing, on both grey matter volume and cortical thickness as some of the results identified in the current study contrast with those of human studies of early life stress.

This research is novel amongst macaque studies in its investigation of cortical thickness, its use of a longitudinal design to investigate weaning x ageing interactions, the age group covered, and its investigation of weaning beyond maternal deprivation immediately post-birth. The findings of the current study give strength to the use of rhesus macaques as model animals for studying early life stress as a number of the findings of previous human studies of early life stress were replicated. Furthermore, the current findings illustrate that even when subjects are weaned later than 6 months there is still an impact on brain structure.

8.4 Key Findings

Firstly, this project provides strong evidence for the use of AutoMacq as a macaque MRI processing pipeline. MRI data from across different sites and scanners was successfully processed through the pipeline and allowed for the investigation of both ageing and early life stress.

Extensive changes in brain structure were identified with ageing during early to mid-adulthood, with cortical thickness showing more widespread changes than grey matter volume. Regions showing age-related changes were identified across the brain, with the temporal and frontal regions appearing to be the most affected, closely followed by parietal regions.

Brain regions affected by early life stress (in the form of early weaning), and early life stress x ageing interactions, were also identified. Only one significant result was identified in terms of grey matter volume, and changes in cortical thickness were less extensive than previously identified with ageing, indicating a relatively smaller impact of early life stress (at least in the form of early weaning) on brain structure. However, it was notable that the majority of regions that showed changes related to early life stress, and early life stress x ageing interactions, are involved in visual

processing. This implies that the visual processing system may be particularly vulnerable to the effects of early life stress.

Overall, the results of this project highlight that: 1) ageing and early-life stress (in the form of early weaning), as well as the interaction between the two, have significant impacts on brain structure prior to late adulthood in rhesus macaques; 2) cortical thickness is a more sensitive measure than grey matter volume; 3) a cross-sectional approach underestimates the impacts on brain structure.

8.5 Future Work

8.5.1 Improvements and adaptations of the AutoMacq pipeline

Though a great deal of optimisation was carried out during this project, as with all analysis pipelines, AutoMacq can be iterated upon and further improved over time. First of all, for this project visual quality control was carried out prior to processing scans through AutoMacq. However, this method is subjective and so could induce some bias in terms of scans being incorrectly included or excluded from the sample. One potential improvement to the AutoMacq pipeline would therefore be the incorporation of quantitative quality control metrics, as this could allow for scans that are of too poor a quality to be accurately processed through the AutoMacq pipeline to be more easily and objectively excluded. The difficulty with this adaptation would likely be ensuring that the metrics are not too strict, as AutoMacq does appear capable of handling a wide variety of scans, including those from awake macaques.

A further possible future improvement to AutoMacq would be the introduction of an automated method of correcting the talairach registration step. This would allow for the entire pipeline, after initial manual reorientation, to be ran automatically and unaided. This improvement would be particularly beneficial for studies utilising very large datasets, as manually correcting the talairach registration step for hundreds or thousands of scans could be quite time consuming. However, though datasets of this size are becoming the norm for human MRI studies, macaque MRI studies still tend to use much smaller datasets.

One other potential improvement that could be made to AutoMacq would be to replace the human atlases used in FreeSurfer with macaque-specific versions. This would not be simple to do in the case of replacing the MNI305 atlas used in

autorecon1, as this would likely require rewriting a lot of the processes carried out during that stage of FreeSurfer processing. However, this improvement may result in more accurate surfaces, which could be particularly useful for longitudinal data. Though in the current project, even with human atlases in the pipeline, the error rates of the surface-based outputs, particularly for cross-sectional data and scans from anaesthetised subjects, tended to be low anyway.

Finally, it is possible that AutoMacq could be adapted for use with MRI data from other species of NHP by using different species-specific atlases and templates. This would allow for both voxel-based and surface-based studies of other common NHP models, such as cynomolgus macaques and marmosets.

8.5.2 Further MRI studies of the impacts of ageing

In terms of voxel-based morphometry, the current study was unsuccessful in identifying age-related changes in grey matter volume using a cross-sectional approach. As this was likely due to the small sample size, repeating the cross-sectional analysis with a larger sample size would allow for comparison with our longitudinal ageing study. This could then allow for identification of any results occurring with a cross-sectional approach which do not represent 'true' ageing effects, as can be identified using a longitudinal approach.

Similar longitudinal studies of other age groups in macaques would also be useful to clarify fully when the brain changes observed in the current study begin, and whether the rates of decline accelerate later in life.

Additionally, as data was available for fewer female subjects than male subjects, the results of the current project may not be fully translatable to female macaques. Further research is therefore needed to determine whether the impacts of ageing during early to mid-adulthood differ in female macaques. However, it should be noted, that though it is well established that female macaques mature at a different rate to male macaques, their developmental trajectories are similar (Knickmeyer *et al.* 2010), and previous human studies found that sex-differences in brain ageing were minimal (Podgórski *et al.* 2021; Cui *et al.* 2023). Consequently, though it is possible that there are sex-differences in brain ageing in rhesus macaques, and this should be investigated, the differences are likely to be minimal.

Investigating brain changes during early to mid-adulthood is of particular interest as it is a life period that usually comes just before the onset of neurodegenerative disorders, such as Alzheimer's Disease, and during which early-onset variants of these disorders can manifest (Edwards-Lee *et al.* 2005; Vo *et al.* 2020). As this project has provided clear evidence for grey matter loss during early to mid-adulthood, future studies are needed to investigate the use of different interventions and preventative measures during this period, to potentially slow the onset of neurodegenerative disorders later in life. These studies could also consider measures to slow the more general cognitive decline that is seen with advancing age, as this too often begins just after mid-adulthood (Aartsen *et al.* 2002; Rönnlund *et al.* 2005). Given our results provide evidence for how well macaques appear to model the impacts of ageing on the human brain, these intervention studies could be carried out using macaques. This would allow for more efficient longitudinal research into any potential benefits of the chosen interventions.

8.5.3 Further MRI studies of the impacts of early life stress

It is hoped that as data sharing becomes more common practise in the field, more datasets with weaning age data will become available, and this research can be replicated with a larger sample size. This will be particularly useful for the investigation of grey matter volume, as the cross-sectional sample in the current study was too small to identify significant results. Ideally, future studies will include more variety in weaning age, with less of a correlation between weaning age and site. This would allow for a clearer picture of the impacts of early weaning to be determined.

Further research is also needed to fully determine whether there is an age at which weaning no longer impacts on brain structure, and is therefore no longer a significant source of stress. Additionally, weaning age studies of different age groups of macaques could help to better elucidate how the impacts of early life stress interact with ageing effects, and studying subjects prior to adulthood could allow for any diminishment or masking of weaning age impacts with ageing to be identified.

As was previously discussed, the sample used for this project was heavily weighted towards male subjects, and so may not be fully translatable to female macaques. Given the fact that in the wild female macaques do not tend to leave their

maternal group, whereas male macaques do leave the maternal group at around the age of 4 to 5 years, it would not be surprising if there was a sex difference in terms of the impacts of early weaning on brain structure (Prescott *et al.* 2012). Further research is therefore needed into potential sex differences in the impacts of weaning age, and early life stress more generally, on brain structure.

Future studies of early life stress in macaques could also investigate other potential stressors besides weaning age, such as conflict, surgeries/periods of anaesthesia or movement between facilities. This would allow for the investigation of whether different stressors have different impacts on brain structure, and therefore whether the results of the current project are specific to a certain kind of stressor. However, these stressors may be less common amongst populations of macaques, and so it may be more difficult to gather a large sample.

8.5.4 Future research using other methods

As well as the previously discussed options for future structural MRI studies off the back of this work, there are also a number of studies that could be undertaken using other methodologies. For example, histology studies could be undertaken in which brain tissue from macaques would be stained for different markers of either ageing (for example, $p16^{INK4a}$ and SIRT1 [Horn *et al.* 2024]) or early life stress (for example, Gas6 [Reemst *et al.* 2022]). This could be done across different regions in order to identify whether regions where significant changes were identified in the current study match regions that show greater staining for these markers. Additionally, functional MRI studies could be undertaken in order to determine whether the regions where structural changes were identified correlate to those where functional changes also occur. In particular, a network based approach would be useful in order to determine whether communication between regions identified in the current study is altered by ageing and/or early life stress.

8.6 To Conclude

As part of this project, an analysis pipeline capable of processing structural MRI data from rhesus macaques was successfully designed, optimised, and implemented. The AutoMacq pipeline can process both cross-sectional and longitudinal data, using both voxel-based and surface-based morphometry, and can

be carried out with minimal manual intervention, without any expert knowledge of macaque neuroanatomy.

Utilising the AutoMacq pipeline, the impacts of ageing and weaning age on brain structure were assessed in macaques during early to mid-adulthood. Significant results were identified across the brain, expanding current knowledge of age-related and ELS-related brain changes during this under-researched life period. Changes were identified the most extensively when cortical thickness was investigated, using a longitudinal approach. This provides support for both the relative insensitivity of grey matter volume as a measure of brain structural changes, and the underestimation of results when using a cross-sectional approach.

With the investigation of ageing, changes were seen across much of the brain, whereas the investigation of early weaning identified changes predominantly in regions involved in visual processing. The similarities of the findings of this project to those of previous studies in humans, in terms of the regions in which significant changes were identified, provides further support for the use of rhesus macaques as model animals in neuroscience research.

References

Aartsen MJ, Smits CH, van Tilburg T, Knipscheer KC, Deeg DJ. Activity in older adults: cause or consequence of cognitive functioning? A longitudinal study on everyday activities and cognitive performance in older adults. J Gerontol B Psychol Sci Soc Sci. 2002 Mar;57(2):P153-62. doi: 10.1093/geronb/57.2.p153.

Alexander GE, Chen K, Aschenbrenner M, Merkley TL, Santerre-Lemmon LE, Shamy JL, Skaggs WE, Buonocore MH, Rapp PR, Barnes CA. Age-related regional network of magnetic resonance imaging gray matter in the rhesus macaque. J Neurosci. 2008 Mar 12;28(11):2710-8. doi: 10.1523/JNEUROSCI.1852-07.2008.

Althubaiti A. Information bias in health research: definition, pitfalls, and adjustment methods. J Multidiscip Healthc. 2016 May 4;9:211-7. doi: 10.2147/JMDH.S104807.

Andersen AH, Zhang Z, Zhang M, Gash DM, Avison MJ. Age-associated changes in rhesus CNS composition identified by MRI. Brain Res. 1999 May 22;829(1-2):90-8. doi: 10.1016/s0006-8993(99)01343-8.

Anderson SW, Barrash J, Bechara A, Tranel D. Impairments of emotion and real-world complex behavior following childhood- or adult-onset damage to ventromedial prefrontal cortex. J Int Neuropsychol Soc. 2006 Mar;12(2):224-35. doi: 10.1017/S1355617706060346.

Andrews-Hanna JR, Reidler JS, Sepulcre J, Poulin R, Buckner RL. Functional-anatomic fractionation of the brain's default network. Neuron. 2010 Feb 25;65(4):550-62. doi: 10.1016/j.neuron.2010.02.005.

Arnsten AFT, Datta D, Leslie S, Yang ST, Wang M, Nairn AC. Alzheimer's-like pathology in aging rhesus macaques: Unique opportunity to study the etiology and treatment of Alzheimer's disease. Proc Natl Acad Sci U S A. 2019 Dec 26;116(52):26230-26238. doi: 10.1073/pnas.1903671116. Epub 2019 Dec 23.

Ashburner J, Friston KJ. Voxel-based morphometry--the methods. Neuroimage. 2000 Jun;11(6 Pt 1):805-21. doi: 10.1006/nimg.2000.0582.

Ashburner J, Ridgway GR. Symmetric diffeomorphic modeling of longitudinal structural MRI. Front Neurosci. 2013 Feb 5;6:197. doi: 10.3389/fnins.2012.00197.

Ausderau KK, Colman RJ, Kabakov S, Schultz-Darken N, Emborg ME. Evaluating depression- and anxiety-like behaviors in non-human primates. Front Behav Neurosci. 2023 Jan 19;16:1006065. doi: 10.3389/fnbeh.2022.1006065.

Avants B.B., Tustison N., Song G. Advanced normalization tools (ANTS) Insight J. 2009;2(365):1–35.

Bainbridge WA, Baker CI. Multidimensional memory topography in the medial parietal cortex identified from neuroimaging of thousands of daily memory videos. Nat Commun. 2022 Oct 31;13(1):6508. doi: 10.1038/s41467-022-34075-1.

Balbastre Y, Rivière D, Souedet N, Fischer C, Hérard AS, Williams S, Vandenberghe ME, Flament J, Aron-Badin R, Hantraye P, Mangin JF, Delzescaux T. Primatologist: A modular segmentation pipeline for macaque brain morphometry. Neuroimage. 2017 Nov 15;162:306-321. doi: 10.1016/j.neuroimage.2017.09.007. Epub 2017 Sep 9.

Barbey AK, Koenigs M, Grafman J. Dorsolateral prefrontal contributions to human working memory. Cortex. 2013 May;49(5):1195-205. doi: 10.1016/j.cortex.2012.05.022. Epub 2012 Jun 16.

Bartzokis G, Beckson M, Lu PH, Nuechterlein KH, Edwards N, Mintz J. Age-related changes in frontal and temporal lobe volumes in men: a magnetic resonance imaging study. Arch Gen Psychiatry. 2001 May;58(5):461-5. doi: 10.1001/archpsyc.58.5.461. Erratum in: Arch Gen Psychiatry 2001 Aug;58(8):774.

Beauchamp A, Yee Y, Darwin BC, Raznahan A, Mars RB, Lerch JP. Whole-brain comparison of rodent and human brains using spatial transcriptomics. Elife. 2022 Nov 7;11:e79418. doi: 10.7554/eLife.79418.

Bengtsson J, Elsenburg LK, Andersen GS, Larsen ML, Rieckmann A, Rod NH. Childhood adversity and cardiovascular disease in early adulthood: a Danish cohort study. Eur Heart J. 2023 Feb 14;44(7):586-593. doi: 10.1093/eurheartj/ehac607.

Bernard C, Dilharreguy B, Helmer C, Chanraud S, Amieva H, Dartigues JF, Allard M, Catheline G. PCC characteristics at rest in 10-year memory decliners. Neurobiol Aging. 2015 Oct;36(10):2812-20. doi: 10.1016/j.neurobiolaging.2015.07.002. Epub 2015 Jul 9.

Bethlehem RAI, Seidlitz J, White SR, Vogel JW, Anderson KM, Adamson C, Adler S, Alexopoulos GS, Anagnostou E, Areces-Gonzalez A, Astle DE, Auyeung B, Ayub M, Bae J, Ball G, Baron-Cohen S, Beare R, Bedford SA, Benegal V, Beyer F, Blangero J, Blesa Cábez M, Boardman JP, Borzage M, Bosch-Bayard JF, Bourke N, Calhoun VD, Chakravarty MM, Chen C, Chertavian C, Chetelat G, Chong YS, Cole JH, Corvin A, Costantino M, Courchesne E, Crivello F, Cropley VL, Crosbie J, Crossley N, Delarue M, Delorme R, Desrivieres S, Devenyi GA, Di Biase MA, Dolan R, Donald KA, Donohoe G, Dunlop K, Edwards AD, Elison JT, Ellis CT, Elman JA, Eyler L, Fair DA, Feczko E, Fletcher PC, Fonagy P, Franz CE, Galan-Garcia L, Gholipour A, Giedd J, Gilmore JH, Glahn DC, Goodyer IM, Grant PE, Groenewold NA, Gunning FM, Gur RE, Gur RC, Hammill CF, Hansson O, Hedden T, Heinz A, Henson RN, Heuer K, Hoare J, Holla B, Holmes AJ, Holt R, Huang H, Im K, Ipser J, Jack CR Jr, Jackowski AP, Jia T, Johnson KA, Jones PB, Jones DT, Kahn RS, Karlsson H, Karlsson L, Kawashima R, Kelley EA, Kern S, Kim KW, Kitzbichler MG, Kremen WS, Lalonde F, Landeau B, Lee S, Lerch J, Lewis JD, Li J, Liao W, Liston C, Lombardo MV, Lv J, Lynch C, Mallard TT, Marcelis M, Markello RD, Mathias SR, Mazoyer B, McGuire P, Meaney MJ, Mechelli A, Medic N, Misic B, Morgan SE, Mothersill D, Nigg J, Ong MQW, Ortinau C, Ossenkoppele R, Ouyang M, Palaniyappan L, Paly L, Pan PM, Pantelis C, Park MM, Paus T, Pausova Z, Paz-Linares D, Pichet Binette A, Pierce K, Qian X, Qiu J, Qiu A, Raznahan A, Rittman T, Rodrigue A, Rollins CK, Romero-Garcia R, Ronan L, Rosenberg MD, Rowitch DH, Salum GA, Satterthwaite TD, Schaare HL, Schachar RJ, Schultz AP, Schumann G, Schöll M, Sharp D, Shinohara RT, Skoog I, Smyser CD, Sperling RA, Stein DJ, Stolicyn A, Suckling J, Sullivan G, Taki Y, Thyreau B, Toro R, Traut N, Tsvetanov KA, Turk-Browne NB, Tuulari JJ, Tzourio C, Vachon-Presseau É, Valdes-Sosa MJ, Valdes-Sosa PA, Valk SL, van Amelsvoort T, Vandekar SN, Vasung L, Victoria LW, Villeneuve S, Villringer A, Vértes PE, Wagstyl K, Wang YS, Warfield SK, Warrier V, Westman E, Westwater ML, Whalley HC, Witte AV, Yang N, Yeo B, Yun H, Zalesky A, Zar HJ, Zettergren A, Zhou JH, Ziauddeen H, Zugman A, Zuo XN; 3R-BRAIN; AIBL; Alzheimer's Disease Neuroimaging Initiative; Alzheimer's Disease Repository Without Borders Investigators; CALM Team; Cam-CAN; CCNP; COBRE; cVEDA; ENIGMA Developmental Brain Age Working Group; Developing Human Connectome Project; FinnBrain; Harvard Aging Brain Study; IMAGEN; KNE96; Mayo Clinic Study of Aging;

NSPN; POND; PREVENT-AD Research Group; VETSA; Bullmore ET, Alexander-Bloch AF. Brain charts for the human lifespan. Nature. 2022 Apr;604(7906):525-533. doi: 10.1038/s41586-022-04554-y. Epub 2022 Apr 6. Erratum in: Nature. 2022 Oct;610(7931):E6

Berman RA, Colby CL. Spatial working memory in human extrastriate cortex. Physiol Behav. 2002 Dec;77(4-5):621-7. doi: 10.1016/s0031-9384(02)00897-1.

Borgeest GS, Henson RN, Kietzmann TC, Madan CR, Fox T, Malpetti M, Fuhrman D, Knights E, Carlin JD, cam-CAN, Kievit RA. A morphometric double dissociation: cortical thickness is more related to aging; surface area is more related to cognition. bioRxiv 2021.09.30.462545; doi: https://doi.org/10.1101/2021.09.30.462545.

Boros BD, Greathouse KM, Gearing M, Herskowitz JH. Dendritic spine remodeling accompanies Alzheimer's disease pathology and genetic susceptibility in cognitively normal aging. Neurobiol Aging. 2019 Jan;73:92-103. doi: 10.1016/j.neurobiolaging.2018.09.003. Epub 2018 Sep 21.

Bounoua N, Miglin R, Spielberg JM, Sadeh N. Childhood assaultive trauma and physical aggression: Links with cortical thickness in prefrontal and occipital cortices. Neuroimage Clin. 2020;27:102321. doi: 10.1016/j.nicl.2020.102321. Epub 2020 Jun 25.

Bourisly AK, El-Beltagi A, Cherian J, Gejo G, Al-Jazzaf A, Ismail M. A voxel-based morphometric magnetic resonance imaging study of the brain detects age-related gray matter volume changes in healthy subjects of 21-45 years old. Neuroradiol J. 2015 Oct;28(5):450-9. doi: 10.1177/1971400915598078.

Bryda EC. The Mighty Mouse: the impact of rodents on advances in biomedical research. Mo Med. 2013 May-Jun;110(3):207-11.

Busso DS, McLaughlin KA, Brueck S, Peverill M, Gold AL, Sheridan MA. Child Abuse, Neural Structure, and Adolescent Psychopathology: A Longitudinal Study. J Am Acad Child Adolesc Psychiatry. 2017 Apr;56(4):321-328.e1. doi: 10.1016/j.jaac.2017.01.013. Epub 2017 Feb 3.

Cardozo-Pelaez F, Brooks PJ, Stedeford T, Song S, Sanchez-Ramos J. DNA damage, repair, and antioxidant systems in brain regions: a correlative study. Free Radic Biol Med. 2000 Mar 1;28(5):779-85. doi: 10.1016/s0891-5849(00)00172-6.

Carmon J, Heege J, Necus JH, Owen TW, Pipa G, Kaiser M, Taylor PN, Wang Y. Reliability and comparability of human brain structural covariance networks. Neuroimage. 2020 Oct 15;220:117104. doi: 10.1016/j.neuroimage.2020.117104.

Carr CP, Martins CM, Stingel AM, Lemgruber VB, Juruena MF. The role of early life stress in adult psychiatric disorders: a systematic review according to childhood trauma subtypes. J Nerv Ment Dis. 2013 Dec;201(12):1007-20. doi: 10.1097/NMD.0000000000000049.

Caruana EJ, Roman M, Hernández-Sánchez J, Solli P. Longitudinal studies. J Thorac Dis. 2015 Nov;7(11):E537-40. doi: 10.3978/j.issn.2072-1439.2015.10.63.

Castelli V, Benedetti E, Antonosante A, Catanesi M, Pitari G, Ippoliti R, Cimini A, d'Angelo M. Neuronal Cells Rearrangement During Aging and Neurodegenerative Disease: Metabolism, Oxidative Stress and Organelles Dynamic. Front Mol Neurosci. 2019 May 28;12:132. doi: 10.3389/fnmol.2019.00132.

Catale C, Bisicchia E, Carola V, Viscomi MT. Early life stress exposure worsens adult remote microglia activation, neuronal death, and functional recovery after focal brain injury. Brain Behav Immun. 2021 May;94:89-103. doi: 10.1016/j.bbi.2021.02.032. Epub 2021 Mar 5.

Cavazzana A, Röhrborn A, Garthus-Niegel S, Larsson M, Hummel T, Croy I. Sensory-specific impairment among older people. An investigation using both sensory thresholds and subjective measures across the five senses. PLoS One. 2018 Aug 27;13(8):e0202969. doi: 10.1371/journal.pone.0202969.

Cerroni AM, Tomlinson GA, Turnquist JE, Grynpas MD. Bone mineral density, osteopenia, and osteoporosis in the rhesus macaques of Cayo Santiago. Am J Phys Anthropol. 2000 Nov;113(3):389-410. doi: 10.1002/1096-8644(200011)113:3<389::AID-AJPA9>3.0.CO;2-I.

Chaudhari PR, Singla A, Vaidya VA. Early Adversity and Accelerated Brain Aging: A Mini-Review. Front Mol Neurosci. 2022 Mar 22;15:822917. doi: 10.3389/fnmol.2022.822917.

Chen MA, LeRoy AS, Majd M, Chen JY, Brown RL, Christian LM, Fagundes CP. Immune and Epigenetic Pathways Linking Childhood Adversity and Health Across the Lifespan. Front Psychol. 2021 Nov 26;12:788351. doi: 10.3389/fpsyg.2021.788351.

Chen X, Errangi B, Li L, Glasser MF, Westlye LT, Fjell AM, Walhovd KB, Hu X, Herndon JG, Preuss TM, Rilling JK. Brain aging in humans, chimpanzees (Pan troglodytes), and rhesus macaques (Macaca mulatta): magnetic resonance imaging studies of macro- and microstructural changes. Neurobiol Aging. 2013 Oct;34(10):2248-60. doi: 10.1016/j.neurobiolaging.2013.03.028. Epub 2013 Apr 24.

Chow N, Hwang KS, Hurtz S, Green AE, Somme JH, Thompson PM, Elashoff DA, Jack CR, Weiner M, Apostolova LG; Alzheimer's Disease Neuroimaging Initiative. Comparing 3T and 1.5T MRI for mapping hippocampal atrophy in the Alzheimer's Disease Neuroimaging Initiative. AJNR Am J Neuroradiol. 2015 Apr;36(4):653-60. doi: 10.3174/ajnr.A4228. Epub 2015 Jan 22.

Colman RJ, Anderson RM, Johnson SC, Kastman EK, Kosmatka KJ, Beasley TM, Allison DB, Cruzen C, Simmons HA, Kemnitz JW, Weindruch R. Caloric restriction delays disease onset and mortality in rhesus monkeys. Science. 2009 Jul 10;325(5937):201-4. doi: 10.1126/science.1173635.

Correia-Melo C, Marques FD, Anderson R, Hewitt G, Hewitt R, Cole J, Carroll BM, Miwa S, Birch J, Merz A, Rushton MD, Charles M, Jurk D, Tait SW, Czapiewski R, Greaves L, Nelson G, Bohlooly-Y M, Rodriguez-Cuenca S, Vidal-Puig A, Mann D, Saretzki G, Quarato G, Green DR, Adams PD, von Zglinicki T, Korolchuk VI, Passos JF. Mitochondria are required for pro-ageing features of the senescent phenotype. EMBO J. 2016 Apr 1;35(7):724-42. doi: 10.15252/embj.201592862.

Croxson PL, Forkel SJ, Cerliani L, Thiebaut de Schotten M. Structural Variability Across the Primate Brain: A Cross-Species Comparison. Cereb Cortex. 2018 Nov 1;28(11):3829-3841. doi: 10.1093/cercor/bhx244.

Cui D, Wang D, Jin J, Liu X, Wang Y, Cao W, Liu Z, Yin T. Age- and sex-related differences in cortical morphology and their relationships with cognitive performance in healthy middle-aged and older adults. Quant Imaging Med Surg. 2023 Feb 1;13(2):1083-1099. doi: 10.21037/qims-22-583. Epub 2022 Dec 13.

Dale AM, Fischl B, Sereno MI. Cortical surface-based analysis. I. Segmentation and surface reconstruction. Neuroimage. 1999 Feb;9(2):179-94. doi: 10.1006/nimg.1998.0395.

Dash S, Park B, Kroenke CD, Rooney WD, Urbanski HF, Kohama SG. Brain volumetrics across the lifespan of the rhesus macaque. Neurobiol Aging. 2023 Jun;126:34-43. doi: 10.1016/j.neurobiolaging.2023.02.002. Epub 2023 Feb 11.

De Brito SA, Viding E, Sebastian CL, Kelly PA, Mechelli A, Maris H, McCrory EJ. Reduced orbitofrontal and temporal grey matter in a community sample of maltreated children. J Child Psychol Psychiatry. 2013 Jan;54(1):105-12. doi: 10.1111/j.1469-7610.2012.02597.x. Epub 2012 Aug 10.

Deen B, Koldewyn K, Kanwisher N, Saxe R. Functional Organization of Social Perception and Cognition in the Superior Temporal Sulcus. Cereb Cortex. 2015 Nov;25(11):4596-609. doi: 10.1093/cercor/bhv111. Epub 2015 Jun 5.

Diana RA, Yonelinas AP, Ranganath C. Medial temporal lobe activity during source retrieval reflects information type, not memory strength. J Cogn Neurosci. 2010 Aug;22(8):1808-18. doi: 10.1162/jocn.2009.21335.

Donahue CJ, Glasser MF, Preuss TM, Rilling JK, Van Essen DC. Quantitative assessment of prefrontal cortex in humans relative to nonhuman primates. Proc Natl Acad Sci USA. 2018 May 29;115(22):E5183-E5192. doi: 10.1073/pnas.1721653115. Epub 2018 May 8

du Boisgueheneuc F, Levy R, Volle E, Seassau M, Duffau H, Kinkingnehun S, Samson Y, Zhang S, Dubois B. Functions of the left superior frontal gyrus in humans: a lesion study. Brain. 2006 Dec;129(Pt 12):3315-28. doi: 10.1093/brain/awl244. Epub 2006 Sep 19.

Duan H, Wearne SL, Rocher AB, Macedo A, Morrison JH, Hof PR. Age-related dendritic and spine changes in corticocortically projecting neurons in macaque monkeys. Cereb Cortex. 2003 Sep;13(9):950-61. doi: 10.1093/cercor/13.9.950.

Dube SR, Fairweather D, Pearson WS, Felitti VJ, Anda RF, Croft JB. Cumulative childhood stress and autoimmune diseases in adults. Psychosom Med. 2009 Feb;71(2):243-50. doi: 10.1097/PSY.0b013e3181907888. Epub 2009 Feb 2.

Edwards-Lee T, Ringman JM, Chung J, Werner J, Morgan A, St George Hyslop P, Thompson P, Dutton R, Mlikotic A, Rogaeva E, Hardy J. An African American family with early-onset Alzheimer disease and an APP (T714I) mutation. Neurology. 2005 Jan 25;64(2):377-9. doi: 10.1212/01.WNL.0000149761.70566.3E.

Ellenbogen MA, Schwartzman AE, Stewart J, Walker CD. Stress and selective attention: the interplay of mood, cortisol levels, and emotional information processing. Psychophysiology. 2002 Nov;39(6):723-32. doi: 10.1111/1469-8986.3960723.

Ellenbroek B, Youn J. Rodent models in neuroscience research: is it a rat race? Dis Model Mech. 2016 Oct 1;9(10):1079-1087. doi: 10.1242/dmm.026120.

Epel ES, Blackburn EH, Lin J, Dhabhar FS, Adler NE, Morrow JD, Cawthon RM. Accelerated telomere shortening in response to life stress. Proc Natl Acad Sci U S A. 2004 Dec 7;101(49):17312-5. doi: 10.1073/pnas.0407162101.

Erb J, Schmitt LM, Obleser J. Temporal selectivity declines in the aging human auditory cortex. Elife. 2020 Jul 3;9:e55300. doi: 10.7554/eLife.55300.

Fang C, Yan K, Liang C, Wang J, Cai X, Zhang R, Lu HD. Function-specific projections from V2 to V4 in macaques. Brain Struct Funct. 2022 May;227(4):1317-1330. doi: 10.1007/s00429-021-02440-3. Epub 2022 Jan 3.

Faravelli C, Pallanti S. Recent life events and panic disorder. Am J Psychiatry. 1989 May;146(5):622-6. doi: 10.1176/ajp.146.5.622.

Farokhian F, Yang C, Beheshti I, Matsuda H, Wu S. Age-Related Gray and White Matter Changes in Normal Adult Brains. Aging Dis. 2017 Dec 1;8(6):899-909. doi: 10.14336/AD.2017.0502.

Fischer, G. Operto, S. Laguitton, M. Perrot, I. Denghien, D. Rivière, and J.-F. Mangin: Morphologist 2012: the new morphological pipeline of BrainVISA, In *Proc. HBM*, 2012.

Fischl B. FreeSurfer. Neuroimage. 2012 Aug 15;62(2):774-81. doi: 10.1016/j.neuroimage.2012.01.021. Epub 2012 Jan 10.

Fischl B, Sereno MI, Dale AM. Cortical surface-based analysis. II: Inflation, flattening, and a surface-based coordinate system. Neuroimage. 1999 Feb;9(2):195-207. doi: 10.1006/nimg.1998.0396.

Fjell AM, Westlye LT, Amlien I, Espeseth T, Reinvang I, Raz N, Agartz I, Salat DH, Greve DN, Fischl B, Dale AM, Walhovd KB. High consistency of regional cortical thinning in aging across multiple samples. Cereb Cortex. 2009 Sep;19(9):2001-12. doi: 10.1093/cercor/bhn232. Epub 2009 Jan 15.

Fjell AM, Grydeland H, Krogsrud SK, Amlien I, Rohani DA, Ferschmann L, Storsve AB, Tamnes CK, Sala-Llonch R, Due-Tønnessen P, Bjørnerud A, Sølsnes AE, Håberg AK, Skranes J, Bartsch H, Chen CH, Thompson WK, Panizzon MS, Kremen WS, Dale AM, Walhovd KB. Development and aging of cortical thickness correspond to genetic organization patterns. Proc Natl Acad Sci USA. 2015 Dec 15;112(50):15462-7. doi: 10.1073/pnas.1508831112.

Frazier-Logue N, Wang J, Wang Z, Sodums D, Khosla A, Samson AD, McIntosh AR, Shen K. A Robust Modular Automated Neuroimaging Pipeline for Model Inputs to TheVirtualBrain. Front Neuroinform. 2022 Jun 14;16:883223. doi: 10.3389/fninf.2022.883223.

Freeman J, Ziemba CM, Heeger DJ, Simoncelli EP, Movshon JA. A functional and perceptual signature of the second visual area in primates. Nat Neurosci. 2013 Jul;16(7):974-81. doi: 10.1038/nn.3402. Epub 2013 May 19.

Fülöp T, Larbi A, Witkowski JM. Human Inflammaging. Gerontology. 2019;65(5):495-504. doi: 10.1159/000497375.

Garcia-Saldivar P, Garimella A, Garza-Villarreal EA, Mendez FA, Concha L, Merchant H. PREEMACS: Pipeline for preprocessing and extraction of the macaque

brain surface. Neuroimage. 2021 Feb 15;227:117671. doi: 10.1016/j.neuroimage.2020.117671. Epub 2020 Dec 24

Gauthier LV, Taub E, Mark VW, Barghi A, Uswatte G. Atrophy of spared gray matter tissue predicts poorer motor recovery and rehabilitation response in chronic stroke. Stroke. 2012 Feb;43(2):453-7. doi: 10.1161/STROKEAHA.111.633255. Epub 2011 Nov 17.

Glasser MF, Sotiropoulos SN, Wilson JA, Coalson TS, Fischl B, Andersson JL, Xu J, Jbabdi S, Webster M, Polimeni JR, Van Essen DC, Jenkinson M; WU-Minn HCP Consortium. The minimal preprocessing pipelines for the Human Connectome Project. Neuroimage. 2013 Oct 15;80:105-24. doi: 10.1016/j.neuroimage.2013.04.127. Epub 2013 May 11.

Good CD, Johnsrude IS, Ashburner J, Henson RN, Friston KJ, Frackowiak RS. A voxel-based morphometric study of ageing in 465 normal adult human brains. Neuroimage. 2001 Jul;14(1 Pt 1):21-36. doi: 10.1006/nimg.2001.0786.

Gorka AX, Hanson JL, Radtke SR, Hariri AR. Reduced hippocampal and medial prefrontal gray matter mediate the association between reported childhood maltreatment and trait anxiety in adulthood and predict sensitivity to future life stress. Biol Mood Anxiety Disord. 2014 Nov 13;4:12. doi: 10.1186/2045-5380-4-12.

Gotlib IH, Miller JG, Borchers LR, Coury SM, Costello LA, Garcia JM, Ho TC. Effects of the COVID-19 Pandemic on Mental Health and Brain Maturation in Adolescents: Implications for Analyzing Longitudinal Data. Biol Psychiatry Glob Open Sci. 2022 Dec 1. doi: 10.1016/j.bpsgos.2022.11.002.

Goto M, Abe O, Hagiwara A, Fujita S, Kamagata K, Hori M, Aoki S, Osada T, Konishi S, Masutani Y, Sakamoto H, Sakano Y, Kyogoku S, Daida H. Advantages of Using Both Voxel- and Surface-based Morphometry in Cortical Morphology Analysis: A Review of Various Applications. Magn Reson Med Sci. 2022 Mar 1;21(1):41-57. doi: 10.2463/mrms.rev.2021-0096. Epub 2022 Feb 18

Grainger SA, Crawford JD, Riches JC, Kochan NA, Chander RJ, Mather KA, Sachdev PS, Henry JD. Aging Is Associated With Multidirectional Changes in Social Cognition: Findings From an Adult Life-Span Sample Ranging From 18 to 101 Years.

J Gerontol B Psychol Sci Soc Sci. 2023 Jan 28;78(1):62-72. doi: 10.1093/geronb/gbac110.

Grieger TA, Cozza SJ, Ursano RJ, Hoge C, Martinez PE, Engel CC, Wain HJ. Posttraumatic stress disorder and depression in battle-injured soldiers. Am J Psychiatry. 2006 Oct;163(10):1777-83; quiz 1860. doi: 10.1176/ajp.2006.163.10.1777.

Hage SR, Nieder A. Single neurons in monkey prefrontal cortex encode volitional initiation of vocalizations. Nat Commun. 2013;4:2409. doi: 10.1038/ncomms3409.

Harman D. The aging process: major risk factor for disease and death. Proc Natl Acad Sci U S A. 1991 Jun 15;88(12):5360-3. doi: 10.1073/pnas.88.12.5360.

Harris ML, Oldmeadow C, Hure A, Luu J, Loxton D, Attia J. Stress increases the risk of type 2 diabetes onset in women: A 12-year longitudinal study using causal modelling. PLoS One. 2017 Feb 21;12(2):e0172126. doi: 10.1371/journal.pone.0172126.

Hedges EP, Dimitrov M, Zahid U, Brito Vega B, Si S, Dickson H, McGuire P, Williams S, Barker GJ, Kempton MJ. Reliability of structural MRI measurements: The effects of scan session, head tilt, inter-scan interval, acquisition sequence, FreeSurfer version and processing stream. Neuroimage. 2022 Feb 1;246:118751. doi: 10.1016/j.neuroimage.2021.118751.

Heim S, Eickhoff SB, Amunts K. Specialisation in Broca's region for semantic, phonological, and syntactic fluency? Neuroimage. 2008 Apr 15;40(3):1362-8. doi: 10.1016/j.neuroimage.2008.01.009. Epub 2008 Jan 19.

Helmeke C, Seidel K, Poeggel G, Bredy TW, Abraham A, Braun K. Paternal deprivation during infancy results in dendrite- and time-specific changes of dendritic development and spine formation in the orbitofrontal cortex of the biparental rodent Octodon degus. Neuroscience. 2009 Oct 20;163(3):790-8. doi: 10.1016/j.neuroscience.2009.07.008. Epub 2009 Jul 8.

Hoffman P, Loginova E, Russell A. Poor coherence in older people's speech is explained by impaired semantic and executive processes. Elife. 2018 Sep 4;7:e38907. doi: 10.7554/eLife.38907.

Hogstrom LJ, Westlye LT, Walhovd KB, Fjell AM. The structure of the cerebral cortex across adult life: age-related patterns of surface area, thickness, and gyrification. Cereb Cortex. 2013 Nov;23(11):2521-30. doi: 10.1093/cercor/bhs231. Epub 2012 Aug 14.

Horn MD, Forest SC, Saied AA, MacLean AG. Astrocyte expression of aging-associated markers positively correlates with neurodegeneration in the frontal lobe of the rhesus macaque brain. Front Aging Neurosci. 2024 Mar 20;16:1368517. doi: 10.3389/fnagi.2024.1368517.

Huneke RB, Foltz CJ, VandeWoude S, Mandrell TD, Garman RH. Characterization of dermatologic changes in geriatric rhesus macaques. J Med Primatol. 1996 Dec;25(6):404-13. doi: 10.1111/j.1600-0684.1996.tb00036.x.

Hurtz S, Woo E, Kebets V, Green AE, Zoumalan C, Wang B, Ringman JM, Thompson PM, Apostolova LG. Age effects on cortical thickness in cognitively normal elderly individuals. Dement Geriatr Cogn Dis Extra. 2014 Jul 1;4(2):221-7. doi: 10.1159/000362872.

Hutton C, Draganski B, Ashburner J, Weiskopf N. A comparison between voxel-based cortical thickness and voxel-based morphometry in normal aging. Neuroimage. 2009 Nov 1;48(2):371-80. doi: 10.1016/j.neuroimage.2009.06.043. Epub 2009 Jun 25.

Jacobs B, Driscoll L, Schall M. Life-span dendritic and spine changes in areas 10 and 18 of human cortex: a quantitative Golgi study. J Comp Neurol. 1997 Oct 6;386(4):661-80.

Jenkinson M, Beckmann CF, Behrens TE, Woolrich MW, Smith SM. FSL. Neuroimage. 2012 Aug 15;62(2):782-90. doi: 10.1016/j.neuroimage.2011.09.015.

Johnson EL, Chang WK, Dewar CD, Sorensen D, Lin JJ, Solbakk AK, Endestad T, Larsson PG, Ivanovic J, Meling TR, Scabini D, Knight RT. Orbitofrontal cortex governs working memory for temporal order. Curr Biol. 2022 May 9;32(9):R410-R411. doi: 10.1016/j.cub.2022.03.074.

Johnson J, Chaudieu I, Ritchie K, Scali J, Ancelin ML, Ryan J. The extent to which childhood adversity and recent stress influence all-cause mortality risk in older adults.

Psychoneuroendocrinology. 2020 Jan;111:104492. doi: 10.1016/j.psyneuen.2019.104492. Epub 2019 Oct 24.

Juruena MF, Bourne M, Young AH, Cleare AJ. Hypothalamic-Pituitary-Adrenal axis dysfunction by early life stress. Neurosci Lett. 2021 Aug 10;759:136037. doi: 10.1016/j.neulet.2021.136037. Epub 2021 Jun 8.

Kassem MS, Lagopoulos J, Stait-Gardner T, Price WS, Chohan TW, Arnold JC, Hatton SN, Bennett MR. Stress-induced grey matter loss determined by MRI is primarily due to loss of dendrites and their synapses. Mol Neurobiol. 2013 Apr;47(2):645-61. doi: 10.1007/s12035-012-8365-7. Epub 2012 Nov 9.

Kaul D, Smith CC, Stevens J, Fröhlich AS, Binder EB, Mechawar N, Schwab SG, Matosin N. Severe childhood and adulthood stress associates with neocortical layer-specific reductions of mature spines in psychiatric disorders. Neurobiol Stress. 2020 Nov 21;13:100270. doi: 10.1016/j.ynstr.2020.100270.

Kautz M, Ered A, Nielsen J, Olino T, Alloy L. The Effect of Early Life Stress During Sensitive Exposure Periods on Orbitofrontal Cortex Thickness. Biol Psychiatry. 2021 Apr; 89(9, Supplement): S278-S279. https://doi.org/10.1016/j.biopsych.2021.02.695.

Kelava I, Lewitus E, Huttner WB. The secondary loss of gyrencephaly as an example of evolutionary phenotypical reversal. Front Neuroanat. 2013 Jun 26;7:16. doi: 10.3389/fnana.2013.00016.

Kelly PA, Viding E, Wallace GL, Schaer M, De Brito SA, Robustelli B, McCrory EJ. Cortical thickness, surface area, and gyrification abnormalities in children exposed to maltreatment: neural markers of vulnerability? Biol Psychiatry. 2013 Dec 1;74(11):845-52. doi: 10.1016/j.biopsych.2013.06.020. Epub 2013 Aug 13.

Kennerley SW, Wallis JD. Reward-dependent modulation of working memory in lateral prefrontal cortex. J Neurosci. 2009 Mar 11;29(10):3259-70. doi: 10.1523/JNEUROSCI.5353-08.2009.

Kessing LV, Agerbo E, Mortensen PB. Does the impact of major stressful life events on the risk of developing depression change throughout life? Psychol Med. 2003 Oct;33(7):1177-84. doi: 10.1017/s0033291703007852.

Kim KN, Hernandez D, Seo JH, Noh Y, Han Y, Ryu YC, Chung JY. Quantitative assessment of phased array coils with different numbers of receiving channels in terms of signal-to-noise ratio and spatial noise variation in magnetic resonance imaging. PLoS One. 2019 Jul 5;14(7):e0219407. doi: 10.1371/journal.pone.0219407.

Kinnunen KM, Greenwood R, Powell JH, Leech R, Hawkins PC, Bonnelle V, Patel MC, Counsell SJ, Sharp DJ. White matter damage and cognitive impairment after traumatic brain injury. Brain. 2011 Feb;134(Pt 2):449-63. doi: 10.1093/brain/awq347. Epub 2010 Dec 29.

Knickmeyer RC, Styner M, Short SJ, Lubach GR, Kang C, Hamer R, Coe CL, Gilmore JH. Maturational trajectories of cortical brain development through the pubertal transition: unique species and sex differences in the monkey revealed through structural magnetic resonance imaging. Cereb Cortex. 2010 May;20(5):1053-63. doi: 10.1093/cercor/bhp166. Epub 2009 Aug 24.

Koch H, McCormack K, Sanchez MM, Maestripieri D. The development of the hypothalamic-pituitary-adrenal axis in rhesus monkeys: effects of age, sex, and early experience. Dev Psychobiol. 2014 Jan;56(1):86-95. doi: 10.1002/dev.21093. Epub 2012 Nov 28.

Koenigs M, Barbey AK, Postle BR, Grafman J. Superior parietal cortex is critical for the manipulation of information in working memory. J Neurosci. 2009 Nov 25;29(47):14980-6. doi: 10.1523/JNEUROSCI.3706-09.2009.

Koo BB, Schettler SP, Murray DE, Lee JM, Killiany RJ, Rosene DL, Kim DS, Ronen I. Age-related effects on cortical thickness patterns of the Rhesus monkey brain. Neurobiol Aging. 2012 Jan;33(1):200.e23-31. doi: 10.1016/j.neurobiolaging.2010.07.010. Epub 2010 Aug 30.

Koo TK, Li MY. A Guideline of Selecting and Reporting Intraclass Correlation Coefficients for Reliability Research. J Chiropr Med. 2016 Jun;15(2):155-63. doi: 10.1016/j.jcm.2016.02.012. Epub 2016 Mar 31. Erratum in: J Chiropr Med. 2017 Dec;16(4):346.

Korkki SM, Richter FR, Jeyarathnarajah P, Simons JS. Healthy ageing reduces the precision of episodic memory retrieval. Psychol Aging. 2020 Feb;35(1):124-142. doi: 10.1037/pag0000432. Epub 2020 Jan 13.

Kravitz DJ, Saleem KS, Baker CI, Ungerleider LG, Mishkin M. The ventral visual pathway: an expanded neural framework for the processing of object quality. Trends Cogn Sci. 2013 Jan;17(1):26-49. doi: 10.1016/j.tics.2012.10.011. Epub 2012 Dec 19.

Kühn S, Brass M, Gallinat J. Imitation and speech: commonalities within Broca's area. Brain Struct Funct. 2013 Nov;218(6):1419-27. doi: 10.1007/s00429-012-0467-5. Epub 2012 Nov 3.

Kumar S, Stecher G, Suleski M, Hedges SB. TimeTree: A Resource for Timelines, Timetrees, and Divergence Times. Mol Biol Evol. 2017 Jul 1;34(7):1812-1819. doi: 10.1093/molbev/msx116.

Lalwani P, Gagnon H, Cassady K, Simmonite M, Peltier S, Seidler RD, Taylor SF, Weissman DH, Polk TA. Neural distinctiveness declines with age in auditory cortex and is associated with auditory GABA levels. Neuroimage. 2019 Nov 1;201:116033. doi: 10.1016/j.neuroimage.2019.116033. Epub 2019 Jul 18.

Lam PY, Yin F, Hamilton RT, Boveris A, Cadenas E. Elevated neuronal nitric oxide synthase expression during ageing and mitochondrial energy production. Free Radic Res. 2009 May;43(5):431-9. doi: 10.1080/10715760902849813.

Leach LS, Butterworth P. Depression and anxiety in early adulthood: consequences for finding a partner, and relationship support and conflict. Epidemiol Psychiatr Sci. 2020 Jul 15;29:e141. doi: 10.1017/S2045796020000530.

Lebel C, Gee M, Camicioli R, Wieler M, Martin W, Beaulieu C. Diffusion tensor imaging of white matter tract evolution over the lifespan. Neuroimage. 2012 Mar;60(1):340-52. doi: 10.1016/j.neuroimage.2011.11.094. Epub 2011 Dec 8

Lee SP, Sung IK, Kim JH, Lee SY, Park HS, Shim CS. The effect of emotional stress and depression on the prevalence of digestive diseases. J Neurogastroenterol Motil. 2015 Mar 30;21(2):273-82. doi: 10.5056/jnm14116.

Lemaire V, Koehl M, Le Moal M, Abrous DN. Prenatal stress produces learning deficits associated with an inhibition of neurogenesis in the hippocampus. Proc Natl Acad Sci U S A. 2000 Sep 26;97(20):11032-7. doi: 10.1073/pnas.97.20.11032.

Lemaitre H, Goldman AL, Sambataro F, Verchinski BA, Meyer-Lindenberg A, Weinberger DR, Mattay VS. Normal age-related brain morphometric changes:

nonuniformity across cortical thickness, surface area and gray matter volume? Neurobiol Aging. 2012 Mar;33(3):617.e1-9. doi: 10.1016/j.neurobiolaging.2010.07.013. Epub 2010 Aug 23.

LeMoult J, Humphreys KL, Tracy A, Hoffmeister JA, Ip E, Gotlib IH. Meta-analysis: Exposure to Early Life Stress and Risk for Depression in Childhood and Adolescence. J Am Acad Child Adolesc Psychiatry. 2020 Jul;59(7):842-855. doi: 10.1016/j.jaac.2019.10.011. Epub 2019 Oct 30.

Lepage C, Wagstyl K, Jung B, Seidlitz J, Sponheim C, Ungerleider L, Wang X, Evans AC, Messinger A. CIVET-Macaque: An automated pipeline for MRI-based cortical surface generation and cortical thickness in macaques. Neuroimage. 2021 Feb 15;227:117622. doi: 10.1016/j.neuroimage.2020.117622. Epub 2020 Dec 8.

Lim L, Radua J, Rubia K. Gray matter abnormalities in childhood maltreatment: a voxel-wise meta-analysis. Am J Psychiatry. 2014 Aug;171(8):854-63. doi: 10.1176/appi.ajp.2014.13101427.

Liu Q, Liu Y, Leng X, Han J, Xia F, Chen H. Impact of Chronic Stress on Attention Control: Evidence from Behavioral and Event-Related Potential Analyses. Neurosci Bull. 2020 Nov;36(11):1395-1410. doi: 10.1007/s12264-020-00549-9. Epub 2020 Sep 15.

Long X, Liao W, Jiang C, Liang D, Qiu B, Zhang L. Healthy aging: an automatic analysis of global and regional morphological alterations of human brain. Acad Radiol. 2012 Jul;19(7):785-93. doi: 10.1016/j.acra.2012.03.006. Epub 2012 Apr 14.

Lovell B, Moss M, Wetherell MA. Perceived stress, common health complaints and diurnal patterns of cortisol secretion in young, otherwise healthy individuals. Horm Behav. 2011 Aug;60(3):301-5. doi: 10.1016/j.yhbeh.2011.06.007. Epub 2011 Jun 22.

Lucassen PJ, Vollmann-Honsdorf GK, Gleisberg M, Czéh B, De Kloet ER, Fuchs E. Chronic psychosocial stress differentially affects apoptosis in hippocampal subregions and cortex of the adult tree shrew. Eur J Neurosci. 2001 Jul;14(1):161-6. doi: 10.1046/j.0953-816x.2001.01629.x.

Lucini D, Di Fede G, Parati G, Pagani M. Impact of chronic psychosocial stress on autonomic cardiovascular regulation in otherwise healthy subjects. Hypertension.

2005 Nov;46(5):1201-6. doi: 10.1161/01.HYP.0000185147.32385.4b. Epub 2005 Oct 3.

Maddock RJ, Garrett AS, Buonocore MH. Remembering familiar people: the posterior cingulate cortex and autobiographical memory retrieval. Neuroscience. 2001;104(3):667-76. doi: 10.1016/s0306-4522(01)00108-7.

Malhi GS, Das P, Outhred T, Bell E, Gessler D, Bryant R, Mannie Z. Significant age by childhood trauma interactions on grey matter volumes: A whole brain VBM analysis. Bipolar Disord. 2023 May;25(3):209-220. doi: 10.1111/bdi.13286. Epub 2023 Jan 22.

Marcus DS, Harwell J, Olsen T, Hodge M, Glasser MF, Prior F, Jenkinson M, Laumann T, Curtiss SW, Van Essen DC. Informatics and data mining tools and strategies for the human connectome project. Front Neuroinform. 2011 Jun 27;5:4. doi: 10.3389/fninf.2011.00004.

Matochik JA, Chefer SI, Lane MA, Woolf RI, Morris ED, Ingram DK, Roth GS, London ED. Age-related decline in striatal volume in monkeys as measured by magnetic resonance imaging. Neurobiol Aging. 2000 Jul-Aug;21(4):591-8. doi: 10.1016/s0197-4580(00)00134-2.

Mattison JA, Vaughan KL. An overview of nonhuman primates in aging research. Exp Gerontol. 2017 Aug;94:41-45. doi: 10.1016/j.exger.2016.12.005. Epub 2016 Dec 10

McLafferty M, Armour C, Bunting B, Ennis E, Lapsley C, Murray E, O'Neill S. Coping, stress, and negative childhood experiences: The link to psychopathology, self-harm, and suicidal behavior. Psych J. 2019 Sep;8(3):293-306. doi: 10.1002/pchj.301. Epub 2019 Jun 25.

McLaren DG, Kosmatka KJ, Oakes TR, Kroenke CD, Kohama SG, Matochik JA, Ingram DK, Johnson SC. A population-average MRI-based atlas collection of the rhesus macaque. Neuroimage. 2009 Mar 1;45(1):52-9. doi: 10.1016/j.neuroimage.2008.10.058. Epub 2008 Nov 14.

McLaughlin KA, Sheridan MA, Winter W, Fox NA, Zeanah CH, Nelson CA. Widespread reductions in cortical thickness following severe early-life deprivation: a neurodevelopmental pathway to attention-deficit/hyperactivity disorder. Biol

Psychiatry. 2014 Oct 15;76(8):629-38. doi: 10.1016/j.biopsych.2013.08.016. Epub 2013 Oct 3.

Meyer JS, Hamel AF. Models of stress in nonhuman primates and their relevance for human psychopathology and endocrine dysfunction. ILAR J. 2014;55(2):347-60. doi: 10.1093/ilar/ilu023.

Milham MP, Ai L, Koo B, Xu T, Amiez C, Balezeau F, Baxter MG, Blezer ELA, Brochier T, Chen A, Croxson PL, Damatac CG, Dehaene S, Everling S, Fair DA, Fleysher L, Freiwald W, Froudist-Walsh S, Griffiths TD, Guedj C, Hadj-Bouziane F, Ben Hamed S, Harel N, Hiba B, Jarraya B, Jung B, Kastner S, Klink PC, Kwok SC, Laland KN, Leopold DA, Lindenfors P, Mars RB, Menon RS, Messinger A, Meunier M, Mok K, Morrison JH, Nacef J, Nagy J, Rios MO, Petkov CI, Pinsk M, Poirier C, Procyk E, Rajimehr R, Reader SM, Roelfsema PR, Rudko DA, Rushworth MFS, Russ BE, Sallet J, Schmid MC, Schwiedrzik CM, Seidlitz J, Sein J, Shmuel A, Sullivan EL, Ungerleider L, Thiele A, Todorov OS, Tsao D, Wang Z, Wilson CRE, Yacoub E, Ye FQ, Zarco W, Zhou YD, Margulies DS, Schroeder CE. An Open Resource for Non-human Primate Imaging. Neuron. 2018 Oct 10;100(1):61-74.e2. doi: 10.1016/j.neuron.2018.08.039. Epub 2018 Sep 27.

Mills KL, Goddings AL, Herting MM, Meuwese R, Blakemore SJ, Crone EA, Dahl RE, Güroğlu B, Raznahan A, Sowell ER, Tamnes CK. Structural brain development between childhood and adulthood: Convergence across four longitudinal samples. Neuroimage. 2016 Nov 1;141:273-281. doi: 10.1016/j.neuroimage.2016.07.044. Epub 2016 Jul 22.

Monninger M, Kraaijenvanger EJ, Pollok TM, Boecker-Schlier R, Jennen-Steinmetz C, Baumeister S, Esser G, Schmidt M, Meyer-Lindenberg A, Laucht M, Brandeis D, Banaschewski T, Holz NE. The Long-Term Impact of Early Life Stress on Orbitofrontal Cortical Thickness. Cereb Cortex. 2020 Mar 14;30(3):1307-1317. doi: 10.1093/cercor/bhz167.

Morozov YM, Datta D, Paspalas CD, Arnsten AFT. Ultrastructural evidence for impaired mitochondrial fission in the aged rhesus monkey dorsolateral prefrontal cortex. Neurobiol Aging. 2017 Mar;51:9-18. doi: 10.1016/j.neurobiolaging.2016.12.001. Epub 2016 Dec 10.

Mulder MJ, Keuken MC, Bazin PL, Alkemade A, Forstmann BU. Size and shape matter: The impact of voxel geometry on the identification of small nuclei. PLoS One. 2019 Apr 12;14(4):e0215382. doi: 10.1371/journal.pone.0215382.

Murphy CFB, Rabelo CM, Silagi ML, Mansur LL, Bamiou DE, Schochat E. Auditory Processing Performance of the Middle-Aged and Elderly: Auditory or Cognitive Decline? J Am Acad Audiol. 2018 Jan;29(1):5-14. doi: 10.3766/jaaa.15098.

Navarro A, López-Cepero JM, Bández MJ, Sánchez-Pino MJ, Gómez C, Cadenas E, Boveris A. Hippocampal mitochondrial dysfunction in rat aging. Am J Physiol Regul Integr Comp Physiol. 2008 Feb;294(2):R501-9. doi: 10.1152/ajpregu.00492.2007.

Nyberg L, Salami A, Andersson M, Eriksson J, Kalpouzos G, Kauppi K, Lind J, Pudas S, Persson J, Nilsson LG. Longitudinal evidence for diminished frontal cortex function in aging. Proc Natl Acad Sci U S A. 2010 Dec 28;107(52):22682-6. doi: 10.1073/pnas.1012651108. Epub 2010 Dec 14.

Öz G, Tkáč I, Uğurbil K. Animal models and high field imaging and spectroscopy. Dialogues Clin Neurosci. 2013 Sep;15(3):263-78. doi: 10.31887/DCNS.2013.15.3/goz.

Papagni SA, Benetti S, Arulanantham S, McCrory E, McGuire P, Mechelli A. Effects of stressful life events on human brain structure: a longitudinal voxel-based morphometry study. Stress. 2011 Mar;14(2):227-32. doi: 10.3109/10253890.2010.522279. Epub 2010 Oct 31.

Parker KJ, Maestripieri D. Identifying key features of early stressful experiences that produce stress vulnerability and resilience in primates. Neurosci Biobehav Rev. 2011 Jun;35(7):1466-83. doi: 10.1016/j.neubiorev.2010.09.003. Epub 2010 Sep 17.

Peelle JE, Cusack R, Henson RN. Adjusting for global effects in voxel-based morphometry: gray matter decline in normal aging. Neuroimage. 2012 Apr 2;60(2):1503-16. doi: 10.1016/j.neuroimage.2011.12.086. Epub 2012 Jan 8.

Peters A, Kemper T. A review of the structural alterations in the cerebral hemispheres of the aging rhesus monkey. Neurobiol Aging. 2012 Oct;33(10):2357-72. doi: 10.1016/j.neurobiolaging.2011.11.015. Epub 2011 Dec 21.

Pfefferle D, Plümer S, Burchardt L, Treue S, Gail A. Assessment of stress responses in rhesus macaques (Macaca mulatta) to daily routine procedures in system neuroscience based on salivary cortisol concentrations. PLoS One. 2018 Jan 2;13(1):e0190190. doi: 10.1371/journal.pone.0190190.

Phillips KA, Bales KL, Capitanio JP, Conley A, Czoty PW, 't Hart BA, Hopkins WD, Hu SL, Miller LA, Nader MA, Nathanielsz PW, Rogers J, Shively CA, Voytko ML. Why primate models matter. Am J Primatol. 2014 Sep;76(9):801-27. doi: 10.1002/ajp.22281. Epub 2014 Apr 10.

Podgórski P, Bladowska J, Sasiadek M, Zimny A. Novel Volumetric and Surface-Based Magnetic Resonance Indices of the Aging Brain - Does Male and Female Brain Age in the Same Way? Front Neurol. 2021 Jun 7;12:645729. doi: 10.3389/fneur.2021.645729.

Poirier G, Papaxanthis C, Mourey F, Gaveau J. Motor Planning of Vertical Arm Movements in Healthy Older Adults: Does Effort Minimization Persist With Aging? Front Aging Neurosci. 2020 Feb 25;12:37. doi: 10.3389/fnagi.2020.00037.

Poplawski J, Montina T, Metz G. Early Life Stress Accelerates Critical Periods and Causes Precocious Visual Cortex Development, 03 April 2023, PREPRINT (Version 1) available at Research Square [https://doi.org/10.21203/rs.3.rs-2715680/v1]

Postelnicu G, Zollei L, Fischl B. Combined volumetric and surface registration. IEEE Trans Med Imaging. 2009 Apr;28(4):508-22. doi: 10.1109/TMI.2008.2004426. Epub 2008 Aug 15.

Prescott MJ, Nixon ME, Farningham DAH, Naiken S, Griffiths MA. Laboratory macaques: When to wean? Applied Animal Behaviour Science. 2012 137(3-4), 194–207. https://doi.org/10.1016/j.applanim.2011.11.001

Prichard JW, Alger JR, Turner R. Brain imaging: the NMR revolution. Interview by Clare Thompson. BMJ. 1999 Nov 13;319(7220):1302. doi: 10.1136/bmj.319.7220.1302.

PRIMatE Data Exchange (PRIME-DE) Global Collaboration Workshop and Consortium. Electronic address: michael.milham@childmind.org; PRIMatE Data Exchange (PRIME-DE) Global Collaboration Workshop and Consortium.

Accelerating the Evolution of Nonhuman Primate Neuroimaging. Neuron. 2020 Feb 19;105(4):600-603. doi: 10.1016/j.neuron.2019.12.023.

Proskovec AL, Rezich MT, O'Neill J, Morsey B, Wang T, Ideker T, Swindells S, Fox HS, Wilson TW. Association of Epigenetic Metrics of Biological Age With Cortical Thickness. JAMA Netw Open. 2020 Sep 1;3(9):e2015428. doi: 10.1001/jamanetworkopen.2020.15428.

R Core Team (2021). R: A language and environment for statistical computing. R Foundation for Statistical Computing, Vienna, Austria. URL https://www.R-project.org/.

Ramanoël S, Hoyau E, Kauffmann L, Renard F, Pichat C, Boudiaf N, Krainik A, Jaillard A, Baciu M. Gray Matter Volume and Cognitive Performance During Normal Aging. A Voxel-Based Morphometry Study. Front Aging Neurosci. 2018 Aug 3;10:235. doi: 10.3389/fnagi.2018.00235.

Reemst K, Kracht L, Kotah JM, Rahimian R, van Irsen AAS, Congrains Sotomayor G, Verboon LN, Brouwer N, Simard S, Turecki G, Mechawar N, Kooistra SM, Eggen BJL, Korosi A. Early-life stress lastingly impacts microglial transcriptome and function under basal and immune-challenged conditions. Transl Psychiatry. 2022 Dec 8;12(1):507. doi: 10.1038/s41398-022-02265-6.

Reuter M, Rosas HD, Fischl B. Highly accurate inverse consistent registration: a robust approach. Neuroimage. 2010 Dec;53(4):1181-96. doi: 10.1016/j.neuroimage.2010.07.020. Epub 2010 Jul 14.

Reuter M, Schmansky NJ, Rosas HD, Fischl B. Within-subject template estimation for unbiased longitudinal image analysis. Neuroimage. 2012 Jul 16;61(4):1402-18. doi: 10.1016/j.neuroimage.2012.02.084. Epub 2012 Mar 10.

Revollo HW, Qureshi A, Collazos F, Valero S, Casas M. Acculturative stress as a risk factor of depression and anxiety in the Latin American immigrant population. Int Rev Psychiatry. 2011;23(1):84-92. doi: 10.3109/09540261.2010.545988.

Robillard KN, Lee KM, Chiu KB, MacLean AG. Glial cell morphological and density changes through the lifespan of rhesus macaques. Brain Behav Immun. 2016 Jul;55:60-69. doi: 10.1016/j.bbi.2016.01.006. Epub 2016 Feb 2.

Roelfsema PR, Treue S. Basic neuroscience research with nonhuman primates: a small but indispensable component of biomedical research. Neuron. 2014 Jun 18;82(6):1200-4. doi: 10.1016/j.neuron.2014.06.003.

Rönnlund M, Nyberg L, Bäckman L, Nilsson LG. Stability, growth, and decline in adult life span development of declarative memory: cross-sectional and longitudinal data from a population-based study. Psychol Aging. 2005 Mar;20(1):3-18. doi: 10.1037/0882-7974.20.1.3.

Rosada C, Bauer M, Golde S, Metz S, Roepke S, Otte C, Buss C, Wingenfeld K. Childhood trauma and cortical thickness in healthy women, women with post-traumatic stress disorder, and women with borderline personality disorder. Psychoneuroendocrinology. 2023 Jul;153:106118. doi: 10.1016/j.psyneuen.2023.106118. Epub 2023 Apr 20.

Rosenbaum RS, Köhler S, Schacter DL, Moscovitch M, Westmacott R, Black SE, Gao F, Tulving E. The case of K.C.: contributions of a memory-impaired person to memory theory. Neuropsychologia. 2005;43(7):989-1021. doi: 10.1016/j.neuropsychologia.2004.10.007. Epub 2005 Jan 12.

Ross MC, Sartin-Tarm AS, Letkiewicz AM, Crombie KM, Cisler JM. Distinct cortical thickness correlates of early life trauma exposure and posttraumatic stress disorder are shared among adolescent and adult females with interpersonal violence exposure. Neuropsychopharmacology. 2021 Mar;46(4):741-749. doi: 10.1038/s41386-020-00918-y. Epub 2020 Dec 3.

RStudio Team (2020). RStudio: Integrated Development for R. RStudio, PBC, Boston, MA URL http://www.rstudio.com/

Ruiz R, Roque A, Pineda E, Licona-Limón P, José Valdéz-Alarcón J, Lajud N. Early life stress accelerates age-induced effects on neurogenesis, depression, and metabolic risk. Psychoneuroendocrinology. 2018 Oct;96:203-211. doi: 10.1016/j.psyneuen.2018.07.012.

Sakai K, Rowe JB, Passingham RE. Active maintenance in prefrontal area 46 creates distractor-resistant memory. Nat Neurosci. 2002 May;5(5):479-84. doi: 10.1038/nn846.

Sakurai Y, Furukawa E, Kurihara M, Sugimoto I. Frontal Phonological Agraphia and Acalculia with Impaired Verbal Short-Term Memory due to Left Inferior Precentral Gyrus Lesion. Case Rep Neurol. 2018 Mar 14;10(1):72-82. doi: 10.1159/000487849.

Saleem KS, Logothetis NK. A combined MRI and histology atlas of the rhesus monkey brain in stereotaxic coordinates. 2nd ed San Diego: Elsevier/Academic press. with Horizontal, Coronal and Sagittal series. 2012.

Saleh A, Potter GG, McQuoid DR, Boyd B, Turner R, MacFall JR, Taylor WD. Effects of early life stress on depression, cognitive performance and brain morphology. Psychol Med. 2017 Jan;47(1):171-181. doi: 10.1017/S0033291716002403. Epub 2016 Sep 29.

Satyjeet F, Naz S, Kumar V, Aung NH, Bansari K, Irfan S, Rizwan A. Psychological Stress as a Risk Factor for Cardiovascular Disease: A Case-Control Study. Cureus. 2020 Oct 1;12(10):e10757. doi: 10.7759/cureus.10757.

Schumacher B, Pothof J, Vijg J, Hoeijmakers JHJ. The central role of DNA damage in the ageing process. Nature. 2021 Apr;592(7856):695-703. doi: 10.1038/s41586-021-03307-7. Epub 2021 Apr 28.

Schweizer S, Stretton J, Van Belle J, Price D, Calder AJ; Cam-CAN; Dalgleish T. Age-related decline in positive emotional reactivity and emotion regulation in a population-derived cohort. Soc Cogn Affect Neurosci. 2019 Aug 7;14(6):623-631. doi: 10.1093/scan/nsz036.

Scott BH, Leccese PA, Saleem KS, Kikuchi Y, Mullarkey MP, Fukushima M, Mishkin M, Saunders RC. Intrinsic Connections of the Core Auditory Cortical Regions and Rostral Supratemporal Plane in the Macaque Monkey. Cereb Cortex. 2017 Jan 1;27(1):809-840. doi: 10.1093/cercor/bhv277.

Setton R, Sheldon S, Turner GR, Spreng RN. Temporal pole volume is associated with episodic autobiographical memory in healthy older adults. Hippocampus. 2022 May;32(5):373-385. doi: 10.1002/hipo.23411. Epub 2022 Mar 5.

Shad MU, Muddasani S, Rao U. Gray matter differences between healthy and depressed adolescents: a voxel-based morphometry study. J Child Adolesc

Psychopharmacol. 2012 Jun;22(3):190-7. doi: 10.1089/cap.2011.0005. Epub 2012 Apr 26.

Shansky RM, Morrison JH. Stress-induced dendritic remodeling in the medial prefrontal cortex: effects of circuit, hormones and rest. Brain Res. 2009 Oct 13;1293:108-13. doi: 10.1016/j.brainres.2009.03.062. Epub 2009 Apr 8.

Sharma RK, Lalwani AK, Golub JS. Prevalence and Severity of Hearing Loss in the Older Old Population. JAMA Otolaryngol Head Neck Surg. 2020 Aug 1;146(8):762-763. doi: 10.1001/jamaoto.2020.0900.

Shields GS, Sazma MA, McCullough AM, Yonelinas AP. The effects of acute stress on episodic memory: A meta-analysis and integrative review. Psychol Bull. 2017 Jun;143(6):636-675. doi: 10.1037/bul0000100. Epub 2017 Apr 3.

Silson EH, Steel AD, Baker CI. Scene-Selectivity and Retinotopy in Medial Parietal Cortex. Front Hum Neurosci. 2016 Aug 18;10:412. doi: 10.3389/fnhum.2016.00412.

Simmons D. The use of animal models in studying genetic disease: transgenesis and induced mutation. Nature Education. 2008 1(1):70.

Simon M, Czéh B, Fuchs E. Age-dependent susceptibility of adult hippocampal cell proliferation to chronic psychosocial stress. Brain Res. 2005 Jul 12;1049(2):244-8. doi: 10.1016/j.brainres.2005.05.006.

Smith CD, Chebrolu H, Wekstein DR, Schmitt FA, Markesbery WR. Age and gender effects on human brain anatomy: a voxel-based morphometric study in healthy elderly. Neurobiol Aging. 2007 Jul;28(7):1075-87. doi: 10.1016/j.neurobiolaging.2006.05.018. Epub 2006 Jun 13.

Smith KE, Pollak SD. Early life stress and development: potential mechanisms for adverse outcomes. J Neurodev Disord. 2020 Dec 16;12(1):34. doi: 10.1186/s11689-020-09337-y.

Smith R, Lane RD, Alkozei A, Bao J, Smith C, Sanova A, Nettles M, Killgore WDS. The role of medial prefrontal cortex in the working memory maintenance of one's own emotional responses. Sci Rep. 2018 Feb 22;8(1):3460. doi: 10.1038/s41598-018-21896-8.

Song X, García-Saldivar P, Kindred N, Wang Y, Merchant H, Meguerditchian A, Yang Y, Stein EA, Bradberry CW, Ben Hamed S, Jedema HP, Poirier C. Strengths and challenges of longitudinal non-human primate neuroimaging. Neuroimage. 2021 Aug 1;236:118009. doi: 10.1016/j.neuroimage.2021.118009. Epub 2021 Mar 29.

Sotoudeh N, Namavar MR, Zarifkar A, Heidarzadegan AR. Age-dependent changes in the medial prefrontal cortex and medial amygdala structure, and elevated plus-maze performance in the healthy male Wistar rats. IBRO Rep. 2020 Aug 13;9:183-194. doi: 10.1016/j.ibror.2020.08.002.

Spinelli S, Chefer S, Suomi SJ, Higley JD, Barr CS, Stein E. Early-life stress induces long-term morphologic changes in primate brain. Arch Gen Psychiatry. 2009 Jun;66(6):658-65. doi: 10.1001/archgenpsychiatry.2009.52.

Stevens FL, Hurley RA, Taber KH. Anterior cingulate cortex: unique role in cognition and emotion. J Neuropsychiatry Clin Neurosci. 2011 Spring;23(2):121-5. doi: 10.1176/jnp.23.2.jnp121.

Stonebarger GA, Bimonte-Nelson HA, Urbanski HF. The Rhesus Macaque as a Translational Model for Neurodegeneration and Alzheimer's Disease. Front Aging Neurosci. 2021 Sep 3;13:734173. doi: 10.3389/fnagi.2021.734173.

Storsve AB, Fjell AM, Tamnes CK, Westlye LT, Overbye K, Aasland HW, Walhovd KB. Differential longitudinal changes in cortical thickness, surface area and volume across the adult life span: regions of accelerating and decelerating change. J Neurosci. 2014 Jun 18;34(25):8488-98. doi: 10.1523/JNEUROSCI.0391-14.2014.

Su FY, Chen JR, Chen CM, Huang YC, Peng SL. Assessing Age-Related Gray Matter Differences in Young Adults with Voxel-Based Morphometry: The Effect of Field Strengths. Brain Sci. 2021 Mar 31;11(4):447. doi: 10.3390/brainsci11040447.

Svoboda K, Li N. Neural mechanisms of movement planning: motor cortex and beyond. Curr Opin Neurobiol. 2018 Apr;49:33-41. doi: 10.1016/j.conb.2017.10.023. Epub 2017 Nov 21.

Taki Y, Goto R, Evans A, Zijdenbos A, Neelin P, Lerch J, Sato K, Ono S, Kinomura S, Nakagawa M, Sugiura M, Watanabe J, Kawashima R, Fukuda H. Voxel-based

morphometry of human brain with age and cerebrovascular risk factors. Neurobiol Aging. 2004 Apr;25(4):455-63. doi: 10.1016/j.neurobiolaging.2003.09.002.

The MathWorks Inc. (2021). MATLAB version: 9.10.0 (R2021a), Natick, Massachusetts: The MathWorks Inc. https://www.mathworks.com

Tisserand DJ, van Boxtel MP, Pruessner JC, Hofman P, Evans AC, Jolles J. A voxel-based morphometric study to determine individual differences in gray matter density associated with age and cognitive change over time. Cereb Cortex. 2004 Sep;14(9):966-73. doi: 10.1093/cercor/bhh057. Epub 2004 Apr 27.

Toft H, Bramness JG, Lien L, Abebe DS, Wampold BE, Tilden T, Hestad K, Neupane SP. PTSD patients show increasing cytokine levels during treatment despite reduced psychological distress. Neuropsychiatr Dis Treat. 2018 Sep 17;14:2367-2378. doi: 10.2147/NDT.S173659.

Tomoda A, Navalta CP, Polcari A, Sadato N, Teicher MH. Childhood sexual abuse is associated with reduced gray matter volume in visual cortex of young women. Biol Psychiatry. 2009 Oct 1;66(7):642-8. doi: 10.1016/j.biopsych.2009.04.021. Epub 2009 Jun 27.

Tomoda A, Polcari A, Anderson CM, Teicher MH. Reduced visual cortex gray matter volume and thickness in young adults who witnessed domestic violence during childhood. PLoS One. 2012;7(12):e52528. doi: 10.1371/journal.pone.0052528. Epub 2012 Dec 26.

Tustison NJ, Avants BB, Cook PA, Zheng Y, Egan A, Yushkevich PA, Gee JC. N4ITK: improved N3 bias correction. IEEE Trans Med Imaging. 2010 Jun;29(6):1310-20. doi: 10.1109/TMI.2010.2046908. Epub 2010 Apr 8.

Tyborowska A, Volman I, Niermann HCM, Pouwels JL, Smeekens S, Cillessen AHN, Toni I, Roelofs K. Early-life and pubertal stress differentially modulate grey matter development in human adolescents. Sci Rep. 2018 Jun 15;8(1):9201. doi: 10.1038/s41598-018-27439-5.

Tymofiyeva O, Hu R, Kidambi R, Nguyen C, Max JE, Yang TT. A meta-analysis of brain morphometric aberrations in adolescents who experienced childhood trauma. Front Hum Neurosci. 2022 Dec 6;16:1022791. doi: 10.3389/fnhum.2022.1022791.

Tyrka AR, Parade SH, Price LH, Kao HT, Porton B, Philip NS, Welch ES, Carpenter LL. Alterations of Mitochondrial DNA Copy Number and Telomere Length With Early Adversity and Psychopathology. Biol Psychiatry. 2016 Jan 15;79(2):78-86. doi: 10.1016/j.biopsych.2014.12.025.

Uddin LQ, Nomi JS, Hébert-Seropian B, Ghaziri J, Boucher O. Structure and Function of the Human Insula. J Clin Neurophysiol. 2017 Jul;34(4):300-306. doi: 10.1097/WNP.0000000000000377.

Van Essen DC, Donahue CJ, Coalson TS, Kennedy H, Hayashi T, Glasser MF. Cerebral cortical folding, parcellation, and connectivity in humans, nonhuman primates, and mice. Proc Natl Acad Sci USA. 2019 Dec 26;116(52):26173-26180. doi: 10.1073/pnas.1902299116.

Verhaeghen P, Geigerman S, Yang H, Montoya AC, Rahnev D. Resolving Age-Related Differences in Working Memory: Equating Perception and Attention Makes Older Adults Remember as Well as Younger Adults. Exp Aging Res. 2019 Mar-Apr;45(2):120-134. doi: 10.1080/0361073X.2019.1586120. Epub 2019 Mar 8.

Villalon J, Joshi AA, Toga AW, Thompson PM. COMPARISON OF VOLUMETRIC REGISTRATION ALGORITHMS FOR TENSOR-BASED MORPHOMETRY. Proc IEEE Int Symp Biomed Imaging. 2011 Mar-Apr;2011:1536-1541. doi: 10.1109/ISBI.2011.5872694.

Vinke EJ, de Groot M, Venkatraghavan V, Klein S, Niessen WJ, Ikram MA, Vernooij MW. Trajectories of imaging markers in brain aging: the Rotterdam Study. Neurobiol Aging. 2018 Nov;71:32-40. doi: 10.1016/j.neurobiolaging.2018.07.001.

Vita A, De Peri L, Deste G, Sacchetti E. Progressive loss of cortical gray matter in schizophrenia: a meta-analysis and meta-regression of longitudinal MRI studies. Transl Psychiatry. 2012 Nov 20;2(11):e190. doi: 10.1038/tp.2012.116. Erratum in: Transl Psychiatry. 2013;3:e275.

Vo VG, Pyun JM, Bagyinszky E, An SSA, Kim SY. Identification of a Pathogenic PSEN1 Ala285Val Mutation Associated with Early-Onset Alzheimer's Disease. Curr Alzheimer Res. 2020;17(5):438-445. doi: 10.2174/1567205017666200626210727.

von Bartheld CS. Myths and truths about the cellular composition of the human brain: A review of influential concepts. J Chem Neuroanat. 2018 Nov;93:2-15. doi: 10.1016/j.jchemneu.2017.08.004. Epub 2017 Sep 2.

Vyas A, Mitra R, Shankaranarayana Rao BS, Chattarji S. Chronic stress induces contrasting patterns of dendritic remodeling in hippocampal and amygdaloid neurons. J Neurosci. 2002 Aug 1;22(15):6810-8. doi: 10.1523/JNEUROSCI.22-15-06810.2002.

Walsh ND, Dalgleish T, Lombardo MV, Dunn VJ, Van Harmelen AL, Ban M, Goodyer IM. General and specific effects of early-life psychosocial adversities on adolescent grey matter volume. Neuroimage Clin. 2014 Jan 11;4:308-18. doi: 10.1016/j.nicl.2014.01.001.

Wang J, Feng X, Wu J, Xie S, Li L, Xu L, Zhang Y, Ren X, Hu Z, Lv L, Hu X, Jiang T. Alterations of Gray Matter Volume and White Matter Integrity in Maternal Deprivation Monkeys. Neuroscience. 2018 Aug 1;384:14-20. doi: 10.1016/j.neuroscience.2018.05.020. Epub 2018 May 23.

Wang X, Cheng Z. Cross-Sectional Studies: Strengths, Weaknesses, and Recommendations. Chest. 2020 Jul;158(1S):S65-S71. doi: 10.1016/j.chest.2020.03.012.

Wang X, Luo Q, Tian F, Cheng B, Qiu L, Wang S, He M, Wang H, Duan M, Jia Z. Brain grey-matter volume alteration in adult patients with bipolar disorder under different conditions: a voxel-based meta-analysis. J Psychiatry Neurosci. 2019 Mar 1;44(2):89-101. doi: 10.1503/jpn.180002.

Wang X, Li XH, Cho JW, Russ BE, Rajamani N, Omelchenko A, Ai L, Korchmaros A, Sawiak S, Benn RA, Garcia-Saldivar P, Wang Z, Kalin NH, Schroeder CE, Craddock RC, Fox AS, Evans AC, Messinger A, Milham MP, Xu T. U-net model for brain extraction: Trained on humans for transfer to non-human primates. Neuroimage. 2021 Jul 15;235:118001. doi: 10.1016/j.neuroimage.2021.118001. Epub 2021 Mar 28

Wang Y, Jiang P, Tang S, Lu L, Bu X, Zhang L, Gao Y, Li H, Hu X, Wang S, Jia Z, Roberts N, Huang X, Gong Q. Left superior temporal sulcus morphometry mediates the impact of anxiety and depressive symptoms on sleep quality in healthy adults. Soc Cogn Affect Neurosci. 2021 May 4;16(5):492-501. doi: 10.1093/scan/nsab012.

Whitwell JL, Crum WR, Watt HC, Fox NC. Normalization of cerebral volumes by use of intracranial volume: implications for longitudinal quantitative MR imaging. AJNR Am J Neuroradiol. 2001 Sep;22(8):1483-9.

Wilson B, Petkov CI. Communication and the primate brain: insights from neuroimaging studies in humans, chimpanzees and macaques. Hum Biol. 2011 Apr;83(2):175-89. doi: 10.3378/027.083.0203.

Wisco JJ, Killiany RJ, Guttmann CR, Warfield SK, Moss MB, Rosene DL. An MRI study of age-related white and gray matter volume changes in the rhesus monkey. Neurobiol Aging. 2008 Oct;29(10):1563-75. doi: 10.1016/j.neurobiolaging.2007.03.022. Epub 2007 Apr 24.

Wise SP. Forward frontal fields: phylogeny and fundamental function. Trends Neurosci. 2008 Dec;31(12):599-608. doi: 10.1016/j.tins.2008.08.008. Epub 2008 Oct 4.

Wooddell LJ, Hamel AF, Murphy AM, Byers KL, Kaburu SSK, Meyer JS, Suomi SJ, Dettmer AM. Relationships between affiliative social behavior and hair cortisol concentrations in semi-free ranging rhesus monkeys. Psychoneuroendocrinology. 2017 Oct;84:109-115. doi: 10.1016/j.psyneuen.2017.06.018. Epub 2017 Jun 29.

Wu Y, Wang J, Zhang Y, Zheng D, Zhang J, Rong M, Wu H, Wang Y, Zhou K, Jiang T. The Neuroanatomical Basis for Posterior Superior Parietal Lobule Control Lateralization of Visuospatial Attention. Front Neuroanat. 2016 Mar 24;10:32. doi: 10.3389/fnana.2016.00032.

Wu Z, Peng Y, Hong M, Zhang Y. Gray Matter Deterioration Pattern During Alzheimer's Disease Progression: A Regions-of-Interest Based Surface Morphometry Study. Front Aging Neurosci. 2021 Feb 3;13:593898. doi: 10.3389/fnagi.2021.593898.

Yoshimura N, Tsuda H, Aquino D, Takagi A, Ogata Y, Koike Y, Minati L. Age-Related Decline of Sensorimotor Integration Influences Resting-State Functional Brain Connectivity. Brain Sci. 2020 Dec 10;10(12):966. doi: 10.3390/brainsci10120966.

Young ME, Ohm DT, Dumitriu D, Rapp PR, Morrison JH. Differential effects of aging on dendritic spines in visual cortex and prefrontal cortex of the rhesus monkey.

Neuroscience. 2014 Aug 22;274:33-43. doi: 10.1016/j.neuroscience.2014.05.008. Epub 2014 May 20.

Yu T, Xu H, Wang W, Li S, Chen Z, Deng H. Determination of endogenous corticosterone in rodent's blood, brain and hair with LC-APCI-MS/MS. J Chromatogr B Analyt Technol Biomed Life Sci. 2015 Oct 1;1002:267-76. doi: 10.1016/j.jchromb.2015.08.035. Epub 2015 Aug 28.

Zeighami Y, Fereshtehnejad SM, Dadar M, Collins DL, Postuma RB, Mišić B, Dagher A. A clinical-anatomical signature of Parkinson's disease identified with partial least squares and magnetic resonance imaging. Neuroimage. 2019 Apr 15;190:69-78. doi: 10.1016/j.neuroimage.2017.12.050. Epub 2017 Dec 19.

Zola-Morgan S, Squire LR, Amaral DG, Suzuki WA. Lesions of perirhinal and parahippocampal cortex that spare the amygdala and hippocampal formation produce severe memory impairment. J Neurosci. 1989 Dec;9(12):4355-70. doi: 10.1523/JNEUROSCI.09-12-04355.1989.

Appendix

AutoMacq: an automatic pipeline to analyse macaque structural MRI data

Nathan Kindred[1], Susanna Carella[1], Professor Martijn P van den Heuvel[2,3], Dr Fabien Balezeau[4], Dr Yujiang Wang[5], Dr Colline Poirier[1]

1- Biosciences Institute & Centre for Behaviour and Evolution, Faculty of Medical Sciences, Newcastle University, United Kingdom.
2- Department of Complex Traits Genetics, Center for Neurogenomics and Cognitive Research, Vrije Universiteit Amsterdam, Amsterdam Neuroscience, Amsterdam 1081 HV, the Netherlands
3- Department of Child Psychiatry, Amsterdam University Medical Center, Location Vrije Universiteit Amsterdam, Amsterdam Neuroscience, Amsterdam 1081 HV, the Netherlands
4- Biosciences Institute, Faculty of Medical Sciences, Newcastle University, United Kingdom.
5- CNNP Lab (www.cnnp-lab.com), Interdisciplinary Complex Systems Group, School of Computing, Newcastle University, United Kingdom.

Abstract

MRI scanning of rhesus macaques is a growing field due to their evolutionary proximity and similar neuroanatomy to humans. As such, there is a need for automatic macaque MRI processing pipelines. AutoMacq is a pipeline capable of processing rhesus macaque MRI data to produce both voxel-based and surface-based metrics. It involves minimal manual intervention and can be carried out without expert knowledge of macaque neuroanatomy. To test the quality of the pipeline, scans from 74 subjects across 8 different sites were processed. Results indicate that over 87% of tissue segmentations and surfaces were of satisfactory quality to not require additional manual correction. Hemispheric comparisons and analyses of scan-rescan data showed strong reliability of the volumetric and surface-based outputs. Finally, to illustrate potential applications of AutoMacq, the change in grey matter volume with ageing was investigated cross-sectionally using subjects aged 3-15 years (corresponding to adolescence until mid-adulthood). The analysis revealed a linear decrease in grey matter volume with age similar to what has been found in humans, reinforcing the value of rhesus macaques as a model of healthy human ageing.

1.

Introduction

Automatic pipelines are the gold standard in MRI data processing as they avoid biases that could be introduced by manual interventions and allow for standardisation of data processing. Many pipelines have been created to automatically process and analyse human MRI data, with minimal manual intervention from the researcher (https://neuro-jena.github.io/cat/; https://surfer.nmr.mgh.harvard.edu/fswiki/FreeSurferAnalysisPipelineOverview; https://www.nipreps.org/smriprep/; https://www.fil.ion.ucl.ac.uk/spm/software/spm12/; Fischer *et al.* 2012; Glasser *et al.* 2013; Reuter *et al.* 2012). They can handle both cross-sectional and longitudinal datasets and allow for investigation of voxel-based morphometry (VBM) and/or surface-based morphometry (SBM).

Over the last couple of decades, MRI scanning of animal models has become a rapidly growing field (Öz, Tkáč and Ugurbill 2013). Non-human primates are of particular comparative and translational interest due to their relative evolutionary proximity to humans. In particular, their similarity to humans in terms of brain anatomy and cognitive abilities have made them crucial model animals in neuroscience research (Phillips *et al.* 2014; Roefsema and Treue 2014; Stonebarger *et al.* 2021). Additionally, Rhesus macaque are of particular value for ageing research due to their comparable life

stages to humans, combined with their accelerated rate of ageing (3-4 times the rate of humans) which can allow for more efficient research (Mattison and Vaughan 2017).

The processing of macaque MRI data comes with unique issues, precluding the use of established human pipelines to process macaque MRI data (Milham et al., 2018; PRIMatE Data Exchange (PRIME-DE) Global Collaboration Workshop and Consortium 2020). Though similar in shape and organisation to the human brain, the macaque brain is around 12-16 times smaller than the human brain (in terms of volume), with specific areas accounting for different proportions of the macaque brain compared to the human brain (Croxson *et al.* 2018). Other differences include differences in the amount of tissue surrounding the brain as well as in tissue contrast, making it more difficult to extract and segment the brain in MRI scans, compared to human scans. Non-standardized surface coil arrangements are common when scanning macaques, and often result in variations in coil coverage and image intensity. Differences between sites in terms of equipment and protocols are also common and result in data across sites that varies greatly in terms of quality and scan parameters (Milham *et al.* 2018). Furthermore, motion artefacts can be an additional issue when scanning awake macaques, with the only current way to minimise these artefacts being through training and/or head fixation (PRIMatE Data Exchange (PRIME-DE) Global Collaboration Workshop and Consortium 2020).

Custom processing pipelines tailored for rhesus macaque MRI data are clearly required, and over the last few years such pipelines have been developed (Balbastre *et al.* 2017; Garcia-Saldivar et al. 2021; Lepage et al. 2021). These pipelines require manual correction of tissue segmentation and surfaces, which relies on expert knowledge of macaque neuroanatomy. Additionally, the currently available macaque processing pipelines implement surface-based morphometry only, with no clear option to carry out voxel-based morphometry, despite the complementarity of the two approaches (Goto *et al.* 2022).

This study therefore aimed to design a processing pipeline for rhesus macaque MRI data that can produce accurate tissue segmentations and surfaces without manual intervention and can produce both voxel-based and surface-based metrics.

2.

Materials and Methods

2.1.

Datasets

Scans from publicly available datasets, as well as those acquired locally or privately shared with the authors, were selected to test the pipeline. Data had been acquired on various scanners with various parameters and coil arrangements. An initial visual quality control of the scans was carried out prior to AutoMacq processing and the following section describes the datasets that were retained (for excluded scans and justification, see Suppl. Fig 1).

Cross-sectional datasets - The AutoMacq pipeline was tested using cross-sectional T1 scans from 8 different sites (N= 74 subjects, see Table 1; detailed scan parameters for each site are provided in suppl. Table 1). One of these datasets was collected at Newcastle University, as part of an ongoing longitudinal project. Three other datasets came from Deutsches Primatenzentrum (DPZ), Germany, the National Institute on Drug Abuse (NIDA), USA, and the University of Oxford, UK. The remaining five cross-sectional datasets were from the primate data exchange (PRIME-DE) (Milham *et al.* 2018): Mount Sinai School of Medicine (MSP and MSS), USA, Stem Cell and Brain Research Institute (SBRI), France, University of California Davis (UCD), USA and University of Western Ontario (UWO), Canada.

For some subjects, T2 data were available alongside the T1 scan (see Table 1). All the scans were acquired with a scanner strength of at least 3T and comprised a combination of scans acquired in anesthetized and awake animals.

Scan-Rescan datasets - For a subselection of data two scans per subject, acquired within one week, were available (N = 13). All data were acquired in awake animals, at Newcastle University. There was some overlap in the scans included in the cross-sectional and scan-rescan datasets from Newcastle University.

Table 1: Description of included datasets after the initial quality control check.

Data Type	Site	Subjects (M/F)	Age Range (in year)	Subjects with T2 data	Awake vs. Anaes.	Scanner Strength
CS	Newcastle	18 (12/6)	5-15	18	Awake	4.7T
CS	DPZ	21 (21/0)	6-11	6	Anaes.	3T
CS	NIDA	6 (6/0)	7-10	0	Anaes.	3T
CS	Oxford	8 (5/3)	5-8	0	Anaes.	3T
CS	MSP	8 (8/0)	3-5	4	Anaes.	3T
CS	MSS	5 (5/0)	5-6	5	Anaes.	3T
CS	SBRI	3 (1/2)	7-14	3	Anaes.	3T
CS	UWO	5 (5/0)	4-8	5	Anaes.	7T
	Total	*74 (63/11)*	*3-15*	*41*		
S-RS	Newcastle	13 (8/5)	5-15	13	Awake	4.7T

CS: cross-sectional datasets and S-RS: scan-rescan dataset. M: male and F: female. Anaes.: anaesthetised.

2.2.

Ethics

Original data were acquired in accordance with the relevant legislation in each country and approved by an ethics committee. The re-use of the data was approved by Newcastle University Animal Welfare Ethical Review Board (reference number 1021).

2.3.

Cross-sectional AutoMacq Pipeline

AutoMacq is optimised for the input of both T1 and T2 images, but can process T1 data alone, and utilises freely available software packages (SPM- https://www.fil.ion.ucl.ac.uk/spm/software/spm12/; FreeSurfer- Fischl 2012; ANTs- Avants *et al.* 2009; FSL- Jenkinson *et al.* 2012; Connectome Workbench- Marcus *et al.* 2011). The pipeline can use any macaque template. For this study, the population-average 112RM-SL template and its prior maps

(McLaren *et al.* 2009) were chosen for testing the pipeline. This template is aligned to the Saleem-Logothetis atlas (Saleem and Logothetis 2012) that provides both high-resolution MRI scans and histological sections to delineate the anatomy of the macaque brain. An Ear Bar Zero (EBZ) coordinate system is employed, meaning that the origin is set to the midpoint of the interaural line (Saleem and Logothetis 2012).

The AutoMacq pipeline is outlined in figure 1, and each step to process cross-sectional data is described in detail below (with step numbers referring to those in Fig. 1). AutoMacq can also process longitudinal structural MRI data from rhesus macaques, and this is discussed in the supplementary materials (see suppl. text, suppl. Table 2 and suppl. Figure 2). A detailed walkthrough, scripts and SPM batches for AutoMacq are available at: https://github.com/Nsk97/AutoMacq.git

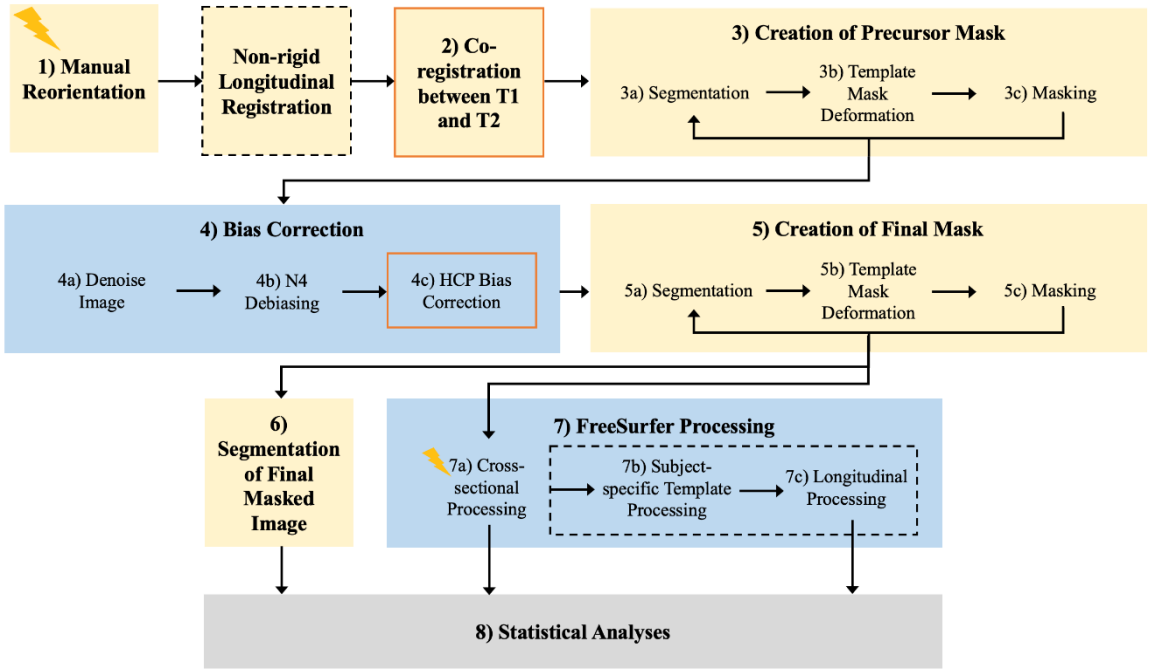

Figure 1: The AutoMacq pipeline. Yellow boxes represent steps carried out using SPM, blue boxes those carried out in a Linux environment (with ANTs, connectome workbench, FSL and FreeSurfer installed). An orange outline represents a step that is skipped if T2 data are not available, and a dashed black outline a step that would only be carried out for longitudinal data. Lightning bolts indicate a manual intervention.

2.3.1.

Cropping and Manual Reorientation (step 1)

Prior to processing through the AutoMacq pipeline, scans with large fields of view are cropped in FreeSurfer. This cropping minimises empty space and tissue outside of the skull. Cropping the field of view allows for more accurate masking later in the pipeline.

Following this, every T1 and, if available, T2 scan is manually reoriented in SPM. This involves rotating the scans and setting the origin to match the orientation and origin of the atlas. This manual reorientation step is simple and does not require any knowledge of macaque neuroanatomy.

2.3.2.

Co-registration between T1 and T2 (step 2)

The next step of AutoMacq consists of co-registering the reoriented T1 and T2 scans to ensure that their orientations precisely match. This step is done using the SPM intra-subject co-registration routine using a rigid-body model and image reslicing (moving the T2 scan to align it with the T1 scan). This step is skipped in the absence of T2 scans.

2.3.3. Brain extraction

To obtain accurate tissue segmentation of macaque data, it is helpful to first mask out non-brain tissues, a process called brain extraction or skull stripping. This is done in 3 steps: (1) the creation of a precursor mask in SPM; (2) bias correction carried out using ANTs, connectome workbench and FSL; and (3) the creation of the final mask in SPM.

Creation of Precursor Mask and initial brain extraction (step 3)

The precursor mask is an approximate, subject-specific mask that can be utilised for bias correction. A precursor mask in the native space is obtained by first creating a mask of the template (by binarising the sum of the grey matter (GM), white matter (WM) and cerebrospinal fluid (CSF) prior maps), and then deforming the template mask to match the subject-specific scan(s). This deformation between the template space and the native space is calculated using the SPM segmentation routine. This routine combines tissue classification of the subject-specific scans (combining information from T1 and T2 scans to improve the segmentation accuracy), correction of intensity non-uniformity (bias correction) and non-rigid co-registration to the template. The segmentation relies on 4 classes of tissue probability maps: GM, WM, CSF, and non-brain tissues (adding the non-brain tissue class was found to improve the quality of the segmentation). The T1 scan (and coregistered T2 scan, if available) is then masked using this approximate precursor mask.

This process (segmentation, mask deformation and masking) can be repeated several times if necessary to further increase the quality of the subject-specific mask, as long as no brain tissues are masked out. Macaque data differs from human in that images are often acquired using non-standardized arrangements of surface coils (Milham et al., 2018), generating increased variation in image intensity. Using the bias correction developed for human data in SPM, no parameter was found to be good enough to produce accurate subject-specific masks. To increase the quality of the mask, the precursor mask was created using little debiasing (heavy regularisation) in SPM and the main debiasing done outside SPM (please note that the precursor mask needs to be resliced to be used by other software).

Bias Correction (step 4)

For the AutoMacq pipeline, the ANTs functions DenoiseImage and N4BiasFieldCorrection are utilised. DenoiseImage removes noise from the scans using a spatially adaptive filter, and N4 debiasing is a variant of non-parametric, non-uniform, normalization (N3) debiasing (Tustison *et al.* 2010). DenoiseImage needs to be applied to the unmasked T1, whereas N4BiasFieldCorrection utilises an unmasked T1 image and the precursor mask as inputs.

To further minimise bias in the images, the program connectome workbench along with the bias correction script from the Human Connectome Pipeline (HCP) can be utilised for subjects with both T1 and T2 scans. This script uses the square root of T1w*T2w in order to correct the bias field, and improvements can be seen when this is used alongside other debiasing steps. The HCP script requires both unmasked and masked T1 images as inputs; the masked T1 is obtained by applying the function fslmaths (from FSL) to the N4 debiasing output.

Creation of Final Mask and Brain extraction (step 5)

A final mask is then created using the same approach described in step 3 but using the debiased scan(s) as input(s) of the segmentation, and a final masked T1 (and T2 if available) is produced which excludes non-brain tissues.

2.3.4.

Tissue segmentation (step 6)

A final segmentation of the masked, debiased T1 scan is then performed in SPM. The output files from this segmentation can then be used to calculate tissues volumes as well as the local amount (or density) of grey matter in each voxel. These metrics can then be analysed statistically for voxel-based morphometry studies.

2.3.5.

Surface-based Cross-Sectional Processing (step 7)

Surface-based processing in AutoMacq utilises custom analysis scripts that adapt the FreeSurfer standard processing stream for human MRI data. For cross-sectional processing, the FreeSurfer stream consists of 3 major stages: autorecon1, autorecon2 and autorecon3. For cross-sectional processing in AutoMacq, modifications are made to the autorecon1 and autorecon2 stages.

Autorecon1

Autorecon1 begins with computation of the affine transformation from the final masked T1 obtained in step 5 to the MNI305 atlas. This is required as atlas coordinates of different brain areas are needed for several downstream functions. The MNI305 is a human brain atlas, so this automatic computation tends to be extremely inaccurate for macaque data, and there is no simple way to substitute a macaque atlas for the MNI305 atlas. However, macaque MRI data can be successfully processed through FreeSurfer by manual correcting the atlas registration. This is done by matching the size and orientation of the masked T1 to the MNI305. Therefore, this manual step does not rely on any knowledge of macaque neuroanatomy and can be carried out quickly and easily by a non-expert. The rest of the autorecon1 stage includes correction of any remaining non-uniformity or fluctuations in intensity (unchanged FreeSurfer standard step). The final step of skull stripping is skipped since images have already been brain extracted in SPM.

Autorecon2

The autorecon2 stage begins with the segmentation of subcortical structures and the computation of their respective volumes. In AutoMacq, the standard stream is adapted to use the manually corrected atlas registration to initialise the subcortical segmentation. Next, WM is segmented to give a WM volume image (cerebellum and brainstem are excluded), which is then used to create the surface encoding the boundary of WM and GM in each hemisphere. These left and right WM surfaces are used as a starting point to generate surfaces encoding the boundary of GM and CSF in each hemisphere ('pial surfaces'). However, this processing in FreeSurfer alone does not always produce accurate surfaces. Instead of manually correcting the white matter surfaces (WM edits), the WM segmentation file produced by SPM (step 6) can be used to re-run the cortical surface generation. To be recognised correctly in FreeSurfer, the WM segment image is first binarized in SPM

(threshold of 0.2). A custom script was written to recognise this binarized WM volume as WM edits. As the last step of autorecon2, a binary mask of the cortical ribbon is then created.

Autorecon3

The autorecon3 stage carries out the co-registration of the GM and WM surfaces to the spherical atlas (spherical morph), in order to label brain regions for cortical parcellation. The entirety of autorecon3 can be ran unchanged from the standard FreeSurfer stream to acquire global brain metrics, but it is also possible to easily replace the human atlas with a macaque parcellation schema in order to acquire macaque parcellations.

2.4.

Statistics

Whole brain measures of GM, WM and CSF were extracted using SPM for every subject. Hemispheric measures of the same metrics were also extracted in SPM, using a hemisphere mask created through manual editing of the Saleem-Logothetis atlas mask. Whole brain and hemispheric measures of grey matter and white matter surface area, as well as cortical thickness were taken from FreeSurfer for every subject. Intraclass correlation coefficient (ICC) was calculated in R, using an absolute-agreement, single-measurement, two-way mixed-effects model, for scan-rescan comparisons. Pearson correlation analyses were carried out in R (https://www.r-project.org/) for hemisphere comparisons. This was used rather than ICC for the hemisphere comparisons as ICC accounts for systematic offsets, which could occur biologically between hemispheres.

The change in GMV with ageing was also investigated in R. Tests for normality and heteroscedasticity were first carried out. A non-linear fit was found to not significantly improve the percentage of variance explained by the model, so a linear model was fitted. Site/scanner was included as a random effect in the model, and total intracranial volume (TIV) was controlled for (fixed effect) in order to account for differences in head size (Whitwell *et al.* 2001).

3.

Results

3.1.

VBM outputs

All of the cross-sectional scans processed through AutoMacq (N=74) produced an accurate brain mask for skull striping (suppl. figure 3). Figure 2 illustrates a representative example of tissue volume outputs (grey matter and white matter volumes) obtained as the result of SPM segmentation. 95.9% of scans (N=71/74) produced tissue volumes of comparable quality to those in figure 2. The remaining scans (4.1%, 3/74) resulted in some errors in the segmentation of grey and white matter (suppl. figure 4).

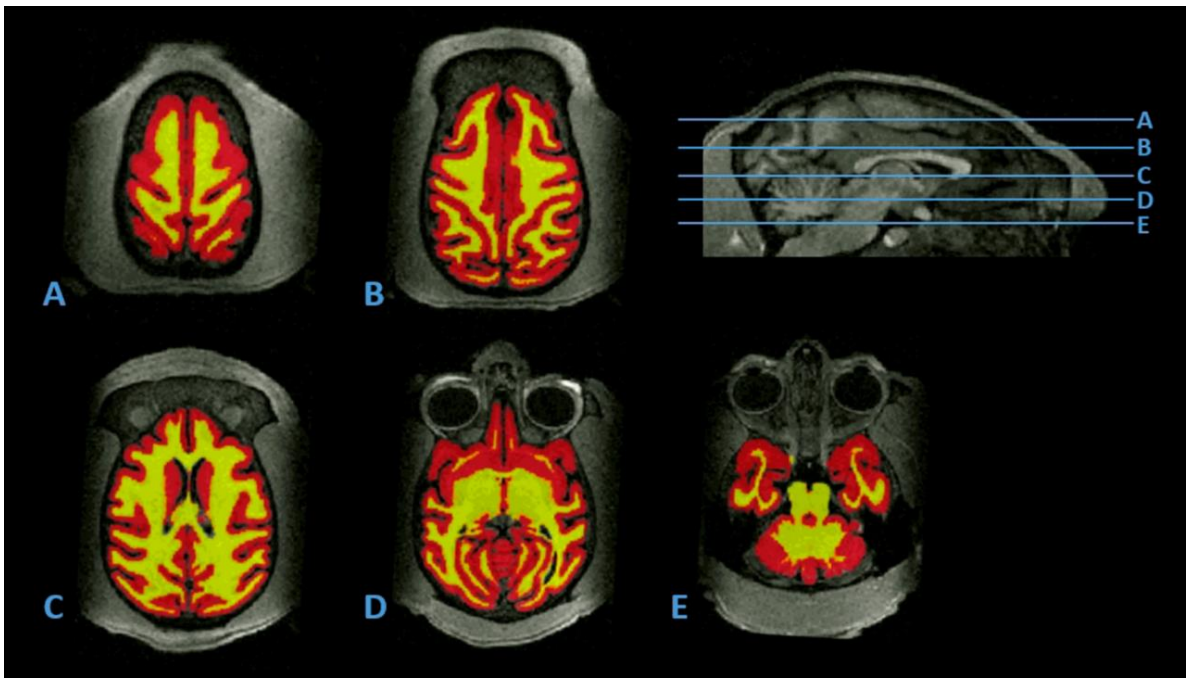

Figure 2: Representative tissue volumes produced by AutoMacq. Horizontal slices of a representative example of GMV (shown in red) and WMV (shown in yellow), produced using the cross-sectional AutoMacq pipeline, displayed on the corresponding T1 scan, and presented alongside a midsagittal image showing where each slice is taken from.

3.2.

SBM output

Figure 3 shows a representative example of FreeSurfer surfaces output from the cross-sectional AutoMacq pipeline, for the same subject for which tissue volume outputs were displayed in figure 2. 87.8% of scans (65/74) processed through AutoMacq resulted in surfaces comparable to those shown in figure 3. This was after the WM segmentation file from SPM was used in place of WM edits in FreeSurfer for 60/74 (81.1%) subjects (the other 14 subjects produced good quality surfaces without this step). This improvement of the surface accuracy with this step is illustrated in figure 4. However, even after the incorporation of the WM segmentation file from SPM, 9/74 (12.2%) subjects still showed some errors in their surfaces (see details in suppl. figure 5).

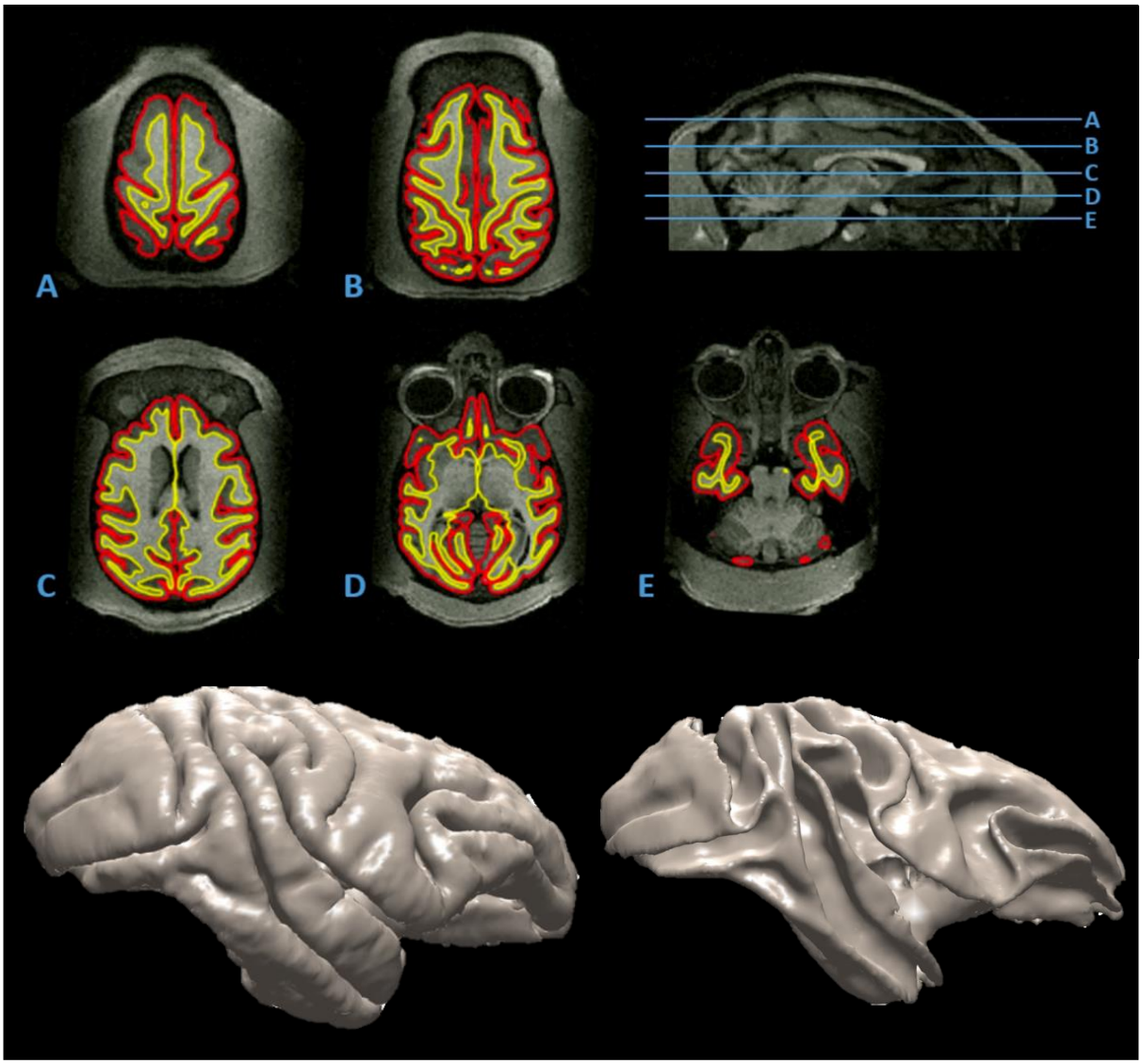

Figure 3: Representative surfaces produced by AutoMacq and 3D models of those surfaces. Horizontal slices of a representative example of pial (shown in red) and white matter (shown in yellow) surfaces, produced using the cross-sectional AutoMacq pipeline. A midsagittal image showing where in the brain each slice is taken from, and 3D models of the surfaces are also presented. The cerebellum and brainstem are excluded during FreeSurfer processing.

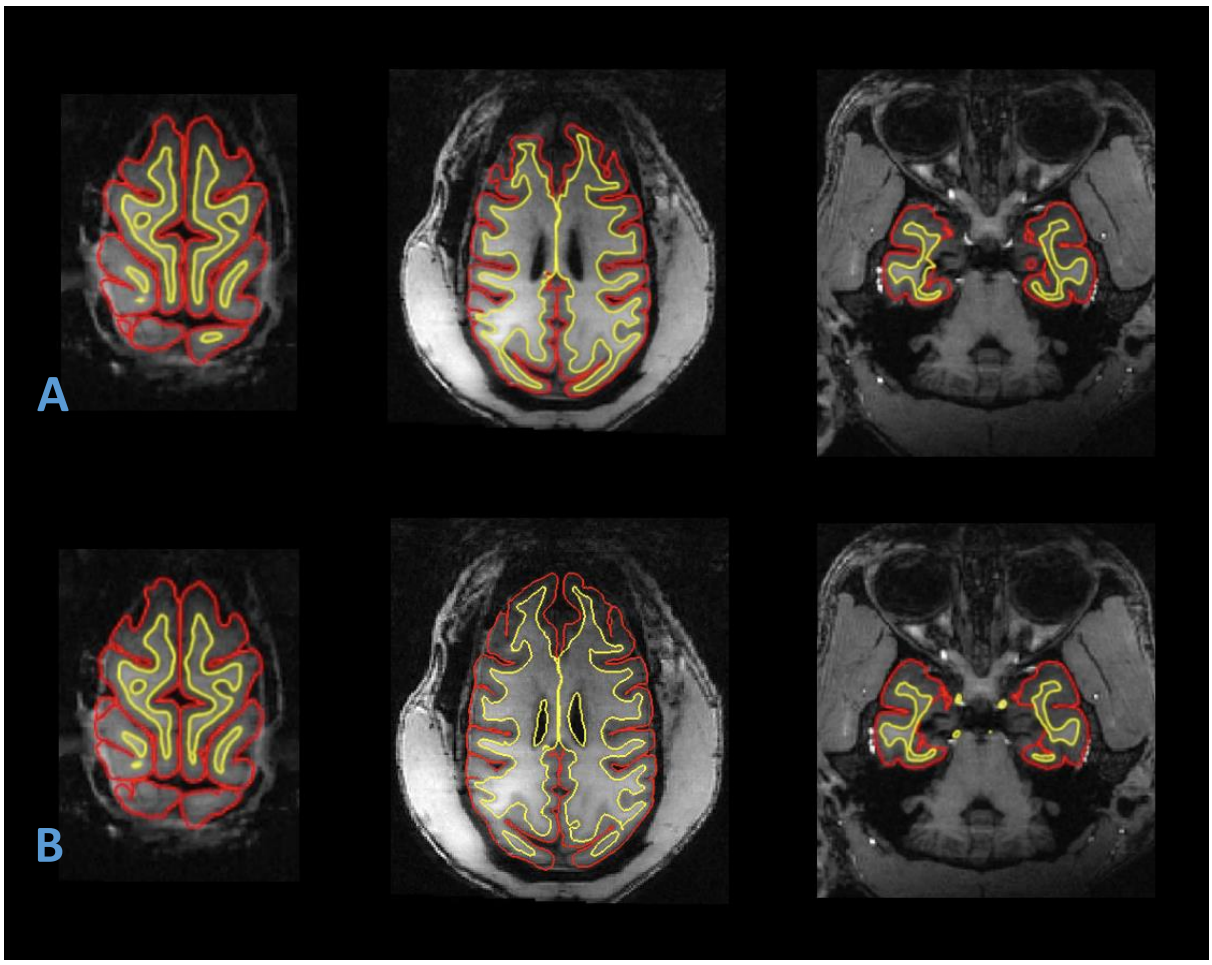

Figure 4: Comparison of surfaces produced with AutoMacq, without and with SPM WM. Horizontal slices of examples of pial (shown in red) and white matter (shown in yellow) surfaces, produced for the same subject using the cross-sectional AutoMacq pipeline, without WM from SPM (A) and with WM from SPM (B).

3.3.

Hemisphere Comparison

To assess the reliability of AutoMacq, various volume-based and surface-based metrics were compared between hemispheres. Considering that hemispheric differences from biological origin are minimal, this analysis allows for quantification of errors mainly due to AutoMacq processing. All of the subjects processed through AutoMacq (including those with errors in their outputs) were included in this analysis.

Results indicate strong correlation between hemispheres for all metrics tested (R values between 0.9 and 0.98, Fig. 5).

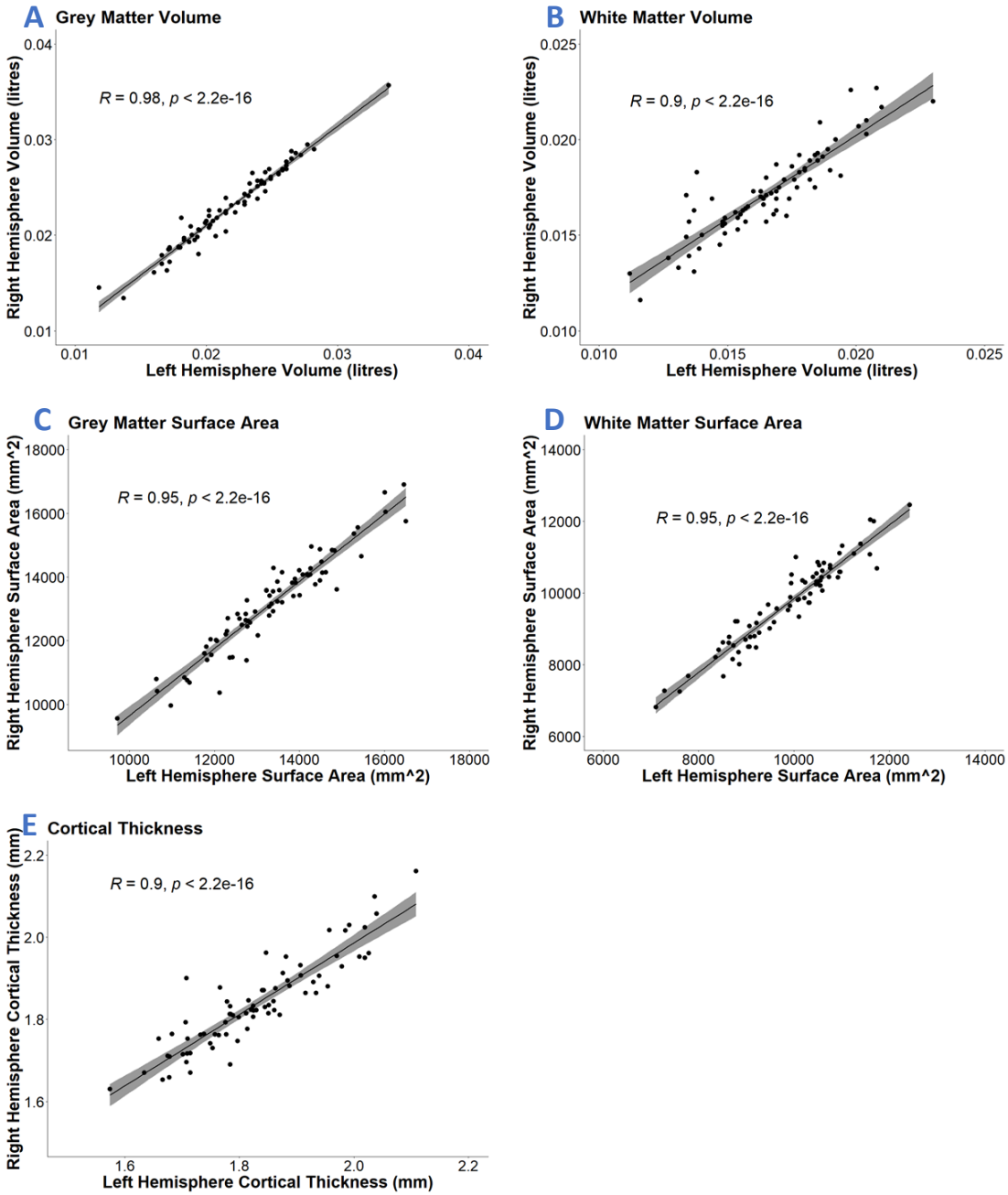

Figure 5: Hemisphere Comparison Graphs. Correlation between left and right hemisphere values for GM volume (A), WM volume (B), GM surface area (C), WM surface area (D) and cortical thickness (E). The linear fit and standard error are plotted, and R and p values are shown on each graph.

3.4.

Scan-Rescan

To further evaluate the reliability of AutoMacq, the scan-rescan dataset was processed to give both volume-based and surface-based outputs. Over such a short span of time between 'scan' and 'rescan' (less than 1 week), noticeable structural brain changes are not expected. Rescan data was available for a subset of 13 Newcastle subjects (8 males and 5 females).

Results indicate strong correlations across metrics despite a modest sample size and the fact that the animals were scanned while awake (ICC values between 0.6 and 0.95, fig. 6).

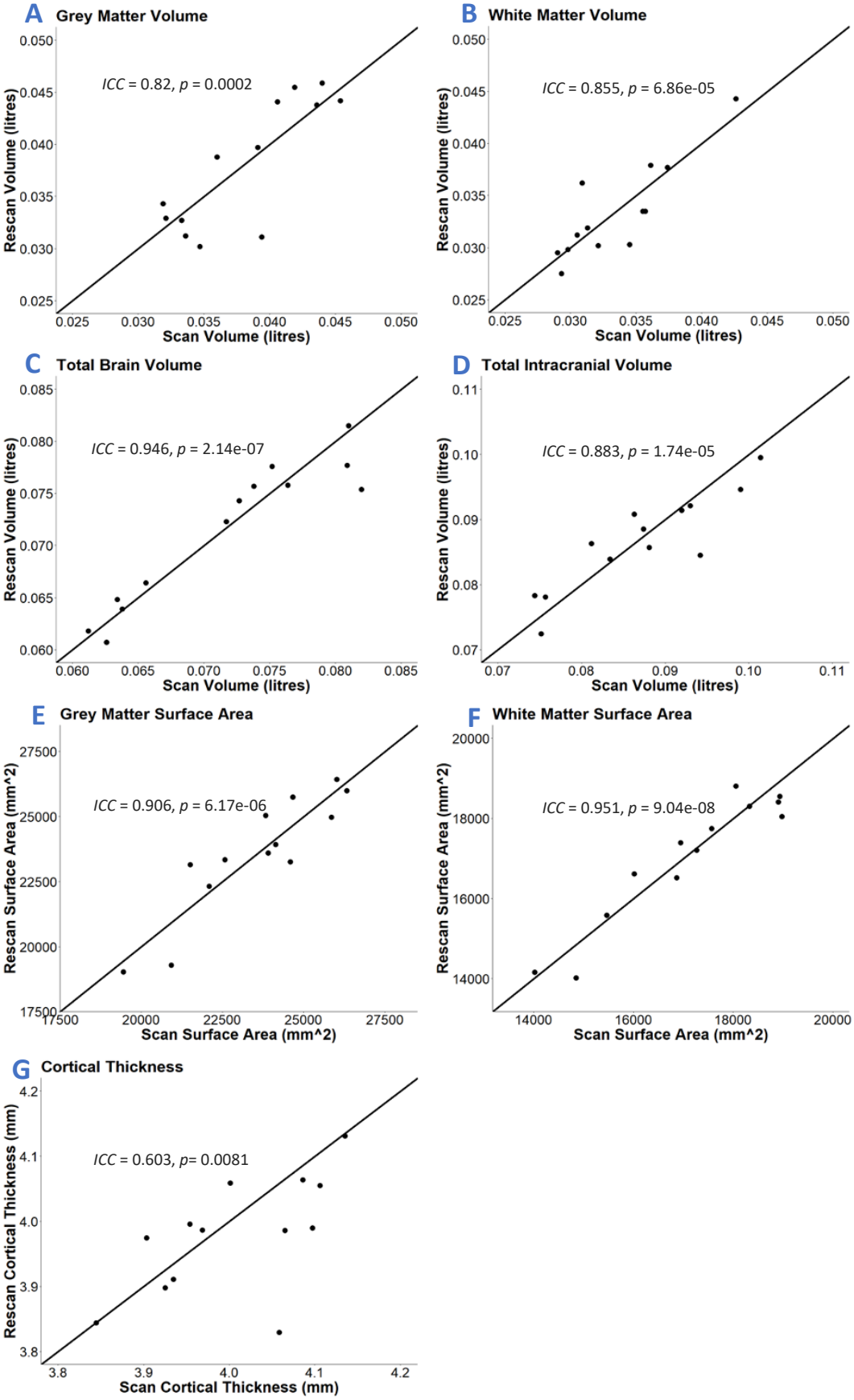
A
Grey Matter Volume
ICC = 0.82, p = 0.0002
Rescan Volume (litres)
Scan Volume (litres)
B
White Matter Volume
ICC = 0.855, p = 6.86e-05
Rescan Volume (litres)
Scan Volume (litres)
C
Total Brain Volume
ICC = 0.946, p = 2.14e-07
Rescan Volume (litres)
Scan Volume (litres)
D
Total Intracranial Volume
ICC = 0.883, p = 1.74e-05
Rescan Volume (litres)
Scan Volume (litres)
E
Grey Matter Surface Area
ICC = 0.906, p = 6.17e-06
Rescan Surface Area (mm^2)
Scan Surface Area (mm^2)
F
White Matter Surface Area
ICC = 0.951, p = 9.04e-08
Rescan Surface Area (mm^2)
Scan Surface Area (mm^2)
G
Cortical Thickness
ICC = 0.603, p= 0.0081
Rescan Cortical Thickness (mm)
Scan Cortical Thickness (mm)

Figure 6: Scan-Rescan Graphs. Graphs of the correlation between the scans and the rescans for GM volume (A), WM volume (B), total brain volume (C), total intracranial volume (D), GM surface area (E), WM surface area (F) and cortical thickness (G). The identity line, ICC value and p value are shown on each graph.

3.5.

Global Brain Changes with Ageing

To demonstrate a possible application of the AutoMacq pipeline, the impact of ageing on total GMV was tested using the male subjects from the cross-sectional datasets. Female subjects were excluded due to the small sample size, and the scans from any site with fewer than 5 male subjects were also excluded so that effect of site could be adequately controlled for in the model. A significant, linear decrease in total GMV with age was found (p=0.0066, fig. 7).

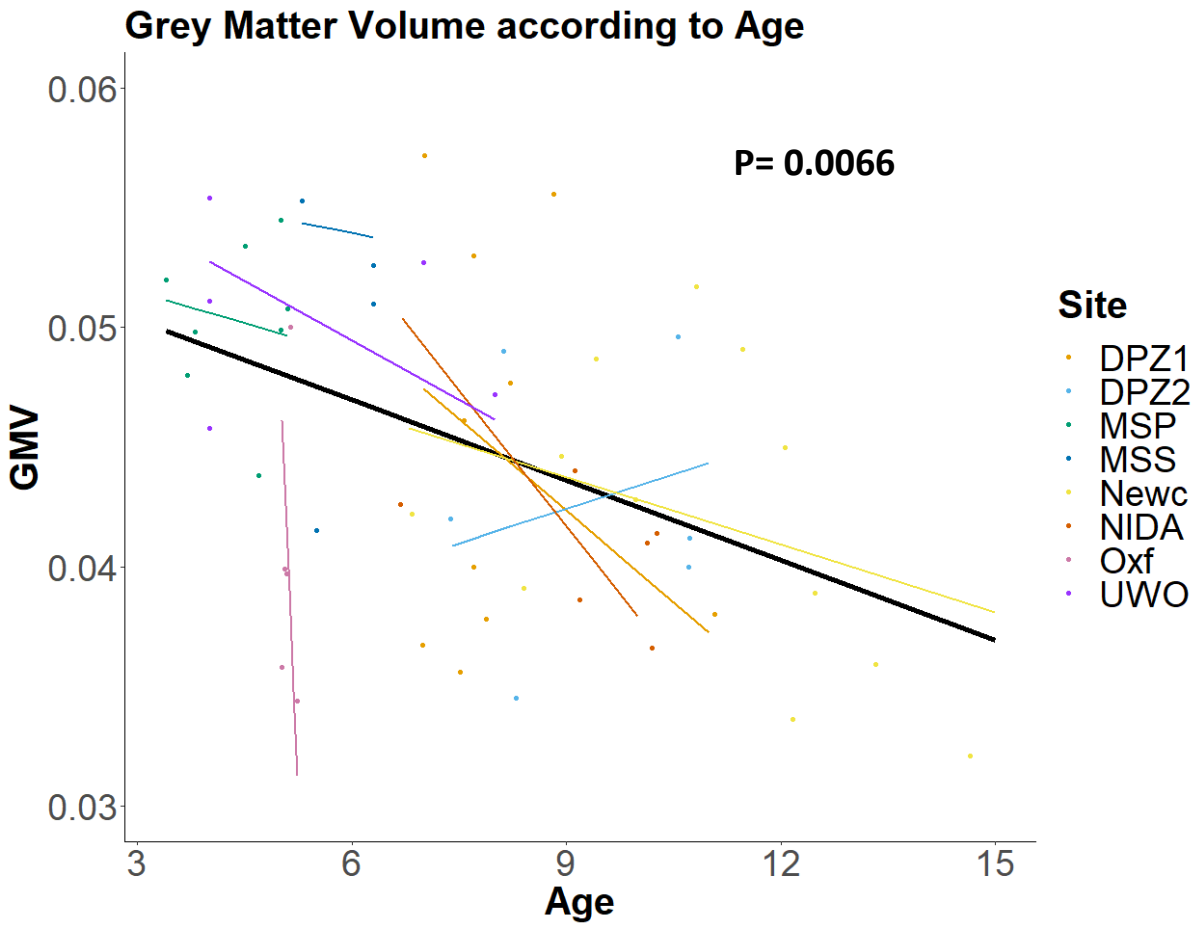

Figure 7: Changes in GM volume according to ageing. The bold black linear line corresponds to the main effect of age, while controlling for TIV and with site/scanner declared as a random effect. The thin coloured lines correspond to linear fits of age effect in each site while controlling for TIV. Dots correspond to raw data (unadjusted for TIV).

4.

Discussion

4.1.

Strengths of AutoMacq

AutoMacq is a robust processing pipeline, capable of successfully processing macaque MRI data with a wide range of quality and scan parameters, with minimal manual intervention. The two manual steps within the pipeline are simple to carry out and do not require any expert knowledge of macaque neuroanatomy. This, coupled with the automation of the rest of pipeline, makes AutoMacq relatively easy to use. Additionally, AutoMacq is unique amongst macaque pipelines in its ability to produce both voxel-based and surface-based metrics (Balbastre *et al.* 2017; Garcia-Saldivar et al. 2021; Lepage et al. 2021), allowing for more avenues of investigation and comparison with a wider range of previous studies (Goto *et al.* 2022).

Both T1 scans alone and datasets of T1 and T2 scans were successfully processed through AutoMacq. 100% of the scans processed through AutoMacq produced an accurate brain mask. This extremely high level of success in terms of brain extraction is better than the one obtained using the FSL bet function (Lepage et al. 2021) and comparable to what can be obtained by more sophisticated deep learning-based approaches (Wang et al., 2021). 95.9% of cross-sectional scans processed through AutoMacq gave good quality volume-based outputs and 87.8% gave good quality surface-based outputs. A good quality output was defined as one not requiring manual correction. The high percentage of good quality outputs produced illustrates AutoMacq's accuracy, with fewer errors in the outputs from AutoMacq than those produced when using other pipelines to process data from various sites (Garcia-Saldivar *et al.* 2021; Lepage et al. 2021). This better performance is likely to come from the use of SPM segmentation routine to identify the GM/WM boundary. AutoMacq was able to handle scans with a wide range of scan parameters and quality, including those known to be difficult to process, such as scans acquired in awake subjects (Newcastle University dataset) and scans from subjects that have open skulls due to head implants (Milham et al., 2018; PRIMatE Data Exchange (PRIME-DE) Global Collaboration Workshop and Consortium 2020). The few scans for which AutoMacq produced outputs with errors were not all from one site, indicating that the poorer outputs were not due to an inability to handle specific scanning parameters but likely due to issues specific to the individual scans themselves.

The present assessment of AutoMacq's quality as a processing pipeline is strengthened by the use of quantitative measures of reliability. The hemisphere comparison resulted in strong correlations for both volume-based and surface-based metrics, despite the fact that problematic volumes and surfaces were not excluded from the analyses. Since only minimal differences from biological origin were expected between hemispheres, this result indicates that AutoMacq produces reliable volume and surface outputs. The reliability of AutoMacq was then further demonstrated by the scan-rescan analysis. This analysis focused on a smaller sample (N=13) from the Newcastle dataset alone. Despite the limited sample size, good to excellent reliability was observed for all of the volume-based metrics tested and 2 of the 3 surface-based metrics, with the correlation for cortical thickness being weaker but still showing moderate reliability (Koo and Li 2016). This weaker correlation is unsurprising given how much influence sample size has in studies of cortical thickness (Pardoe *et al.* 2013), and the strength of this correlation did increase when the outlier was removed. Also, these correlations are fairly strong given the fact that macaques in this subset of data were all scanned whilst awake, and head movements are known to have a major impact on ICC in MRI studies (Hedges *et al.* 2022).

Overall, this scan-rescan analysis provides further evidence for the strong reliability of the AutoMacq pipeline. Both the hemisphere comparison and scan-rescan analysis resulted in similar correlations to what has been seen for human MRI studies (Carmon *et al.* 2020; Hedges *et al.* 2022).

A key strength of AutoMacq is the ability to carry out both VBM and SBM. This is an advantage as it allows for data to be exploited in multiple different ways, and the optional ability to substitute a macaque parcellation schema into the FreeSurfer processing compounds this. Furthermore, the ability to produce both volume-based and surface-based metrics allows for comparison to a wider range of studies, which is particularly important due to the continued publication of both VBM and SBM human studies, especially in clinical populations (Goto *et al.* 2022). Historically, human cortical VBM analyses have been criticised because they tended to suffer from volumetric projection to a template, particularly due to the highly variable cortical folding pattern between subjects, and SBM has been - in part- developed to avoid these issues (Postelnicu *et al.* 2008; Villalon *et al.* 2011). However, the cortical folding pattern in macaques is much more preserved between subjects (Van Essen *et al.* 2019). Additionally, the probability of problems linked to partial volume effects can be mitigated by the use of high magnetic field strengths, allowing the acquisition of images at higher spatial resolution (Milham *et al.* 2018). We therefore suspect that the potential drawbacks of VBM in human data are less likely to be relevant for macaque analyses, which could be tested in future using the AutoMacq pipeline.

4.2.

Limitations of AutoMacq

One limitation of AutoMacq is our use of a human atlas for the FreeSurfer processing. This is what necessitates the manual correction of the atlas registration. The inability to run AutoMacq fully automatically may make processing very large datasets more time consuming, however datasets of hundreds or thousands of macaque MRI scans are relatively rare currently. Additionally, AutoMacq produced good outputs for the vast majority of subjects despite the use of a human atlas. It is possible that substituting in a macaque atlas may result in even fewer errors but given the high success rate already observed this is likely to be unnecessary for most studies.

4.3.

Impact of Ageing on GMV

The impact of ageing on total GMV was investigated using 59 male subjects aged between 3 and 15 years, scanned using 8 different scanners from across 7 different sites. Given macaques age at 4 times the rate of humans during childhood (reaching sexual maturity around 4 and full physical maturity around age 5-6) and 3 times the rate of humans during adulthood (Mattison and Vaughan 2017), the age range tested here can be roughly compared to ages of 12-45 in humans.

A significant linear decrease in GMV was found, indicating that in male rhesus macaques there is a significant decline in GMV prior to reaching mid adulthood. This is a novel finding for this age group and suggests that the age-related decrease in GMV seen in mid/late adulthood in previous studies (Wisco *et al.* 2008; Chen *et al.* 2013) may actually start earlier in the lifespan. This finding fits with what has been seen in human studies, where a decline in GMV has been seen to occur across adolescence and early adulthood (Bartzokis *et al.* 2001; Lebel *et al.* 2012, Bethlehem *et al.* 2022). This study therefore provides further strength to rhesus macaques being models of healthy human ageing (Phillips *et al.* 2014; Roefsema and Treue 2014; Stonebarger *et al.* 2021).

It should be noted that this study only utilised male subjects, as scans were only available from very few females, and it would not have been possible to control for sex. It is therefore not possible to fully generalise these results to female rhesus macaques.

5.

Conclusion

AutoMacq offers a processing pipeline for rhesus macaque MRI data that is easy to use and can be completed without expert knowledge of macaque neuroanatomy. AutoMacq can process data with a wide range of quality and parameters, from across different sites and scanners, with a high level of success. The pipeline is unique amongst macaque processing pipelines in its ability to generate both surface-based and voxel-based metrics, offering two ways to exploit macaque MRI scans and allowing for easier comparison to a wider range of previous research.

6.

Acknowledgements

This study was funded by the MRC DiMeN Doctoral Training Partnership (MR/N013840/1).
With thanks to Dr Dirk Jan Ardesch for his guidance on FreeSurfer and his assistance in writing the initial FreeSurfer scripts. Thank you to Professor Hank P. Jedema and Dr Charles W Bradberry for sharing the NIDA dataset, Dr Jerome Sallet (Dpt of Experimental Psychology, Oxford, UK /INSERM U1208, Bron, France) for sharing the Oxford dataset, and the Cognitive Neuroscience Laboratory at the German Primate Center for sharing the DPZ dataset.

7.

References

Ashburner J, Ridgway GR. Symmetric diffeomorphic modeling of longitudinal structural MRI. Front Neurosci. 2013 Feb 5;6:197. doi: 10.3389/fnins.2012.00197.

Avants B.B., Tustison N., Song G. Advanced normalization tools (ANTS) Insight J. 2009;2(365):1–35.

Balbastre Y, Rivière D, Souedet N, Fischer C, Hérard AS, Williams S, Vandenberghe ME, Flament J, Aron-Badin R, Hantraye P, Mangin JF, Delzescaux T. Primatologist: A modular segmentation pipeline for macaque brain morphometry. Neuroimage. 2017 Nov 15;162:306-321. doi: 10.1016/j.neuroimage.2017.09.007. Epub 2017 Sep 9.

Bartzokis G, Beckson M, Lu PH, Nuechterlein KH, Edwards N, Mintz J. Age-related changes in frontal and temporal lobe volumes in men: a magnetic resonance imaging study. Arch Gen Psychiatry. 2001 May;58(5):461-5. doi: 10.1001/archpsyc.58.5.461. Erratum in: Arch Gen Psychiatry 2001 Aug;58(8):774.

Bethlehem RAI, Seidlitz J, White SR, Vogel JW, Anderson KM, Adamson C, Adler S, Alexopoulos GS, Anagnostou E, Areces-Gonzalez A, Astle DE, Auyeung B, Ayub M, Bae J, Ball G, Baron-Cohen S, Beare R, Bedford SA, Benegal V, Beyer F, Blangero J, Blesa Cábez M, Boardman JP, Borzage M, Bosch-Bayard JF, Bourke N, Calhoun VD, Chakravarty MM, Chen C, Chertavian C, Chetelat G, Chong YS, Cole JH, Corvin A, Costantino M, Courchesne E, Crivello F, Cropley VL, Crosbie J, Crossley N, Delarue M, Delorme R, Desrivieres S, Devenyi GA, Di Biase MA, Dolan R, Donald KA, Donohoe G, Dunlop K, Edwards AD, Elison JT, Ellis CT, Elman JA, Eyler L, Fair DA, Feczko E, Fletcher PC, Fonagy P, Franz CE, Galan-Garcia L, Gholipour A, Giedd J, Gilmore JH, Glahn DC, Goodyer IM, Grant PE, Groenewold NA,

Gunning FM, Gur RE, Gur RC, Hammill CF, Hansson O, Hedden T, Heinz A, Henson RN, Heuer K, Hoare J, Holla B, Holmes AJ, Holt R, Huang H, Im K, Ipser J, Jack CR Jr, Jackowski AP, Jia T, Johnson KA, Jones PB, Jones DT, Kahn RS, Karlsson H, Karlsson L, Kawashima R, Kelley EA, Kern S, Kim KW, Kitzbichler MG, Kremen WS, Lalonde F, Landeau B, Lee S, Lerch J, Lewis JD, Li J, Liao W, Liston C, Lombardo MV, Lv J, Lynch C, Mallard TT, Marcelis M, Markello RD, Mathias SR, Mazoyer B, McGuire P, Meaney MJ, Mechelli A, Medic N, Misic B, Morgan SE, Mothersill D, Nigg J, Ong MQW, Ortinau C, Ossenkoppele R, Ouyang M, Palaniyappan L, Paly L, Pan PM, Pantelis C, Park MM, Paus T, Pausova Z, Paz-Linares D, Pichet Binette A, Pierce K, Qian X, Qiu J, Qiu A, Raznahan A, Rittman T, Rodrigue A, Rollins CK, Romero-Garcia R, Ronan L, Rosenberg MD, Rowitch DH, Salum GA, Satterthwaite TD, Schaare HL, Schachar RJ, Schultz AP, Schumann G, Schöll M, Sharp D, Shinohara RT, Skoog I, Smyser CD, Sperling RA, Stein DJ, Stolicyn A, Suckling J, Sullivan G, Taki Y, Thyreau B, Toro R, Traut N, Tsvetanov KA, Turk-Browne NB, Tuulari JJ, Tzourio C, Vachon-Presseau É, Valdes-Sosa MJ, Valdes-Sosa PA, Valk SL, van Amelsvoort T, Vandekar SN, Vasung L, Victoria LW, Villeneuve S, Villringer A, Vértes PE, Wagstyl K, Wang YS, Warfield SK, Warrier V, Westman E, Westwater ML, Whalley HC, Witte AV, Yang N, Yeo B, Yun H, Zalesky A, Zar HJ, Zettergren A, Zhou JH, Ziauddeen H, Zugman A, Zuo XN; 3R-BRAIN; AIBL; Alzheimer's Disease Neuroimaging Initiative; Alzheimer's Disease Repository Without Borders Investigators; CALM Team; Cam-CAN; CCNP; COBRE; cVEDA; ENIGMA Developmental Brain Age Working Group; Developing Human Connectome Project; FinnBrain; Harvard Aging Brain Study; IMAGEN; KNE96; Mayo Clinic Study of Aging; NSPN; POND; PREVENT-AD Research Group; VETSA; Bullmore ET, Alexander-Bloch AF. Brain charts for the human lifespan. Nature. 2022 Apr;604(7906):525-533. doi: 10.1038/s41586-022-04554-y. Epub 2022 Apr 6. Erratum in: Nature. 2022 Oct;610(7931):E6

Carmon J, Heege J, Necus JH, Owen TW, Pipa G, Kaiser M, Taylor PN, Wang Y. Reliability and comparability of human brain structural covariance networks. Neuroimage. 2020 Oct 15;220:117104. doi: 10.1016/j.neuroimage.2020.117104.

Chen X, Errangi B, Li L, Glasser MF, Westlye LT, Fjell AM, Walhovd KB, Hu X, Herndon JG, Preuss TM, Rilling JK. Brain aging in humans, chimpanzees (Pan troglodytes), and rhesus macaques (Macaca mulatta): magnetic resonance imaging studies of macro- and microstructural changes. Neurobiol Aging. 2013 Oct;34(10):2248-60. doi: 10.1016/j.neurobiolaging.2013.03.028. Epub 2013 Apr 24.

Croxson PL, Forkel SJ, Cerliani L, Thiebaut de Schotten M. Structural Variability Across the Primate Brain: A Cross-Species Comparison. Cereb Cortex. 2018 Nov 1;28(11):3829-3841. doi: 10.1093/cercor/bhx244.

Donahue CJ, Glasser MF, Preuss TM, Rilling JK, Van Essen DC. Quantitative assessment of prefrontal cortex in humans relative to nonhuman primates. Proc Natl Acad Sci U S A. 2018 May 29;115(22):E5183-E5192. doi: 10.1073/pnas.1721653115. Epub 2018 May 8

Fischer, G. Operto, S. Laguitton, M. Perrot, I. Denghien, D. Rivière, and J.-F. Mangin: Morphologist 2012: the new morphological pipeline of BrainVISA, In *Proc. HBM*, 2012.

Fischl B. FreeSurfer. Neuroimage. 2012 Aug 15;62(2):774-81. doi: 10.1016/j.neuroimage.2012.01.021. Epub 2012 Jan 10.

Frazier-Logue N, Wang J, Wang Z, Sodums D, Khosla A, Samson AD, McIntosh AR, Shen K. A Robust Modular Automated Neuroimaging Pipeline for Model Inputs to TheVirtualBrain. Front Neuroinform. 2022 Jun 14;16:883223. doi: 10.3389/fninf.2022.883223.

Garcia-Saldivar P, Garimella A, Garza-Villarreal EA, Mendez FA, Concha L, Merchant H. PREEMACS: Pipeline for preprocessing and extraction of the macaque brain surface. Neuroimage. 2021 Feb 15;227:117671. doi: 10.1016/j.neuroimage.2020.117671. Epub 2020 Dec 24

Glasser MF, Sotiropoulos SN, Wilson JA, Coalson TS, Fischl B, Andersson JL, Xu J, Jbabdi S, Webster M, Polimeni JR, Van Essen DC, Jenkinson M; WU-Minn HCP Consortium. The minimal preprocessing pipelines for the Human Connectome Project. Neuroimage. 2013 Oct 15;80:105-24. doi: 10.1016/j.neuroimage.2013.04.127. Epub 2013 May 11.

Goto M, Abe O, Hagiwara A, Fujita S, Kamagata K, Hori M, Aoki S, Osada T, Konishi S, Masutani Y, Sakamoto H, Sakano Y, Kyogoku S, Daida H. Advantages of Using Both Voxel- and Surface-based Morphometry in Cortical Morphology Analysis: A Review of Various Applications. Magn Reson Med Sci. 2022 Mar 1;21(1):41-57. doi: 10.2463/mrms.rev.2021-0096. Epub 2022 Feb 18

Hedges EP, Dimitrov M, Zahid U, Brito Vega B, Si S, Dickson H, McGuire P, Williams S, Barker GJ, Kempton MJ. Reliability of structural MRI measurements: The effects of scan session, head tilt, inter-scan interval, acquisition sequence, FreeSurfer version and processing stream. Neuroimage. 2022 Feb 1;246:118751. doi: 10.1016/j.neuroimage.2021.118751.

Jenkinson M, Beckmann CF, Behrens TE, Woolrich MW, Smith SM. FSL. Neuroimage. 2012 Aug 15;62(2):782-90. doi: 10.1016/j.neuroimage.2011.09.015.

Koo TK, Li MY. A Guideline of Selecting and Reporting Intraclass Correlation Coefficients for Reliability Research. J Chiropr Med. 2016 Jun;15(2):155-63. doi: 10.1016/j.jcm.2016.02.012. Epub 2016 Mar 31. Erratum in: J Chiropr Med. 2017 Dec;16(4):346.

Lebel C, Gee M, Camicioli R, Wieler M, Martin W, Beaulieu C. Diffusion tensor imaging of white matter tract evolution over the lifespan. Neuroimage. 2012 Mar;60(1):340-52. doi: 10.1016/j.neuroimage.2011.11.094. Epub 2011 Dec 8

Lepage C, Wagstyl K, Jung B, Seidlitz J, Sponheim C, Ungerleider L, Wang X, Evans AC, Messinger A. CIVET-Macaque: An automated pipeline for MRI-based cortical surface generation and cortical thickness in macaques. Neuroimage. 2021 Feb 15;227:117622. doi: 10.1016/j.neuroimage.2020.117622. Epub 2020 Dec 8.

Marcus DS, Harwell J, Olsen T, Hodge M, Glasser MF, Prior F, Jenkinson M, Laumann T, Curtiss SW, Van Essen DC. Informatics and data mining tools and strategies for the human connectome project. Front Neuroinform. 2011 Jun 27;5:4.

Mattison JA, Vaughan KL. An overview of nonhuman primates in aging research. Exp Gerontol. 2017 Aug;94:41-45. doi: 10.1016/j.exger.2016.12.005. Epub 2016 Dec 10

McLaren DG, Kosmatka KJ, Oakes TR, Kroenke CD, Kohama SG, Matochik JA, Ingram DK, Johnson SC. A population-average MRI-based atlas collection of the rhesus macaque. Neuroimage. 2009 Mar 1;45(1):52-9. doi: 10.1016/j.neuroimage.2008.10.058. Epub 2008 Nov 14.

Milham MP, Ai L, Koo B, Xu T, Amiez C, Balezeau F, Baxter MG, Blezer ELA, Brochier T, Chen A, Croxson PL, Damatac CG, Dehaene S, Everling S, Fair DA, Fleysher L, Freiwald W, Froudist-Walsh S, Griffiths TD, Guedj C, Hadj-Bouziane F, Ben Hamed S, Harel N, Hiba B, Jarraya B, Jung B, Kastner S, Klink PC, Kwok SC, Laland KN, Leopold DA, Lindenfors P, Mars RB, Menon RS, Messinger A, Meunier M, Mok K, Morrison JH, Nacef J, Nagy J, Rios MO, Petkov CI, Pinsk M, Poirier C, Procyk E, Rajimehr R, Reader SM, Roelfsema PR, Rudko DA, Rushworth MFS, Russ BE, Sallet J, Schmid MC, Schwiedrzik CM,

Seidlitz J, Sein J, Shmuel A, Sullivan EL, Ungerleider L, Thiele A, Todorov OS, Tsao D, Wang Z, Wilson CRE, Yacoub E, Ye FQ, Zarco W, Zhou YD, Margulies DS, Schroeder CE. An Open Resource for Non-human Primate Imaging. Neuron. 2018 Oct 10;100(1):61-74.e2. doi: 10.1016/j.neuron.2018.08.039. Epub 2018 Sep 27.

Öz G, Tkáč I, Uğurbil K. Animal models and high field imaging and spectroscopy. Dialogues Clin Neurosci. 2013 Sep;15(3):263-78. doi: 10.31887/DCNS.2013.15.3/goz.

Postelnicu G, Zollei L, Fischl B. Combined volumetric and surface registration. IEEE Trans Med Imaging. 2009 Apr;28(4):508-22. doi: 10.1109/TMI.2008.2004426. Epub 2008 Aug 15.

Prichard JW, Alger JR, Turner R. Brain imaging: the NMR revolution. Interview by Clare Thompson. BMJ. 1999 Nov 13;319(7220):1302. doi: 10.1136/bmj.319.7220.1302.

PRIMatE Data Exchange (PRIME-DE) Global Collaboration Workshop and Consortium. Electronic address: michael.milham@childmind.org; PRIMatE Data Exchange (PRIME-DE) Global Collaboration Workshop and Consortium. Accelerating the Evolution of Nonhuman Primate Neuroimaging. Neuron. 2020 Feb 19;105(4):600-603. doi: 10.1016/j.neuron.2019.12.023.

Reuter M, Rosas HD, Fischl B. Highly accurate inverse consistent registration: a robust approach. Neuroimage. 2010 Dec;53(4):1181-96. doi: 10.1016/j.neuroimage.2010.07.020. Epub 2010 Jul 14.

Reuter M, Schmansky NJ, Rosas HD, Fischl B. Within-subject template estimation for unbiased longitudinal image analysis. Neuroimage. 2012 Jul 16;61(4):1402-18. doi: 10.1016/j.neuroimage.2012.02.084. Epub 2012 Mar 10. PMID: 22430496; PMCID: PMC3389460.

Saleem KS, Logothetis NK. A combined MRI and histology atlas of the rhesus monkey brain in stereotaxic coordinates. 2nd ed San Diego: Elsevier/Academic press. with Horizontal, Coronal and Sagittal series. 2012.

Song X, García-Saldivar P, Kindred N, Wang Y, Merchant H, Meguerditchian A, Yang Y, Stein EA, Bradberry CW, Ben Hamed S, Jedema HP, Poirier C. Strengths and challenges of longitudinal non-human primate neuroimaging. Neuroimage. 2021 Aug 1;236:118009. doi: 10.1016/j.neuroimage.2021.118009. Epub 2021 Mar 29.

Stonebarger GA, Bimonte-Nelson HA, Urbanski HF. The Rhesus Macaque as a Translational Model for Neurodegeneration and Alzheimer's Disease. Front Aging Neurosci. 2021 Sep 3;13:734173. doi: 10.3389/fnagi.2021.734173.

Tustison NJ, Avants BB, Cook PA, Zheng Y, Egan A, Yushkevich PA, Gee JC. N4ITK: improved N3 bias correction. IEEE Trans Med Imaging. 2010 Jun;29(6):1310-20. doi: 10.1109/TMI.2010.2046908. Epub 2010 Apr 8.

Van Essen DC, Donahue CJ, Coalson TS, Kennedy H, Hayashi T, Glasser MF. Cerebral cortical folding, parcellation, and connectivity in humans, nonhuman primates, and mice. Proc Natl Acad Sci U S A. 2019 Dec 26;116(52):26173-26180.

Villalon J, Joshi AA, Toga AW, Thompson PM. COMPARISON OF VOLUMETRIC REGISTRATION ALGORITHMS FOR TENSOR-BASED MORPHOMETRY. Proc IEEE Int Symp Biomed Imaging. 2011 Mar-Apr;2011:1536-1541.

Wang X, Li XH, Cho JW, Russ BE, Rajamani N, Omelchenko A, Ai L, Korchmaros A, Sawiak S, Benn RA, Garcia-Saldivar P, Wang Z, Kalin NH, Schroeder CE, Craddock RC, Fox AS, Evans AC, Messinger A,

Milham MP, Xu T. U-net model for brain extraction: Trained on humans for transfer to non-human primates. Neuroimage. 2021 Jul 15;235:118001. doi: 10.1016/j.neuroimage.2021.118001. Epub 2021 Mar 28

Whitwell JL, Crum WR, Watt HC, Fox NC. Normalization of cerebral volumes by use of intracranial volume: implications for longitudinal quantitative MR imaging. AJNR Am J Neuroradiol. 2001 Sep;22(8):1483-9.

Wilson B, Petkov CI. Communication and the primate brain: insights from neuroimaging studies in humans, chimpanzees and macaques. Hum Biol. 2011 Apr;83(2):175-89. doi: 10.3378/027.083.0203.

Wisco JJ, Killiany RJ, Guttmann CR, Warfield SK, Moss MB, Rosene DL. An MRI study of age-related white and gray matter volume changes in the rhesus monkey. Neurobiol Aging. 2008 Oct;29(10):1563-75. doi: 10.1016/j.neurobiolaging.2007.03.022. Epub 2007 Apr 24.